# Investigation of molecular and cellular events associated with beta cell function and elucidation of extracellular RNAs as potential biomarker for diabetes

Sweta Rani

Ph.D. Thesis 2008

**A thesis submitted for the degree of Ph.D.**

**Dublin City University**

**By**

**Sweta Rani, M.Sc.**

**The research work described in this thesis was performed under the supervision of**

**Dr. Lorraine O'Driscoll**

**And**

**Prof. Martin Clynes**

**National Institute for Cellular Biotechnology**

**Dublin City University**

**2008**

I hereby certify that this material, which I now submit for assessment on the programme of study leading to the award of Ph.D. is entirely my own work and has not been taken from the work of others save and to the extent that such work has been cited and acknowledged within the text of my work. Signed: _____ (Candidate) ID No.: _____ Date: _____

# Acknowledgement

This thesis arose in part out of years of research that has been done since I joined NICB. I have worked with a great number of people whose contribution to the research and the making of the thesis deserved special mention. It is a pleasure to convey my gratitude to them all in my humble acknowledgment.

In the first place I would like to record my gratitude to Dr. Lorraine O'Driscoll for her supervision, advice, and guidance for this research as well as giving me extraordinary experiences through out the work. I would like to thank Prof. Martin Clynes for his guidance and support over the course of this project.

Thanks to Dr. Padraig Doolan for his help for processing the microarray chip and Dr. Patrick Gammell for helping with bioanalyzer and siRNA. I must also acknowledge Dr. Niall Barron for helping through qRT-PCR problems and helping me with cloning techniques and thanks to Mr. Mohan Muniyappa as well for helping me with cloning. My gratitude is also extended to Dr. Finbar O'Sullivan and Mr. Kishore Reddy for guiding me through immunohistochemistry and Dr. Annemarie Larkin for helping in immunoprecipitation. Thanks also to Jai for his statistical advice and bioinformatics. I am thankful to Mr. Joseph Carey for preparing media and autoclaving all lab materials. Thanks to Ms. Carol McNamara, Ms. Yvonne Reilly and Ms. Mairead Callan for helping me in day to day work.

My special thanks to former diabetes lab member, Ms Irene Oglesby for training me in all cell related techniques, Elaine Kenny for helping me with conditioned media work and Eadaoin McKiernan for RT-PCR. I would also like to thank our Tissue

Engineering group Erica, for giving me a helping hand whenever I needed, as well as Justine, Serena, Raj and Kishore without whom the lab would be a lonely place to work in. I would also like to thank everyone who contributed in the course of four year of my research at NICB.

Very special thanks to my family members for giving me the much needed support throughout my stay in Dublin. I have run short of words to thank my husband Jai for all his support. One of the best experiences that we lived through in this period was the birth of our daughter Nehal, who provided an additional and joyful dimension to our life mission.

**Abbreviations**

| | |
|---|---|
| AP | Alkaline Phosphatase |
| ATP | Adenosine Triphosphate |
| BSA | Bovine Serum Albumin |
| cAMP | Cyclic Adenosine Monophosphate |
| cDNA | Complementary DNA |
| CEACAM | Carcinoembryonic Antigen-Related Cellular Adhesion Molecule |
| Chgb | Chromogranin B |
| C-peptide | Connecting Peptide |
| cRNA | Complimentary RNA |
| DEPC | Diethyl Pyrocarbonate |
| DM | Diabetes Mellitus |
| DMEM | Dulbecco's Minimal Essential Medium |
| DMSO | Dimethyl Sulphoxide |
| DNA | Deoxyribonucleic Acid |
| dNTP | Deoxynucleotide Triphosphate (N = A, C, T, G) |
| EDTA | Ethylene Diamine Tetraacetic Acid |
| Egr1 | Early growth response 1 |
| ELISA | Enzyme Linked Immunosorbent Assay |
| FCS | Fetal Calf Serum |
| Gad1 | Glutamate Decarboxylase |
| GAPDH | Glyceraldehyde-6-Phosphate Dehydrogenase |
| Gck | Glucokinase |
| GLP1 | Glucagon-like Peptide 1 |
| Glut2 | Glucose Transporter 2 |
| GSIS | Glucose Stimulated Insulin Secretion |
| IAPP | Islet Amyloid Polypeptide |
| IDDM | Insulin Dependent Diabetes Mellitus |
| IL-3 | Interleukin-3 |
| IMS | Industrial Methylated Spirits |
| kDA | Kilo Daltons |
| $k_m$ | Michaelis Constant |
| Min | Minutes |
| MODY | Maturity Onset Diabetes of the Young |

| | |
|---|---|
| mRNA | messenger RNA |
| NAD | Nicotinamide Adenine Dinucleotide |
| NIDDM | Non-Insulin Dependent Diabetes Mellitus |
| Npy | Neuropeptide Y |
| OD | Optical Density |
| PBS | Phosphate Buffered Saline |
| PC1 | Prohormone Convertase 1 |
| PC2 | Prohormone Convertase 2 |
| PCR | Polymerase Chain Reaction |
| Pdx1 | Pancreatic duodenal homeobox factor 1 |
| PKC | Protein Kinase C |
| Pld1 | Phospholipase D1 |
| PLIER | Probe Logarithmic Intensity ERror Estimation |
| PPI | Preproinsulin |
| qRT-PCR | Quantitative real-time PCR |
| Rcf | Rotational Speed at the Relative Centrifugal Force |
| RER | Rough Endoplasmic Reticulum |
| RNA | Ribonucleic Acid |
| RNase | Ribonuclease |
| RNasin | Ribonuclease Inhibitor |
| RPM | Revolutions Per Minute |
| RT-PCR | Reverse Transcriptase Polymerase Chain Reaction |
| TBE | Tris-Boric Acid EDTA Buffer |
| TBS | Tris Buffered Saline |
| TGFβ1 | Transforming growth factor β1 |
| TV | Trypsin Versene |
| UHP | Ultra High Pure Water |

# Abstract

Diabetes is a chronic disorder of glucose metabolism and a major cause of premature mortality. The potential use of replacement beta cells as therapy for diabetes requires an ability to culture such cells while maintaining their functional status. Glucose stimulated insulin secretion (GSIS) is lost in long-term cultured MIN6 heterogeneous cells. MIN6 B1, a clonal sub-line derived from MIN6, has been described as highly glucose-responsive. This study aimed to investigate the GSIS function, changes in gene expression and, subsequently, to develop possible experimental approaches to overcome this loss. Understanding the molecular basis for loss of GSIS may contribute to better culture conditions for islets in transplantation programmes; it may also add to our understanding of beta cell insensitivity to high blood glucose in Type 2 diabetes.

Whole genome microarray analysis on biological triplicate samples of glucose-responsive low passage (p19) (MIN6 B1(GSIS)) and non glucose-responsive high passage (p23) (MIN6 B1(Non-GSIS)) was performed. 111 differentially-regulated genes were identified and 16 gene transcripts were selected based on p-value $<0.05$; fold change $\geq 1.2$; difference $\geq 100$ and validated using qRT-PCR including *Txnip, Gcg* and *Pcsk9*.

*Txnip* was up-regulated whereas *Gcg* and *Pcsk9* were down-regulated in MIN6 B1(Non-GSIS) compared to MIN6 B1(GSIS). siRNA and shRNA silencing of *Txnip* in MIN6(H) (non-responsive) significantly increased the GSIS. Over-expression of *Txnip* cDNA in MIN6(L) (glucose-responsive) caused significant loss of GSIS. siRNA silencing of *Gcg* and *Pcsk9* caused a significant loss of GSIS in MIN6(L) compared to scrambled-transfected cells. Over-expression of *Gcg* cDNA in MIN6(H) increased GSIS.

In parallel, in an attempt to identify more reliable biomarkers for diabetes, we also investigated if extracellular mRNAs are reproducibly detectable in conditioned medium (CM) from a range of insulin-producing cell types and in serum specimens from Type 2 diabetes and controls. *Pdx1*, *Npy*, *Egr1*, *Pld1*, *Chgb*, *Ins1*, *Ins2*, and *beta-actin* from MIN6(L), MIN6(H), and MIN6 B1 cells and their CM suggests that beta cells transcribe and release these mRNAs into their culture environment.This study was subsequently translated to analysis of serum from people with Type 2 diabetes and controls to help establish the clinical relevance of these findings. The result from this clinical phase of the study indicated *Txnip* to be up-regulated and *Egr1* to be down-regulated in Type 2 diabetes compared to controls.

# Section 1.0 Introduction

## 1.1 Diabetes

Diabetes is a chronic disease that occurs when the pancreas does not produce enough insulin or, alternatively, when the body cannot effectively use the insulin it produces. Diabetes currently affects 246 million people worldwide and is expected to affect 380 million by 2025. In 2007, the five countries with the largest numbers of people with diabetes were India (40.9 million), China (39.8 million), the United States (19.2 million), Russia (9.6 million) and Germany (7.4 million). Each year a further 7 million people develop diabetes and 3.8 million deaths are attributable to diabetes. An even greater number die from cardiovascular disease made worse by diabetes-related lipid disorders and hypertension (International Diabetes Federation http://www.idf.org/).

The World Health Organization recognizes three main forms of diabetes (World Health Organisation Department of Non communicable Disease Surveillance http://www.who.int/mediacentre/factsheets/fs312/en/):

- Type 1 diabetes also known as insulin-dependent diabetes mellitus (IDDM),
- Type 2 diabetes non-insulin-dependent diabetes (NIDDM), and
- Gestational diabetes, occurring during pregnancy.

### 1.1.1 Type 1 diabetes

Patients with Type 1 diabetes have a low to zero levels of insulin and C-peptide in blood as the pancreas does not make any insulin (Webb *et al*., 1981; Palmer *et al*., 2004). Type 1 diabetes is characterized by autoimmune destruction of insulin-producing beta cells in the pancreas by CD4+ and CD8+ T cells and macrophages infiltrating the islets (Foulis *et al*., 1991). Genetic factors,

autoantigens and, as yet undefined, environmental triggers act together to initiate the disease (Gillespie, 2006). Susceptibility genes include those within the major histocompatibility complex (MHC)—especially HLA-DR3,DQB1*0201 and HLA-DR4,DQB1*0302, which are present in > 90% of patients with Type 1 DM (Redondo *et al*., 2001; Young *et al*., 2004). Autoantigens include glutamic acid decarboxylase, insulin, insulinoma-associated protein and other proteins in beta cells. These proteins are thought to be exposed or released during normal beta cell injury (Blancou *et al*., 2007). Several viral infections have been associated with subsequent development of human Type 1 diabetes including enterovirus (Lönnrot *et al*., 2000; Salminen *et al*., 2003), rubella (Ginsberg-Fellner *et al*., 1984), mumps (Hyöty *et al*., 1988), rotavirus (Honeyman, 2005) and cytomegalovirus (CMV) (Pak *et al*., 1988; van der Werf *et al*., 2007), but it is unclear which if any of these is the major triggering factor.

Type 1 diabetes accounts for about 5-10% of all diagnosed cases of diabetes (National Diabetes Fact Sheet, 2007). The warning signs for Type 1 diabetes include frequent urination, unusual thirst, extreme hunger, unusual weight loss, extreme fatigue and irritability (Kuzuya, 2000).

**Pathogenesis**

The pathogenesis of the autoimmune beta cell destruction is not fully understood. An examination of islet tissue obtained from pancreatic biopsy from patients with recent onset type 1 diabetes confirmed insulitis. The examination also confirmed presence of CD4 and CD8 T lymphocytes, B lymphocytes and macrophages, suggesting that these cells have a role in destruction of the beta cells (Imagawa *et al*., 1999). The process starts years before overt diabetes

develops and is evident when the beta cell volume is reduced by approximately 80% (Klöppel *et al*., 1985).

### 1.1.2 Type 2 diabetes

Type 2 diabetes is a metabolic disorder that is characterized by insulin resistance (particularly in fat, muscle and liver cells) leading to high levels of glucose in the bloodstream and eventually failure of beta cells. A person with Type 2 diabetes has a normal or high level of C-peptide (Webb *et al*., 1981). The warning signs for Type 2 diabetes are - any of the Type 1 diabetes symptoms, frequent infections, blurred vision, cuts/bruises that are slow to heal; tingling/numbness in the hands/feet; recurring skin, gum, or bladder infections. Sometimes people with Type 2 diabetes have no overt symptoms.

Type 2 diabetes accounts for approximately 90-95% of all diagnosed cases of diabetes (National Diabetes Fact Sheet, 2007; http://www.cdc.gov/diabetes/pubs/pdf/ndfs_2007.pdf). Type 2 diabetes is becoming increasingly common in children. About 40 to 50% of new-onset diabetes mellitus in children is now Type 2 as childhood obesity has become epidemic (Brunton, 2008).

#### Pathogenesis

Insulin resistance: Insulin resistance is regarded as a reduced rate of insulin-mediated glucose uptake in insulin-sensitive tissues of the body including fat, muscle and liver cells (DeFronzo *et al*., 1991; Moller *et al*., 1991).

Beta cell dysfunction: Type 2 diabetes shows marked reduction in first-phase insulin secretion and established diabetes shows attenuated second phase insulin secretion (See Section: 1.3.3.2) (Holt, 2004).

Hyperglycemia develops when insulin secretion can no longer compensate for insulin resistance. Hyperglycemia itself may cause impaired insulin secretion, as high glucose levels desensitize beta cells resulting in beta cell dysfunction or glucose toxicity (Leahy, 1996). Obesity and weight gain are important causative factors for insulin resistance in Type 2 diabetes. Adipose tissue increases plasma levels of free fatty acids leading to impaired insulin-stimulated glucose transport and muscle glycogen synthase activity (Camastra *et al*., 1999).

### 1.1.6 Gestational diabetes

Gestational diabetes is a form of glucose intolerance diagnosed in some women during pregnancy. Gestational diabetes may require treatment to normalize maternal blood glucose levels to avoid complications in the infant. After pregnancy, 5-10% of women with gestational diabetes are found to have Type 2 diabetes. Women who have had gestational diabetes have a 20-50% chance of developing Type 2 diabetes in the next 5-10 years. 70% of women who have had gestational diabetes will develop Type 2 diabetes at some point during their lifetime (National Diabetes Fact Sheet, 2007; http://www.cdc.gov/diabetes/pubs/pdf/ndfs_2007.pdf).

**Pathogenesis**

In the case of gestational diabetes, insulin resistance usually begins in the second trimester and progresses throughout the remainder of the pregnancy. Insulin

resistance and inadequate insulin secretion (to compensate for it) play a central role in the pathophysiology of gestational diabetes. Insulin resistance appears to result from a combination of increased maternal adiposity and the insulin-desensitizing effects of hormonal products of the placenta such as progesterone, cortisol, placental lactogen, prolactin, and growth hormone (Setji *et al*., 2005; Buchanan *et al*., 2005).

### 1.1.7 Health complications

Diabetes can cause many complications. Acute complications (hypoglycaemia, ketoacidosis or nonketotic hyperosmolar coma) may occur if the disease is not adequately controlled. Serious long-term complications include cardiovascular disease (doubled risk), chronic renal failure (diabetic nephropathy is the main cause of dialysis in developed world adults), retinal damage (which can lead to blindness and is the most significant cause of adult blindness in the non-elderly in the developed world), nerve damage (of several kinds), and microvascular damage (Nathan *et al.*, 2005).

The complications of diabetes are not an inevitable outcome, and the risk can be reduced substantially by appropriate therapy. Diabetes therapy is no longer mainly about glucose lowering *per se*, but about overall reduction in the risk factors for diabetic complications (Table: 1.1.4).

**Chronic Complications of Type 1 and Type 2 Diabetes**

* OCULAR COMPLICATIONS
  1. Diabetic cataracts
  2. Diabetic retinopathy
  3. Glaucoma

* DIABETIC NEPHROPATHY
  1. Microalbuminuria
  2. Progressive diabetic nephropathy

* DIABETIC NEUROPATHY
  1. Peripheral neuropathy
     - Distal symmetric polyneuropathy
     - Isolated peripheral neuropathy
     - Painful diabetic neuropathy
  2. Autonomic neuropathy
     - Management of autonomic neuropathy
     - Management of erectile dysfunction

* CARDIOVASCULAR COMPLICATIONS
  1. Heart disease
  2. Peripheral vascular disease

* SKIN AND MUCOUS MEMBRANE COMPLICATIONS
  1. Chronic pyogenic infections of the skin
  2. Necrobiosis lipoidica diabeticorum
  3. Eruptive xanthomas

**Table: 1.1.4 Chronic Complications of Diabetes**

### 1.1.5 Therapy for diabetes

The common therapy for diabetes is daily injections of insulin, but this therapy does not solve serious long-term complication which, as a consequence, results in a shortened life expectancy of diabetic patients (Nathan *et al.*, 1993). Using this form of therapy, it is difficult to provide exact amounts of insulin needed at any given time, resulting in episodes of hyperglycaemia or hypoglycaemia. Hyperglycaemia causes accumulated cell damage in many tissues, leading to the development of long–term complications in IDDM patients. The Diabetes Control and Complications Trial (Centers for Disease Control and Prevention http://www.cdc.gov/) has shown that tight regulation of blood glucose levels can effectively prevent these complications.

Long-term studies strongly suggest that tight control of blood glucose can prevent the development, and retard the progression, of chronic complications of Type 1 diabetes. In contrast to conventional insulin treatment, replacement of a patient's islets of Langerhans either by pancreas organ transplantation or by isolated islet transplantation is the only treatment to achieve a constant normoglycemic state and avoiding hypoglycaemic episodes, a typical adverse event of multiple daily insulin injections (Bretzel *et al.*, 2004).

## 1.2 The Pancreas

The pancreas is an organ in the digestive and endocrine system of vertebrates. It is both exocrine (secreting pancreatic juice containing digestive enzymes) and endocrine (producing several important hormones as detailed below). The endocrine (*i.e*. hormone-producing) cells of the pancreas are grouped in the islets of Langerhans. Discovered in 1869 by the German pathological anatomist Paul Langerhans, the islets of Langerhans constitute approximately 1 to 2% of the mass of the pancreas (Kobayashi *et al.*, 2004) (Fig: 1.2).

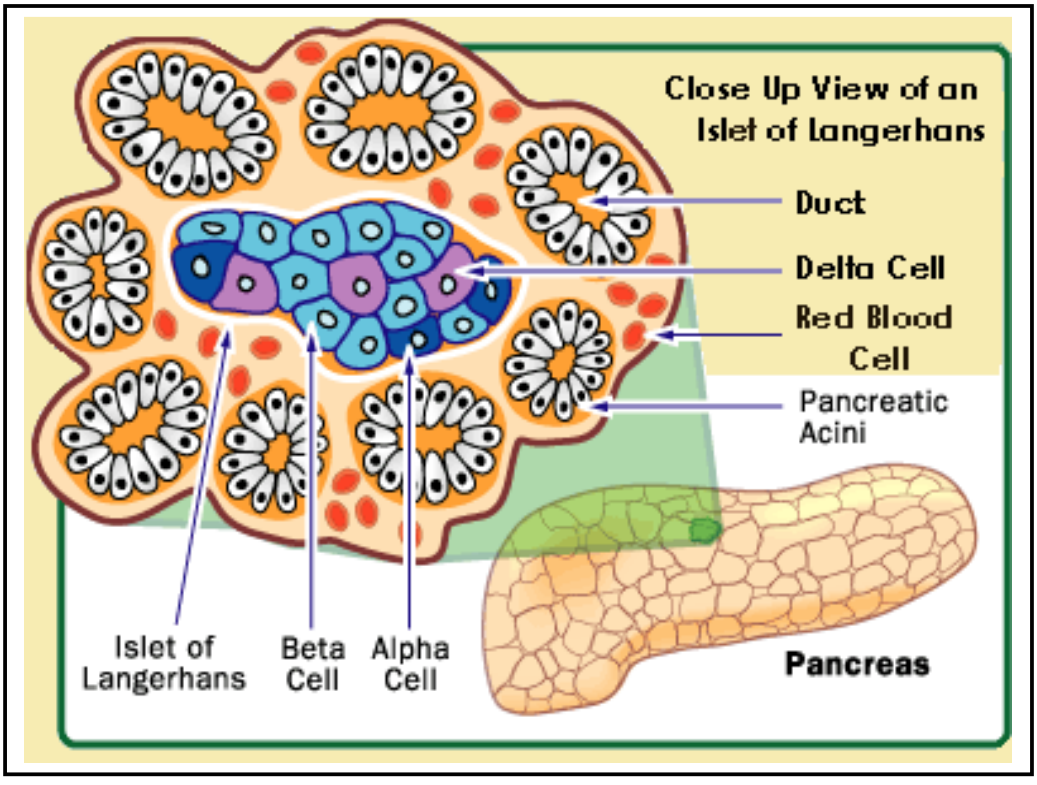


**Fig: 1.2 Structure of pancreas showing different types of cells present (**http://health.howstuffworks.com/diabetes1.htm**).**

Hormones produced in the Islets of Langerhans are secreted directly into the blood flow by at least four different types of cells (Brissova *et al.*, 2005; Kobayashi *et al.*, 2004; Suckale *et al*., 2008) (Fig: 1.2).

- Beta cells producing insulin and amylin (65-80% of the islet cells)
- Alpha cells releasing glucagon (15-20%)
- Delta cells producing somatostatin (3-10%)
- PP cells containing polypeptide (1%)

The beta cells present in pancreatic islet of Langerhans play an important role in glucose haemostasis. Insulin and glucagon directly influence glucose homeostasis, while somatostatin and pancreatic polypeptide have modulatory function. After a carbohydrate-rich meal, beta cells secrete insulin that facilitate glucose uptake by liver, adipose tissue and muscle, thereby reducing glucose concentration in blood. When glucose concentration is decreased, alpha cells secrete glucagon, which increases glucose concentration in blood by activating glycogenolysis and gluconeogenesis. This way both insulin and glucagon maintain blood glucose concentration (Nussey *et al*., 2001).

## 1.3 Insulin

### 1.3.1 Structure of Insulin

Insulin is a small protein of approx. 5.8kDa. Insulin is synthesized by humans and other mammals in the beta cells of pancreas. Insulin, a polypeptide hormone, consists of two polypeptide chains, one 21 amino acids long, called the "A" chain, and a second, the "B" chain, which is 30 amino acids long. The two chains are bound together in their quaternary structure by two disulfide bridges.

The secondary structure of both chains is mostly alpha helical (Fig: 1.3.1). Insulin is created as a single peptide chain, which is looped around, bonded to itself by covalent disulfide bonds between cysteine residues (Brange *et al.*, 1993). In addition, a third disulfide bridge between two amino acids in the "A" chain helps stabilize its tertiary structure (Brange *et al.*, 1993).

Most animals have a single copy of the insulin gene, with the exception of Arctic salmon, African clawed frog and the murine species including rat and mouse (Bell *et al.*, 1980). Apparently insulin gene duplication in mouse resulted from reverse transcription and reintegration of an incompletely processed RNA transcript of the original insulin gene (insulin gene II) (Soares *et al.*, 1985).

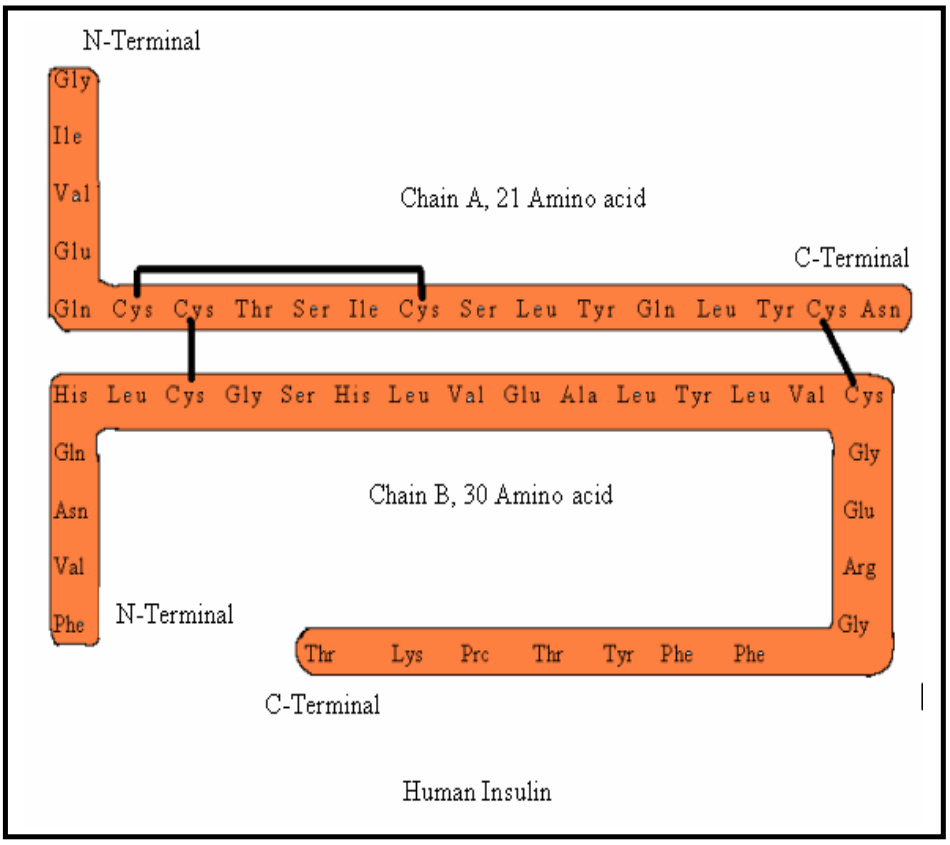


**Fig: 1.3.1 Structure (amino acid sequence) of human insulin. Following post-translational modification of their precursor chains, these are assembled in endoplasmic reticulum. The disulfide bridges, which create the quaternary assembly of this molecule, are shown as black bonds connecting the cysteine (Cys) residues.**

### 1.3.2 Biosynthesis of insulin

The biosynthesis of insulin starts in the nucleus of the beta cells of the pancreas. It is thought that translation of the mRNA into preproinsulin starts while the ribosome is free in the cytosol. The signal sequence of the preproinsulin anchors the ribosome to the membrane of the rough Endoplasmic Reticulum (RER), after which the protein is translocated into the lumen of Endoplasmic Reticulum (ER). Translocation of preproinsulin is mediated by a signal-peptide across the RER (Rhodes *et al.*, 2000). In the RER of beta cells, insulin is synthesized as a single polypeptide chain; preproinsulin precursor molecules are held together by the C-peptide (connecting peptide) and contain a hydrophobic signal peptide, consisting of 23 amino acids at the N- terminal. After preproinsulin is synthesized in the ER, it is converted into proinsulin (Ren *et al*., 2007). The influx of Ca+ from the calcium storehouse ER causes the fusion of secretory vesicles to the plasma membrane (Varadi *et al.*, 2002). Then with the help of secretory vesicle the proinsulin is transported through the Golgi apparatus and packaged into immature clathrin-coated granules. Here the proinsulin is broken down into the center portion of the molecule C-peptide, liberated from the C- and N- terminal ends of the proinsulin. The signal peptide is removed by the action of proteolytic enzymes known as *prohormone convertases* (*PC1* and *PC2*), as well as the exoprotease carboxypeptidase E to produce proinsulin (Nie *et al.*, 2000). The remaining polypeptides (51 amino acids), *i.e*. the B- and A- chains, are held together by disulfide bonds forming mature insulin. At exocytosis, equimolar amounts of insulin and C-peptide are released into the circulation, together with up to 5% proinsulin (Goodman, 2003).

### 1.3.3 Insulin secretion and regulation

Insulin plays a central role in the control of the body's metabolism. It accelerates the glucose uptake into a number of tissues while simultaneously suppressing glucose production and lipolysis. The beta cell glucose transporter, GLUT2, senses the glucose concentration and transports it into the cell. Glucose is phosphorylated into glucose 6-phosphate (G-6-P) by glucokinase, which is a part of the glucose-sensing mechanism (Nilsson *et al.*, 1996). Glucose phosphorylation increases ATP production in the beta cell, increasing the intracellular ratio of ATP/ADP (Ghosh *et al.*, 1991). ATP binds to $K_{ATP}$ channels on the beta cell membrane, probably concomitant with phosphorylation of $K_{ATP}$ channel, closes the channels, resulting in depolarization of the beta cell membrane (Tarasov *et al.*, 2004). When the beta cell membrane potential reaches –30 to –40 mV, the voltage-sensitive calcium channels ($Ca^{2+}$-channels) open leading to an influx of calcium ions. The increase of intracellular calcium ions triggers the exocytosis of insulin granules (Ohara-Imaizumi *et al.*, 2006)**.** In addition, increased $(Ca^{2+})_i$ then activates (opens) voltage-sensitive potassium channels, thereby restoring the resting potential to –70 to -60 mV and increasing the concentration of cytoplasmic free calcium (Ohara-Imaizumi *et al.*, 2006). The final result is insulin exocytosis (Fig: 1.3.3).

After glucose stimulation, insulin secretion from the beta cell is biphasic. The first phase of insulin secretion occurs within 10–15 minutes of stimulation and involves the release of preformed insulin. The second phase, which lasts up to 2 hours, is the release of newly synthesized insulin (Henquin *et al.*, 2000).

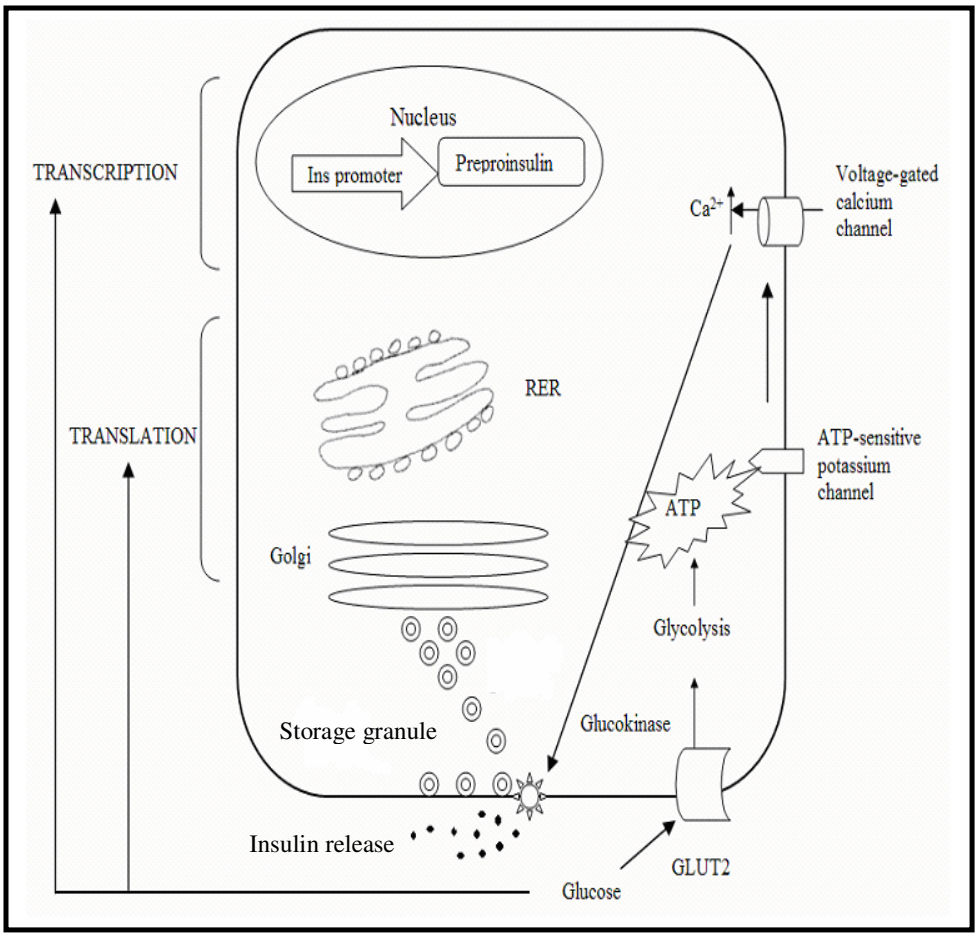


**Fig: 1.3.3 Rising blood glucose levels triggers insulin secretion from beta cells. Starting with the uptake of glucose by the GLUT2 transporter, the glycolytic phosphorylation of glucose causes a rise in the ATP: ADP ratio. This rise inactivates the potassium channels that depolarize the membrane, causing the calcium channel to open up allowing calcium ions to flow inward. The ensuing rise in levels of intracellular calcium leads to the exocytotic release of insulin from their storage granules.**

Gastrointestinal hormones and some amino acids, such as leucine, arginine, and lysine, also stimulate insulin secretion. Gastrointestinal hormones, such as glucose-dependent insulinotropic peptide (GIP), cholecystokinin, glucagon-like peptide-1 (GLP-1) and vasoactive intestinal peptide (VIP), are secreted following ingestion of foods and potentiate insulin secretion (Drucker *et al.*, 2006).

#### 1.3.3.1 Role of Endoplasmic Reticulum (ER) in insulin secretion

One of the salient attribute of beta cells is a highly developed Endoplasmic Reticulum (ER) which helps in its function of glucose response and insulin secretion. ER is entrusted with post-translational modification, folding and assembly of newly synthesized secretory proteins. Proper functioning of ER is essential for cell survival (Webb *et al.,* 2000; Araki *et al.*, 2003). The pancreatic beta cells respond to glucose by the biosynthesis of preproinsulin and the release of insulin. The ER is also responsible for proper three-dimensional folding of precursor insulin (proinsulin) into mature insulin (Fonseca *et al.*, 2005). The correct folding of the proinsulin is essential for the efficient production of insulin (Halban *et al*., 1994).

Preproinsulin is the original single polypeptide used to form mature insulin. It consists of four regions, from N-terminal to C-terminal *i.e.* a hydrophobic signal sequence (SS), B-chain polypeptide, connecting peptide (C-peptide) and A-chain polypeptide. The transcribed mRNA for preproinsulin moves to a ribosome and sequentially binds to the signal recognition particle (SRP) initiating protein translation. The translated SS peptide (also called nascent chain) tags onto the SRP and migrates to a high-affinity receptor for SRP named the SRP docking protein (SRPdp) that is located at the external surface of the RER (Gilmore *et al.,*

1982). Subsequently, the ribosome dissociates from the SRP and SRPdp and is restrained by the ribosome receptor (RR) on the ER membrane. The natural hydrophobic property of SS (22 of 24 amino acids in SS are hydrophobic) facilitates and enhances the binding affinity between ribosome-mRNA complex and the phospholipids bilayer of the ER membrane (Do *et al*., 1996). In addition to SRPdp, other membrane proteins such as translocating-chain associated membrane (TRAM) and Sec61 proteins are essential for directing the ribosome-mRNA complex to the ER membrane (High et al., 1993; Voigt *et al*., 1996; Knight *et al*., 1998). Through the joint interaction of membrane proteins, the complex is placed at the site on the ER membrane termed translocon (McCormick *et al*., 2003) where the SS peptide guides the extension of the preproinsulin polypeptide chain into the ER lumen. The SS peptide is excised by signal peptidase positioned on the inner ER membrane and proinsulin is formed. The proinsulin is then folded by a molecular chaperone (e.g. protein disulfide isomerase, PDI) by the formation of the disulfide bonds (Winter *et al*., 2002). The vesicles filled with proinsulin then bud out from the RER towards the Golgi apparatus where the zinc/calcium environment around the Golgi favours the formation of the zinc-containing proinsulin hexamer (Dodson *et al*., 1998). Proinsulin passes through *cis*, *medial* and *trans* Golgi cisternae and is converted to insulin at the stage of vesicle formation. This transformation is driven by membrane-associated prohormone convertase enzymes (PCs). The catalytic sites targeted by PCs are called the dibasic sites (Goodge *et al*., 2000).

Subsequently the granules are packed with mature insulin coupled with the precipitation of removed C-peptide and are maintained in the cytoplasm as an "insulin secreting vesicles pool" or "readily releasable pool (RRP)". Once the

beta cells sense certain physiological variations of glucose level (high glucose) the insulin is secreted through the release of these primary granules in order to maintain normoglycaemia.

As described above, the release of insulin by beta cells is dependent upon glucose-induced alteration of $Ca^{2+}$. Glucose dependent sequestration of cytosolic $Ca^{2+}$ into ER via activation of the ER $Ca^{2+}$ -ATPase, and its subsequent release, has been demonstrated to play an important role in glucose-activated beta cell $Ca^{2+}$ signalling (Roe *et al.*, 1994).

### 1.3.3.2 Mechanism of glucose-stimulated insulin secretion (GSIS)

The secretion of insulin from pancreatic beta cell is a complex process involving the integration and interaction of multiple external and internal stimuli. The primary stimulus for insulin secretion in the beta cell is to response to changes in ambient glucose (Rajan *et al.*, 2002).

As described in section 1.3.3, insulin secretion in response to glucose in beta cells exhibits two phases. Glucose enters beta cells via the GLUT2 transporter. Glucokinase is the first enzyme of the glycolytic pathway and serves as a glucose sensor. The metabolism of glucose by means of glycolysis and the citric acid cycle generates nicotinamide adenine dinucleotide (NADH) and the reduced form of flavin adenine dinucleotide (FADH2), which donate electrons to the mitochondrial electron-transport chain (ETC). Protons are then pumped out by respiratory chain complexes I, III, and IV, creating a proton electrochemical gradient. When protons re-enter the mitochondrial matrix, through adenosine triphosphate (ATP) synthase, ATP is generated from adenosine diphosphate

(ADP) and inorganic phosphate (Pi) leading to increased cytosolic ATP: ADP ratio (Langin, 2001). Mitochondrial ATP production is essential for GSIS (Wiederkehr *et al*., 2006) (Fig: 1.3.3.2.1 and Fig: 1.3.3.2.2).

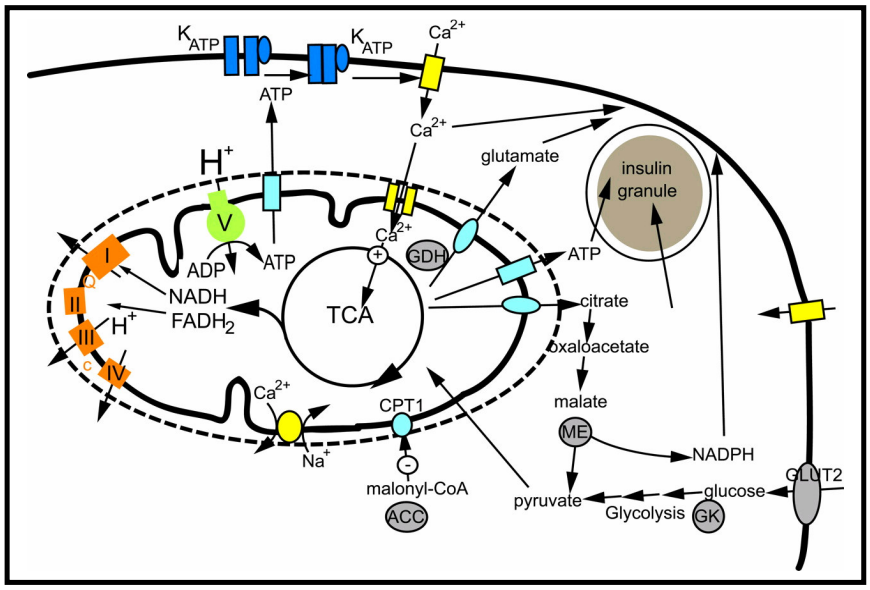


**Fig: 1.3.3.2.1 Role of mitochondria in metabolism and secretion coupling of the beta cell. Respiratory chain complexes I–IV (orange), complex V/ATP synthase (green), calcium transport systems (yellow), transporters/shuttles of the inner mitochondrial membrane (pale blue), and open and closed forms of the $K_{ATP}$ channel (dark blue) are indicated. ACC, Acetyl-CoA carboxylase; GDH, glutamate dehydrogenase; GK, glucokinase; ME, malic enzyme; TCA, TCA cycle (Wiederkehr *et al*., 2006).**

The pancreatic beta cell $K_{ATP}$ channel is comprised of Sulfonylurea receptor -1 (SUR1) and potassium channel Kir6.2. The SUR1 channel maintains a potassium current, generating cell-membrane polarization (Donley *et al*., 2005). This increased cytosolic ATP: ADP ratio in turn results in closure of the SUR1 receptor channel, depolarizing the membrane and initiation of electrical activity (Ren *et al*., 2007). This glucose-induced closure of the $K_{ATP}$ channel activates the $K_{ATP}$ channel-dependent signalling pathway, depolarizing the beta cell to cause increased $Ca^{2+}$ entry via voltage-dependent $Ca^{2+}$ channels and increased [$Ca^{2+}$] ion. In response to the rise in intracellular $Ca^{2+}$, some docked and primed insulin storage granules fuse and release insulin, while storage granules traffic to join the RRP at the cell surface. Insulin secretion from the beta cells is biphasic, with the first phase resulting from the release of insulin granules from an immediate releasable pool pre-primed at the plasma membrane. The second phase only occurs with nutrient stimulation and is thought to represent secretion from those granules which are mobilized to re-fill the readily and immediate releasable pools of granules. This increased [$Ca^{2+}$] ion triggers the exocytosis of a small pool of granules that is responsible for the first phase of insulin release (Straub *et al*., 2002).

Second phase of insulin secretion includes mobilization and trafficking of intracellular storage pools of insulin secretory granules to the plasma membrane (Spurlin *et al*., 2006). The fusion of insulin secretory granules is known to be regulated by soluble N-ethylmaleimide sensitive factor attachment protein receptor (SNARE) protein complexes at the plasma membrane (Spurlin *et al*., 2006).

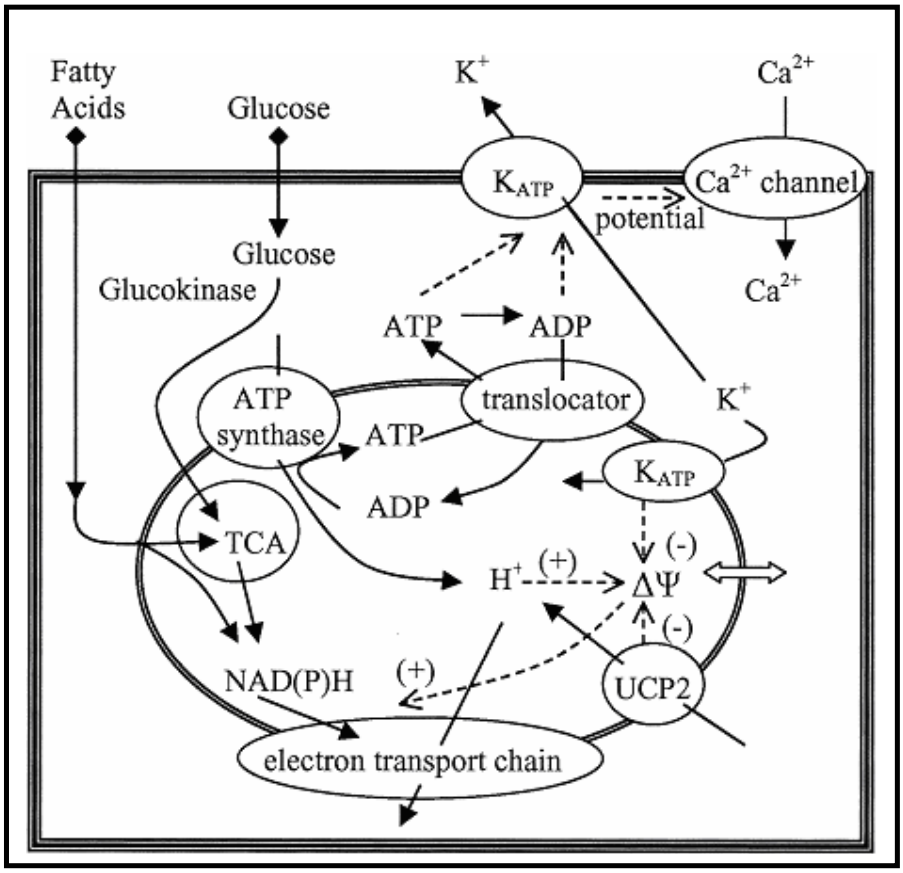


**Fig: 1.3.3.2.2. The various components discussed in the text are illustrated in the cartoon of a beta cell and a mitochondrion within it. Glucose and fatty acid metabolism leads to an increase in NADH and $Ca^{2+}$ and to a decrease in ADP. In turn, decreased ADP leads to increased mitochondrial membrane potential ($\Delta\Psi$). Increased glycolytic flux, decreased ADP concentration, and increased intracellular $Ca^{2+}$ concentration may all contribute to increased GSIS in the electron transport chain (ETC). Solid lines indicate flux of substrates, and dashed lines indicate regulating effects, where (+) represents activation and (–) represents repression (Fridlyand *et al*., 2004).**

Upon stimulation with glucose, the target membrane t-SNARE proteins Syntaxin 1 (Syn1) and SNAP-25 (soluble NSF (N-ethylmaleimide sensitive factor) attachment protein) receptor leads the insulin granules to the plasma membrane through interaction with their cognate vesicle v-SNARE protein, vesicle-associated membrane protein VAMP2. Heterotrimeric SNARE core complex is composed of the vesicle-associated membrane protein (VAMP 2; synaptobrevin) and two predominantly plasma membrane proteins, syntaxin 1 and synaptosomal-associated protein of 25kDa (SNAP-25) (Quetglas *et al*., 2000). SNARE core complex facilitates the fusion of the insulin secretory granule with the plasma membrane and release of insulin from the cell (Spurlin *et al*., 2006).

### 1.3.4 Insulin function

The biological effects of insulin on the integration of fuel metabolism are primarily to promote the storage of glucose as glycogen, amino acids as proteins and fats as triglycerides. Insulin promotes fuel storage via a number of mechanisms.

#### 1.3.4.1 Glucose metabolism

Once in the blood, insulin controls glucose homeostasis by stimulating the uptake of glucose into skeletal muscle and, to a lesser extent, into liver and adipose tissue. In skeletal muscle, heart muscle, and fat this uptake is mediated by the so-called insulin-sensitive glucose transporter GLUT-4 (Shi *et al*., 2008). Once glucose enters the cells it is phosphorylated by hexokinase to glucose-6-phosphate. Glucose-6-phosphate then undergoes glycolysis for energy production or it is stored as glycogen.

#### 1.3.4.2 Lipid metabolism

Lipids are basically insoluble in blood and are transported as lipoproteins. Triglycerides are hydrolysed to fatty acids and glycerol by the action of an enzyme lipoprotein lipase. Insulin stimulates the synthesis of the enzyme lipoprotein lipase (Gibson *et al*., 2002).

#### 1.3.4.3 Protein synthesis

Insulin can stimulate protein synthesis in many types of cells *in vivo* and tissues, including human and rat muscles, and many types of cells in culture. This involves two major kinds of effects: the rapid activation of existing components of the translational apparatus and the longer term increase in the capacity of the cell or tissue for protein synthesis, which includes an increase in ribosome number (Proud, 2006).

### 1.3.5 C-peptide

C-peptide was discovered in 1967 and is a by-product of insulin production (Steiner, 2004). Insulin is synthesized in the pancreatic beta cell as a component of a polypeptide called proinsulin. Proinsulin is subsequently cleaved enzymatically, releasing insulin into the circulation along with a residual 3,000 molecular weight fragment called C-peptide or connecting peptide. It is named connecting peptide as it connects the A chain and B chain of insulin within the proinsulin molecule (Rendell, 1983). Chen *et al*. (2002) reported that the highly conserved acidic N-terminal part of C-peptide plays an important role in insulin precursor folding. C-peptide also has some intramolecular chaperone-like function in the folding of insulin precursor (Chen *et al*., 2002).

As insulin and C-peptide are secreted nearly in equal amounts, measurements of immunoreactive C-peptide release has proven to be useful as a measure of insulin secretory rate *in vivo* in humans (Rubenstein *et al*., 1969). The half-life of insulin is shorter than that of C-peptide approximately 3.0 minutes or less under normal conditions (Rendell, 1983). Beta cell function can be evaluated by calculating insulin secretion rate by deconvolution of peripheral C-peptide concentrations as proposed by Eaton *et al*. (1980) and again by Polonsky *et al*. (1986). Serum/plasma C-peptide assays have enabled evaluation of beta cell reserve in both diabetic and normal subjects (Polonsky *et al*., 1986).

## 1.4 Glucagon

Glucagon was given its name by Kimball and Murlin (Murlin *et al*., 1923). In 1955 Staub *et al*. purified and crystallized glucagon and 2 years later the amino acid sequence of glucagon was reported by Bromer *et al*. (1957).

### 1.4.1 Structure of Glucagon

Glucagon is a polypeptide that consists of a peptide chain of 29 amino acids (Fig: 1.4.1). After cleavage of the signal peptide, proglucagon is cleaved into active glucagon, glucagon-related polypeptide (GRPP) and the major proglucagon fragment (Nussey *et al.,* 2001; Pineda, 2003).

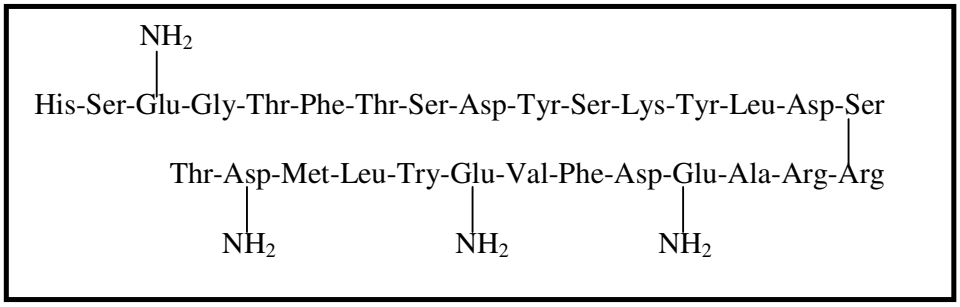


**Fig: 1.4.1 Amino acid sequence of Glucagon**

### 1.4.2 Biosynthesis of Glucagon

Preproglucagon is produced in the alpha cells in pancreatic islets and L cells in the jejunum and ileum. A number of peptides can be produced from preproglucagon depending on posttranslational processing at dibasic amino acid sites. PC2 and PC1/3 is prohormone convertase enzyme and are found in high concentration in islet cells. PC2 converts preproglucagon to glucagon by cleaving the N-terminal part in alpha cells (Porte *et al*., 2003). Whereas PC1/3

cleaves the C-terminal part of preproglucagon, leading to the formation of GLP-1 (Damholt *et al*., 1999) (Fig: 1.4.2).

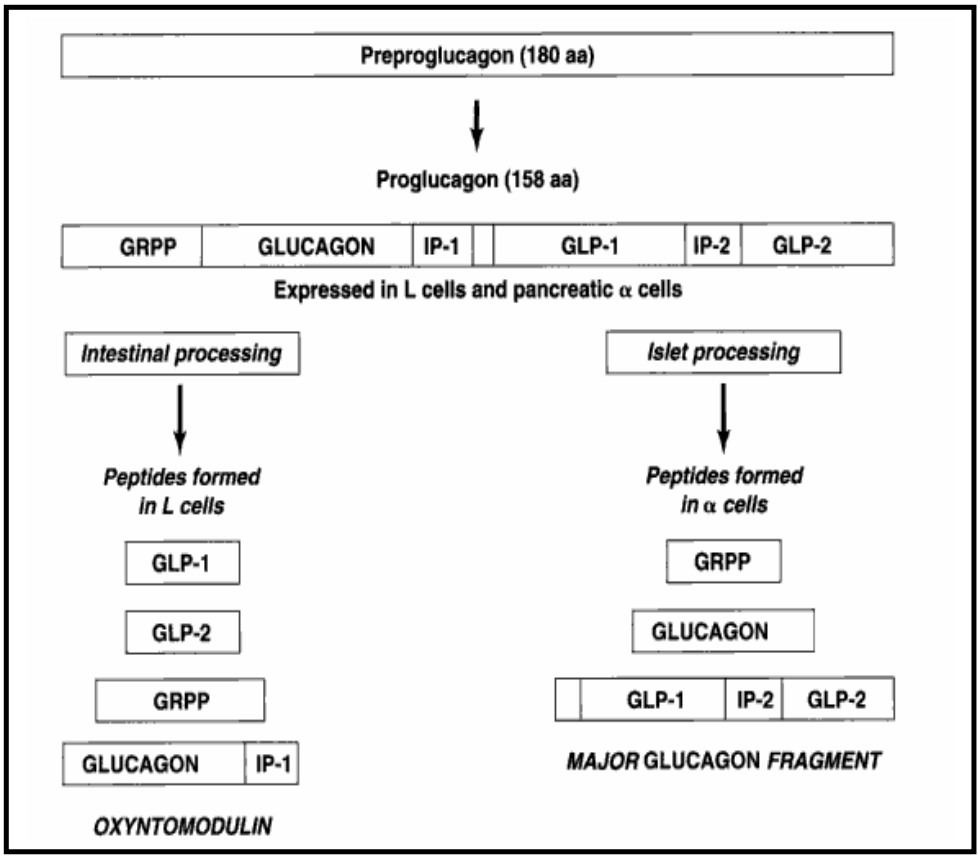


**Fig: 1.4.2 Processing of the proglucagon to peptides in the alpha cells and intestinal L cells. GLP=glucagon-like peptide, GRPP= glicentin-related pancreatic peptide, IP= intervening peptide. The peptides shown are GRPP (proglucagon 1-30), glucagon (proglucagon 33-61), IP-1 (proglucagon 64-69), and MPGF (proglucagon 72-158) (Furuta *et al*., 2001).**

Glucagon is derived from proglucagon which is also known as glicentin. Proglucagon is a 158 amino acid precursor containing glucagon and two related peptide sequences, glucagon-like peptides 1 and 2 (GLP-1 and -2). It is cleaved at a series of dibasic sites and at a single basic site to release a number of peptides, including glucagon, 2 glucagon containing peptides (GLP) and 2 other peptides known as intervening peptides (IP) (Fricker, 1991).

These peptides are separated by three intervening peptides called glucagon-related polypeptide (GRPP), intervening peptide I (IVP-I) and intervening peptide II (IVP-II) (Okamoto, 1990).

In the islet cells of the pancreas the glucagon precursor is cleaved at Lys-Arg sequence thereby giving rise to glucagon and three possible inactive fragments: GRPP, IVP-I and MPGF (major proglucagon fragment). Glucagon and GRPP are released together from the pancreas (Moody *et al.*, 1981).

### 1.4.3 Glucagon secretion

Glucose enters the alpha cell through either of glucose-transporter SLC2A1 or GLUT1. At low-glucose concentrations, the activity of $K_{ATP}$ channels is low rendering a membrane potential of about –60 mV (Gromada *et al.*, 2004). ATP-dependent $K^+$ ($K_{ATP}$) channels play a fundamental role in alpha cells, as they do in beta cells. However, lower ATP concentrations are required to obtain the maximum inhibition of $K_{ATP}$ conductance in alpha cells compared to beta cells (Leung *et al.*, 2005). The voltage-gated $Ca^{2+}$-channels are divided into three subfamilies: 1) L-type $Ca^{2+}$-channel; 2) N-type $Ca^{2+}$-channels and 3) T-type $Ca^{2+}$-channel (Gromada *et al.*, 2007) (Fig: 1.4.3).

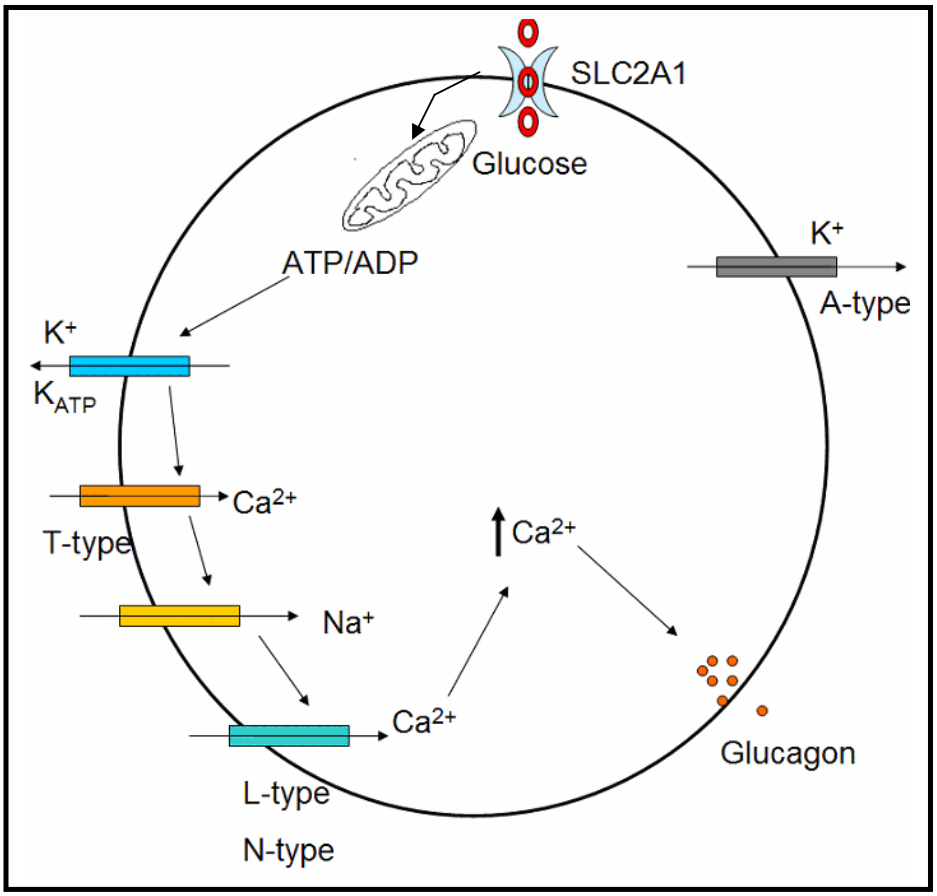


**Fig: 1.4.3 Schematic model for glucose-dependent regulation of glucagon secretion in alpha cell. Glucose enters the alpha cell through glucose-transporter SLC2A1. Glucose uptake and metabolism lead to an increase in the ATP/ADP ratio and closure of ATP-sensitive $K^+$-channels ($K_{ATP}$-channels) leading to membrane depolarization. This membrane depolarization leads to activation of voltage-gated $Ca^{2+}$-channels (T-, L- and N-type) and $Ca^{2+}$ influx. This increase in the $[Ca^{2+}]i$ stimulates exocytosis of the glucagon-containing granules.**

At the potential between –40 and –30 mV, voltage-dependent T-type $Ca^{2+}$-channel opens, depolarizing the plasma membrane. This depolarization leads to activation of N-type $Ca^{2+}$ channels and voltage-dependent $Na^{+}$ channels (MacDonald *et al.*, 2007). Their activation triggers $Ca^{2+}$ influx and exocytosis of glucagon granules (Gromada *et al.*, 2007).

The opening of A-type $K^{+}$ channels is necessary for action potential repolarization (Quesada *et al.*, 2006). However, high-glucose concentrations elevate the intracellular ATP/ADP ratio completely blocking the $K_{ATP}$ channels leading to greater membrane depolarization (MacDonald *et al.*, 2007). The voltage-gated $Ca^{2+}$ and $Na^{+}$ channels therefore become inactivated and electrical activity ceases. This result in reduced $Ca^{2+}$ influx and suppressed glucagon secretion (Gromada *et al.*, 2004; Quesada *et al.*, 2008).

### 1.4.4 Actions of glucagon

The function of glucagon is antagonistic to that of insulin. The release of glucagon is stimulated by hypoglycemia and inhibited by hyperglycemia, insulin and somatostatin (Muñoz *et al*., 2005). The control of glucagon secretion is regulated by low glucose and by intra-islet insulin. The physiological role of glucagon is to stimulate production and secretion of glucose. Glucagon acts primarily on the liver, stimulating glycogenolysis and gluconeogenesis increasing the blood glucose levels (Chiasson *et al*., 1975; Magnusson *et al*., 1995). Glucagon stimulates lipolysis that increases the circulating concentration of free fatty acids. Hormone-sensitive lipase mediates the lipolysis of triacylglycerol into the non-esterified fatty acids and glycerol, which are released from adipocytes. It has been reported that glucagon increases the release of

glycerol from adipocytes (Slavin *et al.,* 1994). It stimulates the hepatic uptake of amino acids for gluconeogenesis in the liver (Goodman, 2003). Glucagon may also be involved in diabetic ketoacidosis, a medical complication in diabetes derived from the overproduction of ketone bodies (Eledrisi *et al.,* 2006).

### 1.4.5 Glucagon in diabetes

Diabetes is the result of an insulin deficiency or resistance along with an absolute or relative excess of glucagon, resulting in a higher rate of hepatic glucose production than glucose utilization, favouring hyperglycaemia. The rate of hepatic glucose output has been correlated with the hyperglycaemia found in animal models of diabetes as well as in human diabetes, and the maintenance of this abnormality has also been associated with hyperglucagonaemia (Dunning *et al*., 2007; Li *et al*., 2008). Lack of suppression of glucagon release is observed in hyperglycaemic conditions, which further contributes to postprandial hyperglycaemia in both Type 1 and Type 2 diabetes (Shah *et al*., 2000.

Impaired insulin secretion is found to mediate both the impaired postprandial suppression of glucagon release (Meier *et al*., 2006) and the impaired glucagon response to hypoglycemia (Gosmanov *et al*., 2005; Raju *et al*., 2005). The glucagon response to hypoglycaemia is known to disappear within a few months after the onset of Type 1 diabetes, whereas the response to other stimuli remains intact (Jauch-Chara *et al*., 2007). Lorenzi *et al*. (1984) also reported that in patients with Type 1 diabetes for more than ten years the glucagon responses to insulin hypoglycemia was severely blunted or absent and also the abrupt restoration of plasma glucose levels was impaired. The loss of the glucagon response to falling plasma glucose concentrations has been observed, which is a

key feature of the pathogenesis of induced hypoglycemia, in insulin-deficient (Type 1 and advanced Type 2) diabetes (Raju *et al*., 2005). Whether all abnormalities of alpha cell function in Type 2 diabetes are secondary to beta cell dysfunction is still controversial (Dunning *et al*., 2007).

## 1.5 Somatostatin

Somatostatin was first discovered in hypothalamic extracts and identified as acting on pituitary to inhibit growth hormones. Subsequently it was also found to be secreted by other extra hypothalamic regions of the central nervous system, present in the cells of peripheral nervous system and in non-neural tissues including thyroid, gut and endocrine pancreas (Srikant, 2004).

### 1.5.1 Structure of Somatostatin

Somatostatin is present in two forms- somatostatin 14 (SST-14) and somatostatin 28 (SST-28), reflecting its amino acid chain length. SST is synthesized from a 116 amino acid peptide, preprosomatostatin by proteolytic cleavages (Funckes *et al*., 1983). In mammals, preprosomatostatin is encoded by a single mRNA sequence (Montminy *et al*., 1984). Proteolytic cleavage of 24 amino acids at the N-terminus of preprosomatostatin leads to the formation of prosomatostatin (Noe *et al*., 1989). Prosomatostatin is processed in two different ways to generate SST-14 and SST-28 (Montminy *et al*., 1984) in a tissue specific manner. SST-14 is synthesized in brain, pancreas and gastric tissue, while SST-28 is mainly synthesized in the intestinal epithelium (McPhee *et al*., 2006).

### 1.5.2 Actions of somatostatin

Somatostatin has an inhibitory effect on the insulin-releasing action of beta cells. It is also found to suppress the activity of glucagon release from adjacent alpha cells (Berts *et al*., 1996). Hypothalamic somatostatin has been established as an inhibitor of growth hormone release from the pituitary cells (Thermos, 2008).

### 1.6 Pancreatic Polypeptide

Pancreatic polypeptide (PP) is a 36 amino acid polypeptide and belongs to the family of regulatory peptides consisting of neuropeptide Y (Npy) and peptide YY (PYY) (Glover *et al*., 1984; Mor *et al*., 1994). PP is produced by PP cells, which are localized in the periphery of pancreatic islets of Langerhans and scattered between the acinar cells of the pancreatic head and uncinate lobe (Larsson *et al*., 1976). More than 95% of PP is of pancreatic origin and the rest is released from the gastrointestinal tract (Liu *et al*., 1999; Stanley *et al*., 2004).

#### 1.6.1 Role of Pancreatic polypeptide

Physiologically, pancreatic polypeptide (PP) is released in response to food ingestion (Dembiński *et al*., 2004). PP reduces the secretion from the exocrine pancreas. It also decreases gall bladder contraction and inhibits gastric and small intestine motility. It also helps to pace the entry of nutrients into the circulation by slowing down the digestive process (Liu *et al*., 1999).

## 1.7 Insulin producing cell lines

In contrast to conventional insulin treatment, either replacement of a patient's islets of Langerhans by whole pancreas transplantation or by isolated islet transplantation is a likely cure for diabetes (Bretzel *et al*., 2007). Isolated islet transplantation has shown success (Shapiro *et al.*, 2000). Islet transplantation was performed on sixty-five patients in Edmonton in 2004. Five-year follow-up study carried on these transplanted patients revealed that approximately 80% had C-peptide present post–islet transplantation, but only a minority (~10%) maintained insulin independence (Ryan *et al.*, 2005). The 2008 CITR report describes 325 islet transplant recipients. Of these recipients, most (86%) received islet-alone infusions, while the others (14%) had previously received a kidney transplant and followed by islet transplant (Collaborative Islet Transplant Registry 2008).

Low numbers of donated pancreas necessitates the search for other beta cell/islet sources. It has been proposed that replacement beta cells may be generated from stem/progenitor cells, from the pancreas and expanded *in vitro*, making it a possibility that enough islets could be produced from a pancreas obtained from a single donor for one or more successful transplants (Ren *et al*., 2007). However, so far, an adequate supply of such cells has not been identified. Another alternative source includes the use of cultured beta cell lines isolated from rodent islets or human islets (Suzuki *et al.*, 2003; Limbert *et al*., 2008).

Cultured beta cell lines are important for research purposes, as they provide a "pure cell" population to work with and great for studying islet cell biology and transcriptional cascade of endocrine differentiation (Limbert *et al*., 2008). However, beta cell lines generated to date lack the characteristics of mature beta

cells and generally demonstrate reduced insulin secretion and some show loss of proliferation (Kayo *et al.*, 1996; O'Driscoll *et al.*, 2006; Limbert *et al*., 2008).

The most widely used insulin-secreting cell lines are RIN, HIT, βTC, MIN6 and INS-1 cells. These cells secrete mainly insulin but are also known to secrete glucagon and somatostatin (Poitout *et al*., 1996; Hohmeier *et al*., 2004). There has been evidence of loss of GSIS along with down-regulation of glucagon mRNA expression with increased passage in MIN6 cells (O'Driscoll *et al*., 2004).

### 1.7.1 MIN6 cell line

MIN6 cell lines have been established from insulinomas obtained by targeted expression of the simian virus 40 T antigen genes in transgenic mice. MIN6 cell line produces insulin and T antigen and have morphological characteristics of pancreatic beta cells. MIN6 cells exhibit GSIS comparable with cultured normal mouse islet cells (Miyazaki *et al.*, 1990) and have been considered as an appropriate model for investigating the mechanism of GSIS. The results indicate that glucose metabolism and the glucose concentration-dependence of insulin secretion from MIN6 cells closely resemble those in normal beta cells, and that this cell line is thus a useful tool for studying GSIS in normal pancreatic beta cells (Ishihara *et al.*, 1993). Previous MIN6 studies showed loss in functional GSIS correlated with changes in morphology, increased proliferation and increased alkaline phosphatase activity, suggesting that the loss of GSIS may be due to de-differentiation of the high passage MIN6 cells (O'Driscoll *et al.*, 2004 and 2006).

### 1.7.2 MIN6 B1 cell line

MIN6 B1 cell line was derived from the mouse pancreatic beta cell line MIN6. MIN6 B1 responded to glucose in a concentration- and cell confluence-dependent manner. MIN6 B1 insulin secretion, when stimulated by glucose in a concentration-dependent fashion, repeatedly reached 12-fold after 1 hour of stimulation with 16.7 vs. 2.8 mmol/L glucose (Lilla *et al.*, 2003).

### 1.7.3 Vero–PPI cell line

Vero cells were derived from epithelial cells of kidney from African green monkey (Cercopithecus aethiops) (Yasumura *et al.*, 1963). In our laboratory this non-beta cell line was engineered by Dr. Lorraine O'Driscoll to produce and process human proinsulin by transfection of the human PPI cDNA. These Vero-PPI cells secreted mature human insulin but failed to show GSIS (O'Driscoll *et al.*, 2002).

### 1.7.4 RIN cell lines

Two cell lines were derived from a transplantable islet-cell tumour. One named RIN-r and maintained in NEDH rats. The other cell line named RIN-m and had been maintained in nude mice (Gazdar *et al*., 1980). Further research on these early cell lines lead to various subclones originating either from the RIN-m line (Bhathena *et al*., 1980) or the RIN-r line (Philippe *et al*., 1986). Low passage of the RINm5F subclone, derived from the RIN-m line, exhibited modest GSIS, with a 50% increase in insulin release between 0 and 1.4mmol/L glucose (Praz *et al*., 1983). RINm5F is a cell line that is less differentiated than the MIN6 cell line (Kayo *et al*., 1996) and show a defective physiological insulin secretory response

to glucose stimulation (Tiedge *et al*., 1996). RINm5F tumour cells can thus be used as a model for studying the glucose-recognition apparatus on glucose-induced insulin biosynthesis and secretion (Tiedge *et al*., 1993).

### 1.7.5 HIT cell lines

Hamster insulinoma (HIT) cells were isolated from Syrian hamster pancreatic islet cells and transformed by infection with simian virus 40. The HIT-T15 line was subcloned from the original cell lines and selected for high insulin content. HIT-T15 cells were reported to be responsive to a glucose stimulus and many other secretagogues (Hohmeier *et al*., 2004). The dose–response curve for glucose showed a threshold of responsiveness below 1 mmol/L (i.e. sub-physiological), with peak stimulation between 7.5 and 10mmol/L, and a half-maximal response at approximately 5mmol/L. The magnitude of responsiveness to glucose was two-fold. However, responses to glucose, as well as other secretagogues, such as arginine and forskolin, were found to decrease with increasing time in culture (Zhang *et al*., 1989).

### 1.7.6 βTC cell lines

The βTC class of insulinoma cell lines was established by targeted expression of the SV40 large T-antigen in beta cells of transgenic mice (Hanahan, 1985). The first cell lines established from these mice (βTC1, βTC2 and βTC3) produced and secreted insulin in response to a glucose stimulus (Efrat *et al*., 1988). However, insulin secretion occurred with a left shift of the dose–response curve, with maximal insulin secretion at 1.25mmol/L glucose. A more detailed analysis of the βTC3 line showed that insulin secretion increased progressively between

glucose concentrations of 0.1 and 16.7mmol/L (D'Ambra et al., 1990) but with a lower threshold for maximal stimulation than that for normal beta cells (Efrat *et al*., 1988). βTC cell lines maintain their features of differentiated beta cells for about 50 passages in culture (Efrat *et al*., 1988).

βTC3 was reported to secrete insulin with increasing glucose concentration and produce significantly higher levels of insulin compared to RIN (rat islet insulinoma) or HIT (hamster islet cell line) cells. βTC3 cells have shown to possess the ATP-dependent K+ ($K_{ATP}$) channel electrical activity and also used for studies of cytoplasmic $Ca^{2+}$ release (Gromada *et al*., 1996; Kozak *et al*., 1998).

### 1.7.7 INS-1 line

A widely used cell line for insulin secretion studies is the INS-1 cell line which was derived from the original radiation induced tumour (Chick *et al*., 1977). The INS-1 cell line was established by growing the tumour material in the presence of 2-mercaptoethanol (2-ME) (Asfari *et al*., 1992).

INS-1 cells express GLUT2 and glucokinase maintaining glucose responsiveness in the physiological range. The maximum glucose stimulated insulin secretion is generally only 2–4-fold (when treated with 3 or 20mmol/L glucose), well below the 15-fold responses observed in freshly isolated rodent islets (Asfari *et al*., 1992; Antinozzi *et al*., 1998).

### 1.7.8 Human beta cell line for transplantation therapy

There is limited donor tissue supply compared to the large number of diabetes patients detected each year. Therefore, great efforts have been undertaken to develop alternative strategies including *ex vivo* expansion of beta cells, *in vitro* differentiation of embryonic/adult stem cells into insulin producing beta cell phenotypes and gene therapy (Giannoukakis *et al*., 2002; Bretzel *et al.*, 2004; Onaca *et al*., 2007; Limbert *et al*., 2008).

Alternative sources of islets have been sought in stem cells (Assady *et al*., 2001; Moritoh *et al*., 2005), porcine islets (Korsgren *et al*., 2003) and beta cell expansion with growth factors (Hayek *et al*., 1995; Beattie *et al*., 2002). Embryonic stem (ES) cells are derived from embryos at the blastocyst-stage and have the ability to differentiate into all cell types. Xu *et al*. (2006) and D'Amour *et al*. in 2006 demonstrated that human ES cells could be differentiated into hormone-expressing endocrine cells. The insulin-positive cells thus generated had insulin content similar to that found in adult islet cells, along with ATP-sensitive potassium channel and voltage-dependent calcium channels. But these cells lacked GSIS and insulin-positive cells made up only about 7% of the differentiated population (Claiborn *et al*., 2008).

Expansion of primary beta cells by growth factors is also hampered by the senescence of the cells (Halvorsen *et al*., 2000). Immortalization of purified beta cells by the addition of genes such as TERT could allow the cells to grow indefinitely; however, immortalized beta cell lines established in this way lose their differentiated function (de la Tour *et al*., 2001).

Kroon *et al*. (2008) reported that glucose-responsive endocrine cells could be generated from human ES cells after implantation into mice. These insulin-

expressing cells that were generated after engraftment showed many properties of functional beta cells, including expression of beta cell transcription factors, processing of proinsulin along with the presence of mature endocrine secretory granules. Upon histopathological analysis Kroon *et al*. (2008) reported that the proportion of endocrine cells within the pancreatic-type tissue was >50%. Glucose stimulation of the implanted mice resulted in secreted human insulin and C-peptide at levels similar to those of mice transplanted with approx 3,000 human islets. Human ES cell–derived endocrine cells as reported in this study were functionally very similar to adult human islets, providing evidence that human ES cells may provide a renewable source of islets for cell replacement therapies (Kroon *et al*., 2008; Stanley *et al*., 2008).

### 1.8 *Thioredoxin-interacting protein (Txnip)*

Thioredoxin-interacting protein (Txnip), also known as Vitamin D (3)-up-regulated protein-1, Vdup1; TRX-binding protein-2, TBP-2, is a ubiquitous protein that binds with high affinity to thioredoxin, and inhibits its ability to reduce sulfhydryl groups via NADPH oxidation (Hui *et al*., 2004). Thioredoxin is an oxidoreductase that reduces oxidized proteins and scavenges free radicals (Muoio et al., 2007) (Fig: 1.8.1). *Txnip* is also found to be stress responsive and inhibits thioredoxin activity (Yamawaki *et al.*, 2005). It is believed that thioredoxin facilitates the processing and maturation of insulin and, thus, may prevent unfolded protein response-induced apoptosis of pancreatic beta cells (Hui *et al*., 2004).

Using FISH Ludwig *et al*. (2001) mapped mouse *Txnip* gene to chromosome 3, a region showing homology of genetic loci to human chromosome 1q21.1. Chromosome 1q21.1 is a region that has shown to be the most consistent linkage to Type 2 diabetes mellitus (T2DM) (Elbein *et al*., 1999; Vionnet *et al*., 2000). The 1q21-1q23 chromosomal area has been implicated in T2DM and localization of *Txnip* on the same chromosome could lead to the hypothesis that variation in *Txnip* gene may affect susceptibility to T2DM (Greevenbroek *et al*., 2007).

*Txnip* is a pro-apoptotic factor and is involved in beta cell glucose toxicity and oxidative stress (Chen *et al*., 2006; Chen *et al*., 2008). *Txnip* is over-expressed in diabetes in the cardiovascular system and has deleterious effects on pancreatic beta cells (Schulze *et al*., 2002). *Txnip* has been identified as the most dramatically glucose-induced gene in human islet microarray study (Minn *et al.*, 2005).

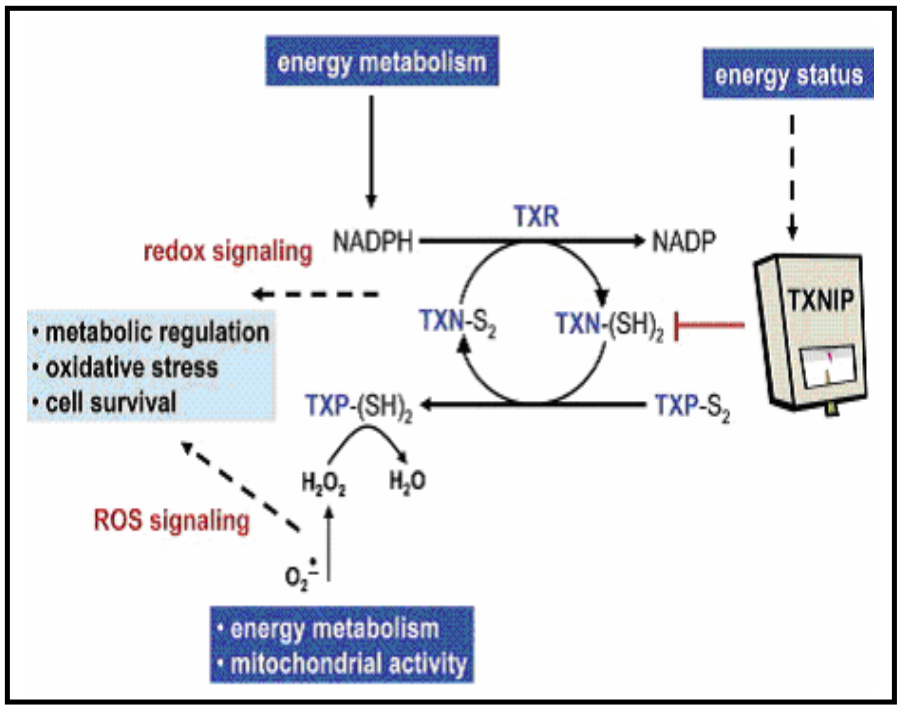


**Fig: 1.8.1 Models of *Txnip* showing the role of *Txnip* in the thioredoxin system. Thioredoxin (TXN) reduces oxidized cysteine residues (protein-S2) on cellular proteins. Reduced TXN (TXN-$(SH)_2$) is regenerated via the action of thioredoxin reductase (TXR) at the expenditure of NADPH. When TXN reduces the oxidized form of thioredoxin peroxidase (TXP), the reduced enzyme (TXP-(SH)2) is available to scavenge reactive oxygen species (ROS) such as hydrogen peroxide ($H_2O_2$) and the superoxide anion ($O_2$•−). *Txnip* binds and inhibits the reduced form of TXN, thereby functioning as a rheostat that modulates both redox status and ROS-mediated signalling to regulate metabolism and other cellular processes. (Dashed arrows indicate unknown mechanisms) (Muoio *et al*., 2007).**

Parikh *et al*., (2007) proposed that *Txnip* functions as a homeostatic regulator that incorporate glucose sensing and insulin signaling to control cellular energy status. They suggested that insulin-mediated suppression of *Txnip* might act as a signal that enhances glucose uptake in the periphery to facilitate post-meal energy uptake. Whereas, surplus intracellular glucose activates *Txnip*, bringing glucose uptake to a halt (Parikh *et al*., 2007) (Fig: 1.8.2).

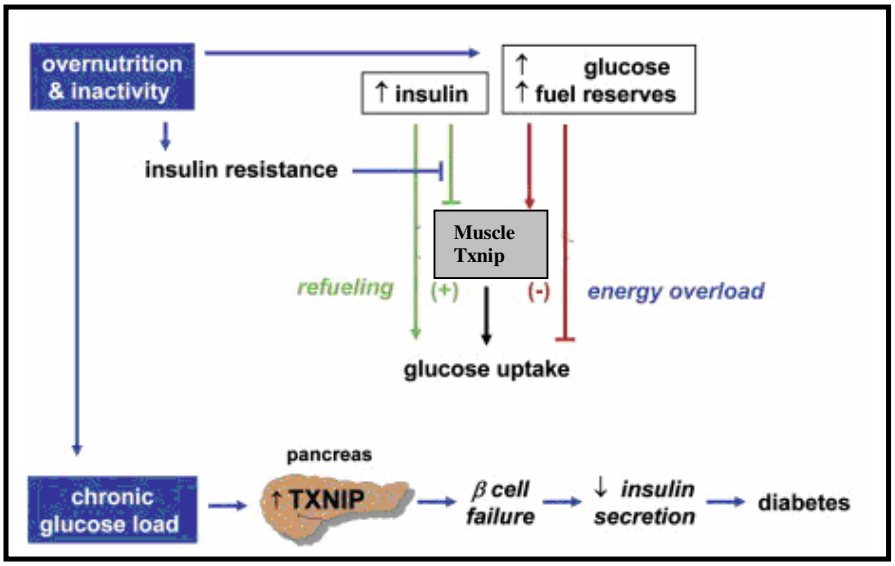


**Fig: 1.8.2 Role of *Txnip* in Type 2 diabetes. Insulin-mediated suppression of muscle *Txnip* serves as a signal to enhance glucose uptake and facilitates post-meal energy uptake. A surplus of glucose activates *Txnip*, which exerts negative feedback (–) to discourage glucose uptake. The energy burden of over nutrition and inactivity (blue lines) leads to high levels of *Txnip* in muscle and is aggravated further by insulin resistance. This leads to a chronic glucose load on the pancreas, triggering *Txnip* -mediated beta cell failure and leading to diabetes (adapted from Muoio *et al*., 2007).**

Hui *et al*. (2004) reported that *Txnip* regulates glycolysis. Over-expression of *Txnip* might signal to reduce uptake of glucose and reduced insulin secretion from the pancreatic beta cells (Fig: 1.8.3).

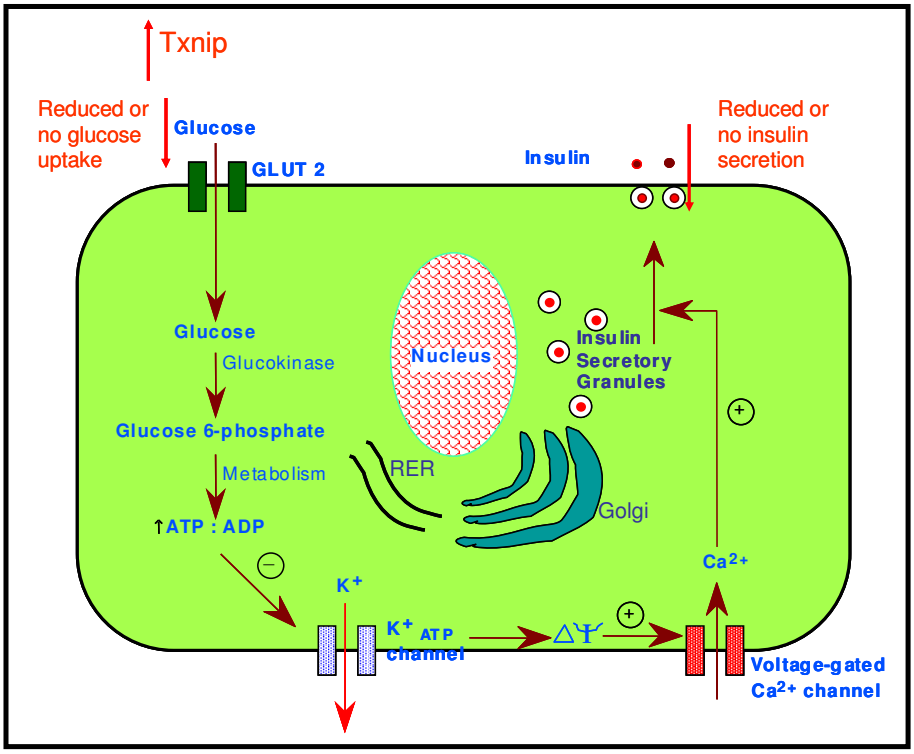


**Fig: 1.8.3 Schematic representation of effect of Txnip on insulin secretion. Increased Txnip reduces the uptake of glucose and thereby may reduce the production of insulin in the pancreatic beta cell.**

It has been proved that, in addition to regulating the cellular redox status, *Txnip* modulates overall gene transcription and thereby may further enhance beta cell death and impair insulin secretion, suggesting that it may be involved in glucose toxicity, beta cell loss and diabetes complications (Minn *et al*., 2005). *Txnip* is elevated in the vasculature and pancreas of diabetic animals, suggesting a broad role in diabetes complications (World *et al*., 2006). Over-expression of *Txnip*

sensitizes various cell types including endothelial cells, pancreatic beta cells and cardiomyocytes to oxidative stress with concomitant induction of apoptosis (World *et al*., 2006; Muoio *et al*., 2007).

Reduced *Txnip* expression is associated with increased tumour cell growth and metastatic potential (Goldberg *et al*., 2003), and this phenomenon has been observed in human breast cancer and colon cancer (Butler *et al*., 2002; Ohta *et al*., 2005). The anti-cancer agent suberoylanilide hydroxamic acid (SAHA) acts in part by increasing *Txnip* expression (Butler *et al*., 2002). *Txnip* leads to cell cycle arrest at the G0/G1 phase (Han *et al*., 2003) and it has been shown to inhibit proliferation in a variety of cells (Junn *et al*., 2000; Schulze *et al*., 2002). Over-expression of *Txnip* renders cells more susceptible to oxidative stress and induces apoptosis (Junn *et al*., 2000; Wang *et al*., 2002; Minn *et al*., 2005).

### 1.9 *Proprotein convertase subtilisin/kexin type 9 (Pcsk9)*

*Proprotein convertase subtilisin/kexin type 9* (*Pcsk9*) is also known as *convertase subtilisin*; *neural apoptosis regulated convertase 1*, *Narc1*; and is located on the chromosome 4. It is a 692-residue extracellular protein expressed primarily in the kidneys, liver and intestines representing the 9th member of the secretory subtilase family. *Pcsk9* gene is a novel putative proprotein convertase belonging to the subtilase subfamily (Seidah *et al.*, 2003). It is synthesized as a soluble zymogen that undergoes autocatalytic intramolecular processing in the endoplasmic reticulum (ER) as a precursor that undergoes autocatalytic processing, intracellular trafficking and finally, release into the extracellular medium (Lambert *et al*., 2006).

The *Pcsk9* protein domains comprises of 30 amino acid signal peptide (SP), the propeptide or inhibitory prodomain consists of 31–152 amino acids, the subtilisin-like catalytic domain (amino acids 153–452), and a cysteine-rich, unique, C-terminal domain (CRD) consists of 453–692 amino acids (Fig: 1.9). The central part of the catalytic domain consists of seven-stranded parallel β-strand sandwiches between sets of alpha-helices. Three disulfide bonds are found within this region (Lopez *et al*., 2008).

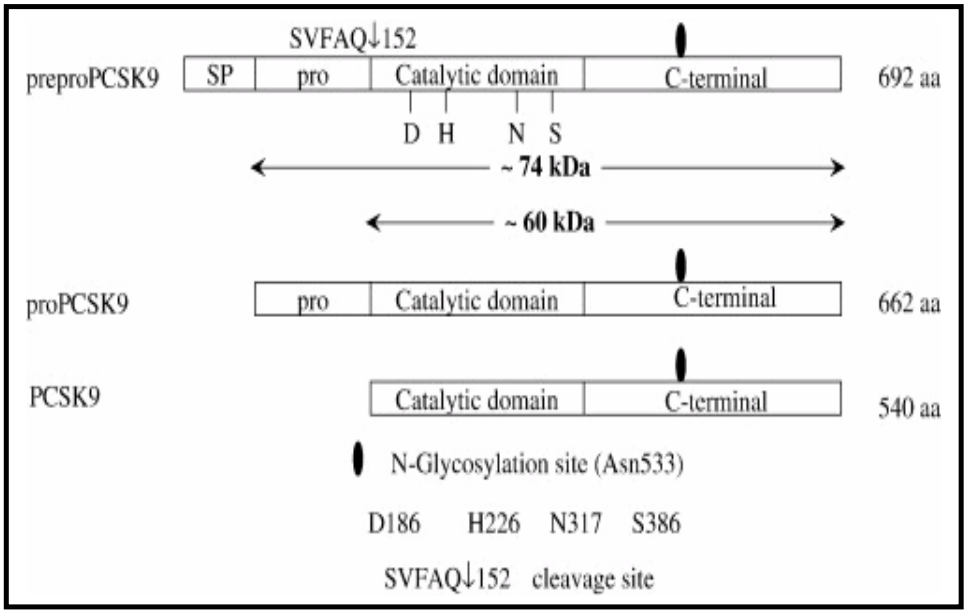


**Fig: 1.9 The protein domains that comprise *Pcsk9* are a 30 amino acid signal peptide (SP), the propeptide, the subtilisin-like catalytic domain, and a cysteine-rich, unique, C-terminal domain. Important residues such as the triad of active site residues: aspartate 186 (D186), histidine 226 (H226) and serine 386 (S386), the highly conserved asparagine 317 (N317), and an N-glycosylation site (Asn533) have been indicated. The autocleavage site has been mapped to SVFAQ↓152 (Lopez *et al*., 2008).**

*Pcsk9* mRNA is expressed in a limited number of tissues including the liver, kidney, cerebellum, and small intestine. It is also found to be transiently expressed in kidney epithelial and brain telencephalon cells (Seidah *et al*., 2003).

## 1.10 Important gene transcripts associated with beta cell

### 1.10.1 *Insulin I* (*Ins1*) and *Insulin II* (*Ins2*)

In contrast to humans, rodents express two proinsulin isoforms. One isoform, proinsulin 1, is expressed exclusively in islet beta cells. The second, proinsulin 2, is expressed in islets and in other tissues, especially the thymus. Both insulin are the product of nonallelic preproinsulin gene and are very similar (Soares *et al*., 1985). *Insulin II* (*Ins2*) is the murine homologue of the human insulin gene and is located on mouse chromosome 7. *Insulin I* (*Ins1*) is thought to have evolved by a gene duplication event, lacks the second intron of the *Ins2* gene, and is located on mouse chromosome 19 (Paronen *et al.*, 2003).

The *Ins1* gene possesses an intron homologous to the 119 base pair (bp) intron of *Ins2*. The *Ins2* gene contains two introns: a 499 bp intron interrupting the region encoding the connecting peptide and a 119 bp intron interrupting the segment encoding the 5 noncoding region of the mRNA. The introns are transcribed and present in a preproinsulin mRNA precursor (Lomedico *et al*., 1979).

### 1.10.2 *Phospholipase D1 (Pld1)*

*Pld1* gene is also known as *choline phosphatase 1* and is located on chromosome 3. Three Pld isoenzymes have been identified: two *Pld1* alternative spliced forms (*Pld1a*, *Pld1b*) and *Pld2*. *Pld1* plays an important role in signal transduction, cell growth, intracellular protein trafficking, secretion and glucose transport (Hughes *et al.*, 2004; Viparelli *et al*., 2008). It has been established that *Pld1* activity is required for both phases of glucose-stimulated insulin release, suggesting its role in exocytosis. The results suggest that phosphatidic acid formation on the granule

membrane by *Pld1* is essential for the regulated secretion of insulin from pancreatic beta cells (Hughes *et al.*, 2004). *Pld1* hydrolyzes membrane phospholipid phosphatidylcholine to generate phosphatidic acid (PA) and choline with subsequent activation of *protein kinase C* and stimulation of insulin release (Du *et al*., 2003; Cho *et al*., 2008).

Hughes *et al*. (2004) suggested *Pld1* to be the predominant isoform in MIN6 cells, and to be located at least partially on insulin granules. Over-expression of wild-type or a dominant negative catalytically inactive mutant of *Pld1* augmented or inhibited, secretagogue-stimulated secretion, respectively (Hughes *et al.*, 2004).

### 1.10.3 *Early growth response 1 (Egr1)*

*Egr1* is also known as *nerve growth factor-induced clone A* (*NGFI-A)* and is located on chromosome 18. It is an immediate-early response gene implicated in the regulation of cell growth, differentiation and apoptosis. In beta cells, *Egr1* induction is specifically associated with insulin secretion. Glucose rapidly and transiently induces *Egr1* mRNA in MIN6 (Josefsen *et al*., 1999). Changes in *Egr1* expression levels, in response to extracellular signals including glucose, regulate *Pdx1* expression and insulin production in pancreatic beta cells. *Egr1* regulates expression of *Pdx1* in pancreatic beta cells by both direct and indirect activation of the *Pdx1* promoter. *Egr1* expression levels may act as a sensor in pancreatic beta cells to translate extracellular signals into changes in *Pdx1* expression levels and pancreatic beta cell function (Eto *et al.*, 2007).

### 1.10.4 *Homeodomain transcription factor pancreas duodenum homeobox-1 (Pdx1)*

The *homeodomain transcription factor pancreas duodenum homeobox-1* is also known as *homeodomain transcription factor*, *IPF1*; *somatostatin transcription factor 1*, *STF1*; *pancreas duodenum homeobox-1*, *Pdx1* and *Idx1*. *Pdx1* gene is located on chromosome 5. *Pdx1* belongs to the antp-family of homeobox proteins (Hui *et al*., 2002).

*Pdx1* is a key regulator of pancreatic beta cell development, function, and survival and is known to serve as "a master control switch" for expression of both the exocrine and endocrine pancreatic cells. During embryogenesis, *Pdx1* is initially expressed by exocrine and endocrine cells of the pancreas and it is important for pancreas development and function of the mature islet cells (Gannon *et al*., 2008).

*Pdx1* expression is restricted to beta and delta cells of the islets (Sharma *et al.*, 1997) and it is required for activating transcription of genes including *insulin*, *somatostatin*, *islet amyloid polypeptide*, *glucose transporter type 2*, and *glucokinase* (Guz *et al.*, 1995). In addition, glucose induces *Pdx1* activity by phosphorylation and nuclear translocation via the PI3-kinase-dependent pathway. On the other hand, chronic hyperglycemia and elevated fatty acid levels down-regulate the expression of *Pdx1* (Harmon *et al.*, 1999). Deficits in *Pdx1* expression result in insulin deficiency and hyperglycemia (Eto *et al.*, 2007).

### 1.10.5 *Chromogranin B (Chgb)*

*Chromogranin B* (*Chgb*) is also known as *secretogranin I* (*scg1*) and is located on chromosome 2 (Jenkins *et al*., 1991). *Chgb* functions as a neuroendocrine secretory granule protein and it may be the precursor for other biologically active peptides. *Chgb* are major $Ca^{2+}$ storage proteins of the secretory granules of neuroendocrine cells (Yoo *et al.*, 2002). Giordano *et al*. (2008) suggested the co-existence of insulin and *chgb* in various insulin-secreting beta cells of various types of secretory granules. They also reported that changes in *chgb* release may result in alterations of insulin secretion and may therefore contribute to various types of metabolic diseases (Giordano *et al*., 2008).

### 1.10.6 *Prohormone convertase 2* (*PC2*)

*Prohormone convertase 2* is now officially known as *proprotein convertase subtilisin/kexin type 2* (*Pcsk2*). It is located on the chromosome 2.

Proinsulin is converted to insulin by the concerted action of two sequence-specific subtilisin-like proteases termed *prohormone convertase 1* (*PC1*) (*PC1* is also known as *PC3*) and *prohormone convertase 2* (*PC2*) (Neerman-Arbez *et al*., 1994). *PC2* is a type II proinsulin-processing enzyme, and it cleaves the proinsulin molecule on the COOH-terminal side of dibasic peptide, Lys [64]-Arg[65], which joins the C-peptide and the A-chain domains (Yoshida *et al*., 1995).

### 1.10.7 *Glutamate decarboxylase (GAD)*

*GAD* is an enzyme found on the surface of beta cells that helps metabolize glutamic acid. There are two forms of *GAD i.e*. *GAD65* (also known as *Glutamic acid decarboxylase 2* (*Gad2*)) and *GAD67* (also known as *Glutamic acid decarboxylase 1* (*Gad1*)). The presences of GAD autoantibodies serve as a marker for the early diagnosis (up to 7 years before the clinical onset) of Type 1 diabetes (Park *et al*., 2006). Ludvigsson *et al*. (2008) assessed the ability of alum-formulated GAD (GAD-alum) to reverse recent-onset Type 1 diabetes patients. They reported that following GAD-alum treatment (subcutaneous injections of GAD-alum) there was slow loss of residual beta cell function up to 30 month compared to placebo (alum alone) patients (Ludvigsson *et al*., 2008). *GAD65* has been assigned to chromosome 10, whereas *GAD67* is located on chromosome 2 (Kelly *et al*., 1992).

### 1.10.8 *Neuropeptide Y (Npy)*

*Neuropeptide Y* (*Npy*) is neuroendocrine regulatory peptide consisting of 36 amino acids. It is present in central nervous system, peripheral nerve fibres, and neuroendocrine tissues, including the pituitary gland and adrenal glands (Terenghi *et al.*, 1987). Synthesis of *Npy* is also demonstrated within rat islets (Jamal *et al.*, 1991; Wang *et al.*, 1994) and in RIN-m5F and INS 1 (Waeber *et al.*, 1993) clonal rat insulinoma cells, suggesting a possible role for *Npy* as a paracrine regulator in the islet. *Npy* has been co-localized, by means of double label immunohistochemistry, with insulin and glucagon in embryonic mouse islets, and it has been identified with glucagon in both adult human and adult mouse alpha cells (Waeber *et al.*, 1995). Hirai *et al*. (2008) reported *Npy* to be a

new potential autoantigen associated with secretory vesicles in Type 1 diabetes. *Npy* was also found to be significantly higher in sera from patients with Type 1 diabetes compared to controls (Hirai *et al*., 2008).

### 1.11 siRNA and shRNA

Small interfering RNA (siRNA) is also known as short interfering RNA or silencing RNA. It is a class of 20-25 nucleotide-long double-stranded RNA molecules. In the late nineties RNA silencing was discovered in plants during the course of transgenic experiments that eventually led to the silencing of the introduced transgene and, in some cases, of homologous endogenous genes or resident transgenes (Matzke *et al*., 1989; Linn *et al*., 1990; Napoli *et al*., 1990; Smith *et al*., 1990; van der Krol *et al*., 1990). However, this approach could not be used in mammalian cells as the long double-stranded RNAs (dsRNAs) triggered a cytotoxic reaction leading to cell death (Hunter *et al*., 1975). Cytotoxic reaction, mediated by the interferon system, protected the organism from RNA viruses by sacrificing the infected cell and thus preventing the spread of the virus (Stark *et al*., 1998). It was later reported that the dsRNAs shorter than 30 nucleotides do not trigger the interferon response; therefore artificially produced siRNAs and their delivery into mammalian cells were able to efficiently induce RNA silencing (Elbashir *et al*., 2001).

siRNA-induced silencing is short-lived and cannot be used to study long-term effects therefore constructs were developed to directly express siRNA-like molecules in cells (Brummelkamp *et al*., 2002). These constructs uses RNA-polymerase III to express a short hairpin RNA (shRNA). This polymerase is specialised to transcribe short templates with a precisely defined termination signal. The resulting transcript is about twice as long as the mature siRNA and folds back upon itself to form a double-stranded precursor with one end exhibiting the 2-nucleotide overhang that is typical for siRNAs, while the other

end forms a bulge. Dicer recognises the open end of this structure and excises the mature siRNA, thus producing a single siRNA from each transcript (Kim *et al*., 2005; Siolas *et al*., 2005) (Fig: 1.11.1).

### 1.11.1 Mechanism of action

Long double-stranded RNA (dsRNA) (typically >200 nt) upon introduction, enters a cellular pathway that is commonly referred to as the RNA interference (RNAi) pathway. During the initiation stage, long dsRNA is cleaved into siRNA (Hamilton *et al*., 2002), mediated by type III RNase Dicer enzyme. RNase III family members are among the few nucleases that show specificity for dsRNAs (Nicholson, 1999) and are evolutionarily conserved in worms, flies, fungi, plants, and mammals (Agrawal *et al*., 2003). Complete digestion by RNase III enzyme results in dsRNA fragments of 23- to 28-mer diced siRNA products (Blaszczyk *et al*., 2001).

During the effector stage, the siRNAs assemble into endoribonuclease-containing complexes known as RNA-induced silencing complexes (RISCs). siRNAs undergo unwinding before being incorporated into a high-molecular-weight protein complex called RISC (Hammond *et al*., 2000). Dicers are part of the RISC complex, which includes several different proteins such as the Argonaute gene family members and an ATP-dependant RNA helicase activity that unwinds the two strands of RNA. Functional RISCs contain only single stranded siRNA (Martinez *et al*., 2002). The siRNA strands subsequently guide the RISC to complementary RNA molecules, where base pairing takes place between the antisense strand of the siRNA and the sense strand of the target mRNA. This leads to endonuclease cleavage of the target RNA (Novina and Sharp, 2004).

Gene silencing by RISC is accomplished via homology-dependent mRNA degradation (Tuschl *et al*., 1999; Hamilton & Baulcombe, 1999), translational repression (Grishok *et al*., 2001) or transcriptional gene silencing (Pal-Bhadra *et al*., 2002) (Figure 1.11.1).

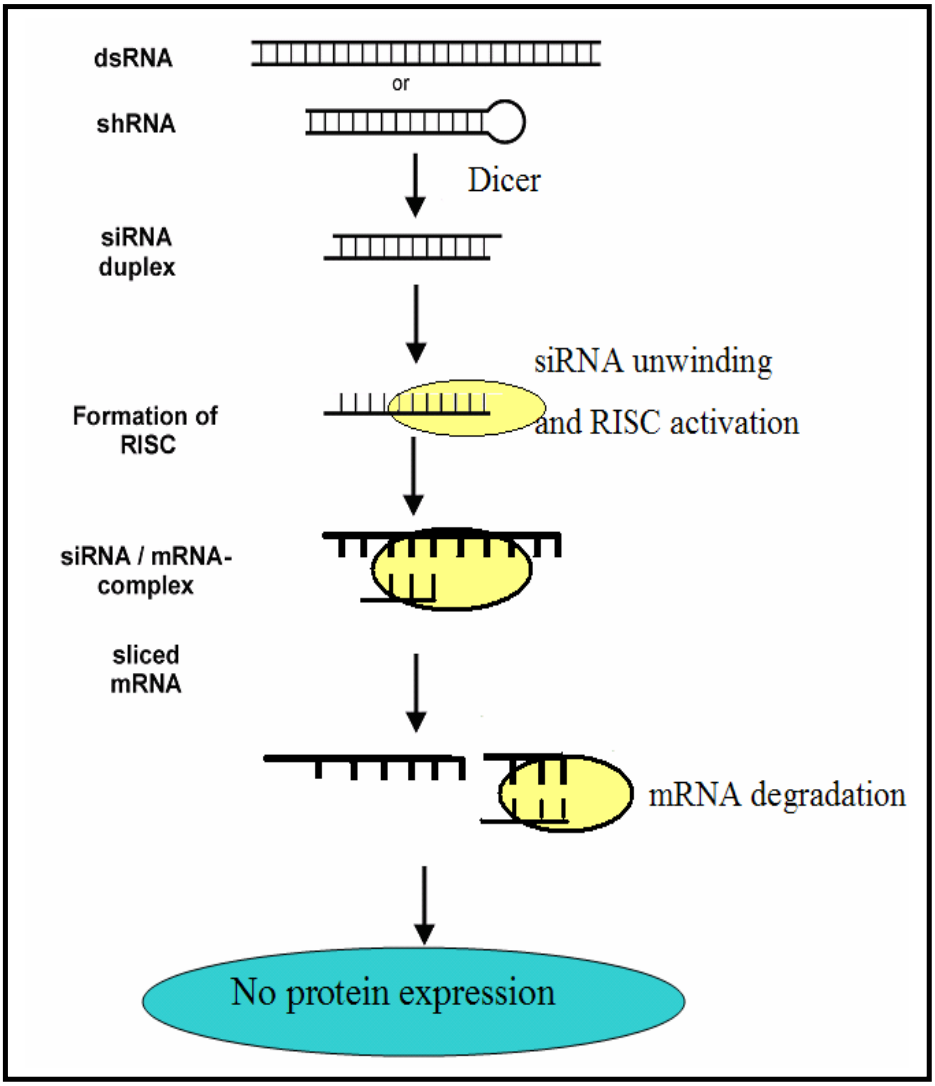


**Fig: 1.11.1 siRNA mechanism of action. dsRNAs are processed by a host Dicer enzyme to form siRNAs. Dicer-processed siRNAs and synthetic siRNAs undergo ATP dependent unwinding before being incorporated into a protein complex called RISC (RNA-induced silencing complex) that contains single stranded siRNAs. The RISC is reconfigured to active RISC which contains the proteins required for cleaving the target mRNA at the point where the antisense siRNA binds. After the cleavage the active RISC is released to cleave additional mRNA molecules whereas the cleaved mRNA is degraded by cellular ribonucleases.**

### 1.12 Biomarkers for diabetes

There are no reported circulating biomarkers for detecting beta cell mass and function. As Type 1 diabetes is usually detected after a loss of about 90-95% of the beta cells (Atkinson *et al.*, 2005), association of gene expression with beta cell loss, if detectable in serum, may aid in early detection of the disease.

Autoimmune processes are involved in pancreatic beta cell destruction in Type 1 diabetes. Autoantibodies including islet cell antibodies (ICA), glutamic acid decarboxylase antibodies (GADA) and antibodies directed against protein tyrosine phosphatase/IA2 (IA2-Ab) have been detected in the circulation years before clinical onset of the disease and are awaiting clinical trial (Gale, 1996).

#### 1.12.1 Circulating extracellular nucleic acid

Mandel and Métais reported the finding of extracellular nucleic acids in plasma in 1948 (Mandel *et al.*, 1948). It was some 30 years later Leon *et al.,* demonstrated elevated circulating cell-free nucleic acid levels in cancer patients when compared with healthy controls. Leon *et al.* (1977) predicted poor survival of cancer patients with higher circulating nucleic acid level after therapies, introducing a profound implication of this area of work in diagnostic medicine.

DNA and mRNA from foetal origin have been discovered in the plasma of pregnant women (Bianchi *et al.*, 1997; Poon *et al.*, 2000; Nancy *et al.*, 2006). Quantitative alterations of cell-free placental-derived mRNA in the maternal circulation are associated with many pregnancy-related disorders, such as preeclampsia and preterm labour (Zhong *et al*., 2008) (Fig: 1.12.1). Plasma levels of endothelial-specific mRNA and DNA was found to be acutely elevated

following burns, and related to the severity in terms of the percentage of total body surface area burn (Fox *et al*., 2008). Significantly higher levels of *rhodopsin* mRNA have been reported in peripheral blood from diabetic individuals compared to healthy controls (Hamaoui *et al.*, 2004). Circulating *TGF-beta1* mRNA has been proposed as sensitive biomarkers for the diagnosis and prognosis of hepatocellular carcinoma (Dong *et al*., 2008). Skvortsova *et al*. (2006) based on their study of circulating DNA proposed that total circulating DNA combined with the quantitative analysis of circulating DNA distribution between cell-bound and cell-free fractions in blood it could be possible to accurately detect and discriminate malignant from benign breast tumours. With recent advances in sensitive and specific analytical techniques, DNA/RNA has potential to be used as a tool for early detection of disease, clinical diagnosis, monitoring treatment and in prognosis of diabetes and oncology (Gahan, 2008).

Many of the developed cancer markers are serum proteins, such as alpha-fetoprotein (AFP) in liver cancer; carcinoembryonic antigen (CEA) in colorectal cancer and prostate-specific antigen (PSA) in prostate cancer (Labrie *et al.*, 2004; Fernandes *et al.*, 2005; Ren *et al.*, 2006). The sensitivity and specificity of these markers are often not satisfactory as some of these markers are also expressed in benign conditions. Moreover, these markers provide little information on the complex molecular progression of the tumour throughout the course of the disease, so the development of a 'molecular marker' is long awaited in diagnostic medicine (Tsang *et al.*, 2007) (Fig: 1.12.1).

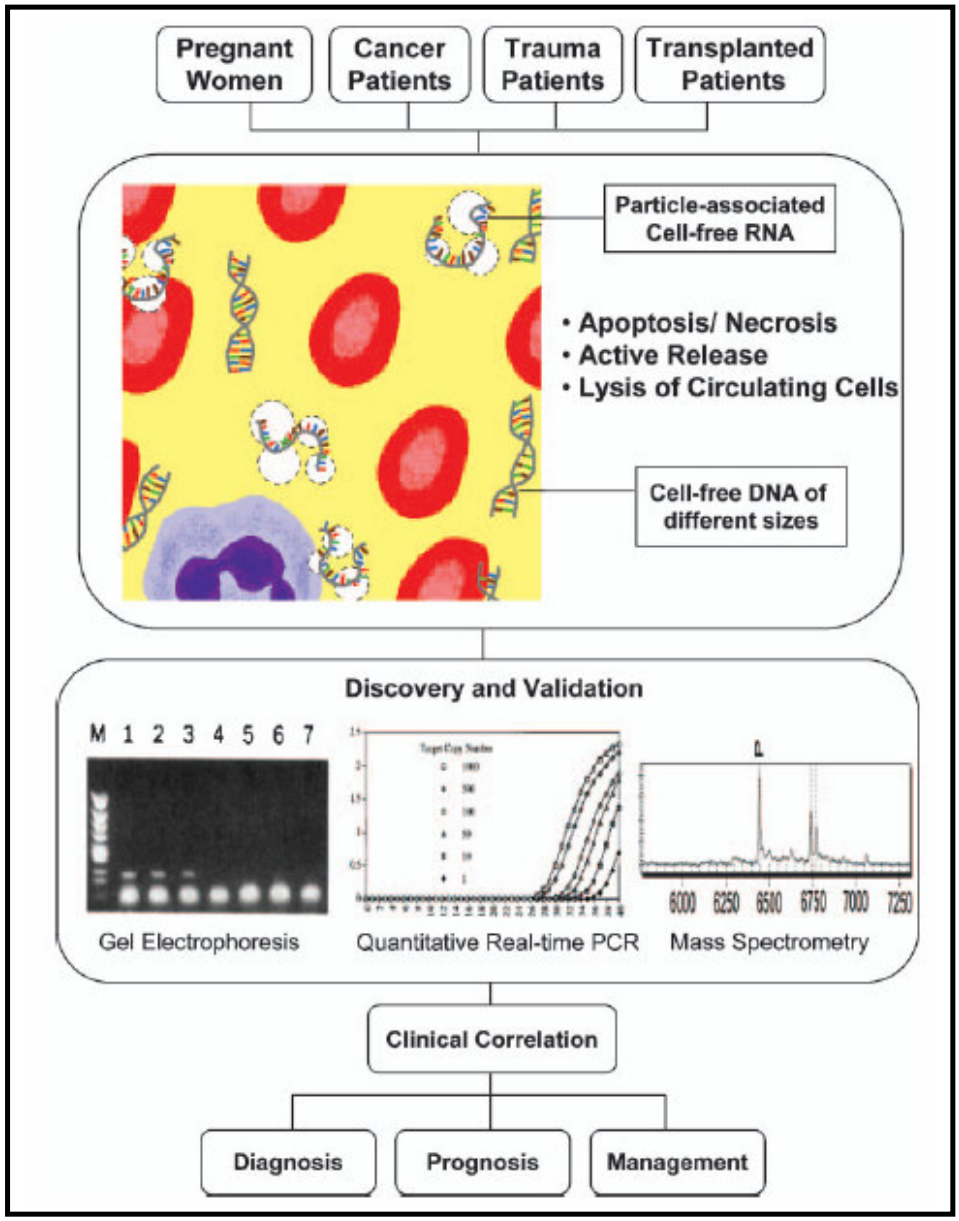


**Fig: 1.12.1 Diagram showing the flow of studies on circulating nucleic acid (Tsang *et al*., 2007).**

#### 1.12.1.1 Extracellular DNA

The presence of cell-free circulating DNA was reported in 1966, when higher levels of circulating DNA were found in patients with systemic lupus erythematosus, compared to healthy individuals (Tan *et al.*, 1966). Similarly, associations between elevated circulating DNA levels and other clinicopathological conditions, including pancreatitis, hepatitis, inflammatory bowel disease, glomerular nephritis, rheumatoid arthritis and cancer (Koffler *et al.*, 1973; Leon *et al.*, 1977) have been reported. Higher levels of circulating DNA were associated with metastatic cancer compared to localised disease and reduced levels of DNA were found following radiotherapy in lymphoma, lung, ovary, uterus and cervical tumours (Anker *et al*., 2001). Elevation of plasma foetal DNA has been observed in a variety of pregnancy complications (Tsang *et al.*, 2007). These findings have also opened up the possibility of predicting the diseases by close monitoring of foetal DNA level and the area is now under investigation (Farina *et al.*, 2004). Neutrophil-derived circulating free DNA has been reported to be of prognostic value in severely injured patients (Margraf *et al*., 2008).

#### 1.12.1.2 Extracellular RNA

Extracellular RNA has been detected in plasma and serum of patients presenting with various forms of cancer (Wieczorek *et al.*, 1987; Kopreski *et al.*, 1999; Hasselmann *et al.*, 2001). Extracellular RNAs have been detected in a range of biological matrices, including serum/plasma, saliva (Li *et al.*, 2004; Li *et al.*, 2004), urine (Bryzgunova *et al.*, 2006), milk (Semenov *et al.*, 2004), bronchial lavage (Schmidt *et al.*, 2005), as well as cell culture supernatants (Stroun *et al.*,

1978; Morozkin *et al.*, 2004; O'Driscoll *et al.*, 2005; O'Driscoll *et al.*, 2008). How they are released from cells – whether that is by active secretion, as a result of apoptosis/necrosis, or some combination of these mechanisms - is not yet defined (Rykova *et al.*, 2006). The protection of extracellular RNA from degradation by RNases may be due to it being packaged into apoptotic bodies (Hasselmann *et al.*, 2001), integrated within nucleoprotein complexes (Sisco *et al.*, 2001), with phospholipids (Wieczorek *et al.*, 1985; Rosi *et al.*, 1988) and proteins (Masella *et al.*, 1989). Rykova *et al*. (2008) proposed that specific RNA quantification in blood plasma could prove to be valuable for discrimination between cancer and benign tumours by analysing extracellular circulating *RASSF1A*, *Cyclin D2* and *RARbeta2* gene transcripts (Rykova *et al*., 2008).

### 1.12.2 Circulating Nucleic acids and diabetic complications

Diabetes is known to cause deleterious effects on almost every organ of the body. Major diabetic complications are retinopathy, coronary heart disease, nephropathy, neuropathy and peripheral vascular disease. Measurement of tissue-specific nucleic acids in the circulation may have some potential for prognostic and diagnostic purposes. It has been shown previously that plasma nucleic acids (DNA and RNA) appear to reflect the amount of cell death occurring in the organism (Stroun *et al*., 2001).

Malik *et al*. (2005) reported an increased plasma protein level of CD105 in diabetic patient with proliferative retinopathy. They also reported higher *VEGF* mRNA levels in the vitreous fluid in patients with advanced retinopathy (Malik *et al*., 2005). As described in section 1.12.1, higher circulating mRNA for *rhodopsin* was reported in diabetic retinopathy (DR) patients and could be used

as an early predictor of DR (Hamaoui *et al*., 2004). *Rhodopsin* mRNA could also be a useful marker in assessment of DR and may also be useful in detection and evaluation of other retinal lesions including maculopathy, glaucoma and pigment lesions. Nephron-specific mRNA (*nephrin*) detected in peripheral blood of diabetic patient suggests a marker for glomerular function in diabetes nephropathy patients (Butt *et al*., 2006). Circulating heat shock protein 27 levels in serum were found to be significantly higher in cases with distal symmetrical polyneuropathy than in controls (Gruden *et al*., 2008).

Several acute-phase proteins e.g. fibrinogen and PAI-1 are elevated in NIDDM (Ganda *et al*., 1992). Serum levels of interleukin-6 and interleukin-6/interleukin-6 receptor complex were also found to be elevated in diabetic patients (Kado *et al*., 1999). Berney *et al*. (2006) reported that circulating *insulin* mRNA was detected using qRT-PCR assay immediately after islet transplantation. They also suggested that detection of *insulin* mRNA in the peripheral blood may be a promising method for predicting islet graft damage (Berney *et al*., 2006). Serum concentration of polyclonal free light chains, a bi-product of normal immunoglobulin synthesis, was found to be significantly raised in Type 2 diabetes patients before overt renal impairment developed (Hutchison *et al*., 2008) compared to controls.

### 1.13 Aims of Thesis

The aim of this project was:-

- To determine if GSIS was lost in MIN6 B1 cells
- To identify the passage number at which glucose-responsiveness was lost
- To investigate the gene expression changes associated with the loss of GSIS phenotype, using whole genome microarray and bioinformatics tools.
- To validate the panel of differentially-regulated genes from the microarray study using quantitative real-time RT-PCR (qRT-PCR).
- To transfect siRNA for gene targets from qRT-PCR validated microarray study to investigate their association with GSIS.
- To over-express gene targets from qRT-PCR validated microarray study by cDNA transfection to investigate their association with GSIS.
- To detect amplifiable mRNA in media conditioned by insulin producing cells.
- To establish if gene transcripts extracellular to beta cells reflect the numbers of insulin-producing cell conditioning the medium.
- To identify gene transcripts extracellular to beta cells showing the functional status of the beta cells (*i.e.* GSIS *vs*. non-GSIS).
- To establish if gene transcripts are detectable in serum from people with diabetes and those without this condition, as control.
- To determine if gene transcripts, which may be potential biomarkers, are differentially-regulated in Type 2 diabetes and control serum.

Previously in our laboratory we found that MIN6, a heterogeneous cell line, lost its GSIS phenotype in long term culture (O'Driscoll *et al.*, 2006). In the present study we aimed to investigate MIN6 B1 cell line, a homogenous cell population, for any changes in the long term culture. Furthermore, we aimed to identify gene transcripts associated with loss of GSIS and to investigate if manipulating such gene transcripts would restore GSIS function. This study would provide an insight into the molecular basis for beta cell dysfunction in Type 2 diabetes.

Earlier in our laboratory, extracellular nucleic acids were amplified in medium conditioned by cancerous cell line (O'Driscoll *et al.*, 2005). Here in this project we tried to detect amplifiable mRNA in medium conditioned by insulin producing cell lines. As Type 1 diabetes is usually diagnosed after a loss of 70% – 80% of the insulin-secreting beta cells in the pancreas (Sia, 2004), detecting an association of gene expression in the circulating serum with beta cell loss could aid in early disease detection. Furthermore detection of extracellular mRNAs indicating impaired beta cell function that might be important for determining beta cell abnormalities in Type 2 diabetes.

# Section 2.0 Materials and Methods

## 2.1 Cell Culture Methods

### 2.1.1 Water

Ultra high pure water (UHP) was used in the preparation of all media and solutions. Pre-treatment of water, involving activated carbon, pre-filtration and anti-scaling was first carried out. This water was then purified by a reverse osmosis system (Millipore Milli-RO 10 Plus, Elgastat UHP), which is low in organic salts, organic matter, colloids and bacteria with a standard of 12 - 18 MΩ/cm resistance.

### 2.1.2 Treatment of Glassware

All solutions for use in cell culture and maintenance were prepared and stored in sterile glass bottles. Bottles, lids and all other glassware used for any cell-related work were prepared as follows: - all glassware and lids were soaked in a 2% (v/v) solution of RBS-25 (AGB Scientific) for at least 1hrs. This is a deproteinising agent, which removes proteineous material from the bottles. Glassware was scrubbed and rinsed several times in tap water; the bottles were then washed by machine using Neodisher detergent, an organic, phosphate-based acid detergent. The bottles were then rinsed twice with distilled water, once with UHP water and sterilised by autoclaving.

### 2.1.3 Sterilisation

Water, glassware and all thermostable solutions were sterilised by autoclaving at 121°C for 20 min under 15 p.s.i. pressures. Thermolabile solutions were filtered through a 0.22 μm sterile filter (Millipore, millex-gv, SLGV-025BS). Low protein-binding filters were used for all protein-containing solutions. Acrodisc (Pall Gelman Laboratory, C4187) 0.8/0.2 μm filters were used for non-serum/protein solutions.

### 2.1.4 Media Preparation

Medium was routinely prepared and sterility checked by Mr. Joe Carey (technician) as in SOP NCTCC 003-02. 10X media were added to sterile UHP water buffered with HEPES (N- [2-Hydroxyethyl]-N'- [2-ethanesulphonic acid]) (Sigma, H-9136) and $NaHCO_3$ (BDH, 30151) and adjusted to a pH of 7.45 - 7.55 using sterile 1.5M NaOH and 1.5M HCl. The media were then filtered through sterile 0.22 μm bell filters (Gelman, 121-58) and stored in 500 ml sterile bottles at 4°C. The basal media used during routine cell culture were prepared according to the formulations shown in Table 2.1.4. Sterility checks were carried out on each 500 ml bottle of medium as described in Section 2.2.6.

The basal media were stored at $4^oC$ up to their expiry dates as specified on each individual 10X medium container. Working stocks of culture media were prepared as 100 ml aliquots and supplemented as required. These were stored for up to 3 weeks at $4^oC$, after this time, fresh culture medium was prepared.

**Table: 2.1.4 Preparation of basal media**

| | **DMEM (Dulbecco's Modified Eagle Medium) (mls)** (Sigma, D-5648) | **MEM** (Gibco, 21430-020) |
|---|---|---|
| 10X Medium | 500 ml | 500 ml |
| Ultra pure $H_20$ | 4300 ml | 4300 ml |
| 1M HEPES* (Sigma, H-9136) | 100 ml | 100 ml |
| 7.5% $NaHCO_3$ (BDH, 30151) | 45 ml | 45 ml |

* The weight equivalent of 1M N- (2-Hydroxyethyl) piperazine-N'- (2-ethanesulfonic acid) (HEPES) was dissolved in an 80% volume of ultra pure water and autoclaved. The pH was adjusted to 7.5 with 5M NaOH.

## 2.2 Maintenance of cell lines

### 2.2.1 Safety Precautions

All cell culture work was carried out in a class II down-flow re-circulating laminar flow cabinet (Nuaire Biological Cabinet) and any work, which involved toxic compounds, was carried out in a cytoguard (Gelman). Strict aseptic techniques were adhered to at all times. The laminar flow cabinet was swabbed with 70% industrial methylated spirits (IMS) before and after use, as were all the items used in the cabinet. Each cell line (including low and high passage cells) was assigned specific media and waste bottles and only one cell line was used at a time in the cabinet, which, was allowed to clear for 15 min between different cell lines. The cabinet and incubators were cleaned each week with industrial detergents (Virkon, Antec. International; TEGO, TH. Goldschmidt Ltd.). A separate Laboratory coat was kept for aseptic work and gloves were worn at all times during cell work.

### 2.2.2 Culture of Adherent Cell Lines

The cell lines used during the course of this study, their sources and their basal media requirements are listed in Table 2.2.2.2. Cell lines were generally maintained in vented 25 $cm^2$ (Costar, 3056) and 75 $cm^2$ flasks (Costar, 3376) and fed every one to three day.

#### 2.2.2.1 Subculture of Adherent Cell Lines

Prior to subculture cells were always monitored for any contamination and were only subcultured when the cells were 70-80% confluent. During routine subculturing or harvesting of adherent cell lines, cells were removed from their flasks by enzymatic detachment.

#### 2.2.2.2 Subculture of Vero-PPI cell line

Culture media from the flasks were removed and discarded in waste bottle. To the T25 $cm^2$ flask 1-2 mls of pre-warmed 1X calcium and magnesium- free ($Ca^{2+}$/$Mg^{2+}$-free) phosphate-buffered saline (Gibco, 14200-067) was added and washed back and forth to remove all the traces of serum and dead cells.

The wash solution was removed and discarded in waste bottle. The purpose of this was to eliminate any naturally occurring TV (Trypsin Versene - TV) inhibitor, which would be present in residual serum. Pre-warmed (37°C) trypsin/EDTA (TV) solution (2.5% trypsin (Gibco, 15090), 0.01% ethylene diamine tetra acetic acid (Sigma, E5134) solution in phosphate buffered saline (PBS) (Oxoid, BR14a)) was then placed on the cells (2 ml/25$cm^2$ flask or 3 ml/75$cm^2$ flask) and the flasks were incubated at 37°C until the cells were seen to have detached (2 min). The TV was deactivated by addition of an equal volume of growth medium (containing serum). The entire solution was transferred to a 30 ml sterile universal tube (Sterilin, 128a) and centrifuged at 900 rpm (revolutions per minute) for 5 min. The resulting cell pellet was re-suspended in pre-warmed (37°C) fresh growth medium, counted (See Section: 2.2.3) and used to re-seed a flask at the required cell density or to set up an assay. Cells were never re-seeded back into the same flask.

**Table: 2.2.2.2 Cell lines used in this study**

| *Cell Line* | **Source of Cell Line** | **Basal medium and additives** | **Cell Type** | **$CO_2$ Requirement** |
|---|---|---|---|---|
| MIN6 | Dr. Per Bendix Jeppesen | DMEM with 20% heat-inactivated at 56°C for 1hrs. fetal calf serum (FCS) | Murine beta Cell Line | 5% $CO_2$ |
| MIN6 B1 | Dr. Valeria Lilla | DMEM with 15% heat inactivated FCS at 56°C for 1hrs. (BioWhittaker, DE14-801F), 1% L-Glut, and ß-mercaptoethanol (Sigma, M-3148) | clonal population of Murine beta Cell Line (MIN6) | 5% $CO_2$ |
| Vero-PPI cells | Vero – ATCC, Vero-PPI Dr Lorraine O'Driscoll | MEM with 5.6mmol/L glucose, 1% nonessential amino acids | Vero cells engineered to produce human insulin | 5% $CO_2$ |

### 2.2.2.3 Subculture of MIN6 and MIN6 B1 Cell Line

MIN6 and MIN6 B1 flasks were emptied of conditioned medium and the cells were rinsed in pre-warmed 1X $Ca^{2+}$/$Mg^{2+}$- free PBS (Gibco, 14200-067). TV (3 ml) was then added and incubated at 37°C for 2 min exactly. The flask was tapped sharply to dislodge the cells and then 3 ml of culture medium was added to inhibit the TV. The cell suspension was aspirated gently and with care to avoid separating the cells in to a single cell suspension. Following this the cells were centrifuged at 900 rpm for 5 min.

The resulting pellet was re-suspended in pre-warmed culture medium, counted (See Section: 2.2.3) and re-seeded to flasks or assay plates. MIN6 and MIN6 B1 cells were never re-seeded back in to the same flask.

### 2.2.3 Cell Counting

Cell counting and viability determinations were carried out using a trypan-blue (Gibco, 15250-012) dye exclusion technique.

An aliquot of trypan-blue was added to a sample from a single cell suspension at a ratio of 1:4. After 3 min incubation at room temperature, a sample of this mixture was applied to the chamber of a haemocytometer over which a glass cover slip had been placed. Trypan-blue only stains dead cells, whereas viable cells appear bright with a halo and remain unstained. Cells in the 16 squares of the four outer corner grids of the chamber were counted microscopically. An average per corner grid was calculated with the dilution factor being taken into account. Final cell numbers were multiplied by $10^4$ to determine the number of cells per ml (volume occupied by sample in chamber is 0.1cm x 0.1cm x 0.01cm *i.e.* 0.0001$cm^3$ therefore cell number x $10^4$ is equivalent to cells per ml). Non-viable cells were those, which stained blue while viable cells excluded the trypan-blue dye and remained unstained.

### 2.2.4 Freezing MIN6 and MIN6 B1 cells

Cryoprotective medium or freezing medium was prepared in complete culture medium containing 20% dimethylsulfoxide (DMSO; Sigma, D-5879) and filter sterilised using 0.22 μm filter and syringe. The freezing medium was then placed on ice until used. Appropriate number of cryogenic vials (Greiner, 122 278) were labelled with the cell line, passage no, date and placed on ice at this point. MIN6 and

MIN6 B1 cells were trypsinised as outlined previously (See Section: 2.2.2.3). The supernatant from the centrifuged cells were removed and re-suspend the cell pellet in 1 ml of fresh media. This solution (20% DMSO) was slowly added drop wise to the cell suspension to give a final concentration to 10% of DMSO, and a final cell concentration of $5 \times 10^6 - 1 \times 10^7$ cells/ml. This step was very important, as DMSO is toxic to cells. When added slowly, the cells had a period of time to adapt to the presence of the DMSO, otherwise cells may have lysed. Then 1.5 to 1.8 mls of the DMSO containing cell suspension was added to each of the vials. The cryovials were cooled on ice for 10 min, and then transferred to a –20°C freezer in a Boehringer Mannheim enzyme box for 30 min. Following this, the cells were placed at –80°C until required.

### 2.2.5 Thawing MIN6 and MIN6 B1 Cells

Prior to thawing 8 mls of culture media was added into the flasks and the flasks was allowed to equilibrate in a 37°C, 5% $CO_2$ humidified incubator for at least 30 min or overnight. A sterile universal tube containing 5 ml growth medium was pre-warmed and prepared for thawing back the cells. This allowed for the rapid transfer and dilution of thawed cells to reduce their exposure time to the DMSO freezing solution (DMSO is toxic at room temperature). The cryovial taken from the –80°C storage was partially thawed and its contents were transferred to the universal. The suspension was centrifuged at 900 rpm for 5 min, the DMSO-containing supernatant was removed and the pellet was then resuspended in fresh growth medium. Viability counts were carried out (See Section: 2.2.3) to determine the efficacy of the freezing/ thawing procedures. A sample was also taken for sterility analysis (See Section: 2.2.6). Thawed cells were placed into tissue culture flasks with the appropriate

volume of medium (3-4 ml/25cm$^2$ flask and 8-10 ml/75cm$^2$ flask) and allowed to attach overnight. 24hrs. after thawing, the cells were re-fed with fresh warmed medium to remove any residual traces of DMSO.

### 2.2.6 Sterility Checks

Sterility checks were routinely carried out on all media, supplements and TV used for cell culture. Samples of basal media were inoculated into Columbia (Oxoid, CM331) blood agar plates, Sabauraud (Oxoid, CM217) dextrose and Thioglycollate (Oxoid, CM173) broth's which should between them detect most contaminants including bacteria, fungus and yeast. Growth media (*i.e.* supplemented with serum) were sterility checked at least 3 days prior to use by incubating samples at 37°C. These were subsequently examined for turbidity and other indications of contamination. Freshly thawed cells were also subjected to sterility checks.

### 2.2.7 *Mycoplasma* Analysis

*Mycoplasma* examinations were carried out routinely (at least every 3 months) on all cell lines used in this study. This analysis was preformed by Michael Henry and Shane Kelly at the National Institute for Cellular Biotechnology (NICB).

#### 2.2.7.1 Indirect Staining Procedure

In this procedure, *Mycoplasma*-negative NRK cells (a normal rat kidney fibroblast line) were used as indicator cells and incubated with supernatant from test cell lines to test for *Mycoplasma* contamination. NRK cells were used for this procedure because cell integrity is well maintained during fixation. A fluorescent Hoechst stain was utilised which binds specifically to DNA and so will stain the nucleus of the cells in

addition to any *Mycoplasma* DNA present. A *Mycoplasma* infection would thus be seen as small fluorescent bodies in the cytoplasm of the NRK cells and occasionally outside the cells.

NRK cells were seeded onto sterile cover slips in sterile Petri dishes (Greiner, 633 185) at a cell density of $2x10^3$ cells per ml and were allowed to attach overnight at 37°C in a 5% $CO_2$, humidified incubator. 1 ml of cell-free (cleared by centrifugation at 1,000 rpm for 5 min) supernatant from each test cell line was then inoculated onto a NRK cover slip and incubated as before until the cells reached 20 - 50% confluency (4-5 days). After this time, the waste medium was removed from the Petri dish; the cover slips (Chance Propper, 22 x 22 mm) were washed twice with sterile PBS, once with a cold PBS/Carnoys (50/50) solution and fixed with 2 ml of Carnoys solution (acetic acid: methanol - 1:3) for 10 min. The fixative was then removed and after air-drying, the cover slips were washed twice in deionised water and stained with 2 ml of Hoechst 33258 dye (BDH) (50 ng/ml) for 10 min.

From this point on, work proceeded in the dark to limit quenching of the fluorescent stain. The cover slips were rinsed three times in PBS. They were then mounted in 50% (v/v) glycerol in 0.05 M citric acid and 0.1 M disodium phosphate and examined using a fluorescence microscope with a UV (ultraviolet) filter.

Prior to removing a sample for *Mycoplasma* analysis, cells were to be passaged a minimum of 3 times after thawing to facilitate the detection of low-level infection. Optimum conditions for harvesting supernatant for analysis occur when the culture is in log-phase near confluency and the medium has not been renewed in 2-3 days.

## 2.3 Specialised techniques in cell culture

### 2.3.1 Proliferation assays experimental protocol

The proliferation rates (doubling times) of the MIN6 low passage (L) cells, high passage (H) cells, MIN6 B1 low passage (MIN6 B1(GSIS)) cells and high passage MIN6 B1(Non-GSIS) cells were determined by monitoring their growth over consecutive 24hrs. time periods. For this, the cells were seeded at $5x10^4$ cells/well in 24-well plates (Costar, 3524). Cells were incubated over-night at 37°C / 5% $CO_2$ and 3 wells were trypsinised and counted on each of the 7 days following seeding. Cell doubling times were calculated from a graph of cell numbers against time.

### 2.3.2 Stimulated Insulin Secretion Analysis of Cultured Cells

MIN6 and MIN6 B1 were seeded at a cell density of 2 x $10^5$ cells/well in a 24-well plate (taking care not to generate a single-cell suspension (See Section: 2.2.2.3)). The GSIS (Glucose-stimulated insulin secretion) profiles of MIN6 B1 cells were analysed at glucose concentrations of 3.3 and 16.7mmol/L. These cells were allowed to grow for 72hrs. prior to the GSIS assay (Fig: 2.3.2.2). Following this, 1xKRB (Krebs-Ringer Buffer) was prepared from an aliquot of frozen 10xKRB stock (Table: 2.3.2.1), BSA (an insulin carrier) was added to a final concentration of 0.1%, and the KRB–BSA was pH-adjusted to 7.36 with 1 mol/L NaOH. This solution was pre-incubated for 30 min at 37°C and 5% $CO_2$ and glucose concentrations of 3.3 and 16.7mmol/L were prepared with KRB solution and were subsequently placed at 37°C and 5% $CO_2$ for 30 min. MIN6 B1 cells to be analysed were rinsed (twice) in 1xKRB and were equilibrated at 3.3mmol/L glucose for 30 min at 37°C. After equilibration, the glucose-containing stimulation medium was added (1 ml/well) and incubated at

37$^{o}$C in 5% $CO_2$ for 60 min. The GSIS assay was then terminated by placing the plate on ice. Supernatant (300 µl) was removed from each well, placed in an ice-cold eppendorf tube, centrifuged at 2000 rpm for 2 min. 200 µl of supernatant was then transferred to a fresh eppendorf tube for analysis by (pro)insulin ELISA (Mercodia, 10-1124-10) (See Section: 2.3.2.4).

**Table : 2.3.2.1 10 X Krebs Ringer Buffer (KRB)**

| Amount | Reagent |
|---|---|
| 36.525g | NaCl |
| 2.2g | KCl |
| 0.941g | $CaCl_2.2H_2O$ |
| 1.22g | $MgCl_2.6H_2O$ |
| 29.8g | HEPES |
| 500 ml | UHP $H_2O$ |

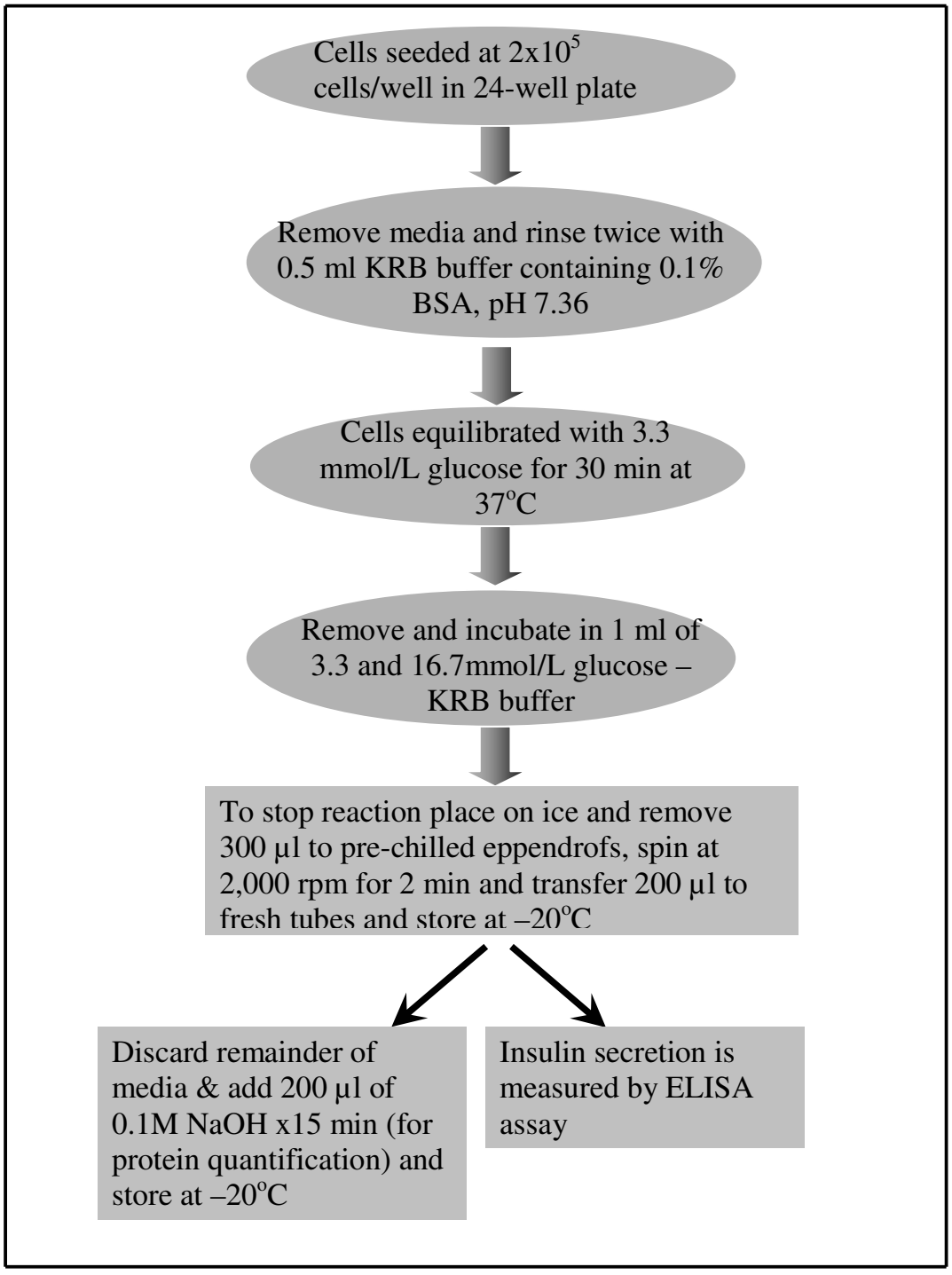


**Fig: 2.3.2.2 GSIS flow chart**

### 2.3.3 Insulin content analysis

MIN6 B1(GSIS) and MIN6 B1(Non-GSIS) cells were re-suspended in 200 µl of 1mM NaOH and left to incubate at room temperature for 5 min. The cells were left to lyse on ice for another 10 min and stored in -20$^{o}$C until used.

### 2.3.4 Protein Quantification

Lysed samples were removed from the freezer and placed on ice. A BSA standard of 1 mg/ml was prepared in UHP. Diluted BSA Standards was prepared and 5 µl of standard and 5 µl of sample were placed in triplicate wells on a 96-well plate (Costar, 3596). The Biorad $D_c$ Protein Assay was used for protein quantification. 25 µl of Reagent A (containing 20 µl Reagent S (Biorad, 500-0115) per ml of Reagent A (500-0113)) followed by 200 µl of Reagent B (Biorad, 500-0114) were added to each test well. The plate was kept at room temperature for 15 min prior to reading on the Spectra Max Plus using a softmax Lowry protein assay (750nm) program.

### 2.3.5 ELISA Analysis for Insulin and Proinsulin

Insulin secretion studies have already been described (See Section: 2.3.21). Analyses on conditioned media were carried out using a proinsulin ELISA kit (Mercodia, 10-1124-10). The kits were supplied with reagents, standards etc. Standard protocol was followed as per manufacturer's instructions. In brief, standards and samples (25 µl) were added directly to the coated plate (mouse monoclonal anti-insulin) in triplicate. 50 µl conjugate solution (enzyme conjugate 11X in enzyme conjugate buffer by dilution of 1 + 10) was then added to the samples and standards. The plate was wrapped in foil (to prevent debris falling into the wells) and incubated at room temperature for 2hrs. on a belly dancer set to maximum speed. Following this, the

conjugate/sample mixes were tapped off into the sink and the wells were washed 6 times with washing solution (wash buffer 21X diluted 1 + 20 in UHP prior to use). Washing was carried out using a wash bottle with a wide bore nozzle and care was taken not to overflow wells during washing (to prevent cross contamination between samples). After washing, the plate was tapped firmly on tissue to remove the excess wash solution. At this point 200 µl peroxidase substrate was added to each well. As it is light sensitive this reaction was allowed to develop in the dark (the plate was wrapped in tinfoil) for 15 - 30 min and stopped by adding 50 µl stop solution per well. The plates were mixed gently and any bubbles were burst manually. The plates were read at 450nm on a plate reader (Labsystems Multiskan Ex) and the data was processed using Excel sheet.

### 2.3.6 Proliferation using Acid Phosphatase assay

Proliferation using Acid Phosphatase assay was performed following siRNA transfection. Cells were incubated for a period of 72hrs. after siRNA transfection. Media was removed from the plates and each well on the plate was washed with 100 µl of PBS. After washing 100 µl of freshly prepared phosphatase substrate (10mM *p*-nitrophenol phosphate (Sigma, 104-0) in 0.1 M sodium acetate (Sigma, S8625), 0.1% triton X-100 (BDH, 30632), pH 5.5) was added to each well. The plates were wrapped in tinfoil and incubated in the dark at 37°C for 2hrs. After incubation the enzymatic reaction was stopped by the addition of 50 µl of 1 M NaOH to each well. The plate was read in a dual beam plate reader at 405nm with a reference wavelength of 620nm.

## 2.4 Sampling different insulin producing cells and their CM

### 2.4.1 Identifying a suitable time point for CM collection (Protocol-1)

The experimental design to identify a suitable time point for CM collection and analysis is shown in Fig: 2.4.1. MIN6 B1 cells were set up in T75cm$^2$ flasks at a density of 5 x $10^6$ cells with 8 mls of media added to it. After each 24hrs, 500 µl of conditioned media (CM) was taken off the cells and replaced by same amount of fresh culture media. CM was filtered with a 0.45 µm filter. Immediately 250 µl aliquots of filtered CM was added in to 750 µl aliquots of TriReagent and stored at -80°C until RNA extraction (See Section: 2.5.1.2.1) was carried out. After 96hrs. the cells were trypsinised, counted and washed twice with PBS. The pellet was stored in 1 ml aliquots of TriReagent at -80°C until RNA extraction.

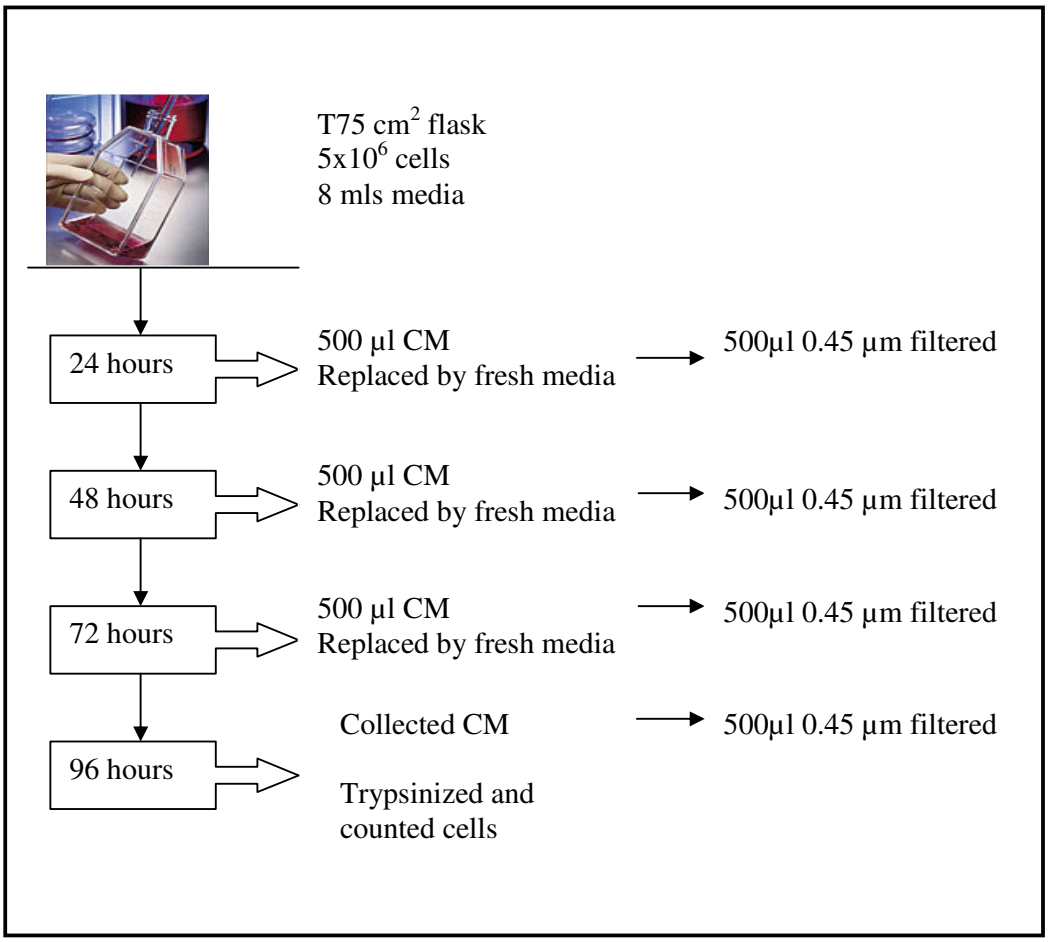


**Fig: 2.4.1 Experimental design of study to identify a suitable time point post cell seeding for CM collection and analysis**

### 2.4.2 Identifying a suitable time point for CM collection (Protocol-2)

The experimental design to identify a suitable time point for CM collection and analysis is shown in Fig: 2.4.2, MIN6 B1 cells were set up in T75cm$^2$ flasks at a density of 5 x 10$^6$ cells and 8 mls of media was added. After each consecutive 24hrs. CM and cells were taken from each of the flask and the same procedure was followed as above (See Section: 2.4.1).

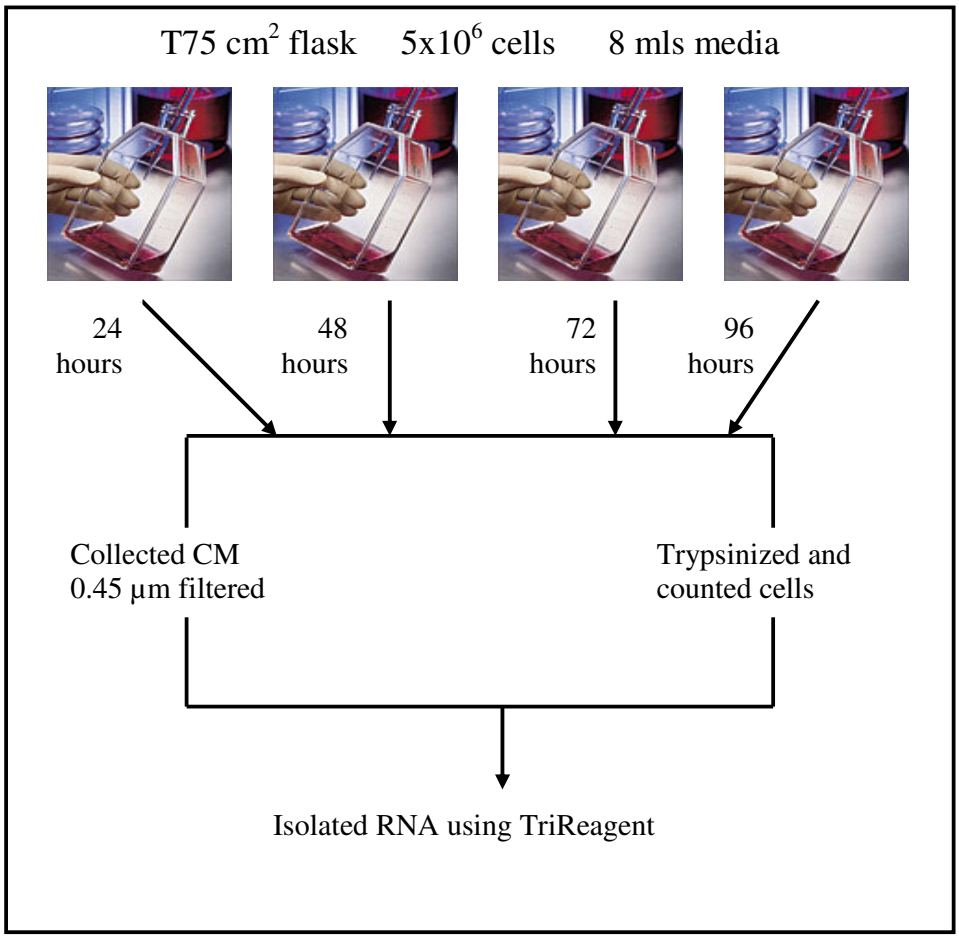


**Fig: 2.4.2 Experimental design of study to identify a suitable time point post cell seeding for CM collection and analysis**

### 2.4.3 Conditioned media (CM) filtration

#### 2.4.3.1 Conditioned media filtration from insulin-producing cells

Insulin-producing MIN6 B1 and Vero-PPI cells were seeded at different densities *i.e.* 1x $10^6$ cells, 5x$10^6$ cells and 1x$10^7$ cells per T25cm$^2$ flask along with a total of 4 mls of culture media. Cells were allowed to grow for 48hrs. Conditioned media was taken off and sterile filtered using 0.45 µm to make sure that there are no cells included.

Cultured cells in the flask was trypsinised, counted and centrifuged at 900 rpm for 5 min to form a pellet. These pellets were washed twice with cold PBS prior to re-

suspending in 1 ml of TriReagent, incubating as above and storing in -80$^{o}$C for further RNA isolation (See Section: 2.5.1.2.1).

#### 2.4.3.2 Conditioned media filtration from MIN6 (L) and (H)

MIN6 (L) and (H) cells were allowed to grow to 80% confluency in 75cm$^2$ flasks and cultured further for 48hrs. in 8mls of media (reaching approximately 90% confluency). CM was removed and passed through 0.45 µm filters to ensure that there were no cells present.

### 2.4.4 Collecting Serum from blood

Two blood specimens of approximately 10 ml were taken with consent from each patient recruited for the Type 2 diabetes and control serum study. From the collected blood samples, the red blood cells were allowed to clot naturally. These specimens were processed within 3-4hrs. of blood draw. Serum specimens from control volunteers (*i.e.* no history or symptoms of diabetes) were also collected and processed in the similar way.

All serum specimens were processed by removing the serum from the clotted blood and placing into a 10 ml centrifuge tube. A balance tube was made by adding an equal amount of water to another 10 ml centrifuge tube. The tubes were then centrifuged at room temperature for 15 min at 400 rcf (relative centrifugal force). After centrifugation the cleared serum was carefully removed and passed through a 0.45 µm filter to further ensure no particles/ platelets were retained. The serum was then aliquoted into 1 ml/1.5 ml aliquots and stored at -80°C until required. RNA extraction from the serum was carried out using a slightly modified version of the optimised TriReagent protocol developed here (See Section: 2.5.1.2.1). In order to minimise the

amount of time the serum was defrosting without protection from RNases, when required, 500 µl of TriReagent was added to the frozen serum specimens and the samples were gently pipetted to ensure thorough mixing. This serum-TriReagent mix was then added in 500 µl aliquots to clean eppendorf tubes containing 250 µl of TriReagent, so that the final ratio of TriReagent to serum was 3:1 (*i.e.*750 µl : 250 µl).

## 2.5 Analytical Techniques and Assays

### 2.5.1 RNA Analysis

#### 2.5.1.1 Preparation for RNA Analysis

RNA is easily degraded by RNase (ribonuclease) enzymes, which are ubiquitous, thus the following precautions were taken prior to RNA work.

All solutions for RNA related work were prepared from sterile UHP $H_2O$ that had been treated with 0.1% diethyl pyrocarbonate (DEPC) (Sigma, D5758) before autoclaving (autoclaving inactivates DEPC). All Eppendorfs, PCR (polymerase chain reaction) tubes etc. were RNase-free and pre-autoclaved prior to use as were Gilson pipette tips. Disposable nitrile gloves were worn at all times during RNA work (to protect the operator and to prevent RNA degradation) and changed frequently.

#### 2.5.1.2 RNA Extraction

RNA was extracted from cultured cells and their conditioned media stored in TriReagent at -80$^{o}$C until required (Fig: 2.5.1.2.1).

##### 2.5.1.2.1 RNA Isolation from CM and Serum samples

The frozen TriReagent samples were allowed to thaw at room temperature and upon thawing, were allowed to sit for at least 5 min to ensure complete dissociation of nucleoprotein complexes. To this was added 0.2 ml of chloroform per ml of TriReagent. Samples were shaken vigorously for 15 sec and allowed to stand for 15 min at room temperature.

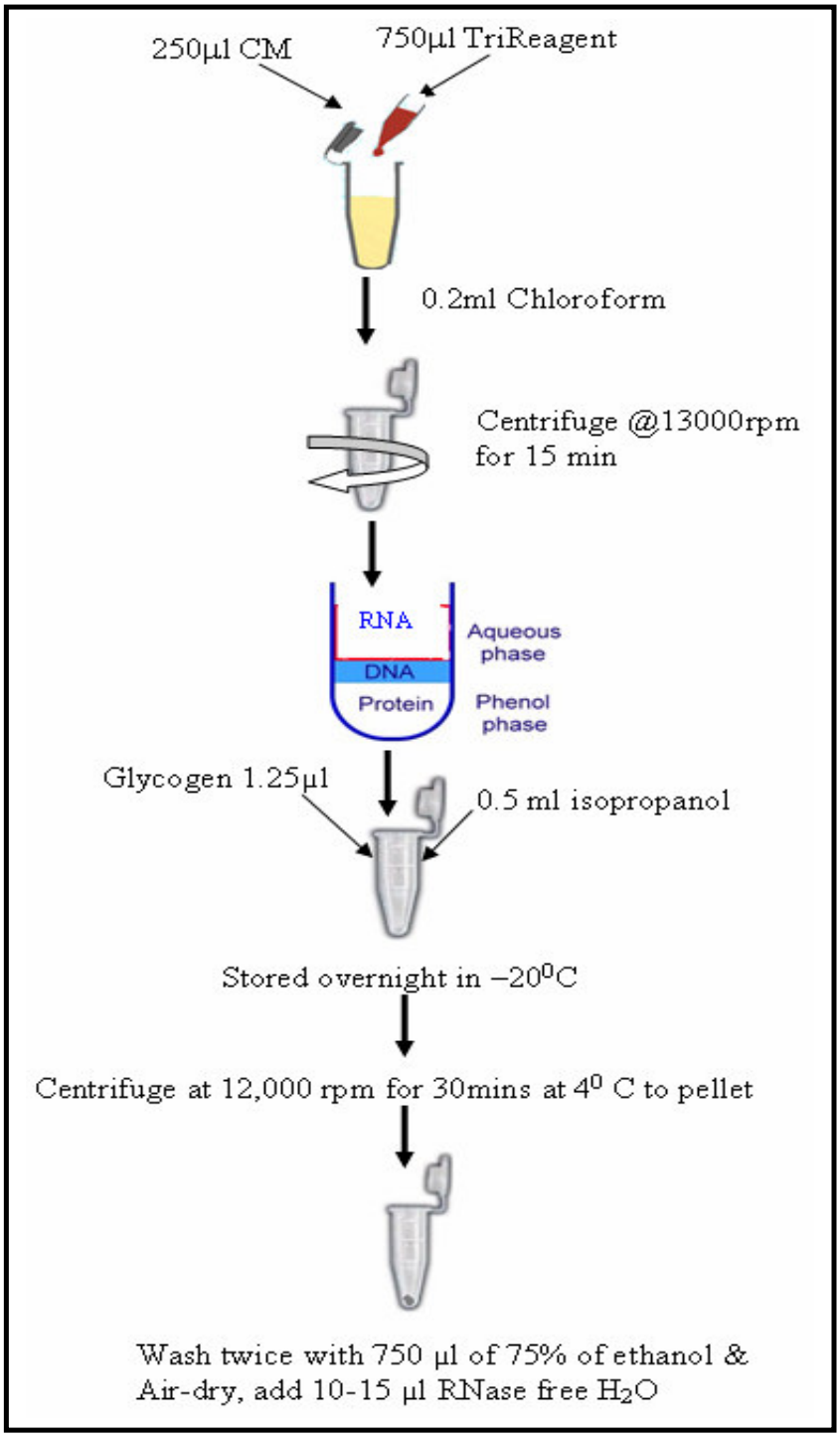


**Fig: 2.5.1.2.1 RNA isolation using TriReagent from cells and CM**

The resulting mixtures were then centrifuged at 13000 rpm in a microfuge for 15 min at 4$^{o}$C. The colourless upper aqueous phase (containing RNA) was removed into a fresh RNase-free 1.5 ml eppendrof tube. Glycogen (Sigma, G1767) 1.25 µl (final concentration 120 µg/ml) and 0.5 ml of ice-cold isopropanol (Sigma, I9516) was added. The samples were mixed and incubated at room temperature for 5-10 min and stored at -20$^{o}$C over-night, to ensure maximum RNA precipitation. The Eppendrof tubes were then centrifuge at 12,000 rpm for 30 min at 4$^{o}$C to pellet the precipitated RNA.

Taking care not to disturb RNA pellet, the supernatant was removed and the pellet was subsequently washed by the addition of 750 µl of 75% of ethanol and vortexed. Centrifugation was followed at 7,500 rpm for 5 min at 4$^{o}$C. The supernatant was removed and the wash step was repeated. The RNA pellet was then allowed to air-dry for 5-10 min and subsequently was re-suspended in 15 µl of DEPC-treated water. To facilitate dissolution repeated pipetting was done (Fig: 2.5.1.2.1).

#### 2.5.1.2.2 RNA Isolation from Cells

Approximately 1x10$^{7}$ cells were trypsinised, washed once with PBS, pelleted and lysed using 1 ml of TriReagent (Sigma, T-9424). The samples were allowed to stand for 5 min at room temperature to allow complete dissociation of nucleoprotein complexes and then stored at –80$^{o}$C. When required, sample was allowed to stand at room temperature for 5-10 min. To this was added 0.2 ml of chloroform per ml of TriReagent was added. Samples were shaken vigorously for 15 sec and allowed to stand for 15 min at room temperature. The resulting mixtures were then centrifuged at 13000 rpm in a microfuge for 15 min at 4$^{o}$C. The colourless upper aqueous phase (containing RNA) was removed into a fresh RNase-free 1.5 ml eppendrof tube. To

this 0.5 ml of ice-cold isopropanol (Sigma, I9516) was added. The samples were mixed and incubated at room temperature for 5-10 min. The eppendrof tubes were then centrifuge at 12,000 rpm for 30 min at 4$^{o}$C to pellet the precipitated RNA. Taking care not to disturb RNA pellet, the supernatant was removed and the pellet was subsequently washed by the addition of 750 µl of 75% of ethanol and vortexed. Centrifugation was followed at 7,500 rpm for 5 min at 4$^{o}$C. The supernatant was removed and the wash step was repeated. The RNA pellet was then allowed to air-dry for 5-10 min and subsequently was re-suspended in 15 µl of DEPC-treated water. To facilitate dissolution repeated pipetting was done.

#### 2.5.1.2.3 Preparation of total RNA from cells using RNeasy Mini Prep Kit® (QIAGEN, 74104)

Alternatively, high quality RNA used for microarray studies was isolated from cells using the RNeasy mini-kit (Qiagen, 74104). Cell pellets for RNA extraction (stored at –80$^{o}$C) were re-suspended in 1.2 ml of buffer RLT (supplemented with 10 µl/ml of β-mercaptoethanol) and vortexed to loosen the pellets. The lysed pellets were aspirated a number of times and vortexed until the samples were completely homogenised. 1 volume (1.2 ml) of 70% ethanol was added to the homogenised samples and mixed well by pipetting. This mixture was then loaded in 700 µl aliquots on to an RNeasy mini column, which was placed in a collection tube and centrifuged at 8,000 x g for 15 sec (this was continued until the entire mixture had been passed through the column). Once all the homogenised cells had been passed through the column, the washes were carried out. Initially 700 µl RW1 was loaded on to the column and centrifuged at 8,000 x g for 15 sec. This was closely followed by 2 washes in buffer RPE (also followed by centrifuging at 8,000 rpm for 15 sec). To completely dry the

spin column, it was placed in a fresh collection tube and centrifuged at full speed for 1 min. The RNA was eluted by passing two lots of 25 µl RNase free water (supplied) through the column by centrifuging it at 8,000 rpm for 1 min. The eluted RNA was then quantified (See Section: 2.5.1.4).

### 2.5.1.3 Treatment of RNA

RNA was treated with DNase and RNase enzyme to establish that RT-PCR signals in this study are from RNA, and not from contaminating DNA. Fig 2.5.1.3 shows experimental design for untreated, DNase and RNase treatments.

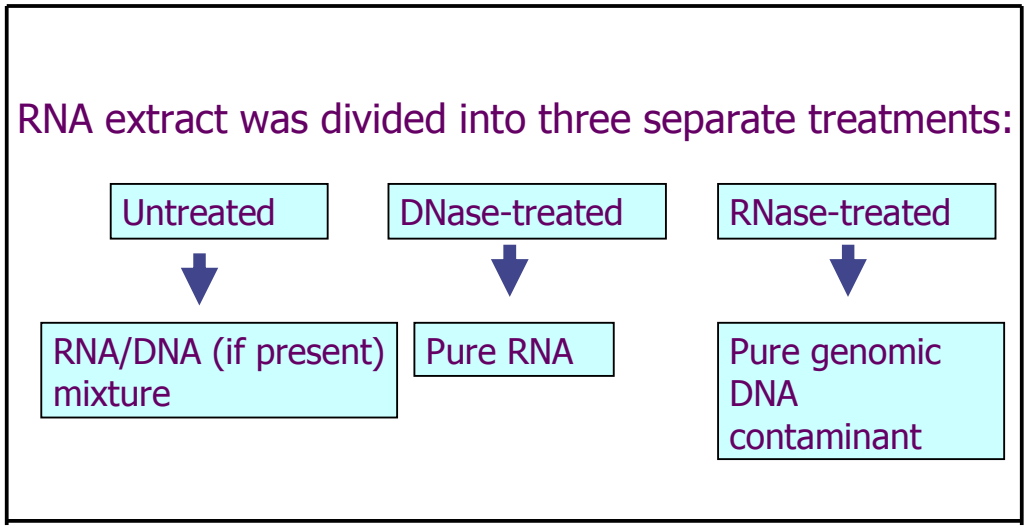


**Fig: 2.5.1.3 Experimental design of RNase- and DNase-treated RNA samples.**

#### 2.5.1.3.1 DNase-treated RNA

In order to remove any contaminating genomic DNA that may be present in the RNA isolates, samples from cells and their corresponding CM was treated with 1U of RNase-free DNase (Promega, M6101) per 1 µg RNA in a reaction mixture of 10 µl including reaction buffer (Promega, M198A) (Table: 2.5.1.3.1). RNA was incubated

at 37$^{o}$C for 30 min in the reaction mixture containing RNase-free DNase (Promega, M6101) as recommended by the manufacturer as follow: -

**Table: 2.5.1.3.1 preparation of master mix for DNA digestion reaction**

| Reagent | Volume |
|---|---|
| RNA in water | 1–8 µl |
| RQ1 RNase-Free DNase 10X Reaction Buffer | 1 µl |
| RQ1 RNase-Free DNase | 1 U/µg RNA |
| Nuclease-free water to a final volume of | 10 µl |

To this mixture was added 1 µl of RQ1 DNase Stop Solution (Promega, M199A) to terminate the reaction and incubated further at 65°C for 10 min to inactivate the DNase.

### 2.5.1.3.2 RNase-treated RNA

To establish that RT-PCR signals in this study are from RNA, and not from contaminating DNA, isolated samples were treated with 1U RNase ONE ribonucleases (Promega, M4261) per 0.1 µg RNA in a 10 µl reaction mixture containing buffer (Promega, M2174) (Table: 2.5.1.3.2). Incubate the RNA at 37$^{o}$C for 30 min in the reaction mixture containing RNase-ONE Ribonuclease (Promega, M4261) as recommended by the manufacturer as follow: -

**Table: 2.5.1.3.2 preparation of master mix for RNA digestion reaction**

| Reagent | Volume |
|---|---|
| RNA in water | 1–8 µl |
| 10X Reaction Buffer | 1 µl |
| RNase-ONE Ribonuclease | 1 U/0.1µg RNA |
| Nuclease-free water to a final volume of | 10 µl |

### 2.5.1.4 RNA Quantification using NanoDrop

The NanoDrop® ND-1000 is a full-spectrum (220-750nm) spectrophotometer that measures 1 µl samples with high accuracy and reproducibility. It uses a sample retention technology that relies on surface tension alone to hold the sample in place eliminating the need for cuvettes and other sample containment devices. In addition, the NanoDrop has the capability to measure highly concentrated samples without dilution (50X higher concentration than the samples measured by a standard cuvette spectrophotometer).

To quantify an RNA sample, 1 µl of the sample is pipetted onto the end of a fibre optic cable (the receiving fibre, Fig: 2.5.1.4.1 (A)). A second fibre optic cable (the source fibre, Fig: 2.5.1.4.1 (B)) is then brought into contact with the liquid sample causing the liquid to bridge the gap between the fibre optic ends. The gap is controlled to a 1mm path (Fig: 2.5.1.4.1 (C)). A pulsed xenon flash lamp provides the light source and a spectrometer utilising a linear CCD array is used to analyse the light after passing through the sample. The instrument is controlled by special software run from a computer, and the data is logged in an archive file on the computer.

When measurement of the sample is complete, the sample can be simply wiped away using a soft laboratory wipe. This is sufficient to prevent sample carryover because each measurement pedestal is a highly polished end of a fibre optic cable, with no cracks or crevices for residual sample to reside in.

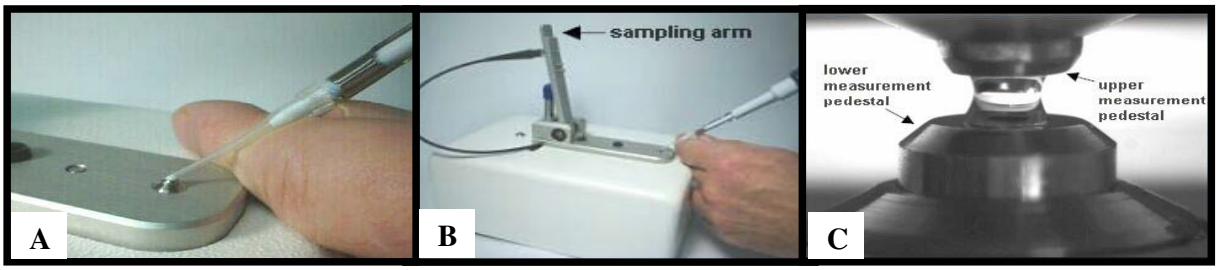


**Fig: 2.5.1.4.1 Samples are quantified by loading 1 µl onto the receiving fibre (A), the source fibre, connected to the sampling arm (B) is brought down into contact with the sample allowing a 1mm gap between the upper and lower pedestal (C), through which the light is passed. (Pictures adapted from ND-1000 Spectrophotometer users manual V 3.1.0).**

RNA (like DNA) was quantified using an ND-1000 spectrophotometer. The ND-1000 software automatically calculated the quantity of RNA in the samples using the $OD_{260}$.

*i.e.* $OD_{260}$ x 40 x Dilution Factor/1000 = RNA content (µg/µl)

The software simultaneously measured the $OD_{280}$ of the samples allowing the purity of the sample to be estimated.

Purity = $OD_{260}/OD_{280}$

This was typically in the range of 1.8-2.0. A ratio of <1.6 indicated that the RNA may not be fully in solution. The RNA was diluted to 1 µg/µl stocks for the reverse transcription (RT).

#### 2.5.1.5 RNA Quality Analysis by Electrophoresis

For RNA quality analysis agarose (Sigma, A-9539) gel electrophoresis was used. 1% agarose gel was prepared in 1X TBE buffer (prepared in autoclaved $dH_2O$), and gel was casted within an RNase-free gel box (soak gel box in 5 mM NaOH overnight and rinse twice with DEPC treated water before use). 5 µl of the sample and 2 µl of dye were loaded. The gel was run at 100 V until the dye reached the end of the gel (~30 min). The RNA gel was observed using a UV gel box.

#### 2.5.1.6 Total RNA Analysis using the Bioanalyzer

The Agilent 2100 Bioanalyzer is a microfluidics-based platform for the analysis of proteins, DNA and RNA. The miniature chips are made from glass and contain a network of interconnected channels and reservoirs. The RNA 6000 Nano LabChip kit enables analysis of samples containing as little as 5 ng of total RNA.

**a) Reagent Preparation:**

The channels are firstly filled with a gel matrix and the sample wells with buffer or sample, there are 12 sample wells per chip. 1 µl of each sample is loaded into a sample well along with a fluorescent dye (marker). An RNA ladder is loaded into another sample well for size comparison. RNA Gel Matrix was prepared fresh just before use.

RNA Gel Matrix was vortexed and aliquoted 550 µl (room temperature), into top receptacle of spin filter and centrifuged at 1500 x g (4000 rpm) for 10 min discarding the spin filter.

Gel-Dye Mix was prepared by using 65 µl filtered Gel Matrix in a microcentrifuge tube. To this is added 1 µl RNA Dye Concentrate after vortexing for 10 sec. It was mixed properly by vortexing and centrifuged for 10 min at 13,000 x g (14,000 rpm).

**b) Sample Preparation**

RNA samples were thawed on ice and 1 µl of RNA was dispensed into each PCR tube. Samples and ladder were heat denatured at 70°C for at least 2 min and then placed on ice for 2 min and centrifuged briefly to collect sample at the bottom of the tube.

**c) Loading the Gel-Dye Mix**

New chip was taken out of its sealed bag and placed on the Chip Priming Station. Then 9.0 µl of the gel-dye mix was pipetted in each of the wells marked G (light letter). Then Chip Priming Station was closed by pressing the plunger until it was held by the clip and was released after 30 sec. Then 9.0 µl of the gel-dye mix was pipetted in each of the wells marked G and discarding the remaining gel-dye mix.

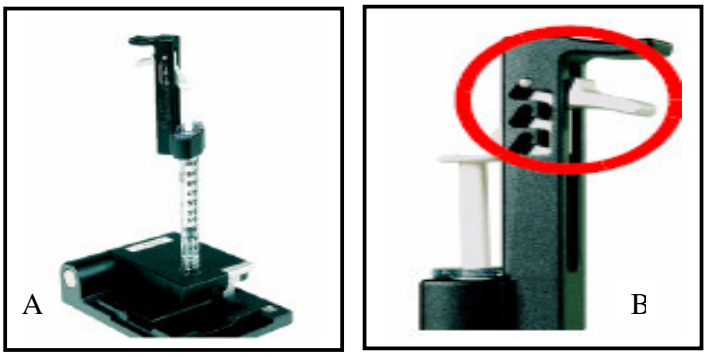


**Fig: 2.5.1.6.1 Picture showing (A) the Chip Priming Station and (B) plunger held by the clip.**

**d) Loading a Primed Chip**

RNA 6000 Nano Marker was pipetted (5 µl) into each well, including the well marked with a ladder. Then 1 µl denatured RNA sample was added into each well, one sample per well and 1 µl denatured ladder into the well marked with a ladder. Care was taken to fill all the unused wells as well. Then the chip was vortexed using chip vortexer. The chip was vortexed at the Set Point indicated on the right side of the dial for one minute.

**e) Running the Agilent 2100 Bioanalyzer**

The channels were firstly filled with a gel matrix and the sample wells with buffer or sample, there are 12 sample wells per chip. 1 µl of each sample was loaded into a sample well along with a fluorescent dye (marker). An RNA ladder was loaded into another sample well for size comparison. When all the samples were loaded, the chip was briefly vortexed and loaded onto the Bioanalyzer machine (Fig: 2.5.1.6.2 for picture of chip).

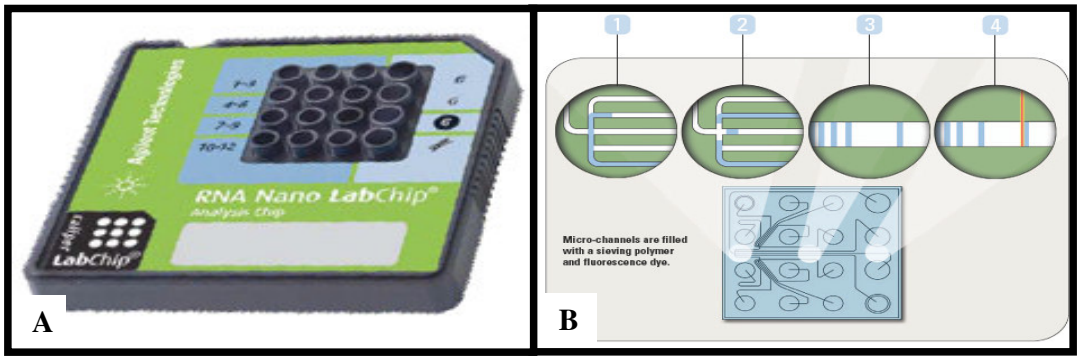


**Fig: 2.5.1.6.2 The RNA 6000 Nano chip, a picture of the front of the RNA Nano chip (A) and a diagram of the microchannels in the chip (B), the sample moves through microchannels (1) and is injected into separation chamber (2) were components are electrophoretically separated (3) and detected by their fluorescence and translated into gel-like images and electropherograms. Both pictures available from** http://www.agilent.com/chem/labonachip

The machine is fully automated and electrophoretically separates the samples by injecting the individual samples contained in the sample wells into a separation chamber. The resulting data was presented as an electropherogram (Fig: 2.5.1.6.3).

The fluorescence was measured on the Y-axis and the time in seconds is measured on the X-axis. The smaller fragments are detected first and are shown on the left-hand side of the electropherogram. Fig. 2.5.1.6.3 is an example of good quality cell RNA, the 18S and 28S ribosomal RNA peaks are quite sharp and the 28S is higher than the 18S peak. As RNA degrades, the 28S RNA peak decreases and smaller fragments are visible.

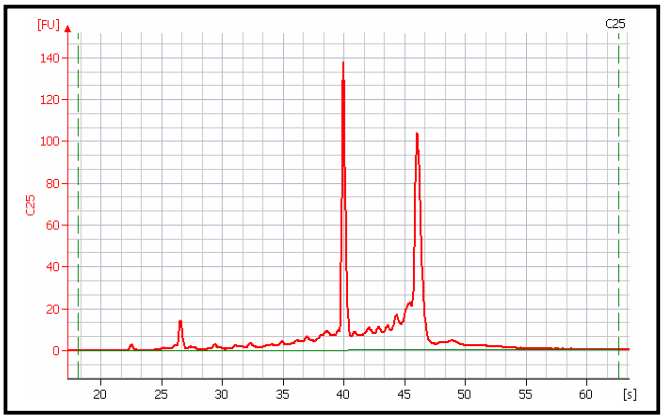


**Fig: 2.5.1.6.3 Examples of electropherogram generated using the Agilent Bioanalyzer. Electropherogram showing first small peak as marker, second peak as 5s RNA, followed by sharp 18S and 28S ribosomal bands. MIN6 B1 cell RNA as evident by the sharp 18S and 28S ribosomal bands.**

## 2.5.2 Reverse-Transcription Polymerase Chain Reaction Analysis

### 2.5.2.1 Reverse Transcription of RNA from cells (cDNA Synthesis)

mRNA was copied to cDNA by reverse transcriptase using an oligo dT primer. First-strand cDNA was synthesised by reverse transcription (RT) by mixing the following components in a 0.5 ml eppendorf tube (Eppendorf, 0030 121 023) and heated at 70$^{o}$C for 10 min followed by cooling on ice. Table 2.5.2.1.1 shows the protocol for preparation cDNA from cell RNA whereas; table 2.5.2.1.2 shows the protocol for preparation of cDNA from CM RNA.

**Table: 2.5.2.1.1 First strand cDNA from cell RNA**

| Volume | Reagents |
|---|---|
| 1 µl | Oligo dT (0.5 µg/µl) (MWG) |
| 1 µl | RNA (1 µg/µl) |
| 3 µl | DEPC-treated $H_2O$ |

**Table: 2.5.2.1.2 First strand cDNA from CM RNA**

| Volume | Reagents |
|---|---|
| 1 µl | Oligo dT (0.5 µg/µl) (MWG) |
| 4 µl | RNA |

This step gets rid of RNA secondary structures and allows the oligo dT to bind the poly $(A)^+$ tail of the RNA. While this mixture was incubated, the following reaction mix was generated (all volumes listed in master mix assume 1 µg total RNA) (Table: 2.5.2.13).

**Table: 2.5.2.1.3 Reverse Transcription Reaction Mixture**

| Volume | Reagents |
|---|---|
| 2 µl | 10X buffer (Sigma, B8559) |
| 1 µl | RNasin (40U/µl) (Sigma, R2520) |
| 1 µl | dNTP (deoxynucleotide triphosphate) (10mM of each dNTP) (Sigma, DNTP100) |
| 10 µl | DEPC -treated water |
| 1 µl | MMLV-RT (200 U/µl) (Sigma, M1302) |
| 15 µl | Total |

Once the RNA mixture had cooled (~2 min) 15 µl of the master mix (Table: 2.5.2.1.3) was added and mixed by flicking. The mixture was centrifuged to collect the material in the bottom of the tube and then incubated at 37$^{o}$C for 1hr. The resultant cDNA was stable overnight at 4$^{o}$C but for prolonged storage it was maintained at –20$^{o}$C.

### 2.5.2.2 Polymerase Chain Reaction

The cDNA was analysed for the expression of genes of interest by PCR. The standardised PCR mix is listed below and did not change significantly with any of the PCRs carried out in this thesis. 2.5 µl cDNA was added to the following reaction mixture (Table: 2.5.2.2). The samples were mixed and centrifuged before being placed on the thermocycler (Biometra).

**Table: 2.5.2.2 PCR Reaction Mixture**

| Volume | Reagents |
|---|---|
| 12.25 µl | $H_2O$ |
| 2.5 µl | 10X PCR buffer (Sigma, P2317) |
| 1.5 µl | 25 mM $MgCl_2$ (Sigma, M8787) |
| 4 µl | 1.25 mM dNTP |
| 0.5 µl | each of the forward and reverse primers (250 ng/µl) for the target gene (MWG) |
| 0.25 µl | Taq Polymerase (5 U/µl) (Sigma, D4545). |
| 20 µl | Total |

A typical PCR protocol is outlined below. However annealing temperatures can vary from primer set to primer set therefore a full list of the primers used in this thesis and the annealing temperatures are listed in Table 2.5.2.5.2.

95°C for 3 min (Denaturation step)

Followed by

25-30 cycles of:

95°C for 30 sec (Denaturation)

52-60°C for 30 sec (Annealing)

72°C for 30 sec (Extension)

And

72°C for 7 min (Extension)

PCR products were stored at 4°C until they were analysed by gel electrophoresis.

* 30 cycles were sufficient when amplifying gene transcripts from cell RNA however; it was necessary to increase this to 45 cycles when using RNA extracted from CM.

**2.5.2.3 Gel Electrophoresis of PCR Products**

Typically, 2% agarose (Sigma, A9539) gels were used for PCR gel electrophoresis, which were prepared and run in 1X TBE (10.8 g Tris base, 5.5 g Boric Acid, 4 ml 0.5 M EDTA (pH 8.0) and made up to 1 L with UHP) and melted in a laboratory microwave. Upon cooling, the gel was supplemented with 5 µl ethidium bromide (10 mg/ml) to allow visualisation of the DNA. Ethidium bromide is a dye that binds to double stranded DNA by interpolation (intercalation) between the base pairs. Here it fluoresces when irradiated in the UV part of the spectrum. The gel was then poured in

to the electrophoresis unit (Biorad) and allowed to set. Sample wells were formed by placing a comb into the top of the gel prior to hardening.

To run the samples, 2 µl of 6X loading buffer (50% Glycerol, 1 mg/ml bromophenol blue, 1 mM EDTA) was added to 10 µl PCR product and the mixture was loaded to the gel with an appropriate size marker (Sigma, D0672). The gels were electrophoresed at 120-150 V for 1 - 2hrs. (depending on size of the target gene, *i.e.* to get adequate separation). Once the internal control and target bands have migrated to the required extent, the gel was taken to the gel analyzer (an EpiChemi II Darkroom, UVP Laboratory Products), photographed and densitometrically analysed using Labworks software (UVP).

#### 2.5.2.4 Densitometry Analysis

Densitometric analysis of the PCR products was carried out using the MS Windows 3.1 compatible Molecular Analyst software/PC image analysis software available for use on the 670 Imaging Densitometer (Bio-Rad. CA) Version 1.3. Developed negatives of gels were scanned using transmission light and the image transferred to the computer. The amount of light blocked by the DNA band is in direct proportion to the intensity of the DNA present. A standard area was set and scanned and a value was taken for the Optical Density (O.D.) of each individual pixel on the screen. The average value of this O.D. (within a set area, usually $cm^2$) is normalised for background of an identical set area. The normalised reading is taken as the densitometric value used in analysis. As a result, these O.D. readings were unitless.

### 2.5.2.5 Primer sequences used for RT-PCR studies

To investigate if any secreted mRNAs detected were likely to be full-length transcripts or fragmented products, PCR primers were designed in such a way as to amplify regions close to the 3' end (e.g. *Pdx1, Pld1, Ppi*), the 5' region (e.g. *Egr 1, Chgb, Pax4*) or stretching along most of the length of the transcript (e.g. *Ins I*, *Ins II*, *Nyp*) (Fig: 2.5.2.5.1). Primers amplifying 4 different regions along the length of the *beta-actin* transcript were evaluated. All primers used in this study are listed in the Table 2.5.2.5.2.

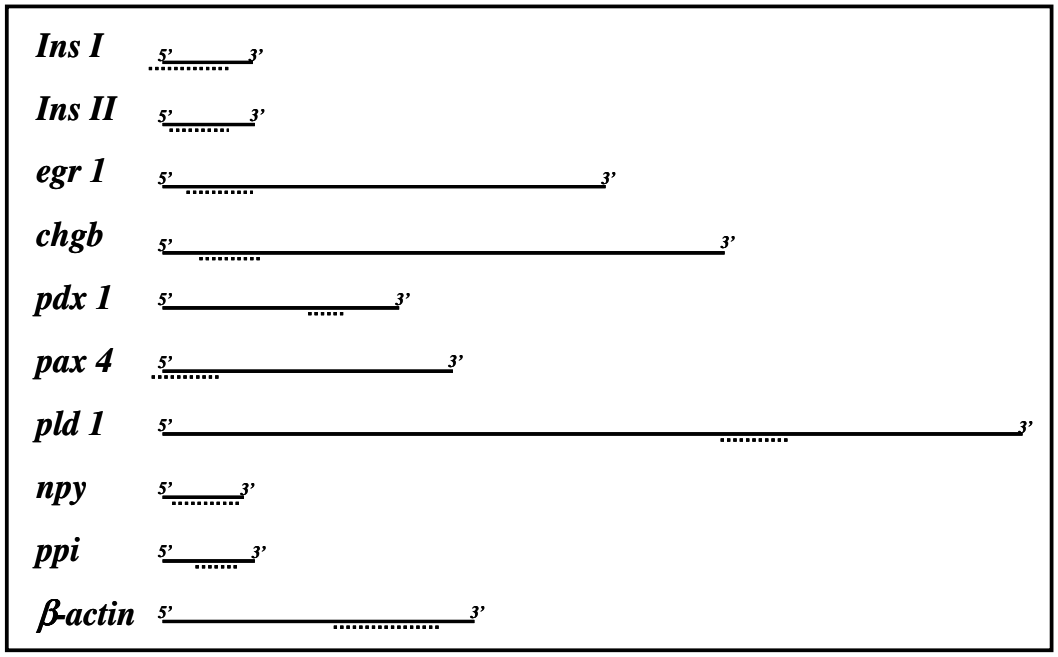


**Fig: 2.5.2.5.1 Location of regions selected for amplification. 5', central or 3' location of the regions selected for the amplification (……) along the coding regions (_____) of transcript analysed.**

| Gene | Sequence (5' to 3') | Annealing Temp.(°C) | RNA Fragment Size (bp) | DNA Fragment Size (bp) | Ref Seq. | Gene ID |
|---|---|---|---|---|---|---|
| *Pdx1* | ggtggagctggcagtgatgtt<br>accgcccccactcggggtcccgc | 60 | 127 | 127 | NM_008814 | 18609 |
| *Gck* | gatgctggatgacagagccaggatg<br>agatgcactcagagatgtagtcga | 54 | 392 | 30,892 | NM_010292 | 103988 |
| *Pax 4* | tggcttcctgtccttctgtgagg<br>tccaagacacctgtgcggtagtag | 52 | 242 | 883 | NM_011038 | 18506 |
| *Npy* | tgaccctcgctctatctctg<br>aagggtcttcaagccttgtt | 58 | 249 | 5,689 | NM_023456 | 109648 |
| *Egr1* | atggacaactaccccaaact<br>attcagagcgatgtcagaaa | 56 | 240 | 918 | NM_007913 | 13653 |
| *Pld1* | tcttatcccttcctgctacc<br>ccaccttgttgaacacaact | 56 | 250 | 11,039 | NM_008875 | 18805 |
| *Chgb* | atccaagtccagtgttccaa<br>tctcattgcctaccttcgtc | 58 | 227 | 6,011 | NM_007694 | 12653 |
| *Gad1* | aaggatgcaaccagatgtgt<br>ttggcgtagaggtaatcagc | 58 | 205 | 22,694 | NM_008077 | 14415 |
| *PC2* | cacagatgactggttcaaca<br>tcacagttgcagtcatcgta | 56 | 359 | Do not amplify | NM_008792 | 18549 |
| *Ppi* | agcgtggcttcttctacacacc<br>ggtgcagcactgatccaccatg | 54 | 158 | 945 | NM_008386/<br>NM_008387 | 16333/<br>16334 |
| *Ins I* | tagtgaccagctataatcagag<br>acgccaaggtctgaaggtcc | 62 | 288 | 407 | NM_008386 | 16333 |
| *Ins II* | ccctgctggccctgctctt<br>aggtctgaaggtcacctgct | 62 | 212 | 701 | NM_008387 | 16334 |
| *beta-actin* | acggccaggtcatcactattg<br>caagaaggaaggctggaaaaga | 60 | 70 | 603 | NM_007393 | 11461 |

**Table: 2.5.2.5.2 Oligonucleotide primers used in RT-PCR analyses showing Gene symbol, nucleotide sequence, annealing temperature, RNA fragment size, Ref Seq. ID and gene ID** .

### 2.5.3 Quantitative real time RT-PCR (qRT-PCR)

TaqMan probes are oligonucleotides that have fluorescent reporter dyes attached to the 5' end and a quencher moiety coupled to the 3' end. These probes are designed to hybridize to an internal region of a PCR product. In the unhybridized state, the proximity of the fluor and the quench molecules prevents the detection of fluorescent signal from the probe. During PCR, when the polymerase replicates a template on which a TaqMan probe is bound, the 5'- nuclease activity of the polymerase cleaves the probe. This decouples the fluorescent dye thus, increasing the fluorescence in each cycle, proportional to the amount of probe cleavage.

#### 2.5.3.1 TaqMan® Real time PCR

RNA was isolated (See Section: 2.5.1.2.3) and cDNA synthesised as per Section 2.5.2.1. In order to exclude any amplification product derived from genomic DNA or any other contaminent that could contaminate the RNA preparation, total RNA without reverse transcription was used as a negative control. Water on its own was amplified as a negative control to rule out presence of any contaminating RNA or DNA in it.

**Table: 2.5.3.1.1 qRT-PCR Reaction Mixture**

| Volume | Reagents |
|---|---|
| 6.8 µl | Nuclease-Free water (Ambion, 9930) |
| 10 µl | TaqMan® Fast Universal PCR master mix (2 X) (Applied BioSystems, 4352042) |
| 0.2 µl | AmpErase® Uracil N-glycosylase (UNG) (Applied BioSystems, N8080096) |
| 1 µl | Assay-on-demand |
| 18 µl | Total |

The TaqMan® Real time PCR analysis was preformed using the Applied BioSystems Assays on Demand PCR Kits, using primer probe pairs as outlined in Table 2.5.3.1.2 and Table 2.5.3.1.3.

2 µl of the cDNA was added to the MicoAmp fast optical 96-well reaction plate (Applied BioSystems, 4346906) followed by 18 µl of reaction master mix (Table: 2.5.3.1.1).

**Table: 2.5.3.1.2 qRT-PCR primer and their assay ID used for microarray validation study.**

| Primer Pair | Supplier | Assay ID |
|---|---|---|
| Thioredoxin interacting protein | Applied BioSystems | Mm00452393_m1 |
| Annexin A2 | Applied BioSystems | Mm00500307_m1 |
| Early growth response 1 | Applied BioSystems | Mm00656724_m1 |
| Kruppel-like factor 4 (gut) | Applied BioSystems | Mm00516104_m1 |
| Thioredoxin domain containing 5 | Applied BioSystems | Mm00520294_m1 |
| FBJ osteosarcoma oncogene | Applied BioSystems | Mm00487425_m1 |
| Growth arrest and DNA-damage-inducible 45 gamma | Applied BioSystems | Mm00442225_m1 |
| FBJ osteosarcoma oncogene B | Applied BioSystems | Mm00500401_m1 |
| Proprotein convertase subtilisin/kexin type 9 | Applied BioSystems | Mm00463738_m1 |
| Solute carrier family 38, member 4 | Applied BioSystems | Mm00459056_m1 |
| Dual specificity phosphatase 1 | Applied BioSystems | Mm00457274_g1 |
| Glucagons | Applied BioSystems | Mm00801712_m1 |
| Jun oncogen | Applied BioSystems | Mm00495062_s1 |
| Immediate early response 5 | Applied BioSystems | Mm00494887_s1 |
| SRY-box containing gene 4 | Applied BioSystems | Mm00486317_s1 |
| Mitogen activated protein kinase 3 | Applied BioSystems | Mm00662375_g1 |
| GAPDH | Applied BioSystems | 4352932E |
| Beta-actin | Applied BioSystems | 4352933E |

**Table: 2.5.3.1.3 qRT-PCR primer and their assay ID used for serum study**

| Primer Pair | Supplier | Assay ID |
|---|---|---|
| Thioredoxin interacting protein | Applied BioSystems | Hs00197750_m1 |
| Early growth response 1 | Applied BioSystems | Hs00152928_m1 |
| Chromogranin B | Applied BioSystems | Hs00174956_m1 |
| Pancreatic and duodenal homeobox 1 | Applied BioSystems | Hs00426216_m1 |
| Phospholipase D1 | Applied BioSystems | Hs00160118_m1 |
| Neuropeptide Y | Applied BioSystems | Hs00173470_m1 |
| Insulin | Applied BioSystems | Hs00355773_m1 |
| Pax4 | Applied BioSystems | Mm01159036_m1 |
| Beta-actin | Applied BioSystems | 4352933E |

Note for table 2.5.3.1.2 and 2.5.3.1.3: - Assay suffix "_m1" means that the probe spans an exon-exon junction and will not detect genomic DNA.

Assay suffix "_s1" means that the primers and probes are designed within a single exon, such assays will, by definition detect genomic DNA

Assay suffix "_g1" means that although the assay probe spans an exon-exon junction, the assay may detect genomic DNA if present in the sample.

**Table: 2.5.3.1.4 Thermal cycling conditions used in this study**

| Step | AmpErase UNG Activation | Denature | PCR | |
|---|---|---|---|---|
| | HOLD | HOLD | CYCLE (40 cycles) | |
| | | | Denature | Anneal/Ext |
| **Time** | 2 min | 20 sec | 3 sec | 30 sec |
| **Temp** | 50°C | 95°C | 95°C | 60°C |

## 2.5.4 Large scale plasmid preparation

Luria-Bertani (LB Broth) was prepared as per table 2.5.4 and was autoclaved. An aliquot of 10 mls LB Broth was taken in a 20 ml universal. Carbenicillin was added to this broth at a concentration of 100 µg/ml and inoculated with 10-20 µl of glycerol stock for one unique clone. This was grown for 6-7hrs. in the upright shaker at 37°C at ~300rpm. This was further inoculated into a 1000 ml flask with 400 mls of LB Broth containing carbenicillin antibiotic (100 µg/ml). The culture was incubated at 37°C with vigorous shaking (~300rpm) for ~8hrs. The bacterial cells were then harvested by centrifugation at 6000x g for 15 min at 4°C. Plasmid DNA was then extracted using the QIAGEN ® Endofree Plasmid Purification Kit (Qiagen, 12362). DNA concentration was determined by measuring using NanoDrop at $OD_{260nm}$ (See Section: 2.5.1.4).

**Table: 2.5.4 2X-LB broth (low-salt) media preparation**

| Reagents | Volume |
|---|---|
| Peptone | 20g/L |
| Yeast Extract | 10g/L |
| NaCl | 5g/L |

### 2.5.4.1 Optimising Antibiotic Selection Conditions

To identify the lowest level of puromycin that kills non-transfected cells within approximately 5 days puromycin concentrations were tested from 1-10 µg/ml keeping all other culture conditions same. Cells were plated $2x10^5$ cells per well in a 24-well plate containing 1 ml of culture medium. After 24hrs., 1ml culture medium containing 1-10 µg/ml puromycin were added to the cells. Cells were cultured for 10–14 days, replacing the puromycin-containing medium every 2- 3 days. Plates were examined for viable cells every 2 days. The lowest puromycin concentration that begins to give massive cell death in approximately 3–5 days were identified and used this puromycin concentration to select cells after transfection.

### 2.5.4.2 Optimisation of plasmid transfection protocol

To determine the optimal conditions for plasmid transfection in 24-well plates, an optimisation with GFP plasmid was carried out for MIN6 cell line. Cell suspensions were prepared at $2x10^5$ cells per 500 µl of plating media. Solutions of GFP plasmid at a concentration of 1-5 µg were prepared in optiMEM (Gibco, 31985). Lipofectamine 2000 (3 µl) solutions were prepared in optiMEM and incubated at room temperature for 5 min. After incubation, lipofectamine solution was added to each GFP plasmid concentrations. These solutions were mixed well and incubated for a further 20 min at

room temperature. 100 µl of the plasmid/lipofectamine solutions were added to a 24-well plate. The cell suspensions were added to each plate at a final cell concentration of $2x10^5$ cells per well. The plates were mixed gently and incubated at 37°C for 24hrs. After 24hrs., the transfection mixture was removed from the cells and the plates were fed with fresh medium. After 72hrs. cells were observed under the fluorescent microscope. Those conditions were used that showed more fluorescent cells and few dead floating cells.

**2.5.4.3 Single cell cloning**

For single cell cloning a cell solution of about 1000 cells / ml was prepared. 100 µl of the cell suspension was added to the first row of wells. 100 µl of the culture media was added to the rest of the 96-well plate. Then using the single channel pipettor 40 µl of the cell suspension was transfered from the first row of wells to the second row of wells and mixed by gently pipetting avoiding bubbles. Using the same tip this was repeated down the entire column.

Clones were then chosen by microscopy after 4 to 5 days. Each wells were checked and marked that contained just a single colony. These colonies were then subcultured from the 96-well plates into 24-well plate. Each clone was transferred into a single well in a 24-well plate.

**2.5.5 RNA interference (RNAi)**

RNAi using small interfering RNAs (siRNAs) was carried out to silence specific genes. The siRNAs used were purchased from Ambion Inc. These siRNAs were 21-23 bp in length and were introduced to the cells via reverse transfection with the

transfection agent *Neo*FX (Ambion Inc., 4511) and lipofectamine 2000 (Invitrogen, 11668-027).

#### 2.5.5.1 Transfection optimisation

##### 2.5.5.1.1 24-well plate optimisation using *Neo*FX Transfection Reagent

To determine the optimal conditions for siRNA transfection in 24-well plates, an optimisation with a siRNA for *Gapdh* (Ambion Inc., 4605) was carried out for MIN6 cell line. Cell suspensions were prepared at $2x10^5$ cells per 500 µl of plating media. Solutions of negative control *i.e.* scrambled siRNA and *Gapdh* siRNAs at a final concentration of 50nM were prepared in optiMEM (Gibco, 31985). *Neo*FX solutions at a range of concentrations were prepared in optiMEM and incubated at room temperature for 10 min (Table: 2.5.5.1.1). After incubation, both negative control and *Gapdh* siRNA solution was added to each *Neo*FX concentration. These solutions were mixed well and incubated for a further 10 min at room temperature. 100 µl of the siRNA/*Neo*FX solutions were added to a 24-well plate. The cell suspensions were added to each plate at a final cell concentration of $2x10^5$ cells per well. The plates were mixed gently and incubated at 37°C for 24hrs. After 24hrs., the transfection mixture was removed from the cells and the plates were fed with fresh medium. After 72hrs. cells were removed for protein extraction and western blot analysis was carried out. Optimal conditions for transfection were determined as the combination of conditions that gave the greatest reduction of Gapdh protein as determined by western blotting after *Gapdh* siRNA transfection and the least cell kill in the presence of transfection reagent (Table: 2.5.5.1.4).

**Table: 2.5.5.1.1 Different conditions used for siRNA optimization in 24-well plate**

| Cell No | SiRNA Concentration | Transfecting reagent | Transfection type |
|---|---|---|---|
| 2x $10^5$ | 50nm *Gapdh* | NeoFX 1 and 2 µl | Reverse transfection |
| 2x $10^5$ | 100nm *Gapdh* | NeoFX 1 and 2 µl | Reverse transfection |
| 2x $10^5$ | 50nm *Gapdh* | NeoFX 1 and 2 µl | Direct transfection |
| 2x 105 | 50nm *Gapdh* | Lipofectamine 2000 1, 2 and 4 µl | Reverse transfection |
| 2x $10^5$ | 50nm *Gapdh* | Lipofectamine 2000 1, 2 and 4 µl | Direct transfection |

### 2.5.5.1.2 24-well plate optimisation using *Lipofectamine 2000* Transfection Reagent

To determine the optimal conditions for siRNA transfection in 24-well plates, an optimisation with a siRNA for *Gapdh* (Ambion Inc., 4605) was carried out for each cell line. Cell suspensions were prepared at $2x10^5$ cells per 500 µl of plating media. Solutions of negative control (scrambled siRNA) and *Gapdh* siRNAs at a final concentration of 50nM were prepared in optiMEM (Gibco, 31985) lipofectamine (Invitrogen, 11668-027) solutions range of concentrations were prepared in optiMEM and incubated at room temperature for 5 min. After incubation lipofectamine solution was added to each negative control and *Gapdh* siRNA solution. These solutions were mixed well and incubated for a further 20 min at room temperature. 100 µl of the siRNA/lipofectamine solutions were added to a 24-well plate. The cell suspensions were added to each plate at a final cell concentration of $2x10^5$ cells per well. The

plates were mixed gently and incubated at 37°C for 24hrs. After 24hrs. the transfection mixture was removed from the cells and the plates were fed with fresh medium. After 72hrs. cells were removed for protein extraction and western blot analysis carried out. Optimal conditions for transfection were determined as the combination of conditions that gave the greatest reduction of Gapdh protein as determined by western blotting after *Gapdh* siRNA transfection and the least cell kill in the presence of transfection reagent (Table: 2.5.4.1.4).

#### 2.5.5.1.3 96-well plate optimisation using *Neo*FX Transfection Reagent

In order to determine the optimal conditions for siRNA transfection in 96-well plates, an optimisation with a siRNA for kinesin (Ambion Inc., 16704) was carried out for each cell line. Cell suspensions were prepared at $5x10^3$, $1x10^4$ and $5x10^4$ cells per ml. Solutions of negative control and *kinesin* siRNA at a final concentration of 50nM were prepared in optiMEM (Gibco, 31985).

*Neo*FX solutions at a range of concentrations were prepared in optiMEM in duplicate and incubated at room temperature for 10 min. After incubation, either negative control or kinesin siRNA solution was added to each NeoFX concentration. These solutions were mixed well and incubated for a further 10 min at room temperature (Table: 2.5.5.1.3). 50 µl of the siRNA/NeoFX solutions were added to a 96-well plate. The cell suspensions were added to each plate at a final cell concentration of $5x10^3$, $1x10^4$ and $5x10^4$ cells per well. The plates were mixed gently and incubated at 37°C for 24hrs. After 24hrs, the transfection mixture was removed from the cells and the plates were fed with fresh medium. The plates were assayed for changes in proliferation at 72hrs. using the acid phosphatase assay (See Section: 2.3.3). Optimal conditions for transfection were determined as the combination of conditions that

gave the greatest reduction in cell number after *kinesin* siRNA transfection and the least cell kill in the presence of transfection reagent (Table: 2.5.4.1.4).

**Table: 2.5.5.1.3 Different conditions used for siRNA optimization in 96-well plate**

| Cell No | SiRNA Concentration | Transfecting reagent | Transfection type |
|---|---|---|---|
| $5x10^3$ | 50nm *Kinesin* | NeoFX 0.5, 0.75 and 1µl | Reverse transfection |
| $1x\ 10^4$ | 50nm *Kinesin* | NeoFX 0.5, 0.75 and 1µl | Reverse transfection |
| $5x\ 10^4$ | 50nm *Kinesin* | NeoFX 0.5, 0.75 and 1µl | Reverse transfection |
| $5x10^3$ | 50nm *Kinesin* | Lipofectamine 2000 0.5, 0.75 and 1µl | Reverse transfection |
| $1x\ 10^4$ | 50nm *Kinesin* | Lipofectamine 2000 0.5, 0.75 and 1µl | Reverse transfection |
| $5x\ 10^4$ | 50nm *Kinesin* | Lipofectamine 2000 0.5, 0.75 and 1µl | Reverse transfection |

### 2.5.5.1.4 96-well plate optimisation using *Lipofectamine 2000* Transfection Reagent

In order to determine the optimal conditions for siRNA transfection in 96-well plates, an optimisation with siRNA for *kinesin* (Ambion Inc., 16704) was carried out for each cell line. Cell suspensions were prepared at $5x10^3$, $1x10^4$ and $5x10^4$ cells per ml. Solutions of negative control and *kinesin* siRNA at a final concentration of 50nM were prepared in optiMEM (Gibco, 31985). Lipofectamine 2000 solutions at a range of concentrations were prepared in optiMEM in duplicate and incubated at room

temperature for 5 min. After incubation, either negative control or *kinesin* siRNA solution was added to each Lipofectamine 2000 concentration. These solutions were mixed well and incubated for a further 20 min at room temperature (Table: 2.5.5.1.3). 50 µl of the siRNA/ Lipofectamine 2000 solutions were added to a 96-well plate. The cell suspensions were added to each plate at a final cell concentration of $5x10^3$, $1x10^4$ and $5x10^4$ cells per well. The plates were mixed gently and incubated at 37°C for 24hrs. After 24hrs, the transfection mixture was removed from the cells and the plates were fed with fresh medium. The plates were assayed for changes in proliferation at 72hrs. using the acid phosphatase assay (See Section: 2.3.3). Optimal conditions for transfection were determined as the combination of conditions that gave the greatest reduction in cell number after kinesin siRNA transfection and the least cell kill in the presence of transfection reagent (Table: 2.5.5.1.4).

**Table: 2.5.5.1.4 Optimised conditions for siRNA transfection**

| **Seeding density per well** | **Volume *Lipofectamine2000* per well (µl)** | **Plate type** |
|---|---|---|
| $5x\ 10^4$ | 0.5 µl | 96-well plate |
| $2x\ 10^5$ | 1 µl | 24-well plate |

### 2.5.6 Western Blot analysis

#### 2.5.6.1 Lysis of cell pellet

Stock of lysis buffer was prepared using the reagents as shown in the Table 2.5.6.1.1. Working lysis buffer was prepared fresh every time before use as shown in the table 2.5.6.1.2.

**Table: 2.5.6.1.1 NP40 Lysis Buffer Stock**

| Reagents | Volume |
|---|---|
| 1M Tris pH 7.4 | 2 ml |
| 3M NaCl | 1.66 ml |
| 1M NaF | 5 ml |
| 10% NP40 | 1 ml |
| $H_2O$ | 90.34 ml |
| Total | 100 ml |

**Table: 2.5.6.1.2 Working Lysis Buffer**

| Reagents | Volume |
|---|---|
| 100 mM Sodium Orthovanidate | 10 µl |
| 100 mM PMSF | 10 µl |
| Protease Inhib Cocktail | 40 µl |
| NP40 Lysis Buffer | 940 µl |
| Total | 1000 µl |

After 72hrs. of transfection cells were lysed in the 24-well plate. Prior to lysis, plate was washed twice with cold PBS and drained off of all supernatant. Cold lysis buffer was added to the cells, dropping it evenly over the whole well/plate (20 µl). The cells were scraped from the well and all the lysed/scraped cells gathered in one corner of the well. The solution was pipetted up and down without frothing and placed in a pre-chilled eppendorf tube. The tube was vortexed for 30-60 sec until the solution was homogenised. The tube was placed on ice for 20 min and the tube was centrifuged at maximum in a microfuge for 15 min. The supernatant was transferred to a fresh

chilled eppendorf tube and immediately quantified for the protein (See Section: 2.3.2.3). The samples were prepared with 2-5X loading buffer (Sigma, S-3401) and water was added to make all the samples at the same concentration. Parafilm was wrapped around the lids of the eppendorfs (to avoid evaporation) and the samples were boiled for 3-5 min. If not used immediately the samples were stored at –20$^{o}$C until needed.

### 2.5.6.2 Gel electrophoresis

Proteins for Western blot analysis were separated by SDS-polyacylamide gel electrophoresis (SDS-PAGE). Resolving and stacking gels were prepared as outlined in Table 2.5.6.3.1 and poured into clean 10 cm x 8 cm gel cassettes, separated by 0.75 cm plastic spacers. The plates were cleaned by tap water, followed by UHP. After drying, the plates were wiped down in one direction using tissue paper soaked in 70% Industrial Methylated Spirits (IMS). The spacers and comb used were also cleaned in this way. After these had dried, the resolving gel was poured first and allowed to set for 20 min at room temperature. The stacking gel was then poured and a comb was placed into the stacking gel in order to create wells for sample loading. Once set, the gels could be used immediately or wrapped in wet tissue paper and stored at 4$^{o}$C for 24hrs.

1X running buffer (Table: 2.5.6.2) was added to the running apparatus before samples were loaded. The samples were loaded onto the stacking gels, in equal amounts relative to the protein concentration of the sample. The empty wells were loaded with loading buffer.

**Table: 2.5.6.2 Running Buffer**

| Reagents | Volume |
|---|---|
| Glycine | 14.4 g |
| Tris | 3.03 g |
| SDS | 1g |
| $H_2O$ | 1L |

The samples were loaded including 7 µl of molecular weight colour protein markers (New England Biolabs, P7708S). The gels were run at 200 V, 45 mA for approximately 1.5hrs. When the bromophenol blue dye front was seen to have reached the end of the gels, electrophoresis was stopped.

**2.5.6.3 Western blotting**

Following electrophoresis, the acrylamide gels were equilibrated in transfer buffer (25 mM Tris, 192 mM glycine (Sigma, G-7126) pH 8.3-8.5 without adjusting) for 10 min. Protein in gels were transferred onto nitrocellulose membranes (Boehringer Mannheim, 1722026) by semi-dry electroblotting. Eight sheets of Whatman 3 mm filter paper (Whatman, 1001824) were soaked in transfer buffer and placed on the cathode plate of a semi-dry blotting apparatus (Biorad). Excess air was removed from between the filters by rolling a universal tube over the filter paper. A piece of nitrocellulose membrane, cut to the same size of the gel, was prepared for transfer (soaked in transfer buffer) and placed over the filter paper, making sure there were no air bubbles.

The acrylamide gel was placed over the nitrocellulose membrane and eight more sheets of pre-soaked filter paper were placed on top of the gel. Excess air was again

removed by rolling the universal over the filter paper. The proteins were transferred from the gel to the nitrocellulose at a current of 34 mA at 15V for 24-25 min.

All incubation steps from now on, including the blocking step, were carried out on a revolving apparatus (Stovall, Bellydancer) to ensure even exposure of the blot to all reagents. The nitrocellulose membranes were blocked for 2hrs. at room temperature with fresh 5% non-fat dried milk (Cadburys, Marvel skimmed milk) in Tris-buffered saline (TBS) with 0.5% Tween (Sigma, P-1379). After blocking, the membranes was washed 3 x 5 min using 1X TBS/PBS. The membrane was then incubated with 5 to 10 mls primary antibody (concentration of primary antibody was used as in Table 2.5.6.3.2) for 1hr. The membrane was again washed 3 x 5 min using 1X TBS/PBS. It was then incubated in secondary antibody and the specific conditions for each antibody are outlined in Table 2.5.6.3.3 below. Finally the membrane was washed 3 x 5 min using 1X TBS/PBS. Bound antibody was detected using enhanced chemiluminescence (ECL) (Amersham, RPN2109).

**Table: 2.5.6.3.1 Preparation of electrophoresis gels**

| **Components** | **Resolving gel (7.5%)** | **Resolving gel (12%)** | **Stacking gel** |
|---|---|---|---|
| Acrylamide stock* (Sigma, A3574) | 3.8 mls | 5.25 mls | 0.8 mls |
| Ultra pure water | 8.0 mls | 6.45 mls | 3.6 mls |
| 1.5M-Tris/HCl, pH 8.8 (BioRad, 161-0798) | 3.0 mls | 3.0 mls | - |
| 1.25M-Tris/HCl, pH 6.8 (BioRad, 161-0799) | - | - | 0.5 mls |
| 10% SDS (Sigma, L-4509) | 150 mls | 150 mls | 50 mls |
| 10% Ammonium persulphate (Sigma, A-1433) | 60 mls | 60 mls | 17 mls |
| TEMED (Sigma, T-8133) | 10 mls | 10 mls | 6 mls |

Note: *Acrylamide stock solution consists of 29.1g acrylamide (Sigma, A8887) and 0.9g NN'-methylene bis-acrylamide (Sigma, 7256) dissolved in 60ml UHP water and made up to 100ml final volume. The solution was stored in the dark at $4^{o}$C for up to 1 month. All components were purchased from Sigma, SDS (L-4509), $NH_4$-persulphate (A-1433) and TEMED, N,N,N,N'-tetramethylethylenediamine (T-8133).

**Table 2.5.6.3.2 List of primary antibodies used for western blot analysis**

| Antibody | Dilution/ Concentration | supplier | Cat. No. |
|---|---|---|---|
| Anti-VDUP-1/Txnip (Mouse monoclonal IgG2b) | 10 µg/ml | MBL | K0204-3 |
| Glucagon (Mouse monoclonal IgG2a) | 1/1000 | abcam | ab23468 |
| Pcsk9 (Rabbit polyclonal IgG) | 1 µg/ml | abcam | ab31762 |
| GAPDH (Mouse monoclonal IgG2b) | 1/10000 | abcam | ab9482 |
| α tubulin (Mouse monoclonal IgG1) | 1/5000 | abcam | ab7291 |

**Table 2.5.6.3.3 List of secondary antibodies used for western blot analysis**

| Antibody | Dilution/ Concentration | supplier | Cat. No. |
|---|---|---|---|
| Mouse | 1/1000 | Dako Cytomation | P 0260 |
| Rabbit | 1/1000 | Dako Cytomation | P0448 |

### 2.5.6.4 Enhanced chemiluminescence detection

Protein bands were developed using the Enhanced Chemiluminescence Kit (ECL) (Amersham, RPN2109) according to the manufacturer's instructions. The blot was removed to a darkroom for all subsequent manipulations. A sheet of parafilm was flattened over a smooth surface, e.g. a glass plate, making sure all air bubbles were removed. The membrane was placed on the parafilm, and excess fluid removed. 1.5 mls of ECL detection reagent 1 and 1.5 mls of reagent 2 were mixed and covered over

the membrane. Charges on the parafilm ensured the fluid stayed on the membrane. The reagent was removed after one minute and the membrane covered in cling film. The membrane was exposed to autoradiographic film (Boehringer Mannheim, 1666916) in an autoradiographic cassette for various times, depending on the signal (30 – 15 min). The autoradiographic film was then developed.

The exposed film was developed for 5 min in developer (Kodak, LX24, and diluted 1:6.5 in water). The film was briefly immersed in water and fixed (Kodak, FX-40, diluted 1:5 in water), for 5 min. The film was transferred to water for 5 min and then air-dried.

### 2.5.7 Immunoprecipitation

The cells were washed three times with PBS and suspend in a cold Lysis buffer (Table: 2.5.6.2.2). This was incubated on ice for 30 min and centrifuged at 12,000 x g for 10 min at 4$^{o}$C. The supernatant was then transferred to a fresh eppendorf tube. Primary antibody was added (2 µg / 200 µl of cell extract) to the cell extract. After mixing it by pipetting up and down it was incubated on a revolving apparatus for 30-120 min at 4$^{o}$C. 20 µl of 50% protein A agarose beads resuspended in the cold Lysis buffer was added to the cell extract mix. After mixing, it was incubated with gentle agitation on revolving apparatus for 60 min at 4$^{o}$C. This mixture was then centrifuged at 5000 rpm for 5 min. The beads were washed 3-5 times with the cold Lysis buffer and centrifuged 5000 rpm for 5 min. the beads were resuspended in 20 µl of Laemmli's sample buffer and boiled for 3-5 min, and centrifuged for 5 min. 10 µl of the samples were loaded per lane in a SDS-polyacrylamide gel for electrophoresis (See Section: 2.5.6.3). The protein was then blotted to a nitrocellulose paper (See Section: 2.5.6.4). The membrane was then blocked for 10% skimmed milk (in PBS)

for 1hr at room temperature. The membrane was then washed three times and incubated with primary antibody diluted with PBS, containing 1% skimmed milk as suggested in the table 2.5.6.3.2 for 1hr at room temperature or over night at 4$^{o}$C. The membrane was then washed using PBS for 5 min x 3 times and incubated in secondary antibody diluted with 1% skimmed milk (in PBS) (Table: 2.5.6.3.3) for 1hr at room temperature. The membrane was again washed with PBS (5 min x 3 times) and were developed using the Enhanced Chemiluminescence Kit (See Section: 2.5.6.5).

### 2.5.8 Immunofluorescence

Cells are allowed to adhere to glass slides overnight. The slides where then washed twice for 5 min in PBS and fixed using methnol for 10 min or 4% paraformaldehyde (Sigma, P6148) (45 min at 4$^{o}$C). Samples were blocked in relevant serum overnight and the following morning the serum was removed. The slide was then washed using PBS/PHEM-0.2% Tween at 5 min per wash and the primary antibody was applied (antibodies and dilutions are listed in Table 2.5.8.1). This was incubated overnight at 4$^{o}$C in a moist environment. The following day, the primary antibody was removed and the slides were washed three times in PBS/PHEM-0.2% Tween at 5 min per wash. The fluorescent secondary antibodies (light sensitive) were prepared in the dark room under dim conditions and were coated in foil. The cells were incubated with secondary antibodies (Table: 2.5.8.2) for 60 min in the dark. All work from this point onwards was carried out in the dark to prevent 'quenching' fluorescent signal. After 60 min incubation the antibodies were removed and the slides were washed three times in PBS/PHEM-0.2% Tween. The cells were then counterstained for nuclei with DAPI and mounted using vectashield (4', 6-diamidino-2-phenylindole) (Vector,

H1000) and covered with cover slips (Chance Propper). Slides were examined by Leica TCS AOBS.

**Table 2.5.8.1 List of primary antibodies used for immunofluorescence analysis**

| Antibody | Dilution | supplier | Cat. No. |
|---|---|---|---|
| Insulin + proinsulin | 1/1250 | abcam | ab8304 |
| Glucagon | 1/200 | cell signalling | #2760 |

**Table: 2.5.8.2 List of primary antibodies used for immunofluorescence analysis**

| Antibody | Dilution | supplier | Cat. No. |
|---|---|---|---|
| Alexa Fluor® 488 goat anti-mouse IgG | 1/1000 | Molecular Probes | A21121 |
| Alexa Fluor® 488 goat anti-rabbit IgG | 1/1000 | Molecular Probes | A31566 |

### 2.5.9 Determination of reactive oxygen species (ROS) by fluorescence

For this assay, 1.875 x $10^5$ cells were seeded per well in a 24-well plate and incubated for 48hrs. at 37°C. 2′,7′-dichlorodihydrofluorescein diacetate (DCFHDA) was then added to three of the six wells at a final concentration of 30 mM and incubated for 40 min. The plate was then washed three times with PBS. Fluorescence was then read at 485 nm excitation and 535 nm emissions in a fluorescence plate reader (Synergy HT, Bio-Tek, USA). The wells containing no DCFHDA acted as blanks for each sample. ROS production was expressed as % increase in fluorescence relative to empty

shRNA transfected cells.

DCFHDA is a non-fluorescent compound that easily enters the cell by free diffusion through the plasmatic membrane; once inside the cytoplasm, this compound loses the diacetyl radical by reaction with cellular esterases and remains inside the cell. The resulting product, 2',7'-dichlorodihydrofluorescein (DCFH) is not fluorescent /per se/, but upon reaction with reactive oxygen species (ROS), particularly hydroxyl radical and superoxide, it is converted to the fluorescent compound dichlorofluorescein.

## 2.6 Affymetrix GeneChips®

The microarray gene expression experiments of this study were performed using the GeneChip® Mouse Genome 430 2.0 Array. The GeneChip® Mouse Genome 430A 2.0 Array is a single array representing approximately 34,000 well-characterized mouse genes.

The GeneChip® Mouse Genome 430 2.0 Array is a single array that contains over 45,000 probe sets analyze the expression level of over 39,000 transcripts and variants from over 34,000 well-characterized mouse genes that can be used to explore mechanisms behind biological and disease processes. All probe sets on the GeneChip Mouse Expression Array 430A are represented on the GeneChip Mouse Genome 430 2.0 Array. It provides coverage of well-substantiated genes in the transcribed mouse genome on a single array. This chip leverages the Power of the Probe Set to obtain multiple independent measurements for each transcript, delivering the greatest accuracy and reproducibility of any microarray platform

Sequences used in the design of the array were selected from GenBank®, dbEST, and RefSeq. The sequence clusters were created from the UniGene database (Build 107, June 2002) and then refined by analysis and comparison with the publicly available draft assembly of the mouse genome from the Whitehead Institute Center for Genome Research (MSCG, April 2002). Oligonucleotide probes complementary to each corresponding sequence are synthesized in situ on the array. Eleven pairs of oligonucleotide probes are used to measure the level of transcription of each sequence represented on the GeneChip Mouse Genome 430 2.0 Array.

**Table: 2.6 Equipment and Chemicals required for Microarray experiment**

| Item | Catalogue No. | Supplier |
|---|---|---|
| 20X SSPE | US51214 | CAMBREX |
| Anti-Strep Biotinylated Ab (Goat) | BA-0500 | LABKEM |
| Wheaton 1L Sterile Bottles | 219980 | SHAW SCIENTIFIC |
| (Paul Hennessy) | | |
| Herring Sperm DNA | D1816 | MSC |
| 10% Tween 20 | 28320 | MSC |
| BSA | 15561-020 | BIOSCIENCES |
| R-Phycoerythro Streptavidin | S-866 | BIOSCIENCES |
| GeneChip® | | |
| Mouse Genome 430 2.0 Array | 900496 | AFFYMETRIX |
| Test3 Array | 900341 | AFFYMETRIX |
| One-Cycle Target Labelling Kit | 900493 | AFFYMETRIX |
| Two-Cycle Target Labelling Kit | 900494 | AFFYMETRIX |
| 0.5M EDTA | E7889 | SIGMA |
| MES Free Acid Monohydrate | M5287 | SIGMA |
| MES Sodium Salt | M3058 | SIGMA |
| DMSO | D5879 | SIGMA |
| Goat IgG | I5256 | SIGMA |
| Sodium Hypochlorite | 42,504-4 | SIGMA |
| 20X SSPE | 85637 | SIGMA |

| Item | Catalogue No. | Supplier |
|---|---|---|
| 5M NaCl | 9759 | AMBION |
| 1.5 ml Eppys | 12400 | AMBION |
| 0.5 ml Eppys | 12300 | AMBION |
| RNase Zap | 9780 | AMBION |
| RNA ladder | 7152 | AMBION |
| 0.5M EDTA | 9260G | AMBION |
| RNase-free UHP | 9932 | AMBION |
| 5X Megascript T7 kit | 1334 (or B1334-5) | AMBION |
| RNeasy Mini Kit | 74106 | QIAGEN |
| QIA Shredder | 79656 | QIAGEN |
| Eppendorf Eppy | 0030-120-191 | UNITECH |
| RNA 6000 Nano chip Kit | 5065-4476 | AGILENT |

### 2.6.1 First-Strand cDNA synthesis for hybridisation to Affymetrix array chips

cDNA synthesis was carried out using One-cycle cDNA synthesis kit. Total RNA (1-8 µg) was placed in an RNase-free 0.5 ml microfuge tubes. To each tube following reagents was added (Table: 2.6.1.1)

**Table: 2.6.1.1 First-Strand cDNA Synthesis**

| Reagents | Amount |
|---|---|
| Poly-A RNA Control | 2 µl |
| T7-Oligo (dT) Primer (50 µM) | 2 µl |
| RNA + RNase-free water | 8 µl |

The tube were gently flicked a few times to mix, and then centrifuged briefly to collect the reaction mixture at the bottom of the tube. The reaction mixture was incubated for 10 min at 70°C and then cooled at 4°C for at least 2 min.

The tube was centrifuged briefly to collect the sample at the bottom of the tube. In a separate tube, the First-Strand Master Mix was assembled for all of the RNA samples. The master mix for single reaction was prepared as in Table: 2.6.1.2.

**Table: 2.6.1.2 1st strand master mix**

| Reagents | Amount |
|---|---|
| 5X 1st strand buffer | 4 µl |
| DTT (0.1M) | 2 µl |
| dNTP (10 mM) | 1 µl |
| Total | 7 µl |

A total volume of 7 µl of master mix was added to each RNA/T7-Oligo (dT) Primer mix for a final volume of 19 µl. The tubes were mixed thoroughly by flicking a few times, centrifuged briefly, and immediately placing the tubes at 42°C incubating it for 2 min. To each RNA sample, SuperScript II was added for a final volume of 20 µl.

The samples were mixed thoroughly by flicking and centrifuged briefly. The tubes were incubate for 1hr at 42°C and then cooled for at least 2 min at 4°C.

### 2.6.2 Second-Strand cDNA Synthesis

In a separate tube second-strand master mix was assembled (Table: 2.6.2). To the master mix following reagents were added.

**Table: 2.6.2 Second-strand master mix**

| Reagents | Amount |
|---|---|
| RNase-free Water | 91 µl |
| 5X 2nd Strand Reaction Mix | 30 µl |
| dNTP (10 mM) | 3 µl |
| E. coli DNA ligase | 1 µl |
| E. coli DNA Polymerase | 4 µl |
| RNase H | 1 µl |
| Total Volume | 130 µl |

The tubes were mixed well by gently flicking and centrifuged briefly. To each first-strand synthesis sample, 130 µl of second-strand master mix was added (Table: 2.6.2). The tubes were mixed well by gently flicking, centrifuged briefly and incubated for 2hrs. at $16^0$C. After incubation, 2 µl of T4 DNA Polymerase was added to each sample and incubated for 5 min at 16°C. After incubation with T4 DNA Polymerase, 10 µl of EDTA (0.5M) was added to the sample tube.

### 2.6.3 Cleanup of Double-Stranded cDNA

For cleaning up of synthesized double-stranded cDNA the sample cleanup module was used. cDNA binding buffer (600 µl) was added to the double-stranded cDNA synthesis preparation and mixed by vortexing for 3 sec. The cDNA Cleanup Spin Column sitting in a 2 ml collection tube was taken and to it was added 500 µl of the sample, centrifuged for 1 min at ≥ 8,000 x g (≥ 10,000 rpm) and the flow-through was discarded. The spin column was reloaded with the remaining sample and centrifuged as above discarding the flow-through and Collection Tube. The spin column was transferred into a new 2 ml collection tube. To the column, 750 µl of the cDNA wash buffer was added, centrifuged for 1 min at ≥ 8,000 x g (≥ 10,000 rpm) and flow-through was discarded. The tubes were centrifuged for 5 min at maximum speed with caps opened. The flow-through and collection tube were discarded. Spin column was transferred into a 1.5 ml collection tube. Care was taken to ensure that the cDNA elution buffer was dispensed directly onto the spin column membrane. The tubes were incubated for 1 min at room temperature and centrifuged for 1 min at maximum speed (≤ 25,000 x g) to elute.

### 2.6.4 Synthesis of Biotin-Labeled cRNA

GeneChip IVT Labeling Kit was used for the IVT labeling step for generating biotin-labeled cRNA. About 12 µl of template cDNA was transferred to 0.5 ml RNase-free microfuge tubes. To carry out the IVT reaction all the reagents were added to the cDNA as in the Table 2.6.4.

**Table: 2.6.4 Master Mix of IVT reaction**

| Reagents | Amount |
|---|---|
| RNase-free water | 14 µl |
| 10X IVT labeling buffer | 4 µl |
| IVT labeling NTP mix | 12 µl |
| IVT labeling enzyme mix | 4 µl |

The reagents were carefully mixed and collected at the bottom of the tube by brief microcentrifugation. The reaction tubes are then incubated at 37°C for 16hrs. to maximize the labeled cRNA yield with high-quality array results.

### 2.6.5 Cleanup and Quantification of Biotin-Labelled cRNA

Sample Cleanup Module was used for cleaning up the biotin-labelled cRNA, to remove unincorporated NTPs. this protocol was performed at room temperature. To the labelled cRNA, 60 µl of RNase-free water was added and mixed by vortexing for 3 sec. To the sample was added 350 µl of IVT cRNA binding buffer and mixed by vortexing for 3 sec. A volume of 250 µl ethanol (96-100%) was added to the lysate, and mixed well by pipetting. This sample was then applied (700 µl) to the IVT cRNA cleanup spin column sitting in a 2 ml collection tube. It was then centrifuged for 15 sec at ≥ 8,000 x g (≥ 10,000 rpm) discarding the flow-through and collection tube. The spin column was transferred into a new 2 ml collection tube. Onto the spin column, 500 µl of IVT cRNA wash buffer was added. This column was centrifuged for 15 sec at ≥ 8,000x g (≥ 10,000 rpm) to wash discarding the flow-through. To the spin column, 500 µl of 80% (v/v) ethanol was added and centrifuged for 15 sec at ≥ 8,000x g (≥ 10,000 rpm) discarding the flow-through. The spin column was again

centrifuged for 5 min at maximum speed with open caps to allow the membrane to dry, discarding the flow-through and collection tube. Spin column was transferred into a new 1.5 ml collection tube, and 11 µl of RNase-free water was added directly onto the spin column membrane ensuring that the water was dispensed directly onto the membrane. Tube was centrifuged for 1 min at maximum speed (≤ 25,000 x g) to elute. Further 10 µl of RNase-free water was added directly onto the spin column membrane ensuring that the water was dispensed directly onto the membrane. Tube was again centrifuged for 1 min at maximum speed (≤ 25,000 x g) to elute. The eluted cRNA was diluted 1:100 fold for quantification using Nanodrop. A 1:2 dilution of the cRNA was also analysed on the Bioanalyzer.

### 2.6.6 Fragmentation of the cRNA

Fragmentation of cRNA target was carried out before hybridisation onto GeneChip probe arrays using the sample clean up module. cRNA samples at a final concentration of 0.5 µg/µl was used for fragmentation and incubated at 94°C for 35 min in 5X fragmentation buffer.

### 2.6.7 Hybridisation of cRNA to GeneChips

To each tube of fragmented cRNA (15 µg), 270 µl of hybridization cocktail for single probe array was added. Hybridization cocktail contained following reagents per reaction as shown in Table 2.6.7

**Table: 2.6.7 Hybridization cocktail**

| Reagents | Amount |
|---|---|
| Control Oligonucleotide B2 3 nM | 5 µl |
| 20X Eukaryotic Hybridization controls | 15 µl |
| Herring Sperm DNA (10 mg/mL) | 3 µl |
| BSA (50 mg/ml) | 3 µl |
| 2X Hybridization Buffer | 150 µl |
| DMSO | 30 µl |
| $H_2O$ | 34 µl |
| Total | 270 µl |

The probe array was equilibrated to room temperature immediately before use by leaving it for 30 min for the rubber septa to equilibrate to room temperature preventing cracking and leading to leaks. The arrays were wetted by filling with 200 µl of 1X hybridization buffer and incubating it at 45°C for 10 min at a rotation speed of 60 rpm. The hybridization cocktail was heated to 99°C for 5 min in a heat block and then cooled to 45°C heat block for 5 min. Hybridization cocktail was spinned at maximum speed in a microcentrifuge for 5 min to remove any insoluble material. The buffer solution from the probe array cartridge was removed and filled with 300 µl of the clarified hybridization cocktail, avoiding any insoluble matter at the bottom of the tube. Then probe arrays were loaded in a balanced configuration around the axis set to 45°C, rotated at 60 rpm and hybridized for 16hrs.

### 2.6.8 Probe Array Washing and Staining

After hybridization, the hybridization cocktail was removed from the probe array and the probe array was completely filled with the appropriate volume of Non-Stringent Wash Buffer (Wash Buffer A). The SAPE (Streptavidin Phycoerythrin) stain solution was prepared fresh (Table: 2.6.8.1). This was mixed well and divided into two aliquots of 600 µl per array.

**Table: 2.6.8.1 SAPE (Streptavidin Phycoerythrin) stain solution**

| Reagents | Amount |
|---|---|
| 2X Stain Buffer | |
| (100 mM MES, 1M [Na+], 0.05% Tween-20) | 600 µl |
| BSA (50 mg/ml) | 48 µl |
| Streptavidin Phycoerythrin (SAPE; 1 mg/ml) | 12.0 µl |
| Deionised (DI) $H_20$ | 540 µl |
| Total volume | 1200 µl |

Antibody solution mix was prepared as follows (Table: 2.6.8.2):

**Table: 2.6.8.2 Antibody solution**

| Reagents | Amount |
|---|---|
| 2X Stain Buffer | 300µl |
| BSA | 24 µl |
| Goat IgG Stock (10 mg/ml) | 6 µl |
| Biotinylated antibody (0.5 mg/ml) | 3.6 µl |
| DI $H_20$ | 266.4 µl |
| Total volume | 600 µl |

The Affymetrix GeneChip® Operating Software (GCOS) manages the fluidics protocol. The Fluidics Station was prepared by running a priming protocol, which ensures that the lines of the fluidics station are filled with the appropriate buffers and the fluidics station is ready for running. From the Protocol drop-down list, Prime_450 was chosen and buffer reservoir A was changed to Non-Stringent Wash Buffer, and intake buffer reservoir B to Stringent Wash Buffer and then the protocol was run. When primed, each module was set up with one GeneChip, two vials of SAPE solution and one vial of antibody solution. The antibody amplification for Eukaryotic targets protocol was initiated. The details of the protocol EukGE-WS2v4 has been listed in the following Table 2.6.8.3. This process takes about 75 min to complete.

**Table: 2.6.8.3**

| **Fluidics Protocols** | **EukGE-WS2v4** |
|---|---|
| Post Hyb Wash #1 | 10 cycles of 2 mixes/cycle with Wash Buffer A at 25°C |
| Post Hyb Wash #2 | 4 cycles of 15 mixes/cycle with Wash Buffer B at 50°C |
| Stain | Stain the probe array for 10 min in SAPE solution at 25°C |
| Post Stain Wash | 10 cycles of 4 mixes/cycle with Wash Buffer A at 25°C |
| 2nd Stain | Stain the probe array for 10 min in antibody solution at 25°C |
| 3rd Stain | Stain the probe array for 10 min in SAPE solution at 25°C |
| Final Wash | 15 cycles of 4 mixes/cycle with Wash Buffer A at 30°C. The |
| Hold | Holding temperature is 25°C |

### 2.6.9 Probe Array Scan

After staining and washing, the chips were scanned using an Affymetrix® GeneChip® Scanner 3000. The sample door on the scanner was opened and the probe array was inserted into the holder. The Data was organized by GCOS. It saves images of the scanned probe array in a data file (*.dat). The software derives the *.cel (Cell Intensity File) file from a *.dat file and automatically creates it upon opening a *.dat file. It contains a single intensity value for each probe cell delineated by the grid (calculated by the Cell Analysis algorithm). The Chip File (*.chp) generated from the analysis of a probe array contains qualitative and quantitative analysis for every probe set. Report File (*.rpt) generated by GCOS summarizes the data quality information for a single experiment. The report is generated from the analysis output file (*.chp).

## 2.7 Quality assessment of Affymetrix microarray chips

The quality of the data generated with Affymetrix microarray chips was assessed based on different criteria including the scaling factor, background and noise levels, GAPDH 3'/ 5' ratios and the %Present call.

**Scaling factor:** The scaling factor was the multiplication factor applied to each signal value on an array. A scaling factor of 1.0 indicates that the average array intensity was equal to the target intensity. Scaling factors vary across different samples and so there were no set guidelines for any particular sample type. However, Affymetrix advise that for replicates and comparisons involving a relatively small number of changes, the scaling/normalization factors (calculated by the global method) should be comparable among arrays. Larger discrepancies among scaling/normalization factors (e.g., three-fold or greater) may indicate significant assay variability or sample degradation leading to noisier data.

**Background and noise levels:** Although there are no official guidelines regarding background, Affymetrix has found that typical Average Background values range from 20 to 100 for arrays scanned with the GeneChip® Scanner 3000. Arrays being compared should ideally have comparable background values. A high background implies that impurities, such as cell debris and salts, are binding to the probe array in a non-specific manner, and that these substances are fluorescing at 570nm (the detection wavelength). These non-specific binding causes a low signal-to-noise ratio (SNR), meaning that transcripts present at very low levels in the sample may be incorrectly called as "Absent". High background creates an overall loss of sensitivity in the experiment. The noise is a measure of the pixel-to-pixel variation of probes

cells on a GeneChip array.

**GAPDH 3'/ 5' ratios:** β-actin and GAPDH are used to assess RNA sample and assay quality for the majority of GeneChip® expression arrays. Specifically, the Signal values of the 3' probe sets for β-actin and GAPDH are compared to the Signal values of the corresponding 5' probe sets. The ratio of the 3' probe set to the 5' probe set is generally no more than 3 for the 1-cycle assay. A high 3' to 5' ratio may indicate degraded RNA or inefficient transcription of ds cDNA or biotinylated cRNA. 3' to 5' ratios for internal controls are displayed in the Expression Report (.rpt) file.

**%Present call:** The number of probe sets called "Present" relative to the total number of probe sets on the array is displayed as a percentage in the Expression Report (.rpt) file. Percent present (%P) values depend on multiple factors including cell/tissue type, biological or environmental stimuli, probe array type, and overall quality of RNA. Replicate samples should have similar %P values. Extremely low %P values are a possible indication of poor sample quality.

## 2.8 Microarray Data Normalisation

The purpose of data normalisation is to minimise the effects of experimental and technical variation between microarray experiments so that meaningful biological comparisons can be drawn from the data sets and that real biological changes can be identified in microarray experiments. Several approaches have been demonstrated to be effective and beneficial.

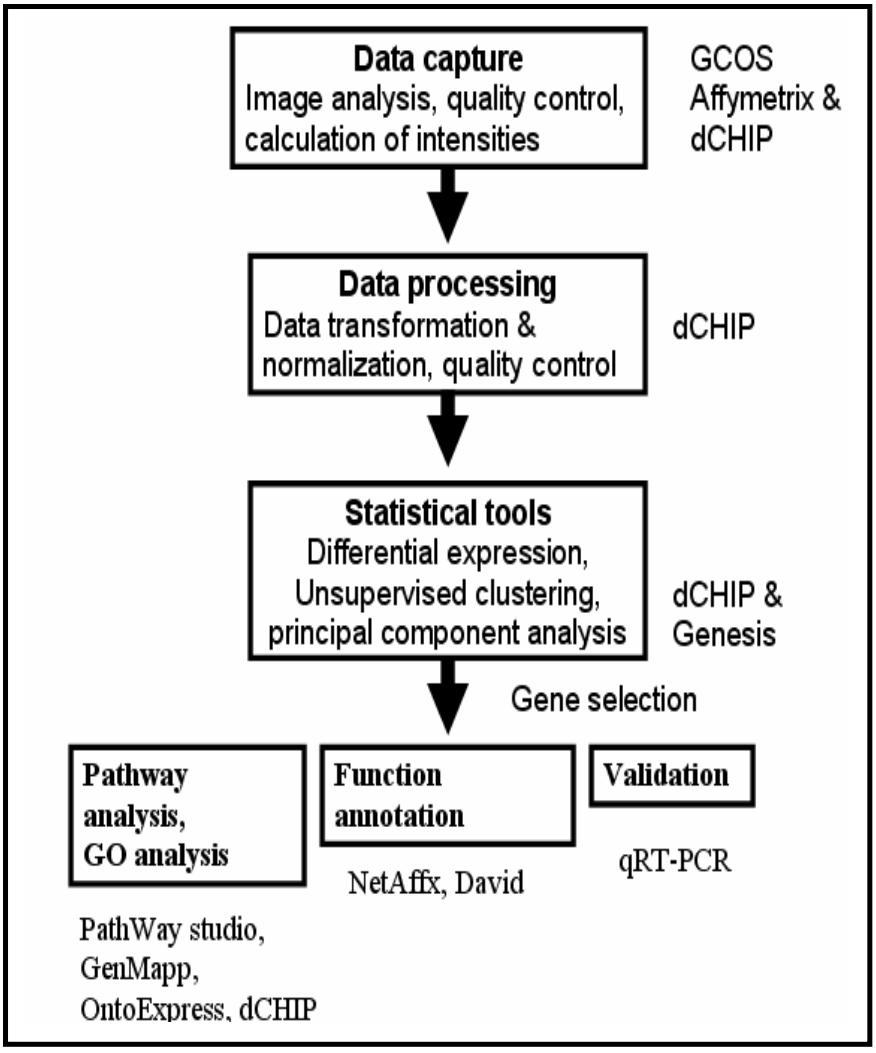


**Fig: 2.8 Flow chart showing expression analysis and interpretation of microarray data**

### 2.8.1 Normalization and Quantification using dChip

DNA-Chip Analyzer (dChip) is a software package implementing model-based expression analysis of oligonucleotide arrays (Li and Wong, 2001) and several high-level analysis procedures. This model-based approach allowed probe-level analysis on multiple arrays. In this normalisation procedure an array with median overall intensity is chosen as the baseline array against which other arrays are normalised at probe level intensity. Subsequently a subset of PM probes, with small within-subset rank difference in the two arrays, serves as the basis for fitting a normalisation curve.

#### 2.8.1.1 Quality inspection

The following Quality Control were taken to estimate the quality of chip

- Median Intensity: Median intensity is the median intensity of the un-normalized probe values.
- P call %: Calls indicate if the transcript is expressed or not. It can be 'P' for present, 'M' for marginally present and 'A' for absent. Total P calls in an array can vary widely based on the different nature of samples.
- % Signal outlier: The signal value greater than $80^{th}$ percentile multiplied by 3 is taken as signal outlier and is represented as % signal outlier.
- % Array outlier: The array-outliers are the arrays whose probe pattern for selected probe set is different from the consensus probe pattern seen in most arrays.
- Warning: If the array outlier increases over 5%, the chip is marked as outlier chip and is marked by '*', indicating potential image contamination or sample hybridization problem of that arrays

Manual inspection: Apart from the above parameters manual inspection was also done to estimate the quality of individual chips. A sample of good and bad quality chip is shown below (Fig 2.8.1.1a and Fig 2.8.1.1b).

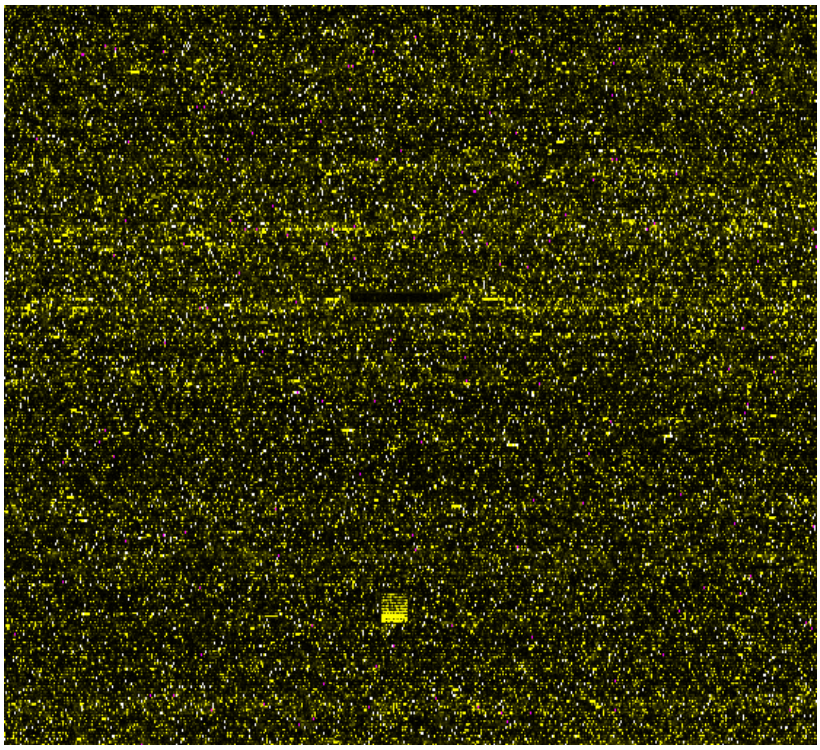

**Fig: 2.8.1.1a An example of a good chip (image simulated by dChip)**

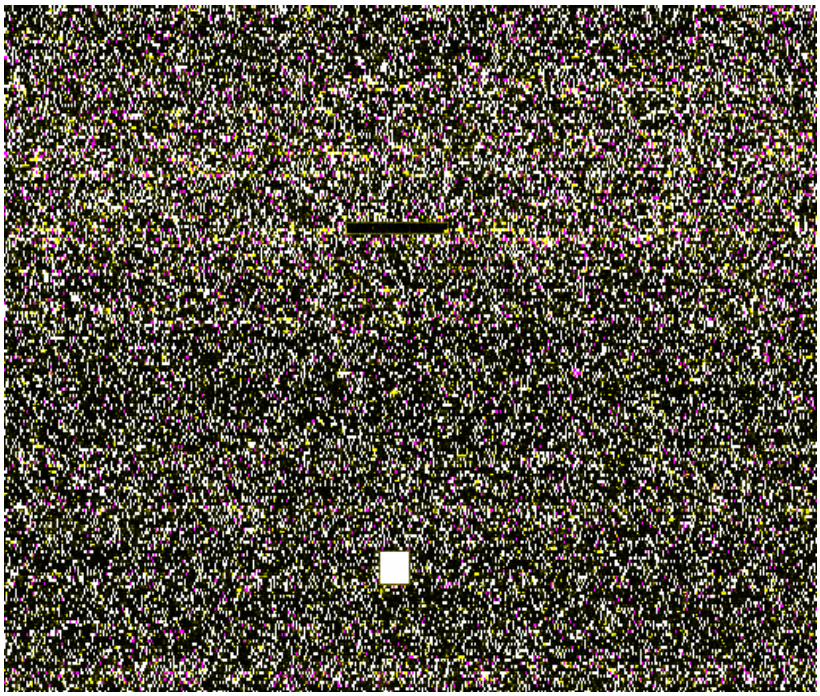

**Fig: 2.8.1.1b A chip with very high background (image simulated by dChip)**

### 2.8.1.2 Hierarchical Clustering

Hierarchical clustering is a mathematical technique whereby the samples/genes are connected iteratively based on their similarity. The sample/genes with similar expression patterns are grouped together and are connected by a series of branches, which is called dendrogram (or clustering tree). Hierarchical clustering was used to see how well the replicates samples cluster, identify any sub-groups in the samples and identify correlated genes.

### 2.8.1.3 Finding significant genes

For most of the places a combination of filtration criteria was used to pick up the differentially-regulated genes. These criteria are discussed below.

**Fold change**

Fold change is the ratio of mean of experimental group to that of baseline. It's a metric to define the gene's mRNA-expression level between two distinct experimental conditions. Fold change of 1.2 and 2 was used for different types of analysis.

**Difference**

The difference of Affymetrix expression units was also taken for finding differentially-regulated genes. Difference of 100 was taken for most of the comparisons.

**t-test:** The t-test assesses whether the means of two groups are statistically different from each other. The output of the t-test is the p-value. The p-value of less than 0.05 was taken as significantly different.

Combination of Fold change ≥1.2, difference≥100 and p-value <0.05 was taken for up-regulated genes. Similarly the combination of Fold change ≤1.2, Difference ≤100 and p-value < 0.05 was taken for down-regulated genes.

### 2.8.2 Microsoft access

This is a database-building package that was used in analysis to compare different gene lists. Access allowed comparison of like genes across multiple lists. It allowed comparison of genes and also relevant information such as probe sets, difference of mean and p-value. Apart from this it was widely used for merging two tables and adding annotation to the genelists.

### 2.8.3 GenMAPP

GenMAPP is a free computer application designed to visualize gene expression and other genomic data on maps representing biological pathways and groupings of genes.

A MAPP is a GenMAPP-produced file format that showed biological relationships between genes or gene products. MAPPs could be used to group genes and view data by any organizing principle. Examples of the types of MAPPs represented in GenMAPP are metabolic pathways, signal transduction cascades, subcellular locations, or gene families. GenMAPP automatically linked each gene on a MAPP to data from gene expression experiments which had been imported. A sample result is shown below.

Integrated with GenMAPP were programs to perform a global analysis of gene expression or genomic data in the context of hundreds of pathway MAPPs and thousands of Gene Ontology Terms. MAPPFinder created a global gene-expression profile across all areas of biology by integrating the annotations of the Gene Ontology (GO) Project with GenMAPP. The results were displayed in a searchable browser, allowing rapid identification of GO terms with over-represented numbers of gene-expression changes. Clicking on GO terms generated GenMAPP graphical files where gene relationships could be explored and annotated. GenMAPP was downloaded from http://www.genmapp.org

**MappFinder:**

MAPPFinder is an accessory program that works with GenMAPP and the annotations from the Gene Ontology (GO) Consortium to identify global biological trends in gene expression data. MAPPFinder relates microarray data meeting a user-defined criterion

for a "significant" change to each term in the Gene Ontology hierarchy, calculating the percentage of genes changed for each GO biological process, cellular component, and molecular function term. MAPPFinder then calculates a cumulative total of genes changed for a parent GO term and all of its children and a statistical score, giving a complete picture of the gene expression changes associated with a particular GO term. Furthermore, this MAPPFinder analysis can be performed on a set of MAPPs local to a user's computer, calculating the percentage of genes meeting the criterion for each MAPP.

The calculations made by MAPPFinder are intended to give you an idea of the relative amount of genes meeting your criterion that are present in each GO term or Local MAPP. The figure below shows a sample line from the MAPPFinder Browser with the different numbers that are calculated. Each number displayed in the MAPPFinder results and the Calculation Summary is defined below.

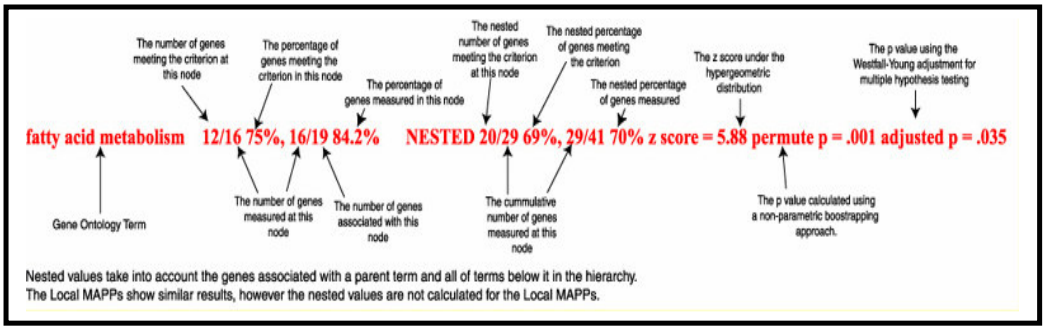


**Genes meeting the criterion**: The number of distinct genes that met the user-defined criterion in the Expression Dataset. This may also be referred to as "genes changed."

**Genes measured:** The number of distinct genes in your Expression Dataset that were found to link to this GO term or MAPP.

**Genes associated with this GO term or MAPP**: The number of genes assigned to this GO term or on this MAPP. Also referred to as the number of "Genes in GO" for a specific term.

**% genes meeting the criterion**: Genes meeting the criterion/genes measured * 100

**% genes measured:** genes measured/genes associated * 100

**Nested numbers**: The same 5 calculations are repeated, but as nested numbers. The GO is arranged in a hierarchy, with child terms having a "is a" or "part of" relationship with the parent. As a result, in order to get the full number of genes associated with a particular node, it calculates the number of genes in the parent node along with its children, grandchildren, etc. MAPPFinder traverses the tree for each node to calculate the cumulative, or "nested", number of genes at that node. As genes are typically assigned to the most specific category possible, the nested numbers give a more accurate representation of the number of genes involved in any biological process, cellular component, or molecular function.

**Z score:** A positive Z score indicates that there are more genes meeting the criterion in a GO term/MAPP than would be expected by random chance. A negative Z score indicates that the there are fewer genes meeting the criterion than would be expected by random chance. A Z score or 1.96 or -1.96 would correlate with a p-value of 0.05.

**Permute P and Adjusted P:** Based on the Z-score permute P and adjusted P values are calculated.

The results of MAPPFinder analysis are both exported as a text file and displayed in a searchable MAPPFinder Browser, allowing the user to quickly identify those areas of biology that show correlated gene expression changes. Clicking on a GO term in the

MAPPFinder Browser window opens a MAPP in GenMAPP that lists all the genes associated with that GO term so that the user can view the individual genes. MAPPFinder creates a gene expression profile across all areas of biology represented in the GO, allowing the user to view at a glance where the largest correlated gene expression changes are occurring in the data. A sample result file is shown below.

### 2.8.4 Onto-Express

Intelligent Systems and Bioinformatics Laboratory, Computer Science Department, Wayne State University developed Onto-Express (OE) as a novel tool able to automatically translate lists of gene transcripts from microarray experiments of differentially-regulated gene transcripts into functional profiles characterising the impact of the condition studied. The software is freely available to academic users from http://vortex.cs.wayne.edu:8080/ontoexpress/servlet/UserInfo. OE constructs functional profiles (using Gene Ontology terms) for the categories: biochemical function, biological process, cellular role, cellular component, molecular function and chromosome location. Statistical significance values are calculated for each category (Draghici *et al*., 2003; Khatri *et al.*, 2005).

#### 2.8.4.1 Pathway-Express

Pathway-Express (PE) is a new tool in the Onto-Tools ensemble (http://vortex.cs.wayne.edu/ontoexpress/servlet/UserInfo). The Pathway-Express works on a list of genes and the system performs a search and builds a list of all associated pathways. After generating a list of pathways for the input list of genes from the Onto-Tools database, PE first calculates a perturbation factor PF (g) for each input gene. This perturbation factor takes into account the (i) normalized fold change

of the gene and (ii) the number and amount of perturbation of genes downstream from it. This gene perturbation factor reflects the relative importance of each differentially-regulated gene. The impact factor of the entire pathway includes a probabilistic term that takes into consideration the proportion of differentially regulated genes on the pathway and gene perturbation factors of all genes in the pathway. The impact factors of all pathways are used to rank the pathways before presenting them to the user (Khatri *et al*., 2005).

### 2.8.5 DAVID

Gene and protein identifiers are not mutually mapped to each other and could be obtained from three independent resources, NCBI, PIR and UniProt. DAVID is the freely available software and has a maximally integrated DAVID Knowledgebase that is useful for converting gene/protein identifiers from one type to another (Huang *et al*., 2007). The probe set ID from microarray study and the protein ID was converted into entrez ID using DAVID to compare the differentially-regulated genes. (http://david.abcc.ncifcrf.gov/).

### 2.8.6 MedScan

Pathway Studio text-mining functions are powered by MedScan text-to-knowledge technology. MedScan helps in mining current literature and helps in building pathways related to the topic of interest, such as disease, phenotype, or physiological process. With the Update Pathway tool, the software downloads all PubMed abstracts since the last update, extract relations from them, and add them to the selected pathway.

### 2.8.7 Statistical analyses

Student's t test, mean and standard deviation was performed using excel.

The correlation between two variables reflects the degree to which the variables are related. The most common measure of correlation is the Pearson Product Moment Correlation (or called Pearson's correlation). A correlation is a number between -1 and +1 that measures the degree of association between two variables.

Homeostasis Model Assessment (HOMA) estimates steady state beta cell function (%B) and insulin sensitivity (%S), as percentages of a normal reference population. HOMA %B and HOMA %S was calculated using HOMA Calculator v2.2.2 that can be downloaded from this site http://www.dtu.ox.ac.uk/index.php?maindoc=/ukpds/

# Section 3.0 RESULTS

### 3.1 Phenotypic changes occurring in cultured cells

#### 3.1.1 Phenotypic changes occurring in cultured MIN6 B1 cells

Continuous culture of MIN6 B1 cells results in many phenotypic changes. The most notable change of MIN6 B1 is in its morphology and growth patterns. Morphological analysis, using phase contrast light microscopy, indicated that MIN6 B1 cells grow as tight, rounded, localised clumps at low passages (MIN6 B1(GSIS), passage 19). MIN6 B1(GSIS) does not tend to form a monolayer over the tissue culture surface as seen in Fig: 3.1.1 (A). As the cells grow towards high passages (MIN6 B1(Non-GSIS), passage 23), the cells no longer tend to be associated in clumps and are found to form a monolayer of "flat", stretched, cells (Fig: 3.1.1 (B)).

**MIN6 B1 p 19 (low passage)** **MIN6 B1 p 23 (high passage)**

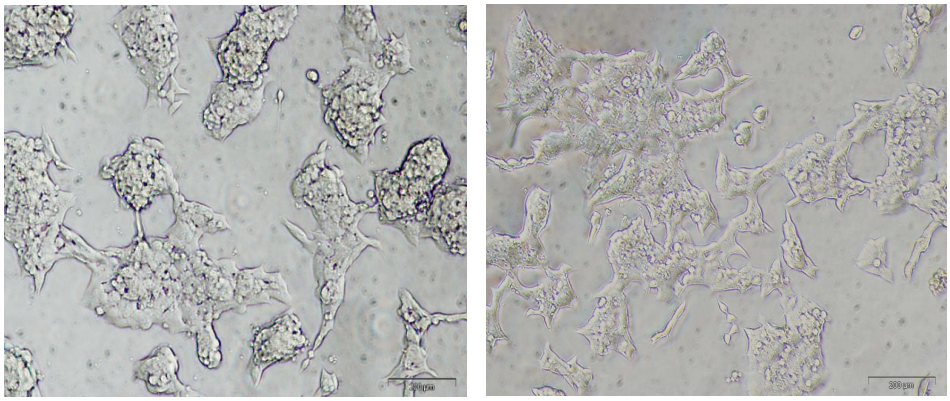

**A** **B**

**Fig: 3.1.1 MIN6 B1 cells seen as grown in T75cm$^2$ vented flask, cultured from low passage (p 19) to high passage (p 23) and were photographed through a microscope, using phase-contrast. (Magnification = 20X; scale bar = 200 µM)**

### 3.1.2 Phenotypic changes occurring in cultured MIN6 (heterogeneous) cells

Continuous culture of MIN6 cells results in many phenotypic changes, including in its morphology and growth patterns. Morphological analysis, using phase contrast light microscopy, has shown a notable deviation between MIN6 cells grown at low (MIN6 (L)) versus high passage (MIN6 (H)). MIN6 (L) cells grow as tight, rounded, localised clumps and do not form a monolayer over the tissue culture surface (Fig: 3.1.2 (A)). Whereas, MIN6 (H) cells no longer tend to be associated in clumps and are found to form a monolayer of "flat", stretched, cells (Fig: 3.1.2 (B)).

**MIN6 p 16** **MIN6 p 40**

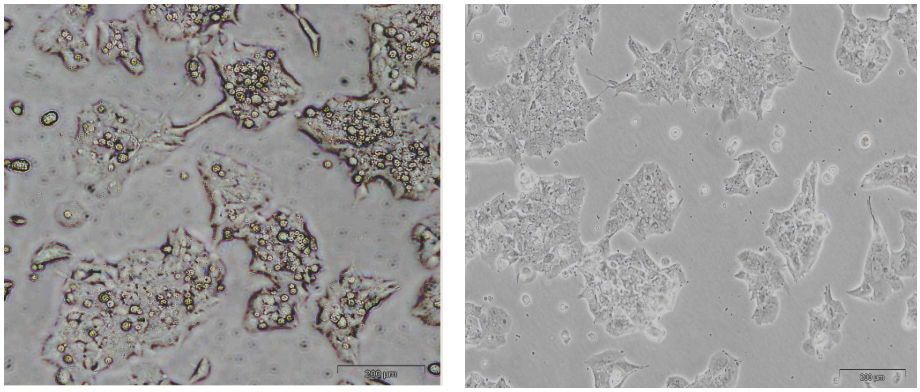

**A** **B**

**Fig: 3.1.2 MIN6 cells seen as grown in T75cm$^2$ vented flask, cultured from low passage (p 16) to high passage (p 40) and were photographed through a microscope, using phase-contrast. (Magnification = 20X; scale bar = 200 µM)**

### 3.2 Results from Measurement of Cellular Proliferation

#### 3.2.1 Proliferation Assay on MIN6 B1 cell line

Continuous sub-culturing of homogenous clonal population of the murine pancreatic beta cell line MIN6 B1 resulted in an increase in proliferation rate. Growth curves were plotted over 7 days following seeding at a density of 5 X $10^4$ cells/well (24-well plate). An increased proliferation rate was observed as MIN6 B1 cells, as they were passaged from low (p 19) to high (p 23) passage. MIN6 B1(Non-GSIS) showed significantly increased (p-value=0.02 at 168hrs. time point) proliferation compared to that of MIN6 B1(GSIS) cells (approximately 2-fold) (Fig: 3.2.1).

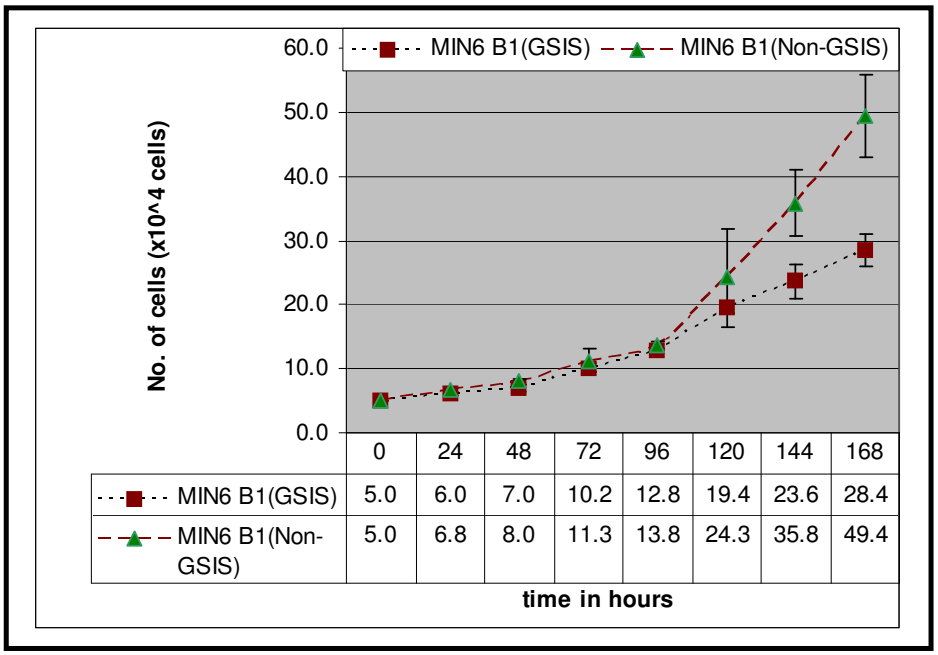


| | 0 | 24 | 48 | 72 | 96 | 120 | 144 | 168 |
|---|---|---|---|---|---|---|---|---|
| MIN6 B1(GSIS) | 5.0 | 6.0 | 7.0 | 10.2 | 12.8 | 19.4 | 23.6 | 28.4 |
| MIN6 B1(Non-GSIS) | 5.0 | 6.8 | 8.0 | 11.3 | 13.8 | 24.3 | 35.8 | 49.4 |

**Fig: 3.2.1 Graph showing comparison of proliferation assay done on MIN6 B1 low and high passage cells. MIN6 B1 high passage cells (p 23) are shown as ( —▲— ) and low passage cells (p 19) are shown as ( - ■ - ).Mean = ± S.D and n=3.**

### 3.2.2 Proliferation Assay on MIN6 cells

Continuous culture of MIN6 cells results in phenotypic changes, most notably deviation from characteristic MIN6 morphology and growth patterns. Continuous sub-culturing resulted in an increase in proliferation rate. Growth curves, plotted over 7 days, following seeding at a density of 5 x$10^4$ cells/well (24-well plate), indicated that the rate of proliferation in the high passage cells was approximately 2.4-fold greater than that observed in the low passage cells (Fig: 3.2.2). Proliferation of MIN6 cells was carried out at passage 18 for low passage and at passage 40 for high passage cells.

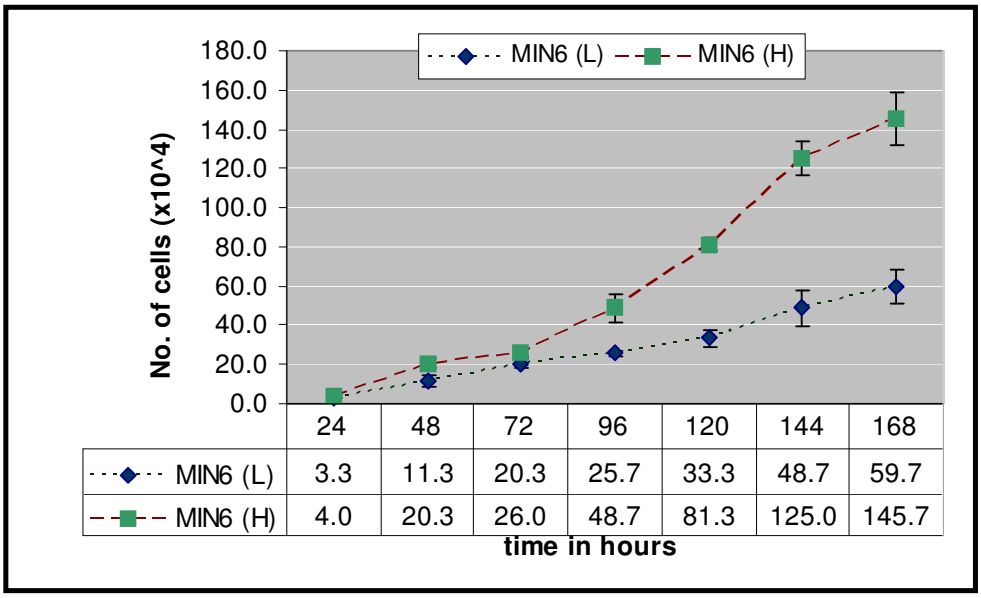


| | 24 | 48 | 72 | 96 | 120 | 144 | 168 |
|---|---|---|---|---|---|---|---|
| MIN6 (L) | 3.3 | 11.3 | 20.3 | 25.7 | 33.3 | 48.7 | 59.7 |
| MIN6 (H) | 4.0 | 20.3 | 26.0 | 48.7 | 81.3 | 125.0 | 145.7 |

**Fig: 3.2.2 Graph showing comparison of proliferation assay done on MIN6 low (L) and high (H) passage cells. MIN6 (H) (p 40) are shown as ( — ■ — ) and MIN6 (L) (p 18) are shown as ( - -◆- - ). Mean = ± S.D and n=3.**

### 3.3 Glucose-Stimulated Insulin Secretion (GSIS)

#### 3.3.1 Glucose-Stimulated Insulin Secretion in MIN6 B1

The MIN6 B1 cell line is described in the literature as a good model for insulin-producing pancreatic beta cells (Lilla *et al*., 2003). MIN6 B1 cell lines have been shown to secrete insulin in response to elevated extracellular glucose concentrations and retain their differentiated phenotypes in short-term culture. However, when passaged repeatedly, we observed that they start losing their function of glucose responsiveness. So in order to determine the passage at which the glucose-stimulated insulin secretion (GSIS) was lost, GSIS assays were performed at alternate passage as the cells were grown from lower (passage 17) to higher passage (passage 27). GSIS assays, commencing at passage 17, were done at alternate passage to subsequently identify gene transcripts associated with the mechanism of loss of glucose response. Cells were seeded in a 24-well plate (cell density of $2 \times 10^5$ cells/well), and grown for 72hrs. Glucose concentration of 3.3mmol/L and 16.7mmol/L were prepared in 1 X KRB. GSIS assay was performed as described in section 2.3.2.1. Conditioned medium was analysed using ELISA at every alternate passages. At passage 17, MIN6 B1 cells showed a 2.9-fold insulin secretion when 3.3mmol/L was compared with 16.7mmol/L glucose (Fig: 3.3.1). However, at passage 21 MIN6 B1 cells started losing their function of GSIS showing 1.2-fold insulin secretion only (Fig: 3.3.1). These cells produced an approximate 2.15-fold GSIS at passage 19; this was reduced to 1.35-fold within 4 passages (passage 23). A significant loss of GSIS (p-value=0.01) was observed in MIN6 B1(Non-GSIS) compared to MIN6 B1(GSIS) just 4 passages apart.

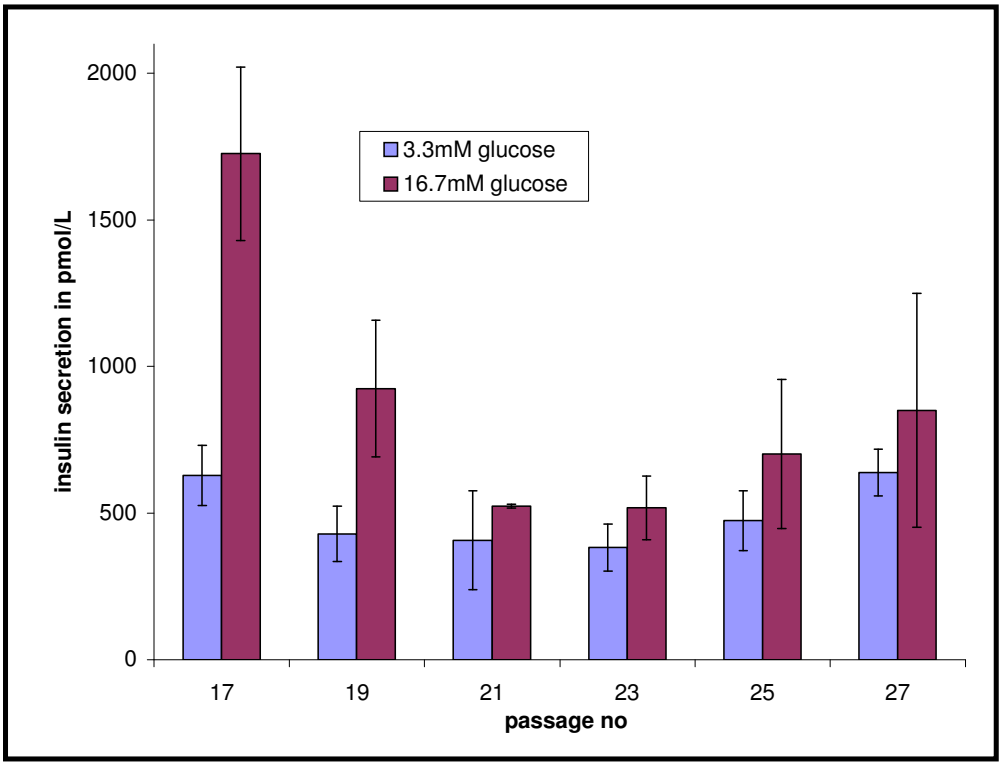


**Fig: 3.3.1 Graph showing GSIS in MIN6 B1 cells using glucose as stimulating agent. GSIS assays were performed at alternate passage numbers between p 17 and p 27 inclusively. Results represent mean of n=3 biological repeats ±SD.**

## 3.4 Analytical Techniques and Assays

### 3.4.1 RNA Quality Analysis by Electrophoresis

As indicated in section 3.3, MIN6 B1 cells were grown from low passage (p 17) to high passage (p 27) and GSIS was performed at every alternate passage. The graph (Fig: 3.3.1) showed a gradual loss of GSIS as the cells were grown from low passage to high passage. To investigate the gene transcript associated with the loss of GSIS, triplicates of p 19 low passage (subsequently termed as MIN6 B1(GSIS)) and p 23 high passage (subsequently termed as MIN6 B1(Non-GSIS)) were selected for microarray experiment. RNA was isolated, using RNeasy kit (See Section: 2.5.1.2.3) from biological triplicate of MIN6 B1(GSIS) (A19, B19 and C19) and MIN6 B1(Non-GSIS) (A23, B23 and C23) cells for microarray hybridization.

The RNA quality was analysed by electrophoresis gel prior to gene expression analysis by microarray experiment (See Section: 2.5.1.5). Total RNA run on a 1% electrophoresis gel showed sharp 28S and 18S rRNA (ribosomal RNA) bands (Fig: 3.4.1.).

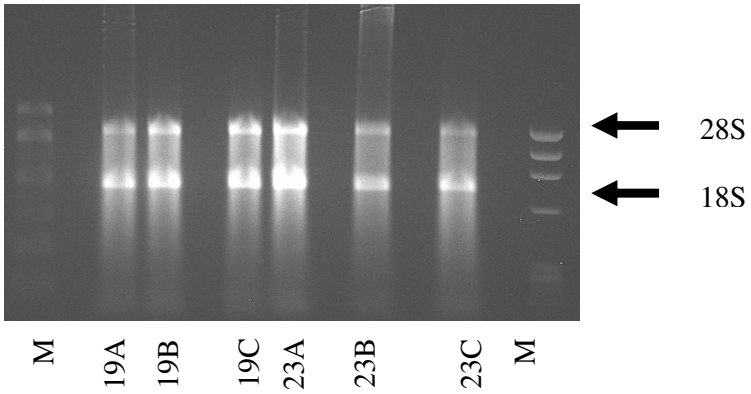


**Fig: 3.4.1 Image typical of total RNA analyzed using 1% agarose gel electrophoresis. M = molecular weight marker: ΦX174 DNA Hae III digest. 19A, 19B and 19C are biological repeats of MIN6 B1(GSIS); 23A, 23B and 23C are biological repeats of MIN6 B1(Non-GSIS).**

### 3.4.2 RNA Quality Analysis by Bioanalyzer

#### 3.4.2.1 Cell RNA quality analysis

RNA quality were also analysed using Bioanalyzer. As described in section 2.5.1.6 the Agilent 2100 Bioanalyzer measures the quantity, integrity and purity of RNAs.

RNA aliquots of each biological triplicate of MIN6 B1(GSIS) (A19, B19 and C19) and MIN6 B1(Non-GSIS) (A23, B23 and C23) were run on an Agilent Bioanalyzer RNA Nano chip to check the RNA integrity. The electropherogram from all triplicate samples of MIN6 B1(GSIS) and MIN6 B1(Non-GSIS) (Fig. 3.4.2.1) shows a typical Bioanalyzer tracing indicating good quality cellular RNA. Integrity of this RNA is measured by 18S and 28S ribosomal bands that

**MIN6 B1(GSIS)** **MIN6 B1(Non-GSIS)**

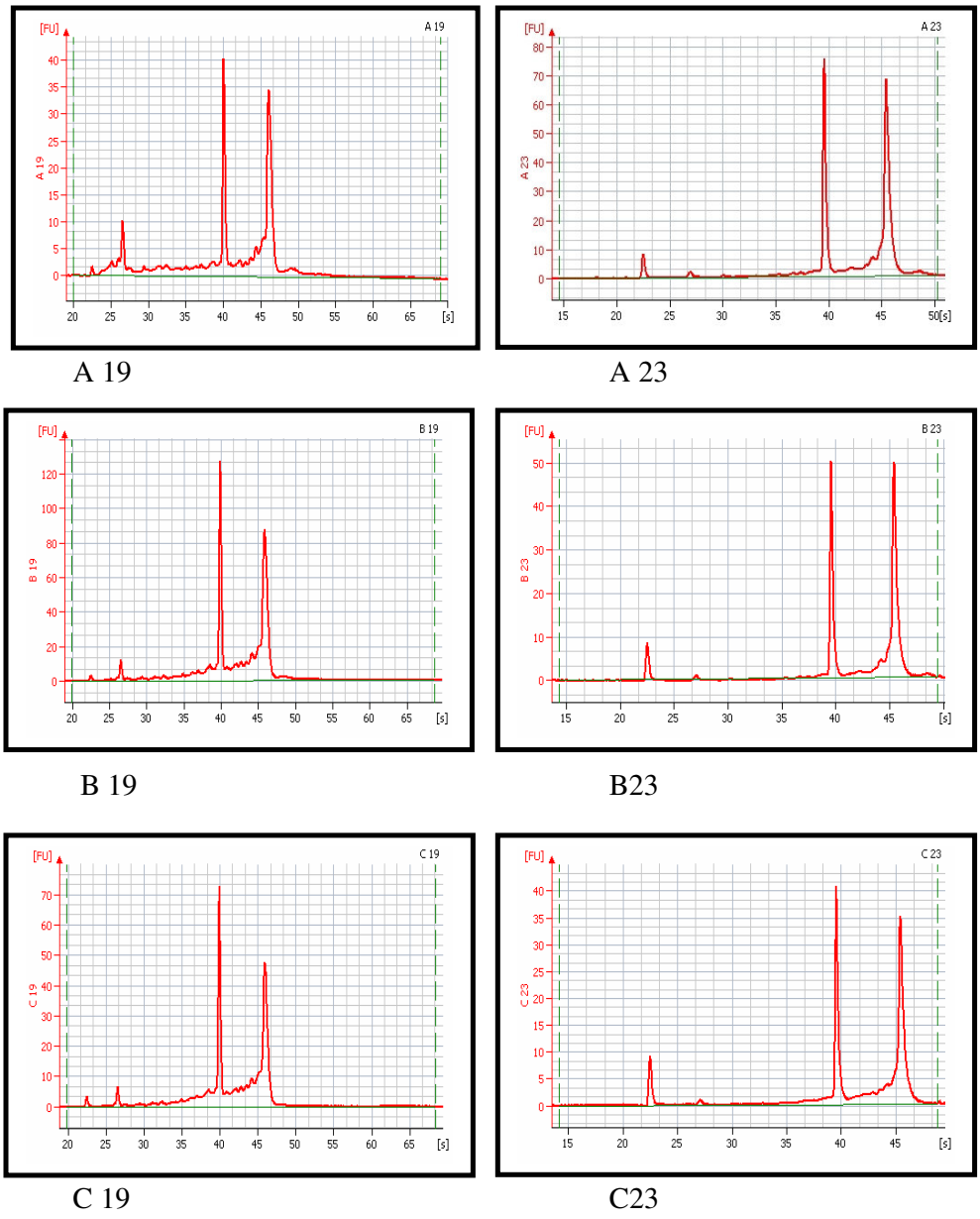


**Fig: 3.4.2.1 Electrophorogram showing first small peak as marker, second peak as 5s RNA, followed by sharp 18S and 28S ribosomal bands. Quality of MIN6 B1 cell RNA was evident by the sharp 18S and 28S ribosomal bands. A19, B19 and C19 are biological triplicate of MIN6 B1(GSIS) whereas A23, B23 and C23 are from MIN6 B1(Non-GSIS) cell RNA.**

appear at 40 and 47 seconds (time is plotted on the X-axis) correlating to 2000 and 4000 nucleotides in length, respectively.

### 3.4.2.2 Fragmented RNA quality analysis

Before hybridization to a microarray chip, the cRNA was fragmented to sizes ranging from 50–200 bases long to improve target specificity (See Section: 2.6.6). A quality check of the fragmented cRNA was performed using Agilent 2100 Bioanalyzer to check that the samples have fragmented as required.

Fragmented cRNA aliquots from each biological triplicate of MIN6 B1(GSIS) (A19, B19 and C19) and MIN6 B1(Non-GSIS) (A23, B23 and C23) were run on an Agilent Bioanalyzer RNA Nano chip to check the cRNA integrity. The electropherogram from all triplicate samples of MIN6 B1(GSIS) and MIN6 B1(Non-GSIS) (Fig. 3.4.2.2) shows the size of cRNA. The fragmentation procedure usually produces a distribution of RNA fragment sizes from approx. 35-200 bases.

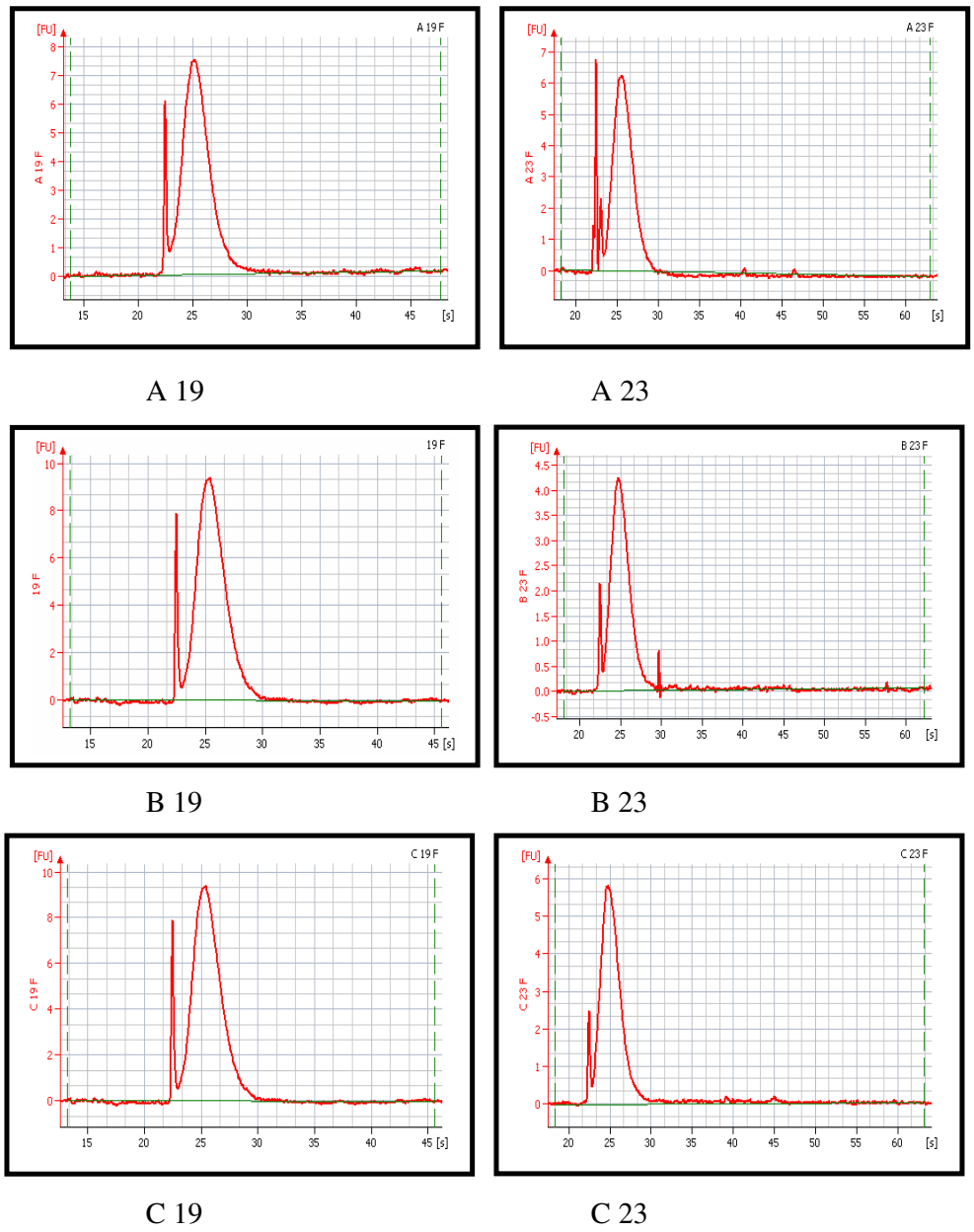


**Fig: 3.4.2.2 Bioanalyzer electropherogram for fragmented labelled cRNA from MIN6 B1 low and high passage cells total RNA. A19, B19 and C19 are biological triplicate of MIN6 B1(GSIS), whereas A23, B23 and C23 are from MIN6 B1(Non-GSIS) fragmented cRNA.**

### 3.4.3 Microarray studies

#### 3.4.3.1 Microarray Q.A results by dChip

The following Quality Control was performed to estimate the quality of data from microarray chip.

- Median Intensity (unnormalised)
- P call %
- % Array outlier
- % Single outlier
- Warning

The sample quality output file is shown in Table: 3.4.3.1.

| Array | Median Intensity (unnormalised) | P call % | % Array outlier | % Single outlier |
|---|---|---|---|---|
| 19-A | 84 | 57.7 | 0.08 | 0.263 |
| 23-A | 70 | 55.1 | 0.142 | 0.229 |
| 19-B | 82 | 57.2 | 0.129 | 0.421 |
| 23-B | 77 | 58.9 | 0.078 | 0.166 |
| 19-C | 73 | 58.3 | 0.106 | 0.19 |
| 23-C | 68 | 57.9 | 0.146 | 0.209 |

**Table: 3.4.3.1 Quality parameters from dChip. 19-A, 19-B and 19-C are biological triplicate of MIN6 B1(GSIS), whereas 23-A, 23-B and 23-C are from MIN6 B1(Non-GSIS).**

**Median intensity:** The median intensity is computed using un-normalized probe values by selecting a probe for every 5 by 5 region on the array. This may give slightly different result from using all probes for computing the median.

**P call:** Calls indicate if the transcript is expressed or not. It can be 'P' for present, 'M' for marginally present and 'A' for absent. Total P calls in an array can vary widely based on the different nature of samples.

**Single outlier:** Single outliers are identified using absolute residuals. The 80th percentile of the absolute residuals of the data points in one array (probe) multiplied by 3 is called the array-wise (probe-wise) residual threshold. If a data point has its absolute residual exceeding both the corresponding array-wise residual threshold and the probe-wise residual threshold, it is called as a single outlier.

**Array outlier:** When fitting the model to a probe set, dChip uses the outlier detection algorithm to detect array-outliers for this probe set. The array-outliers are the arrays whose probe response pattern for this probe set is different from the consensus probe response pattern seen in most arrays. After the model is fitted for all probe sets by "Analysis/Model-based expression", the percentage of probe sets called as array-outlier in one array is reported as "array outlier percentage". If this percentage exceeds 5% in an array, the array is called as an "outlier array". For such "outlier arrays", A "*" is shown in the "Warning" column of "array summary file", and the corresponding array icon in the left pane become dark blue, indicating potential image contamination or sample hybridization problem of these arrays.

### 3.4.3.2 Microarray Q.A results by GCOS

Affymetrix GeneChip Operating Software (GCOS) automates the control of GeneChip® Fluidics Stations and Scanners. GCOS acquires data, manages sample and experimental information. It also performs gene expression data analysis. Table 3.4.3.2 shows the quality parameters as determined by the GCOS software.

| Sample name | Scaling factor | Noise | Background | % Present | 3'/5' Ratio GAPDH |
|---|---|---|---|---|---|
| A19 | 1.00 | 1.25 | 46.5 | 47.1 | 0.93 |
| B19 | 1.00 | 1.27 | 44.37 | 46.2 | 0.94 |
| C19 | 1.00 | 1.20 | 44.58 | 48.2 | 0.85 |
| A23 | 1.00 | 1.16 | 42.44 | 44.7 | 0.87 |
| B23 | 1.00 | 1.20 | 41.07 | 48.7 | 0.87 |
| C23 | 1.00 | 1.16 | 39.95 | 47.8 | 0.90 |

**Table: 3.4.3.2 Quality parameters from Affymetrix GeneChip Operating Software (GCOS). A19, B19 and C19 are biological triplicate of MIN6 B1(GSIS), whereas A23, B23 and C23 are from MIN6 B1(Non-GSIS).**

### 3.4.4 Hierarchical clustering

Only those gene transcript which had a Standard deviation/Mean of less than 0.5 and P calls (P call means transcript present or expressed) in at least 20% of the samples and expression values of minimum 20 in 50% of the samples were selected for Hierarchical clustering. The total number of gene transcripts that passed the above criteria was 214 and was used for hierarchical clustering (Fig: 3.4.4). This stringent criterion was taken as there were very few differentially-regulated genes in this microarray study. The Hierarchical clustering was Average linkage clustering and the distance Metric was Correlation distance.

Sample 23 C did not clustered with its replicates, so this sample was not included for further analysis as it could be a potential outlier. This was also evident from the qRT-PCR data (Fig: 3.4.6.1).

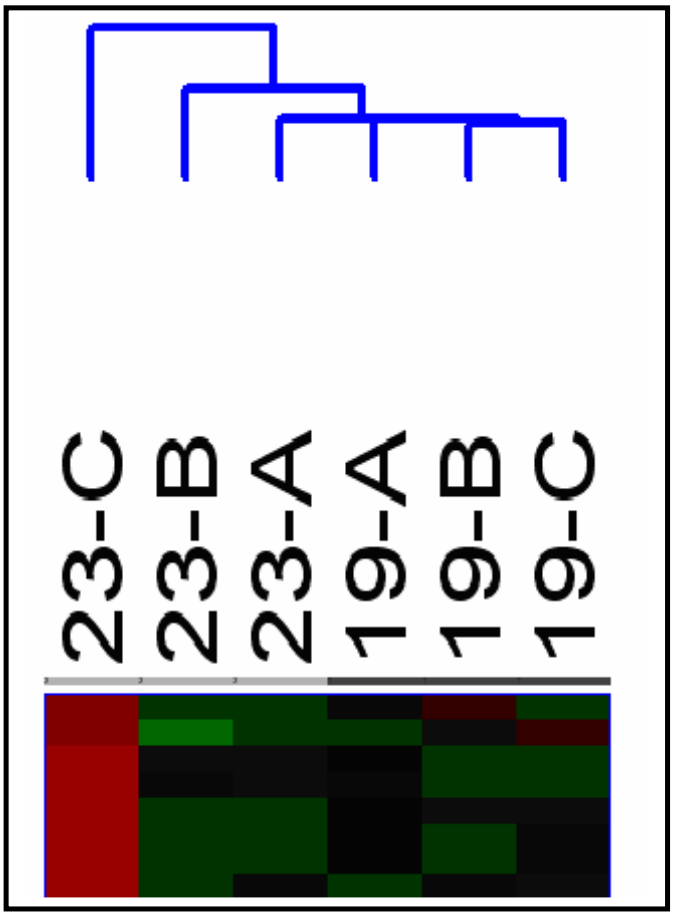


**Fig: 3.4.4 Hierarchical clustering of the MIN6 B1(GSIS) and MIN6 B1(Non-GSIS) cells. 23-A, 23-B and 23-C represents MIN6 B1(Non-GSIS) whereas, 19-A, 19-B and 19-C represents MIN6 B1(GSIS) cells.**

### 3.4.5 Gene lists generated after normalization

As explained gene expression changes associated with the loss of GSIS were investigated using microarray technology. Gene lists were generated after normalizing the data obtained from the microarray study. dChip was used to compare gene expression profiles of MIN6 B1(GSIS) and MIN6 B1(Non-GSIS) samples to identify gene transcripts that were differentially-expressed. In this study, 111 genes were found to be differentially-regulated with 53 genes found to be up-regulated (Table: 3.4.5.1) and 58 genes to be down-regulated (Table: 3.4.5.2) in high passage compared to low passage MIN6 B1 cells. Gene transcripts were considered differentially-expressed if the p-value was less than 0.05, fold change of greater than or equal to 1.2, and difference of greater than 100. Table 3.4.5.1 lists significantly up-regulated gene transcripts with the fold change $\geq$1.2, p-value $<$ 0.05 and difference of $>$100. The Table 3.4.5.2 lists significantly down-regulated gene transcripts with the fold change $\geq$1.2, p-value $<$ 0.05 and difference of $>$100.

| Probe set | Gene | F C | Difference of means | P value |
|---|---|---|---|---|
| 1415997_at | thioredoxin interacting protein | 5.25 | 167.59 | 0.003 |
| 1422134_at | FBJ osteosarcoma oncogene B | 4.63 | 429.35 | 0.013 |
| 1417409_at | Jun oncogene | 2.73 | 1101.34 | 0.045 |
| 1448694_at | Jun oncogene | 2.67 | 485.15 | 0.024 |
| 1417394_at | Kruppel-like factor 4 (gut) | 2.36 | 370.13 | 0.008 |
| 1417395_at | Kruppel-like factor 4 (gut) | 2.25 | 200.1 | 0.004 |
| 1448830_at | dual specificity phosphatase 1 | 2.15 | 933.63 | 0.028 |
| 1423100_at | FBJ osteosarcoma oncogene | 2.12 | 1754.64 | 0.036 |
| 1418025_at | basic helix-loop-helix domain containing, class B2 | 2.04 | 168.67 | 0.014 |
| 1448285_at | regulator of G-protein signaling 4 | 2.02 | 257.74 | 0.015 |
| 1417065_at | early growth response 1 | 1.98 | 1513.88 | 0.034 |
| 1419157_at | SRY-box containing gene 4 | 1.89 | 132.54 | 0.044 |
| 1449556_at | histocompatibility 2, T region locus 23 | 1.82 | 122.18 | 0.021 |
| 1416287_at | regulator of G-protein signaling 4 | 1.75 | 401.72 | 0.007 |
| 1455010_at | RIKEN cDNA 1500012F01 gene | 1.71 | 302.38 | 0.025 |
| 1450376_at | Max interacting protein 1 | 1.7 | 126.34 | 0.038 |
| 1453851_a_at | growth arrest and DNA-damage-inducible 45 gamma | 1.59 | 116.24 | 0.042 |
| 1424880_at | tribbles homolog 1 (Drosophila) | 1.56 | 107.84 | 0.048 |
| 1417612_at | immediate early response 5 | 1.51 | 133.79 | 0.040 |
| 1422825_at | cocaine and amphetamine regulated transcript | 1.48 | 242.39 | 0.003 |
| 1460645_at | cysteine and histidine-rich domain (CHORD)-containing, zinc-binding protein 1 | 1.45 | 148.71 | 0.033 |
| 1416286_at | regulator of G-protein signaling 4 | 1.43 | 599.47 | 0.048 |
| 1417719_at | sin3 associated polypeptide | 1.42 | 136.84 | 0.039 |
| 1418835_at | pleckstrin homology-like domain, family A, member 1 | 1.42 | 210.02 | 0.007 |
| 1449482_at | histone 3, H2ba | 1.42 | 135.06 | 0.018 |
| 1450084_s_at | influenza virus NS1A binding protein | 1.42 | 375.64 | 0.029 |

| | | | | |
|---|---|---|---|---|
| 1416756_at | DnaJ (Hsp40) homolog, subfamily B, member 1 | 1.4 | 112.9 | 0.036 |
| 1423825_at | RIKEN cDNA 5031439A09 gene | 1.38 | 112.54 | 0.040 |
| 1419091_a_at | annexin A2 | 1.37 | 119.33 | 0.036 |
| 1415688_at | ubiquitin-conjugating enzyme E2G 1 (UBC7 homolog, C. elegans) | 1.36 | 197.23 | 0.035 |
| 1433668_at | proline-rich nuclear receptor coactivator 1 | 1.36 | 210.43 | 0.034 |
| 1453481_at | zinc finger, DHHC domain containing 2 | 1.36 | 147.12 | 0.040 |
| 1418191_at | ubiquitin specific peptidase 18 | 1.35 | 122.85 | 0.015 |
| 1437234_x_at | heterogeneous nuclear ribonucleoprotein methyltransferase-like 1 (S. cerevisiae) | 1.35 | 117.92 | 0.036 |
| 1424638_at | Cyclin-dependent kinase inhibitor 1A (P21) | 1.34 | 322.81 | 0.027 |
| 1453326_at | RIKEN cDNA 3300001A09 gene | 1.33 | 346.91 | 0.024 |
| 1425927_a_at | activating transcription factor 5 | 1.31 | 422.03 | 0.049 |
| 1428850_x_at | RIKEN cDNA 2410026K10 gene | 1.29 | 107.59 | 0.027 |
| 1449509_at | small EDRK-rich factor 1 | 1.29 | 108.06 | 0.009 |
| 1420088_at | nuclear factor of kappa light chain gene enhancer in B-cells inhibitor, alpha | 1.28 | 148.62 | 0.037 |
| 1426378_at | eukaryotic translation initiation factor 4B | 1.28 | 161.64 | 0.040 |
| 1419595_a_at | gamma-glutamyl hydrolase | 1.27 | 125.79 | 0.013 |
| 1427060_at | mitogen activated protein kinase 3 | 1.27 | 162.24 | 0.021 |
| 1434642_at | dehydrogenase/reductase (SDR family) member 8 | 1.27 | 186.79 | 0.035 |
| 1416924_at | brain protein I3 | 1.25 | 235.53 | 0.040 |
| 1426547_at | Group specific component | 1.25 | 269.83 | 0.021 |
| 1424233_at | mesenchyme homeobox 2 | 1.23 | 128.32 | 0.048 |
| 1448987_at | acetyl-Coenzyme A dehydrogenase, long-chain | 1.23 | 140.63 | 0.049 |
| 1431665_a_at | translocase of inner mitochondrial membrane 8 homolog b (yeast) | 1.22 | 167.02 | 0.036 |
| 1452655_at | zinc finger, DHHC domain containing 2 | 1.22 | 132.21 | 0.023 |

| | | | | |
|---|---|---|---|---|
| 1432264_x_at | cytochrome c oxidase subunit VIIa polypeptide 2-like | 1.21 | 255.99 | 0.038 |
| 1436915_x_at | lysosomal-associated protein transmembrane 4B | 1.21 | 148.76 | 0.021 |
| 1448493_at | polyadenylate-binding protein-interacting protein 2 | 1.21 | 186.71 | 0.042 |

**Table: 3.4.5.1 Gene transcripts significantly up-regulated in Min6 B1(Non-GSIS) compared to MIN6 B1(GSIS). The list of gene transcripts was sorted by F C (fold change) (1.2-fold or more) in descending order. Identity of columns, from left to right: probe set, name of gene, averaged fold change, difference of means and p-value.**

| Probe set | Gene | Fold change | Difference of means | P-value |
|---|---|---|---|---|
| 1450734_at | leucine zipper transcription regulator 2 | -2.65 | -149.95 | 0.018 |
| 1439618_at | phosphodiesterase 10A | -1.78 | -104.29 | 0.042 |
| 1418890_a_at | RAB3D, member RAS oncogene family | -1.62 | -237.15 | 0.021 |
| 1455643_s_at | expressed sequence | -1.62 | -133.81 | 0.040 |
| 1433502_s_at | expressed sequence | -1.6 | -136.9 | 0.027 |
| 1428154_s_at | phosphatidic acid phosphatase type 2 domain containing 1 | -1.58 | -227.39 | 0.028 |
| 1425952_a_at | Glucagons | -1.55 | -998 | 0.016 |
| 1443609_s_at | synovial apoptosis inhibitor 1, synoviolin | -1.54 | -186.43 | 0.043 |
| 1418891_a_at | RAB3D, member RAS oncogene family | -1.51 | -272.47 | 0.014 |
| 1452830_s_at | carbamoyl-phosphate synthetase 2, aspartate transcarbamylase, and dihydroorotase | -1.5 | -205.35 | 0.016 |
| 1428070_at | synovial apoptosis inhibitor 1, synoviolin | -1.48 | -174.24 | 0.042 |
| 1423914_at | RIKEN cDNA C630004H02 gene | -1.44 | -163.36 | 0.031 |
| 1418141_at | doublecortin | -1.43 | -356.27 | 0.024 |
| 1428111_at | Solute carrier family 38, member 4 | -1.43 | -153.92 | 0.012 |
| 1427294_a_at | RIKEN cDNA 1810073N04 gene | -1.41 | -231.45 | 0.013 |
| 1435247_at | ubiquitin-activating enzyme E1-domain containing 1 | -1.41 | -134.29 | 0.042 |
| 1423730_at | RIKEN cDNA C130052I12 gene | -1.4 | -308.1 | 0.023 |
| 1456397_at | cadherin 4 | -1.4 | -250.13 | 0.021 |
| 1424024_at | multiple coagulation factor deficiency 2 | -1.39 | -266.45 | 0.014 |
| 1434698_at | RIKEN cDNA 9130229H14 gene | -1.37 | -115.47 | 0.028 |
| 1451254_at | inhibitor of kappa light polypeptide enhancer in B-cells, kinase complex-associated protein | -1.37 | -102.19 | 0.017 |
| 1454810_s_at | expressed sequence AI315068 | -1.37 | -106.84 | 0.044 |
| 1428112_at | arginine-rich, mutated in early stage tumours | -1.36 | -768.66 | 0.049 |
| 1448704_s_at | histocompatibility 47 | -1.35 | -394.94 | 0.027 |
| 1427295_at | RIKEN cDNA 1810073N04 gene | -1.34 | -146.01 | 0.023 |

| | | | | |
|---|---|---|---|---|
| 1448411_at | Wolfram syndrome 1 homolog (human) | -1.34 | -125.52 | 0.045 |
| 1451091_at | thioredoxin domain containing 5 | -1.34 | -134.3 | 0.018 |
| 1418139_at | doublecortin | -1.33 | -144.76 | 0.046 |
| 1416949_s_at | solute carrier family 39 (zinc transporter), member 7 | -1.32 | -232.58 | 0.021 |
| 1456175_a_at | coatomer protein complex, subunit beta 2 (beta prime) | -1.32 | -137.06 | 0.048 |
| 1415670_at | coatomer protein complex, subunit gamma | -1.31 | -268.62 | 0.048 |
| 1456393_at | RIKEN cDNA 2310002J21 gene | -1.31 | -430.03 | 0.043 |
| 1440849_at | Adult male medulla oblongata cDNA | -1.3 | -148.01 | 0.031 |
| 1417763_at | Signal sequence receptor, alpha | -1.29 | -336.47 | 0.030 |
| 1418774_a_at | ATPase, Cu++ transporting, alpha polypeptide | -1.29 | -143.63 | 0.038 |
| 1451967_x_at | karyopherin (importin) beta 1 | -1.29 | -153.85 | 0.016 |
| 1417542_at | ribosomal protein S6 kinase, polypeptide 2 | -1.28 | -127.3 | 0.044 |
| 1437620_x_at | Aldehyde dehydrogenase 18 family, member A1 (Aldh18a1), transcript variant 2, mRNA | -1.26 | -155.74 | 0.026 |
| 1438510_a_at | histidyl-tRNA synthetase | -1.26 | -123 | 0.045 |
| 1435050_at | DNA segment, Chr 10, Brigham & Women's Genetics 1379 expressed | -1.26 | -160.6 | 0.045 |
| 1416395_at | guanylate kinase 1 | -1.25 | -129.64 | 0.044 |
| 1455066_s_at | RIKEN cDNA 9130229H14 gene | -1.25 | -292.77 | 0.022 |
| 1417710_at | RIKEN cDNA 0610012D09 gene | -1.24 | -195.99 | 0.046 |
| 1426674_at | eukaryotic translation initiation factor 3, subunit 9 (eta) | -1.24 | -105.26 | 0.027 |
| 1427347_s_at | TUBULIN BETA CHAIN (T BETA-15) | -1.24 | -224.42 | 0.044 |
| 1423670_a_at | signal recognition particle receptor ('docking protein') | -1.23 | -279.61 | 0.012 |
| 1427464_s_at | heat shock 70kD protein 5 (glucose-regulated protein) | -1.23 | -588.19 | 0.012 |
| 1450675_at | stromal membrane-associated protein 1-like | -1.23 | -123.64 | 0.049 |

| | | | | |
|---|---|---|---|---|
| 1451255_at | liver-specific bHLH-Zip transcription factor | -1.23 | -112.78 | 0.044 |
| 1452230_at | RIKEN cDNA 1200006L06 gene | -1.23 | -127.05 | 0.042 |
| 1452767_at | ribosome binding protein 1 | -1.23 | -180.53 | 0.027 |
| 1419287_at | HSPC171 protein | -1.22 | -106.87 | 0.034 |
| 1423030_at | valosin containing protein | -1.22 | -412.44 | 0.035 |
| 1435277_x_at | expressed in non-metastatic cells 1, protein | -1.22 | -222.04 | 0.039 |
| 1438225_x_at | translocating chain-associating membrane protein 1 | -1.22 | -196.84 | 0.037 |
| 1452102_at | coatomer protein complex, subunit beta 2 (beta prime) | -1.22 | -194.57 | 0.031 |
| 1417287_at | histocompatibility 13 | -1.2 | -273.34 | 0.012 |
| 1424255_at | Suppressor of Ty 5 homolog (S. cerevisiae) | -1.2 | -100.82 | 0.037 |

**Table: 3.4.5.2 Gene transcripts significantly down-regulated in MIN6 B1(Non-GSIS) compared to MIN6 B1(GSIS). The list of gene transcripts was sorted by fold change (1.2-fold or more) in descending order. Identity of columns, from left to right: probe set, name of gene, averaged fold change, difference of means and p-value.**

### 3.4.6 Gene Ontology

#### 3.4.6.1 GenMAPP (Gene Microarray Pathway Profiler)

The 111 differentially-regulated genes from the microarray study on MIN6 B1 cells were analysed using freely available software GenMAPP. The gene expression changes associated with a particular GO term was identified by MAPPFinder. MAPPFinder compares the genes that are differentially-regulated to the total number of input genes.

Fig 3.4.6.1.1 shows the percentage of down-regulated genes associated with the following GO categories: protein targeting to ER, endoplasmic reticulum lumen, signal sequence binding, secretory pathway, protein transport, intracellular protein transport, cell adhesion, Miscellaneous and Unknown (Fig: 3.4.6.1.1).

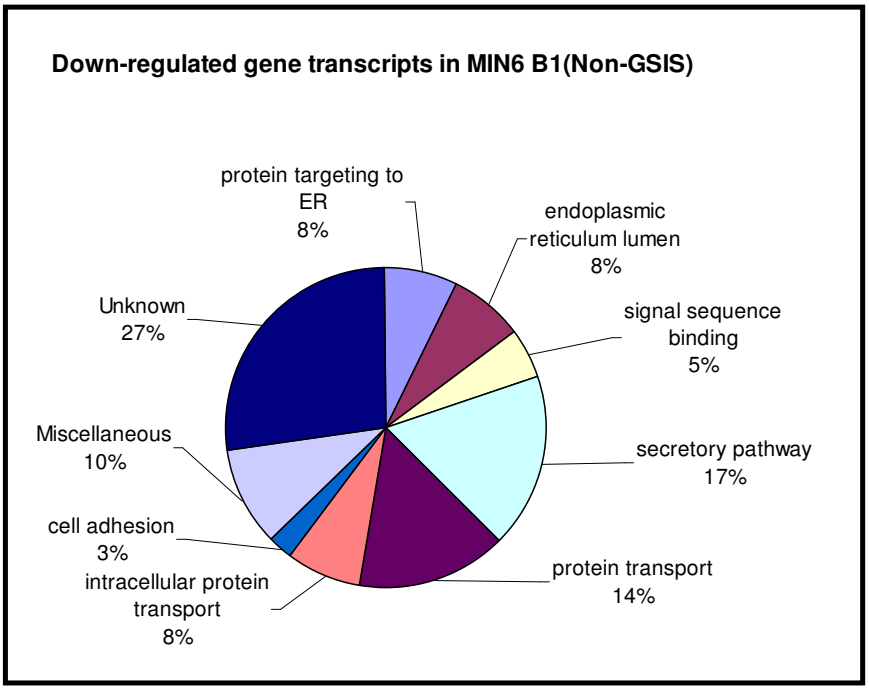


**Fig: 3.4.6.1.1 Representation of down-regulated categories of gene transcripts in MIN6 B1(Non-GSIS) compared to MIN6 B1(GSIS).**

Fig 3.4.6.1.2 shows the percentage of up-regulated genes associated with the following GO categories: transcription factor activity, regulation of protein kinase activity, DNA damage, Response to stress, Oxidoreductase activity, Signal transduction, GTPase activity, Translation, Metabolic, Zinc ion binding, Ubiquitin cycle, Miscellaneous and Unknown (Fig: 3.4.6.1.2). Table 3.4.6.1.3 shows the list of gene transcripts associated with different GO categories.

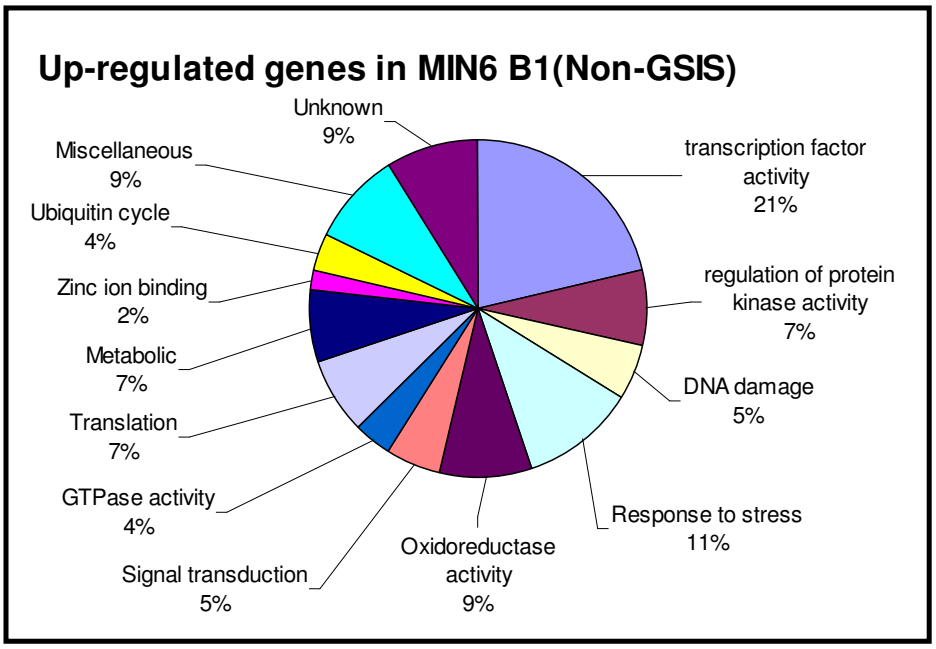


**Fig: 3.4.6.1.2 Representation of up-regulated categories of gene transcripts in MIN6 B1(Non-GSIS) compared to MIN6 B1(GSIS).**

| Gene name | Affy –ID | Gene Symbol | Fold change |
|---|---|---|---|
| **Protein targeting to ER/protein targeting to membrane** | | | |
| Translocating chain-associating membrane protein 1 | 1438225_x_at | Tram1 | -1.22 |
| Signal recognition particle receptor ('docking protein') | 1423670_a_at | Srpr | -1.23 |
| Signal sequence receptor, alpha | 1417763_at | Ssr1 | -1.29 |
| **Endoplasmic reticulum lumen** | | | |
| Heat shock 70kD protein 5 (glucose-regulated protein) | 1427464_s_at | Hspa5 | -1.23 |
| Signal recognition particle receptor ('docking protein') | 1423670_a_at | Srpr | -1.23 |
| Thioredoxin domain containing 5 | 1451091_at | Txndc5 | -1.34 |
| Signal sequence receptor, alpha | 1417763_at | Ssr1 | -1.29 |
| Karyopherin (importin) beta 1 | 1451967_x_at | Kpnb1 | -1.29 |
| **Secretory pathway** | | | |
| Coatomer protein complex, subunit beta 2 (beta prime) | 1452102_at | Copb2 | -1.22 |
| Translocating chain-associating membrane protein 1 | 1438225_x_at | Tram1 | -1.22 |
| Signal recognition particle receptor ('docking protein') | 1423670_a_at | Srpr | -1.23 |
| Signal sequence receptor, alpha | 1417763_at | Ssr1 | -1.29 |
| Multiple coagulation factor deficiency 2 | 1424024_at | Mcfd2 | -1.39 |
| Glucagon | 1425952_a_at | Gcg | -1.55 |
| RAB3D, member RAS oncogene family | 1418891_a_at | Rab3d | -1.62 |
| **Protein transport** | | | |
| Nuclear factor of kappa light chain gene enhancer in B-cells | 1420088_at | Nfkbia | 1.28 |
| Translocase of inner mitochondrial membrane 8 homolog b (yeast) | 1431665_a_at | Timm8b | 1.22 |
| Ribosome binding protein 1 | 1452767_at | Rrbp1 | -1.23 |
| Guanylate kinase 1 | 1416395_at | Guk1 | -1.25 |
| Histocompatibility 47 | 1448704_s_at | H47 | -1.35 |

| | | | |
|---|---|---|---|
| **Intracellular protein transport** | | | |
| Coatomer protein complex, subunit beta 2 (beta prime) | 1456175_a_at | Copb2 | -1.22 |
| Signal recognition particle receptor ('docking protein') | 1423670_a_at | Srpr | -1.23 |
| Coatomer protein complex, subunit gamma | 1415670_at | Copg | -1.31 |
| **Response to unfolded protein** | | | |
| DnaJ (Hsp40) homolog, subfamily B, member 1 | 1416756_at | Dnajb1 | 1.4 |
| Valosin containing protein | 1423030_at | Vcp | -1.22 |
| Heat shock 70kD protein 5 (glucose-regulated protein) | 1427464_s_at | Hspa5 | -1.23 |
| Synovial apoptosis inhibitor 1, synoviolin | 1428070_at | Syvn1 | -1.54 |
| **Cell adhesion** | | | |
| Cadherin 4 | 1456397_at | Cdh4 | -1.4 |
| **Transcription factor activity** | | | |
| FBJ osteosarcoma oncogene | 1422134_at | Fos | 4.63 |
| Jun oncogene | 1417409_at | Jun | 2.73 |
| Kruppel-like factor 4 (gut) | 1417394_at | Klf4 | 2.36 |
| Basic helix-loop-helix domain containing, class B2 | 1418025_at | Bhlhb2 | 2.04 |
| Early growth response 1 | 1417065_at | Egr1 | 1.98 |
| SRY-box containing gene 4 | 1419157_at | Sox4 | 1.89 |
| Max interacting protein 1 | 1450376_at | Mxi1 | 1.7 |
| Sin3 associated polypeptide | 1417719_at | Sap30 | 1.42 |
| Influenza virus NS1A binding protein | 1450084_s_at | Ivns1abp | 1.42 |
| Activating transcription factor 5 | 1425927_a_at | Atf5 | 1.31 |
| Mesenchyme homeobox 2 | 1424233_at | Meox2 | 1.23 |
| Inhibitor of kappa light polypeptide enhancer in B-cells | 1451254_at | Ikbkap | -1.37 |
| **Regulation of protein kinase activity** | | | |
| Regulator of G-protein signaling 4 | 1448285_at | Rgs4 | 2.02 |
| Growth arrest and DNA-damage-inducible 45 gamma | 1453851_a_at | Gadd45g | 1.59 |
| Tribbles homolog 1 (Drosophila) | 1424880_at | Trib1 | 1.56 |

| | | | |
|---|---|---|---|
| Cyclin-dependent kinase inhibitor 1A (P21) | 1424638_at | Cdkn1a | 1.34 |
| **DNA damage** | | | |
| Growth arrest and DNA-damage-inducible 45 gamma | 1453851_a_at | Gadd45g | 1.59 |
| Mitogen activated protein kinase 3 | 1427060_at | Mapk3 | 1.27 |
| Valosin containing protein | 1423030_at | Vcp | -1.22 |
| **Response to stress** | | | |
| Thioredoxin interacting protein | 1415997_at | Txnip | 5.25 |
| Dual specificity phosphatase 1 | 1448830_at | Dusp1 | 2.15 |
| Growth arrest and DNA-damage-inducible 45 gamma | 1453851_a_at | Gadd45g | 1.59 |
| DnaJ (Hsp40) homolog, subfamily B, member 1 | 1416756_at | Dnajb1 | 1.4 |
| Annexin A2 | 1419091_a_at | Anxa2 | 1.37 |
| Mitogen activated protein kinase 3 | 1427060_at | Mapk3 | 1.27 |
| **Oxidoreductase activity** | | | |
| Cytochrome c oxidase subunit VIIa polypeptide 2-like | 1432264_x_at | Cox7a2l | 1.21 |
| Liver-specific bHLH-Zip transcription factor | 1451255_at | Lsr | -1.23 |
| Aldehyde dehydrogenase 18 family, member A1 (Aldh18a1) | 1437620_x_at | Aldh18a1 | -1.26 |
| Ribosomal protein S6 kinase, polypeptide 2 | 1417542_at | Rps6ka2 | -1.28 |
| Solute carrier family 39 (zinc transporter), member 7 | 1416949_s_at | Slc39a7 | -1.32 |
| **Signal transduction** | | | |
| DNA segment, Chr 10, Brigham & Women's Genetics 1379 D10 | 1435050_at | Bwg1379 e | -1.26 |
| Doublecortin | 1418139_at | Dcx | -1.43 |
| Phosphodiesterase 10A | 1439618_at | Pde10a | -1.78 |
| **GTPase activity** | | | |
| Stromal membrane-associated protein 1-like | 1450675_at | Smap1l | -1.23 |
| Expressed in non-metastatic cells 1, protein | 1435277_x_at | Nme1 | -1.5 |
| **Translation** | | | |
| Histidyl-tRNA synthetase | 1438510_a_at | Hars | 1.28 |
| Eukaryotic translation initiation factor 3, | 1426674_at | Eif3b | 1.21 |

| | | | |
|---|---|---|---|
| subunit 9 (eta) | | | |
| Polyadenylate-binding protein-interacting protein 2 | 1448493_at | Paip2 | -1.24 |
| Eukaryotic translation initiation factor 4B | 1426378_at | Eif4b | -1.26 |
| **Metabolic** | | | |
| Gamma-glutamyl hydrolase | 1419595_a_at | Ggh | 1.27 |
| ATPase, Cu++ transporting, alpha polypeptide | 1418774_a_at | Atp7a | 1.27 |
| Dehydrogenase/reductase (SDR family) member 8 | 1434642_at | Hsd17b11 | 1.27 |
| Acetyl-Coenzyme A dehydrogenase, long-chain | 1448987_at | Acadl | -1.41 |
| **Zinc ion binding** | | | |
| Cysteine and histidine-rich domain (CHORD)-containing | 1460645_at | Chordc1 | -1.29 |
| **Ubiquitin cycle** | | | |
| Ubiquitin specific peptidase 18 | 1418191_at | Usp18 | 1.45 |
| Ubiquitin-activating enzyme E1-domain containing 1 | 1435247_at | Ube1dc1 | -1.41 |
| **Miscellaneous** | | | |
| Cocaine and amphetamine regulated transcript | 1422825_at | Cartpt | 1.48 |
| Wolfram syndrome 1 homolog (human) | 1448411_at | Wfs1 | 1.42 |
| Zinc finger, DHHC domain containing 2 | 1453481_at | Zdhhc11 | 1.36 |
| Leucine zipper transcription regulator 2 | 1450734_at | Sec16b | 1.36 |
| Heterogeneous nuclear ribonucleoprotein methyltransferase-like 1 | 1437234_x_at | Prmt2 | 1.35 |
| Carbamoyl-phosphate synthetase 2, aspartate transcarbamylase | 1452830_s_at | Cad | -1.22 |
| Histone 3, H2ba | 1449482_at | Hist3h2ba | -1.28 |
| Histocompatibility 2, T region locus 23 | 1449556_at | H2-23 | -1.34 |
| Ubiquitin-conjugating enzyme E2G 1 (UBC7 homolog) | 1415688_at | Ube2g1 | -2.65 |
| **Unknown** | | | |
| Immediate early response 5 | 1417612_at | Ier5 | 1.51 |
| Pleckstrin homology-like domain, family A, | 1418835_at | Phlda1 | 1.42 |

| | | | |
|---|---|---|---|
| member 1 | | | |
| Proline-rich nuclear receptor coactivator 1 | 1433668_at | Pnrc1 | 1.36 |
| Small EDRK-rich factor 1 | 1449509_at | Serf1 | 1.29 |
| Brain protein I3 | 1416924_at | Bri3 | 1.25 |
| Histocompatibility 13 | 1417287_at | H13 | -1.2 |
| HSPC171 protein | 1419287_at | Hspc171 | -1.22 |
| Methyltransferase like 9 | 1417710_at | Mettl9 | -1.24 |
| Melanoma inhibitory activity 3 | 1434698_at | Mia3 | -1.25 |
| Adult male medulla oblongata cDNA | 1440849_at | 6330417G04Rik | -1.3 |
| RIKEN cDNA 2310002J21 gene | 1456393_at | 2310002J21Rik | -1.31 |
| RIKEN cDNA 1810073N04 gene | 1427295_at | 1810073N04Rik | -1.34 |
| Arginine-rich, mutated in early stage tumours | 1428112_at | Armet | -1.36 |
| CLPTM1-like | 1423730_at | Clptm1l | -1.4 |
| RIKEN cDNA C630004H02 gene | 1423914_at | C630004H02Rik | -1.44 |
| Phosphatidic acid phosphatase type 2 domain containing 1 | 1428154_s_at | Ppapdc1 | -1.58 |

**Table: 3.4.6.1.3 111 gene transcripts up- or down-regulated MIN6 B1(Non-GSIS) compared to MIN6 B1(GSIS) associated with overall GO categories. List of mRNAs that increased or decreased by 1.2-fold in MIN6 B1(Non-GSIS) compared to MIN6 B1(GSIS). Identity of columns, from left to right: functional cluster assignment and name of gene, gene symbol and averaged fold change.**

### 3.4.7 Pathway analysis

#### 3.4.7.1 Pathway-Express

To determine if differentially-expressed genes were associated with any well-known pathways, David software was used. This software graphically displays the distribution of differentially-expressed genes (Fig: 3.4.7.1.1.2 and Fig: 3.4.7.1.2.1).

The differentially-expressed genes in MIN6 B1(GSIS) and MIN6 B1(Non-GSIS) were analysed using David software. The pathway associated with these differentially-regulated genes is listed in the Table: 3.4.7.1 and the software calculates and gives the impact factor to the entire pathway. The impact factor of the entire pathway includes a probabilistic term that takes into consideration the proportion of differentially-regulated genes on the pathway and relative importance of each differentially-regulated gene in the pathway. The impact factors of all pathways are used to rank the pathways (Table: 3.4.7.1).

| Pathway Name | Impact Factor |
|---|---|
| MAPK signaling pathway | 7.111 |
| mTOR signaling pathway | 6.518 |
| B cell receptor signaling pathway | 5.816 |
| Colorectal cancer | 5.188 |
| Toll-like receptor signaling pathway | 5.044 |
| T cell receptor signaling pathway | 4.656 |
| Long-term potentiation | 3.337 |
| Prion disease | 2.969 |
| Gap junction | 2.835 |
| GnRH signaling pathway | 2.691 |
| Circadian rhythm | 2.606 |
| Neurodegenerative disorders | 1.95 |
| Type II diabetes mellitus | 1.701 |
| Focal adhesion | 1.572 |
| Adipocytokine signaling pathway | 1.291 |
| Antigen processing and presentation | 1.291 |
| VEGF signaling pathway | 1.291 |
| Long-term depression | 1.254 |
| Fc epsilon RI signaling pathway | 1.23 |
| Adherens junction | 1.23 |
| TGF-beta signaling pathway | 1.163 |
| Apoptosis | 1.153 |
| Natural killer cell mediated cytotoxicity | 0.971 |
| Insulin signaling pathway | 0.783 |
| Axon guidance | 0.777 |
| Cell adhesion molecules (CAMs) | 0.772 |
| Wnt signaling pathway | 0.708 |
| Regulation of actin cytoskeleton | 0.512 |
| Neuroactive ligand-receptor interaction | 0.328 |

**Fig: 3.4.7.1 Pathway-Express (PE), using DAVID software performs a pathway level impact analysis and orders the affected pathways in the decreasing order of their expected importance for the given condition.**

#### 3.4.7.1.1 MAPK signalling pathway

Signal transduction cascades activated for mitogen-activated protein kinase (MAP kinase) pathways are stimulated by different stimuli such as growth factors, stress, cytokines and inflammation. These are stress-activated kinases and are also induced by hyperglycemia and high glucose, which increases ROS production and causes oxidative stress. Oxidative stress induces MAPK-signalling pathway, which causes insulin resistance and beta cell dysfunction. Table 3.4.7.1.1.1 includes the differentially-regulated genes in MIN6 B1(GSIS) and MIN6 B1(Non-GSIS) associated with MAPK-signalling pathway.

| KEGG_PATHWAY:MMU04010:MAPK SIGNALING PATHWAY; 8 Gene(s) | | |
|---|---|---|
| **AFFY_ID** | **Gene Name** | **F C** |
| 1423100_at | FBJ osteosarcoma oncogene B | 4.63 |
| 1417409_at, 1448694_at | Jun oncogen | 2.73 |
| 1448830_at | Dual specificity phosphatase 1 | 2.15 |
| 1453851_a_at | Growth arrest and DNA-damage-inducible 45 gamma | 1.59 |
| 1420088_at | Nuclear factor of kappa light | 1.28 |
| 1427060_at | Mitogen activated protein kinase 3 | 1.27 |
| 1427464_s_at | Heat shock 70kD protein 5 (glucose-regulated protein) | -1.23 |
| 1417542_at | Ribosomal protein S6 kinase | -1.28 |

**Table: 3.4.7.1.1.1 Differentially-regulated genes between MIN6 B1(GSIS) and MIN6 B1(Non-GSIS) cells, associated with MAPK-signalling pathway**

Fig 3.4.7.1.1.2 graphically represent gene transcript associated with the MAP kinase pathway. White and yellow coloured gene transcript are the differentially-regulated genes in MIN6 B1(GSIS) and MIN6 B1(Non-GSIS).

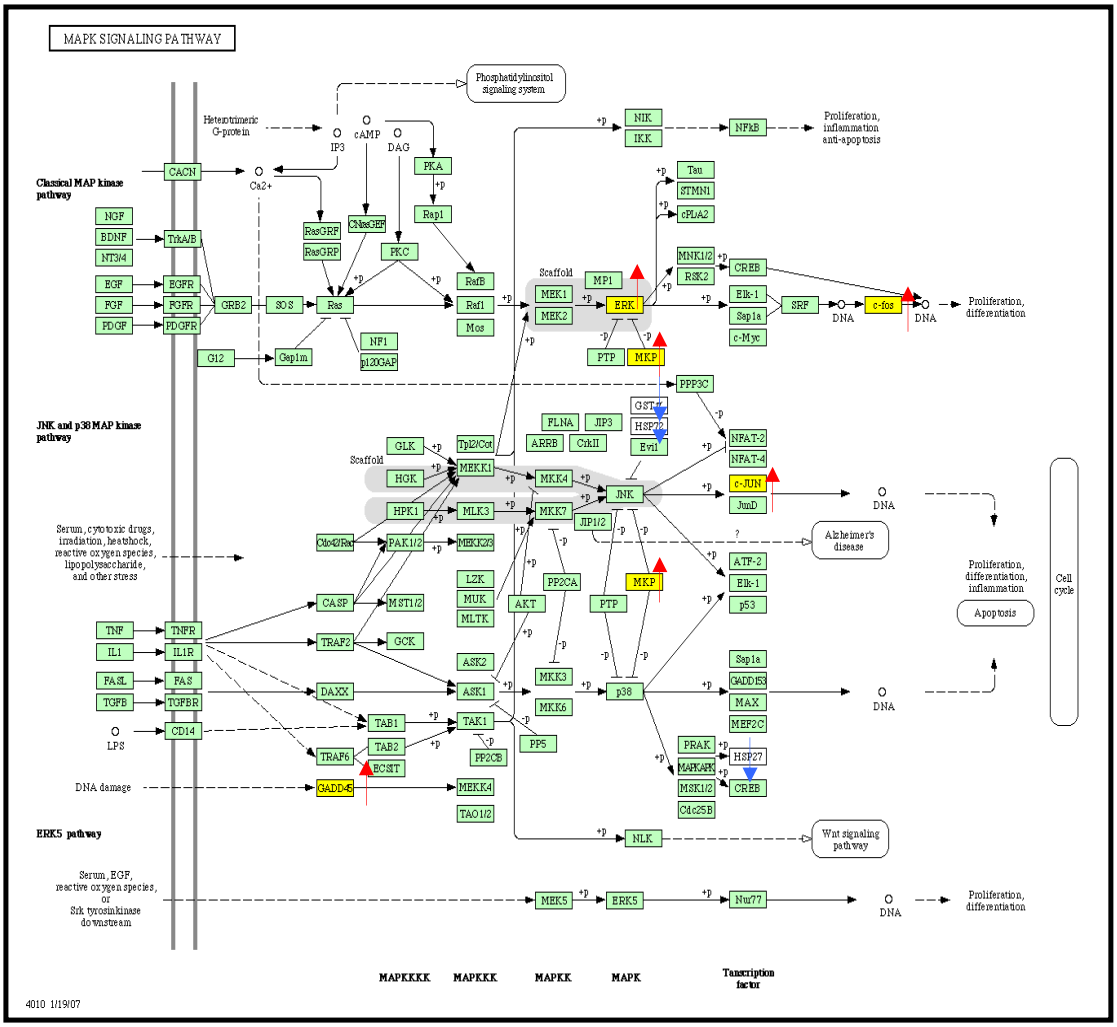


**Fig: 3.4.7.1.1.2 Differentially-regulated genes associated with MAPK signalling pathway. Yellow coloured genes with red arrow ( ↑ ) represent up-regulated gene transcripts and white coloured genes with blue arrow ( ↓ ) represent down-regulated genes associated MIN6 B1 microarray study.**

### 3.4.7.1.2 Insulin signalling pathway

Signalling through the insulin pathway is critical for the regulation of intracellular and blood glucose levels and the avoidance of diabetes. Insulin signalling is mediated by a complex, highly integrated network that controls several processes (Fig: 3.4.7.1.2.1). Fig 3.4.7.1.2.1 represent various gene transcript associated with insulin signalling pathway. Gene transcript circled with white line are the gene transcript that were found to up-regulated in the microarray study in MIN6 B1(Non-GSIS) compared to MIN6 B1(GSIS).

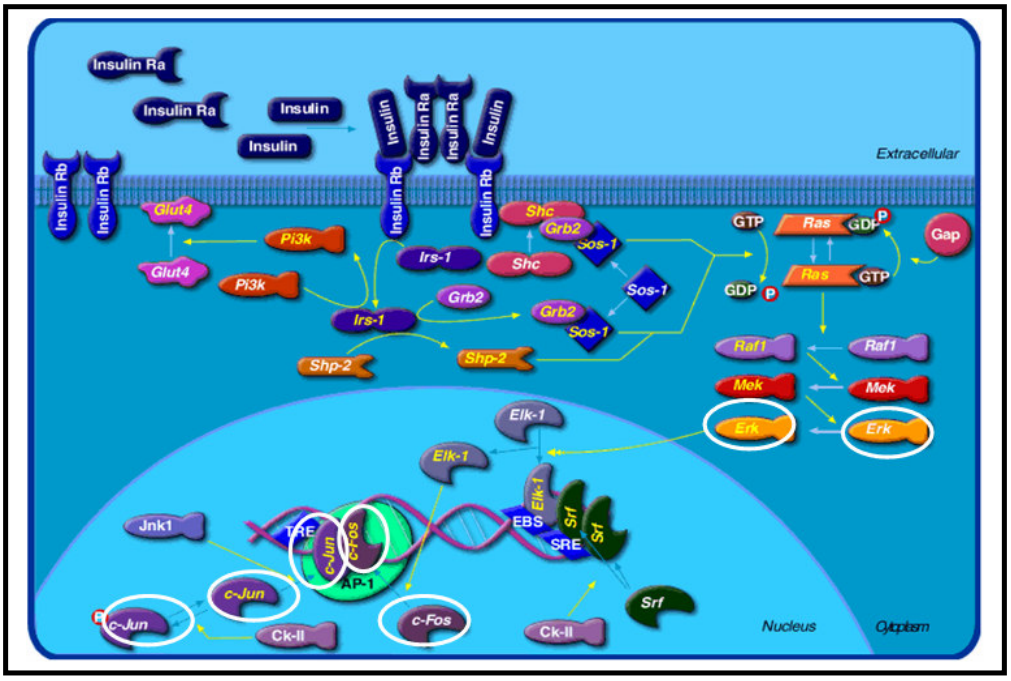


**Fig: 3.4.7.1.2.1 Differentially-regulated genes associated with Insulin signalling pathway. Genes circled in white are the up-regulated genes associated with MIN6 B1 microarray study.**

Table 3.4.7.1.2.2 shows the up-regulated genes associated with insulin signalling pathway. High glucose induces the expression of *c-fos* and *c-jun*. *c-jun* and *c-fos*

represses human insulin promoter (Susini *et al*., 1998). Research has shown that MAP-kinase mediate transcription of immediate early genes like *c-fos* and *c-jun* (Yao *et al*., 1995).

| BIOCARTA:m_insulinPathway:Insulin Signaling Pathway: 3 Gene(s) | | |
|---|---|---|
| **AFFY_ID** | **Gene Name** | **F C** |
| 1423100_at | FBJ osteosarcoma oncogene | 4.63 |
| 1417409_at | Jun oncogen | 2.73 |
| 1427060_at | Mitogen activated protein kinase 3 | 1.27 |

**Table: 3.4.7.1.2.2 Differentially-regulated genes associated with insulin signalling pathway. Genes are arranged by fold change (FC) in descending order.**

### 3.4.8 qRT-PCR validation of the microarray data

To validate the microarray results, twelve up-regulated genes, *Fos*, *Egr1*, *Txnip*, *Sox4*, *Gadd45g*, *Mapk3*, *Jun*, *Anxa2*, *Dusp1*, *Ier5*, *Klf4* and *Fosb,* and four down-regulated genes, *Gcg*, *Slc38a4*, *Txndc5* and *Pcsk9* were selected for qRT-PCR analysis. qRT-PCR was performed in triplicate for each gene transcript (See Section: 2.5.3), and the fold change was determined after normalization to the expression of a housekeeping gene, *Beta-actin*. Comparison of qRT-PCR data with microarray data demonstrated matching trends in expression changes for both methods.

An internal housekeeping gene control was selected based on the expression levels, of which were not significantly different between MIN6 B1(GSIS) and MIN6 B1(Non-GSIS) cells. qRT-PCR was performed on MIN6 B1(GSIS) and MIN6 B1(Non-GSIS) cell RNA to see if there were difference in the expression of *Beta-actin* and *Gapdh*. There was no significant difference in the expression of either *Beta-actin* or *Gapdh*,

therefore *Beta-actin* as a housekeeping gene was included to normalise any possible differences in RNA isolation and RNA degradation (Table: 3.4.8.1).

| | MIN6 B1(Non-GSIS) | MIN6 B1(GSIS) |
|---|---|---|
| Beta-actin | 18.317 | 17.795 |
| Gapdh | 18.078 | 18.66 |

**Table: 3.4.8.1 Shows the cycle threshold (ct) values of *Beta-actin* and *Gapdh* in MIN6 B1(GSIS) and MIN6 B1(Non-GSIS).**

To exclude any amplification product derived from genomic DNA or any other contaminent that could contaminate the RNA preparation, total RNA without reverse transcription and water on its own was amplified as a negative control (See Section: 2.5.3.1). Fig 3.4.8.2 shows the detection of target gene transcript, control, -RT control and water control.

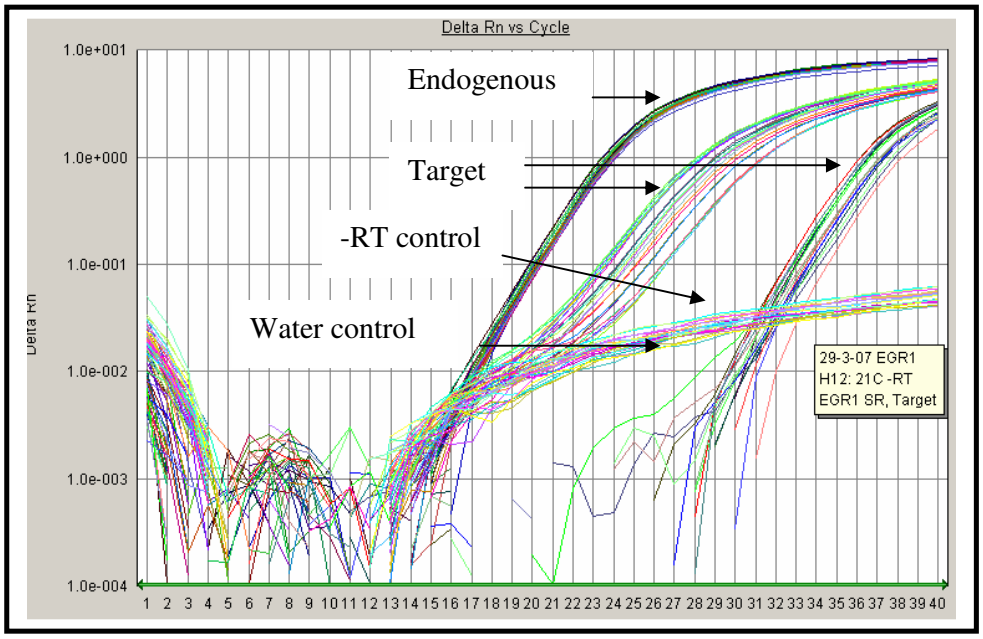


**Table: 3.4.8.2 Detection of target gene transcript, endogenous control, -RT control and water control.**

qRT-PCR validation was performed on the same samples of RNA that were used for microarray study. P-value and fold change was calculated using 19A, B and C VS. 23A and B. 23C sample was not included in the study as it did not cluster with its replicates in the microarray study. Standard deviation shown was calculated on triplicate technical repeat analysis of samples 23A and B (Table: 3.4.8.3). The fold change for both qRT-PCR and microarray study was calculated using 19A, 19B and 19C vs. 23A and 23B only. Table 3.4.8.4 shows the fold change from microarray and qRT-PCR validation study. qRT-PCR study confirmed the trends observed in the microarray experiment for the gene transcripts studied (Table: 3.4.8.4). Fig 3.4.8.5 compares the fold change from microarray and qRT-PCR studies (i.e. table 3.4.8.3 in graphical form).

| Gene | MIN6 B1(GSIS) RQ value | | | MIN6 B1(Non-GSIS) RQ value | | | Average Repeat 1+2 | F C | P-value | S.D |
|---|---|---|---|---|---|---|---|---|---|---|
| | 19A | 19B | 19C | 23A | 23B | 23C | | | | |
| **Up-regulated** | | | | | | | | | | |
| *Anxa A2* | 1 | 1 | 1 | 1.83 | 1.67 | 1.41 | 1.75 | 1.75 | 0.001 | 0.113 |
| *Dusp1* | 1 | 1 | 1 | 3.51 | 3.73 | 0.66 | 3.62 | 3.60 | 0.000 06 | 0.154 |
| *Egr1* | 1 | 1 | 1 | 4.14 | 5.14 | 0.48 | 4.64 | 4.64 | 0.002 | 0.709 |
| *Fos* | 1 | 1 | 1 | 6.03 | 6.94 | 0.29 | 6.49 | 6.49 | 0.001 | 0.641 |
| *FosB* | 1 | 1 | 1 | 55.01 | 62.98 | 0.39 | 58.99 | 58.9 | 0.000 | 5.636 |
| *Gadd45g* | 1 | 1 | 1 | 1.47 | 1.70 | 0.81 | 1.59 | 1.59 | 0.006 | 0.159 |
| *Ier-5* | 1 | 1 | 1 | 1.83 | 1.94 | 0.54 | 1.89 | 1.89 | 0.000 | 0.078 |
| *Jun* | 1 | 1 | 1 | 2.54 | 3.32 | 0.35 | 2.93 | 2.93 | 0.007 | 0.554 |
| *Klf4* | 1 | 1 | 1 | 2.49 | 2.44 | 0.43 | 2.47 | 2.47 | 0.000 | 0.037 |
| *Mapk3* | 1 | 1 | 1 | 1.23 | 1.10 | 0.54 | 1.16 | 1.16 | 0.043 | 0.093 |
| *Sox4* | 1 | 1 | 1 | 1.39 | 1.93 | 0.68 | 1.66 | 1.66 | 0.044 | 0.375 |
| *Txnip* | 1 | 1 | 1 | 2.90 | 3.80 | 0.99 | 3.35 | 3.35 | 0.006 | 0.636 |
| **Down-regulated** | | | | | | | | | | |
| *Gcg* | 1 | 1 | 1 | 0.72 | 0.39 | 0.915 | 0.555 | 1.803 | 0.036 | 0.233 |
| *Pcsk9* | 1 | 1 | 1 | 0.45 | 0.32 | 1.133 | 0.386 | 2.591 | 0.001 | 0.091 |
| *Slc38a4* | 1 | 1 | 1 | 0.81 | 0.63 | 1.065 | 0.719 | 1.392 | 0.026 | 0.129 |
| *Txndc5* | 1 | 1 | 1 | 0.85 | 0.68 | 0.791 | 0.764 | 1.309 | 0.037 | 0.124 |

**Table: 3.4.8.3 RQ (relative quantification) of transcript expression in MIN6 B1 samples as determined by qRT-PCR. RQ of MIN6 B1(GSIS) was set to 1. 19A, 19B and 19C are biological replicates of MIN6 B1(GSIS) cells whereas 23A, 23B and 23C are biological replicates of MIN6 B1(Non-GSIS) cells. p-value and fold change was calculated using 19A, B and C VS. 23A and B. 23C (shown in red font) sample was not included in the study as it did not cluster with its replicates in the microarray study. Standard deviation shown was calculated on triplicate technical repeats of samples 23A and B.**

| | Gene Transcripts | qRT-PCR | Microarray |
|---|---|---|---|
| **Up-regulated** | *Anxa A2* | 1.75 | 1.37 |
| | *Dusp1* | 3.62 | 2.15 |
| | *Egr1* | 4.64 | 1.98 |
| | *Fos* | 6.49 | 2.12 |
| | *FosB* | 59.00 | 4.63 |
| | *Gadd45g* | 1.59 | 1.59 |
| | *Ier-5* | 1.89 | 1.51 |
| | *Jun* | 2.93 | 2.73 |
| | *Klf4* | 2.47 | 2.36 |
| | *Mapk3* | 1.17 | 1.27 |
| | *Sox4* | 1.66 | 1.89 |
| | *Txnip* | 3.11 | 5.25 |
| **Down-regulated** | *Gcg* | -1.80 | -1.55 |
| | *Pcsk9* | -2.59 | -1.5 |
| | *Slc38a4* | -1.39 | -1.43 |
| | *Txndc5* | -1.31 | -1.34 |

**Table: 3.4.8.4 Validation of microarray data by qRT-PCR. Comparison of fold change from qRT-PCR and microarray study, showing gene transcripts up- or down-regulated in MIN6 B1(Non-GSIS) compared to MIN6 B1(GSIS).**

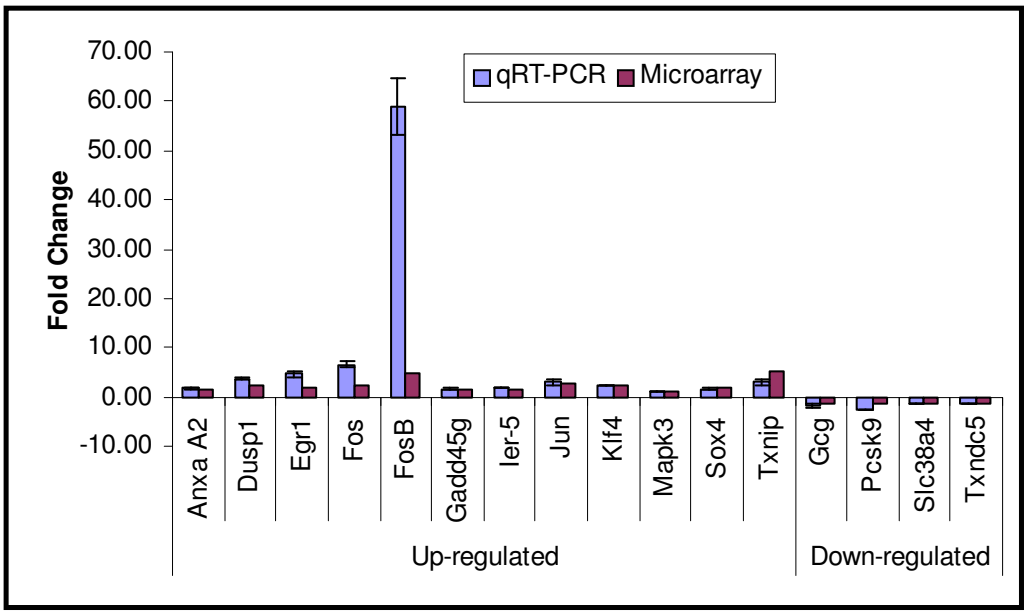


**Fig: 3.4.8.5 Comparison of microarray expression data and qRT-PCR data for selected differentially expressed genes identified by microarray analysis of MIN6 B1(Non-GSIS) and MIN6 B1(GSIS) cells. Range of expression from qRT-PCR analysis was relative to the corresponding microarray expression data. Results are included for *Anxa2*, *Dusp1*, *Egr1*, *Fos*, *Fosb*, *Gadd45g*, *Ier5*, *Jun*, *Klf4*, *Mapk3*, *Sox4*, *Txnip*, *Gcg*, *Pcsk9 Slc38a4*, and *Txndc5.* qRT-PCR was performed on biological triplicates of MIN6 B1(GSIS) and MIN6 B1(Non-GSIS) cells. p-value and fold change for both qRT-PCR and microarray was calculated using 19A, B and C VS. 23A and B. 23C sample was not included in the study as it did not cluster with its replicates in the microarray study. Standard deviation shown was calculated triplicate technical repeats on samples 23A and B.**

### 3.4.9 Comparison of MIN6 and MIN6 B1 microarray data with protein

Changes in the proteome between glucose-responsive MIN6 (L) and glucose non-responsive MIN6 (H) cells were studied using 2D-DIGE (2-D difference gel electrophoresis). A total of 3551 protein spots in the pH range of 4-7 were identified. A criteria of fold change ≥ 1.2 and p-value <0.01 was used to identify differentially-regulated proteins. A total of 35 proteins were identified that passed the above criteria, 18 were down-regulated, whereas 17 were found to be up-regulated in MIN6 (H) compared to MIN6 (L) cells.

MIN6 and MIN6 B1 probe set identifiers (ID) were converted to Entrez ID, using freely available software DAVID (http://david.abcc.ncifcrf.gov/). The same was done with protein ID and was compared using access.

| Name | p-value | FC |
|---|---|---|
| Ubiquitin thiolesterase | 1.70E-10 | 2.98 |
| Phosphoglycerate mutase 1 | 2.00E-06 | 2.95 |
| 3-phosphoglycerate dehydrogenase | 0.00087 | 2.65 |
| Chromogranin A precursor (CgA) | 3.00E-07 | 2.47 |
| protein 1 homolog gamma (HP1 gamma) | 1.10E-07 | 2.41 |
| High mobility group box 1 (Amphoterin) | 8.20E-10 | 2.18 |
| Annexin A4 | 0.00032 | 1.99 |
| Chromatin assembly factor 1 subunit C (CAF-1 subunit) | 2.40E-08 | 1.85 |
| Ubiquinol-cytochrome-c-reductase complex core protein 1 | 2.80E-07 | 1.6 |
| Stathmin 1 | 3.50E-05 | 1.57 |
| Tropomyosin alpha 3 chain | 3.40E-06 | 1.53 |
| Transaldolase 1 | 0.0048 | 1.5 |
| S-adenosylhomocysteine hydrolase | 2.60E-06 | 1.45 |
| deoxyuridine triphosphatase | 4.00E-07 | 1.41 |

| | | |
|---|---|---|
| Prohibitin | 7.30E-05 | 1.31 |
| protein phosphatase 1, catalytic subunit, beta | 0.0019 | 1.25 |
| Chaperonin subunit 2 (beta) | 0.0051 | 1.22 |
| bisphosphate 3'-nucleotidase 1 | 0.0047 | -1.24 |
| proteasome(prosome, macropain) subunit, alpha type 1 | 0.00018 | -1.29 |
| 6-phosphogluconolactonase | 0.00019 | -1.31 |
| proteasome (prosome, macropain) 28 subunit | 0.00015 | -1.33 |
| Enolase 1, alpha non-neuron | 2.10E-05 | -1.53 |
| Malate dehydrogenase, cytoplasmic | 5.50E-06 | -1.61 |
| 6-pyruvoyl-tetrahydropterin synthase/dimerization cofactor | 4.90E-07 | -1.75 |
| Hypoxanthine guanine phosphoribosyl transferase | 6.60E-05 | -1.75 |
| Superoxide dismutase 1, soluble | 2.50E-08 | -1.97 |
| Stromal cell -derived growth factor | 4.00E-10 | -2.28 |
| Endoplasmic reticulum protein ERp29 precursor | 8.90E-12 | -2.34 |
| Prolyl 4-hydrolase, beta polypeptide;protein disulfide isomerase | 1.40E-07 | -2.44 |
| Succinyl-CoA ligase [GDP-forming] beta chain | 9.80E-05 | -2.59 |
| Glucose Regulated Protein 94 | 1.60E-06 | -2.73 |
| Peroxiredoxin 4 | 1.10E-13 | -2.77 |
| galactose-4-epimerase, UDP | 0.00018 | -2.86 |
| heat shock 70kDa protein 5 (glucose-regulated protein) | 9.30E-07 | -2.91 |
| carbonyl reductase 3 | 3.40E-07 | -3.56 |

**Table: 3.4.9 List of 35 differentially expressed proteins in MIN6 (H) cells *versus* MIN6 (L) cells. Identity of columns, from left to right: protein name, p-value and FC (fold change).**

### 3.4.9.1 Common genes in MIN6 Microarray and MIN6 protein study

MIN6 probe set ID from the microarray study and protein ID, from the protein study performed on MIN6 (H) passage 40 and MIN6 (L) passage 18, was converted to entrez ID and compared using access. There were 12 common gene transcripts in MIN6 microarray study and MIN6 protein study (Fig: 3.4.9.1.1). Table 3.4.9.1.2

shows the lists of common gene transcripts that were differentially regulated in MIN6 microarray and MIN6 protein study.

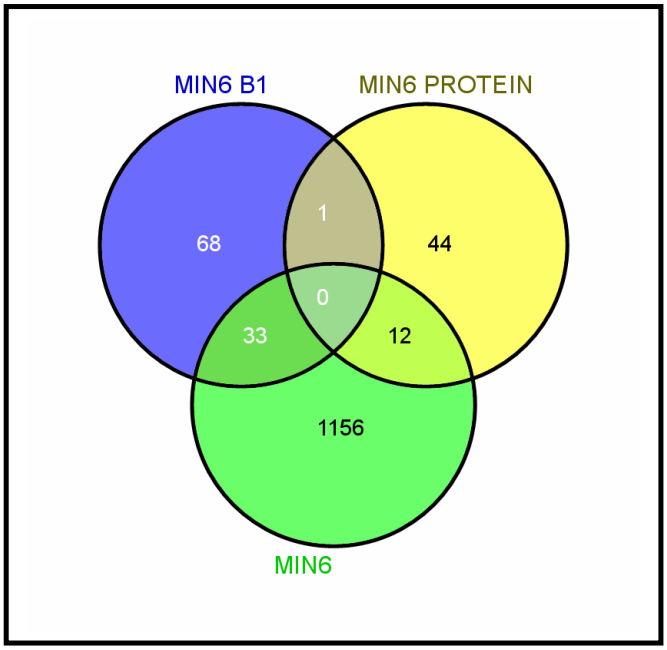


**Fig: 3.4.9.1.1 Venn diagram showing common genes in MIN6, MIN6 B1 microarray study and MIN6 protein study.**

| Probe set | Gene name | F C | Entrez ID | Input ID |
|---|---|---|---|---|
| 96244_at | ubiquitin carboxy-terminal hydrolase L1 | 1.79 | 22223 | *Q9R0P9 |
| 100584_at | annexin A4 | 1.68 | 11746 | *33416530 |
| 93265_at | tropomyosin 5 | 1.49 | 59069 | *20178336 |
| 95066_at | transaldolase 1 | 1.47 | 21351 | *33859640 |
| 96892_at | proteasome (prosome, macropain) subunit, alpha type 1 | 1.45 | 26440 | *33563282 |
| 160272_at | Chromobox homolog 3 | 1.44 | 12417 | *P23198 |
| 95654_at | Cluster Incl AF109905: | 1.31 | 114584 | *15617203 |
| 97909_at | leukemia-associated gene | 1.25 | 16765 | *Q91XT3 |
| 96318_at | DNA segment, Chr 17, Wayne State University 104, expressed | -1.27 | 28106 | *17027227 |
| 93495_at | peroxiredoxin 4 | -1.53 | 53381 | *O08807 |
| 160428_at | Succinate-coenzyme A ligase, GDP-forming, Beta subunit | -1.89 | 20917 | *52788304 |

**Table: 3.4.9.1.2 List of genes and their fold change differentially regulated in microarray and protein study performed on MIN6 (H) passage 40 and MIN6 (L) passage 18. Identity of columns, from left to right: probe set, gene name, F C (fold change), Entrez ID and Input ID.**

### 3.4.9.2 Common genes in MIN6 and MIN6 B1 microarray study

Previously microarray study was performed on long-term cultured MIN6 cells to identify genes associated with loss of GSIS. This microarray study was done on heterogeneous population of MIN6 cells and was about 22 passages apart. Present study was designed on homogenous population of cells (MIN6 B1) that were very limited passage numbers apart (4 passage apart) and the experiment was performed using whole genome microarray. A set of 33 common differentially-regulated gene

transcripts were found in MIN6 and MIN6 B1 microarray study (Fig: 3.4.9.2.1). Table 3.4.9.2.2 shows the lists of common gene transcripts that were differentially-expressed in the MIN6 and MIN6 B1 microarray study. There were 7 common up-regulated and 18 down-regulated genes in MIN6 and MIN6 B1 cells. There were 8 gene transcripts that were down-regulated in MIN6 but were up-regulated in MIN6 B1 cells and 1 gene transcript that was down-regulated in MIN6 B1 and up-regulated in MIN6 cells.

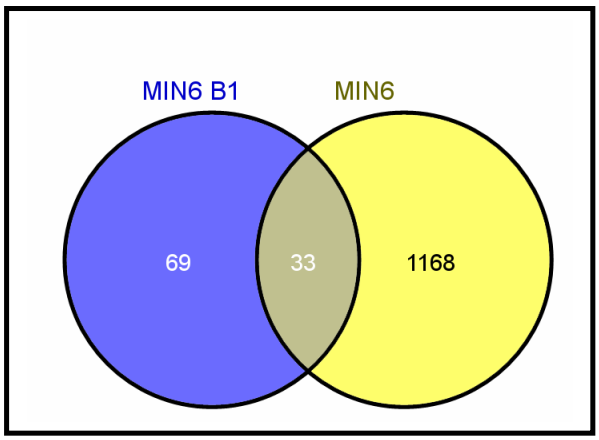


**Fig: 3.4.9.2.1 Venn diagram showing common genes in MIN6, MIN6 B1 microarray study and MIN6 protein study.**

| MIN6 B1 Probe ID | MIN6 B1 Gene Name | Entrez ID | MIN 6 B1 F C | MIN6 Probe ID | MIN6 Gene Name | MIN6 F C |
|---|---|---|---|---|---|---|
| 1415997 _AT | thioredoxin interacting protein | 56338 | 5.25 | 160547 _s_at | NA | 2.28 |
| 1417065 _AT | Early growth response 1 | 13653 | 1.98 | 98579_ at | Early growth response 1 | -4.62 |
| 1449556 _AT | histocompatibility 2, T region locus 23 | 15040 | 1.82 | 98472_ at | histocompatibility 2, T region locus 23 | -2.19 |

| | | | | | | |
|---|---|---|---|---|---|---|
| 1460645_AT | cysteine and histidine-rich domain (CHORD)-containing, zinc-binding protein 1 | 66917 | 1.45 | 160330_at | NA | 1.44 |
| 1417719_AT | sin3 associated polypeptide | 60406 | 1.42 | 160068_at | NA | 2.14 |
| 1418835_AT | pleckstrin homology-like domain, family A, member 1 | 21664 | 1.42 | 160829_at | NA | 3 |
| 1423825_AT | RIKEN cDNA 5031439A09 gene | 68151 | 1.38 | 101001_at | RIKEN cDNA 5031439A09 gene | -2.89 |
| 1415688_AT | ubiquitin-conjugating enzyme E2G 1 | 67128 | 1.36 | 93312_at | RIKEN cDNA 2700059C12 gene | 1.49 |
| 1424638_AT | cyclin-dependent kinase inhibitor 1A (P21) | 12575 | 1.34 | 94881_at | cyclin-dependent kinase inhibitor 1A (P21) | 1.37 |
| 1419595_A_AT | gamma-glutamyl hydrolase | 14590 | 1.27 | 93575_at | gamma-glutamyl hydrolase | -3.75 |
| 1434642_AT | dehydrogenase/reductase (SDR family) member 8 | 114664 | 1.27 | 102370_at | Cluster Incl AA822174 | -8.65 |
| 1426547_AT | group specific component | 14473 | 1.25 | 99197_at | group specific component | -12.93 |
| 1431665_A_AT | translocase of inner mitochondrial membrane 8 homolog b (yeast) | 30057 | 1.22 | 97477_at | translocase of inner mitochondrial membrane 8 homolog b (yeast) | 1.39 |
| 1432264_X_AT | cytochrome c oxidase subunit VIIa polypeptide 2-like | 629383 | 1.21 | 160383_at | NA | -1.51 |
| 1436915_X_AT | lysosomal-associated protein | 114128 | 1.21 | 100571_at | Cluster Incl AW123934 | -1.32 |

| | | | | | | |
|---|---|---|---|---|---|---|
| | transmembrane 4B | | | | | |
| 1417287_AT | histocompatibility 13 | 14950 | -1.2 | 96117_r_at | histocompatibility 13 | -1.44 |
| 1438225_X_AT | translocating chain-associating membrane protein 1 | 72265 | -1.22 | 160936_at | NA | -1.8 |
| 1452102_AT | coatomer protein complex, subunit beta 2 (beta prime) | 50797 | -1.22 | 93340_f_at | coatomer protein complex, subunit beta 2 (beta prime) | -1.73 |
| 1423670_A_AT | signal recognition particle receptor | 67398 | -1.23 | 93757_at | RIKEN cDNA 1300011P19 gene | -1.31 |
| 1451255_AT | liver-specific bHLH-Zip transcription factor | 54135 | -1.23 | 162274_f_at | NA | 1.68 |
| 1452767_AT | RIKEN CDNA 5730465C04 GENE | 81910 | -1.23 | 92850_at | RIKEN cDNA 5730465C04 gene | -2.22 |
| 1455066_S_AT | RIKEN CDNA 9130229H14 GENE | 236520 | -1.25 | 103295_at | Cluster Incl AI854482: r | -1.69 |
| 1417542_AT | ribosomal protein S6 kinase, polypeptide 2 | 20112 | -1.28 | 98007_at | ribosomal protein S6 kinase | -1.34 |
| 1456175_A_AT | coatomer protein complex, subunit beta 2 | 50797 | -1.32 | 93340_f_at | coatomer protein complex, subunit beta 2 | -1.73 |
| 1448411_AT | Wolfram syndrome 1 homolog (human) | 22393 | -1.34 | 103824_at | Wolfram syndrome 1 homolog (human) | -1.91 |
| 1451091_AT | thioredoxin domain containing 5 | 105245 | -1.34 | 98918_at | DNA segment, Chr 13, | -1.42 |
| 1434698_AT | RIKEN CDNA 9130229H14 GENE | 236520 | -1.37 | 103295_at | Cluster Incl AI854482: | -1.69 |
| 1424024_AT | RIKEN CDNA 1810021C21 | 193813 | -1.39 | 97451_at | Cluster Incl AI837599: | -1.4 |

| | | | | | | |
|---|---|---|---|---|---|---|
| | GENE | | | | | |
| 1427294_A_AT | RIKEN CDNA 1810073N04 GENE | 72055 | -1.41 | 160414_at | NA | -1.43 |
| 1435247_AT | ubiquitin-activating enzyme E1-domain containing 1 | 66663 | -1.41 | 102812_i_at | RIKEN cDNA 5730525G14 gene | -1.57 |
| 1428111_AT | solute carrier family 38, member 4 | 69354 | -1.43 | 104286_at | RIKEN cDNA 1700012A18 gene | -1.61 |
| 1452830_S_AT | carbamoyl-phosphate synthetase 2, aspartate transcarbamylase, and dihydroorotase | 69719 | -1.5 | 96827_at | RIKEN cDNA 2410008J01 gene | -1.43 |
| 1425952_A_AT | Glucagon | 14526 | -1.55 | 94633_at | glucagon | -2.59 |
| 1418890_A_AT | RAB3D, member RAS oncogene family | 19340 | -1.62 | 97415_at | RAB3D, member RAS oncogene family | -3.14 |

**Table: 3.4.9.2.2 List of genes and their fold change differentially regulated in microarray and protein study. Identity of columns, from left to right: MIN6 B1 Probe ID, MIN6 B1 Gene Name, Entrez ID, MIN6 B1 F C, MIN6 Probe ID, MIN6 Gene Name and MIN6 F C (F C= fold change; NA= no name were given to these Probe ID).**

### 3.4.9.3 Common genes in MIN6 protein and MIN6 B1 microarray study

A comparison of MIN6 protein study and MIN6 B1 microarray study resulted in a single common gene. It was down-regulated in both protein and microarray study (Table: 3.4.9.3).

| Probe ID | Gene Name | Entrez ID | F C | Protein ID |
|---|---|---|---|---|
| 1427464_S_AT | HEAT SHOCK 70KD PROTEIN 5 (GLUCOSE-REGULATED PROTEIN) | 14828 | -1.23 | *31981722 |

**Table: 3.4.9.3 Gene transcript and its fold change differentially-regulated in microarray and protein study. Identity of columns, from left to right: Probe ID, Gene Name, Entrez ID, F C and Protein ID (F C=fold change).**

### 3.5 siRNA analysis of target genes for their effect on GSIS

Microarray was done on MIN6 B1 cells whereas siRNA knock-down was carried out on MIN6 cells. The reason for switching from MIN6 B1 to MIN6 cells was that MIN6 B1 did not survive after thawing back at the later (functional validation) part of the study. MIN6 B1 was also unavailable to borrow from other laboratory and/or to buy.

Based on the results from microarray analysis and qRT-PCR validation of MIN6 B1(GSIS) and MIN6 B1(Non-GSIS), siRNA targets were chosen. The levels of silencing vary between species, cells and tissues due to differences in the efficiency with which the siRNAs are taken up by target cells. To minimise this problem, conditions for siRNA transfection into MIN6 cell line were optimised in 24-well plates using *Gapdh* as positive control and scrambled siRNA as a negative control.

For every siRNA transfection carried out, both non-transfected (NT) cells and a scrambled (Scr) siRNA transfected cells were used as controls. Scrambled siRNA can be any sequence that does not have homology to any genomic sequence. The scrambled non-targeting siRNA used in this study was commercially produced and promised limited sequence similarity to known genes and their products. It has also been functionally proven to have minimal effects on cell proliferation and viability. For each set of experiments investigating the effect of siRNA, the cells transfected with target-specific siRNA were compared to cells transfected with scrambled siRNA. This took account of any effects due to the transfection reagents and also any non-specific effects caused by introduction of short RNA oligos.

Transfections were carried out in 24-well plates (See Section: 2.5.4.1). In order to determine the success of transfection *Gapdh* siRNA was used for optimization in 24-

well plates. *Gapdh* silencing was seen as a measure of the successful achievement of suitable transfection conditions. Western blots (See Section: 2.5.5) were used to determine if siRNA had an effect at a protein level.

### 3.5.1 Transfection optimization using *Gapdh* siRNA

*Gapdh* siRNA was transfected in MIN6 cell line for optimization in 24-well plates. Western blots (See Section: 2.5.5) were performed to determine if siRNA had an effect at a protein level (Fig: 3.5.1). α-tubulin was used as a loading control for the samples. Down-regulation of Gapdh protein was observed in *Gapdh* siRNA-transfected cells whereas no down-regulation of protein was observed in non-transfected cells and scrambled siRNA-transfected cells.

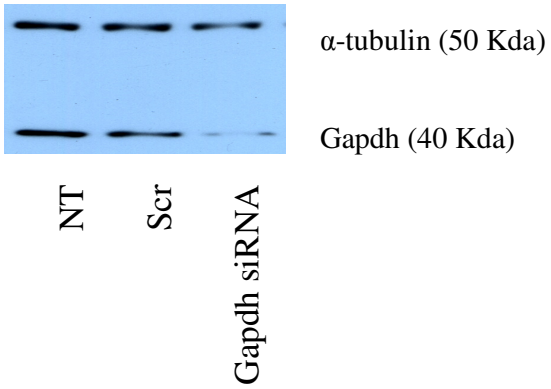


**Fig: 3.5.1 Western blot showing protein expression of *Gapdh* after *Gapdh* siRNA transfection in MIN6 cell line. NT = Non-transfected, Scr = Scrambled, and Gapdh siRNA.**

### 3.6 Glucagon (*Gcg*)

Microarray and qRT-PCR analysis showed *Gcg* was down-regulated in the MIN6 B1(Non-GSIS) cells compared to MIN6 B1(GSIS) cells. The microarray study showed a 1.55-fold, and qRT-PCR showed 1.8-fold, down-regulation of *Gcg* in MIN6 B1(Non-GSIS) compared to MIN6 B1(GSIS) cells. Therefore it was planned to knock-down *Gcg* in glucose-responsive MIN6 cells to determine if *Gcg* likely played an active role in GSIS.

#### 3.6.1 Proliferation assay

Cells grown in 96-well plates were assayed for changes in proliferation at 72hrs. using the acid phosphatase assay (See Section: 2.3.3). Proliferation assays were carried out on MIN6 low passage cells transfected with three *Gcg*-specific siRNA including *Kinesin* siRNA as a positive control. Cellular arrest in the presence of *Kinesin* siRNA was taken as confirmation of efficient transfection conditions. Significantly reduced growth (p-value = 0.02) of *Kinesin* siRNA-transfected cells compared to scrambled siRNA-transfected cells was observed. There was no significant effect in growth when transfected with *Gcg* siRNA compared to scrambled siRNA-transfected cells (Fig: 3.6.1.1).

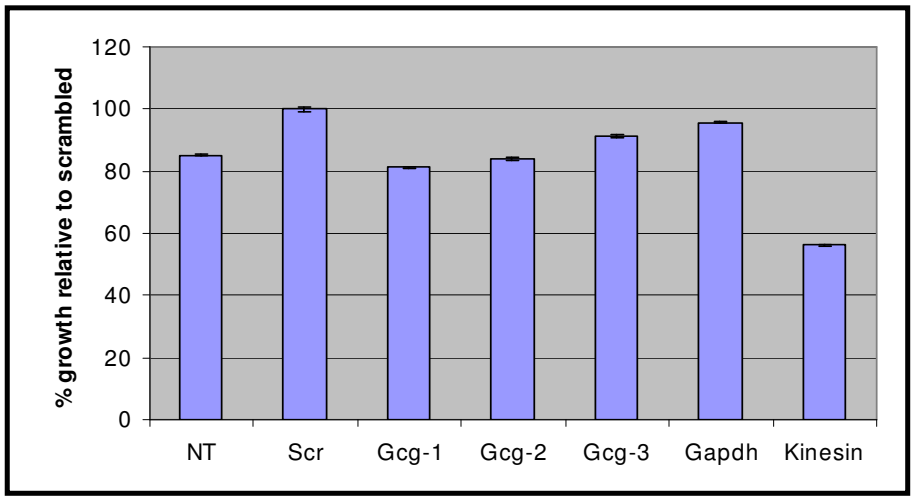


**Fig: 3.6.1.1 Growth rate of MIN6 low passage cells after siRNA transfection using Gcg (n=3), Scrambled, *Gapdh* and *Kinesin*. NT=non-transfected cells, Scr= scrambled transfected, *Gcg*-1, 2, 3= 3 different siRNA.**

There was no change in the morphology of the cells after siRNA transfection except for *kinesin*-transfected cells that showed a rounded morphology, indicating cell cycle arrest (Fig: 3.6.1.2).

**Effect of siRNA on cell morphology**

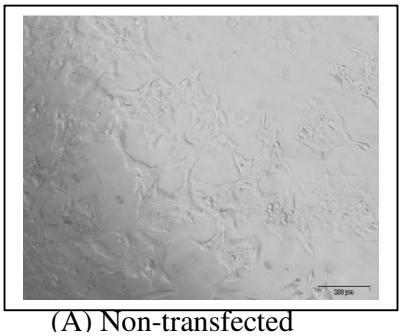

(A) Non-transfected

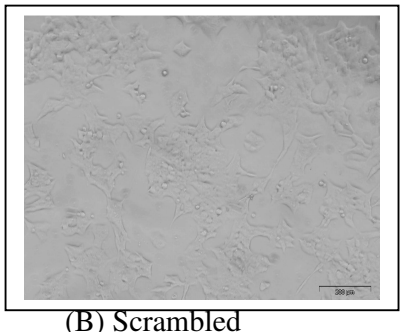

(B) Scrambled

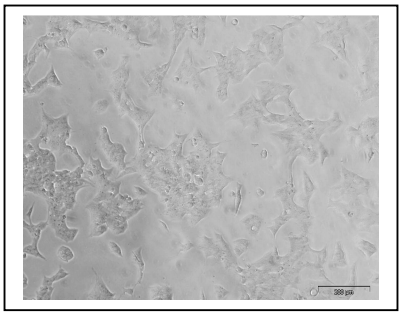

(C) *Gcg*-1

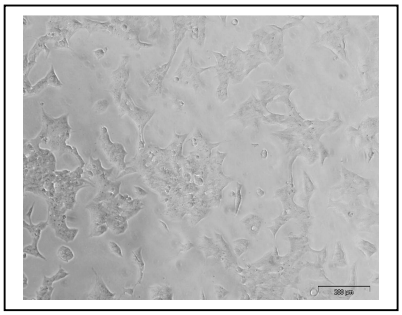

(D) *Gcg*-2

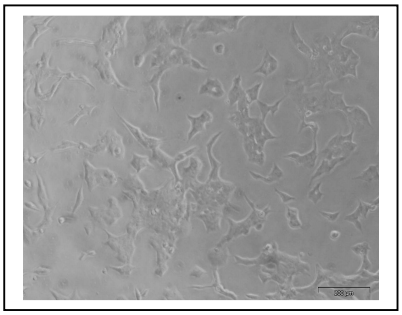

(E)*Gcg*-3

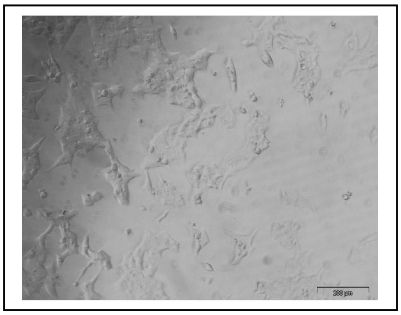

(F) *Gapdh*

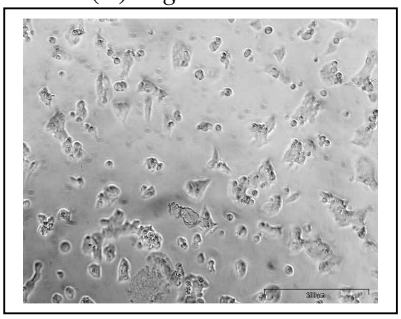

(G) Kinesin

**Fig: 3.6.1.2 Photographs (A) Non-transfected, (B) scrambled, (C) *Gcg*-1, (D) *Gcg*-2, (E) Gcg-3 (F) *Gapdh* and (G) *kinesin* siRNA transfected cells. Rounded morphology of cells indicates cell growth arrest.**

### 3.6.2 qRT-PCR after siRNA transfection

qRT-PCR was carried out on MIN6 low passage cells (passage 35) transfected with 3 independent *Gcg*-specific siRNA. RNA was isolated (See Section: 2.5.1.2.3) from the non-transfected, scrambled siRNA-transfected, *Gcg* siRNA-transfected and *Gapdh* siRNA-transfected cells after 72hrs. of transfection. Fig: 3.6.2 shows a knock-down of *Gcg* mRNA in *Gcg* siRNA-transfected cells compared to scrambled-transfected cells. *Gcg*-1 and *Gcg*-2 siRNA transfection showed a knock-down of approx. 32% and 27%, respectively, whereas no knock-down was seen with the *Gcg*-3 siRNA transfection compared to scrambled siRNA-transfected cells (Fig: 3.6.2).

To exclude any amplification product derived from genomic DNA that could contaminate the RNA preparation –RT and water was used as negative control. For -RT control total RNA from *Gcg*, *Gapdh*, scrambled siRNA-transfected and non-transfected cells were amplified without reverse transcriptase enzyme. Water was also amplified as a control to exclude any contamination in it.

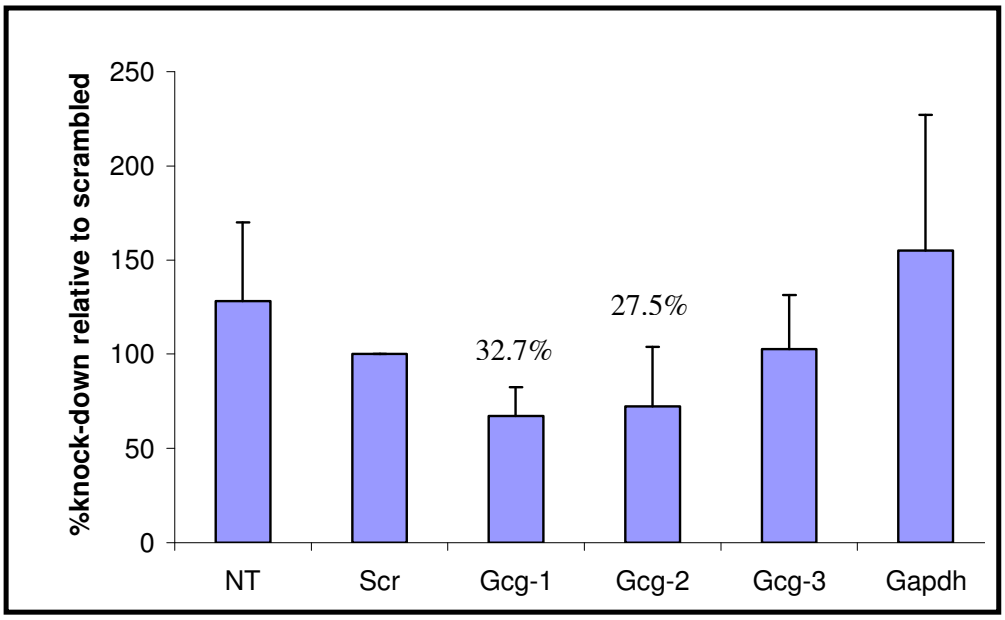


**Fig: 3.6.2 MIN6 low passage cells were transfected with *Gcg*, Scr and *Gapdh*. After 72hrs. of siRNA transfection RNA was isolated and qRT-PCR was performed for *Gcg* mRNA level. Gcg-1 induced 32.7%, Gcg-2 induced 27.5% whereas Gcg-3 showed no knock-down in MIN6 low passage cells. NT=non-transfected, Scr= Scrambled, Gcg-1, 2, 3= Gcg siRNA (n=3) and Gapdh= Gapdh siRNA transfected cells. Results represent mean ± S.D from three different experiments.**

### 3.6.3 GSIS after *Gcg* siRNA

These three *Gcg*-specific siRNA were transfected in MIN6 low passage cells to determine if silencing of *Gcg* affects GSIS. GSIS assay (See Section: 2.3.2.1) was performed after 72hrs. of siRNA transfection (See Section: 2.5.4.1.2). The three *Gcg*-transfected MIN6 low passage cells along with *Gapdh*-transfected cells, scrambled-transfected cells and non-transfected cells were incubated in 3.3 and 16.7mmol/L glucose for 1hr (See Section: 2.3.2.1). Insulin secretion was determined using ELISA (See Section: 2.3.2.4) and normalised to total protein.

There was significant loss of GSIS in *Gcg*-1 (p-value=0.00009), *Gcg*-2 (p-value=0.015) and *Gcg*-3 (p-value= 0.032) siRNA transfected MIN6 low passage cells (Fig: 3.6.3) compared to cells transfected with the scrambled sequence. *Gcg*-1 showed 1.0-fold, *Gcg*-2 showed 1.2-fold and *Gcg*-3 showed 1.4-fold GSIS, whereas non-transfected and scrambled-transfected cells showed 2.2-fold and 2.3-fold GSIS, respectively (Fig: 3.6.3).

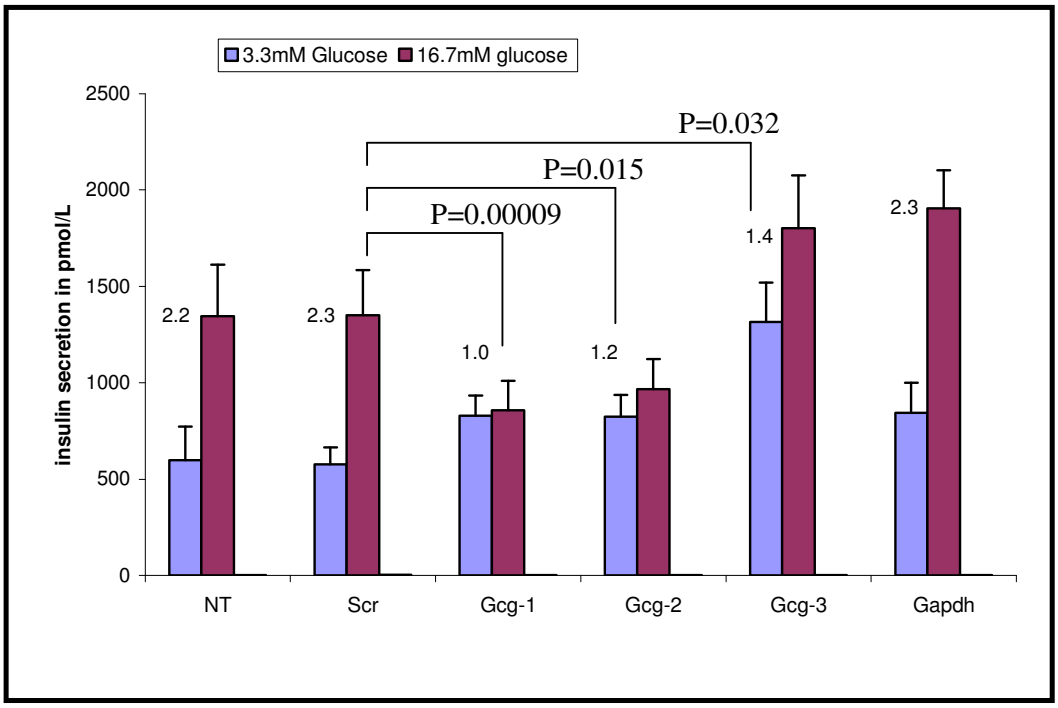


**Fig: 3.6.3 siRNA-mediated knockdown of *Gcg* led to a significant loss of GSIS in MIN6 low passage cells (Gcg-1 (p-value= 0.00009), Gcg-2 (p-value= 0.015), Gcg-3 (p-value=0.032)). GSIS was quantitated in non-transfected MIN6 low passage cells and MIN6 cells transfected with either scrambled siRNA, *Gcg* siRNA or the *Gapdh* siRNA. GSIS assay was performed 72hrs. after transfection. Insulin secretion was measured by ELISA and normalised to total cellular protein. The other numbers near the bars shows the GSIS fold change. NT= non-transfected, Scr= scrambled transfected, Gcg-1, 2, 3= *Gcg* siRNA (n=3), Gapdh= *Gapdh* siRNA transfected cells. Results represent mean ± S.D from three different experiments.**

### 3.6.4 qRT-PCR after cDNA over-expression

qRT-PCR was carried out on *Gcg* cDNA over-expressed MIN6 high passage cells (passage 47) along with empty plasmid-transfected and non-transfected cells. RNA was isolated (See Section: 2.5.1.2.3) and treated with DNase enzyme (See Section: 2.5.1.3.1). cDNA was prepared from the treated RNA (See Section: 2.5.2.1). Fig: 3.6.4 shows a 10.9-fold increase of *Gcg* mRNA in MIN6 high passage cells 72hrs. after *Gcg* cDNA over-expression compared to empty plasmid transfected cells. To exclude any amplification product derived from genomic DNA or any other contaminent that could contaminate the DNase-treated RNA preparation, DNase-treated RNA without reverse transcriptase enzyme and water on its own was amplified as a negative control (See Section: 2.5.3.1).

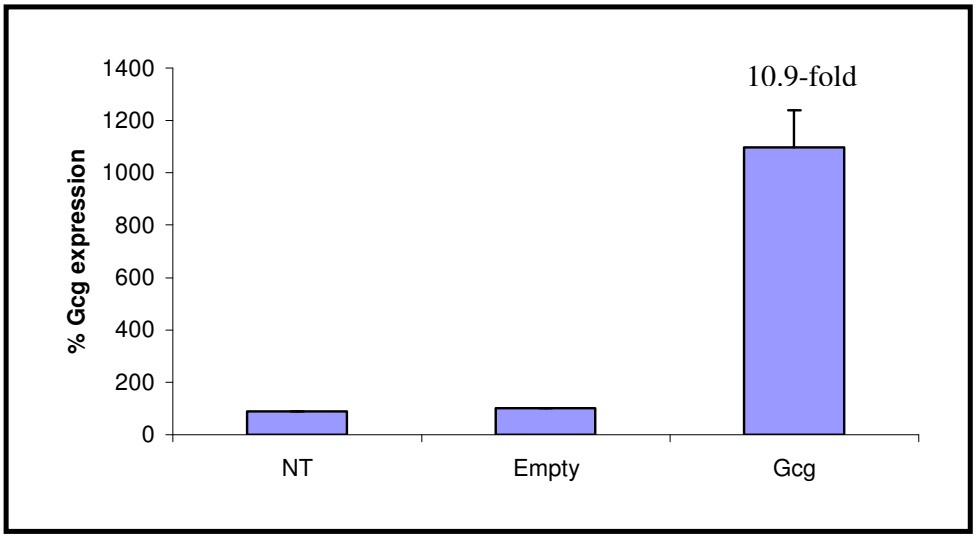


**Fig: 3.6.4 MIN6 high passage cells were transfected with empty plasmid and *Gcg* plasmid. qRT-PCR for *Gcg* mRNA level was performed after 72hrs. of cDNA over-expression in MIN6 high passage cells. A 10.9-fold increased *Gcg* mRNA was observed in Gcg plasmid-transfected cells compared to empty plasmid-transfected cells The results represent mean ± S.D from three different experiments.**

### 3.6.5 GSIS after *Gcg* cDNA over-expression

*Gcg* cDNA over-expression was performed on MIN6 high passage cells (passage 47) as shown in section 3.6.4. GSIS assay (See Section: 2.3.2.1) was performed 72hrs. after transfection. There was an increase in GSIS in *Gcg* over-expressed cells (1.43-fold) compared to empty plasmid transfected-cells (1.16) (Fig: 3.6.5).

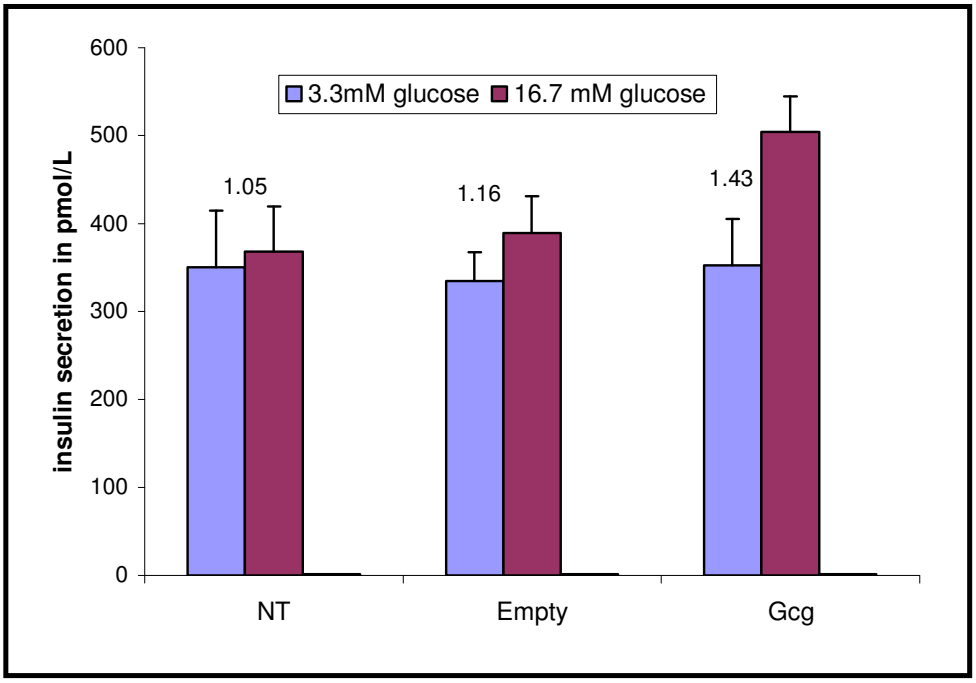


**Fig: 3.6.5 Over-expression of *Gcg* increases GSIS in MIN6 high passage cells. GSIS was quantitated in non-transfected MIN6 high passage cells and MIN6 cells transfected with either empty plasmid or the *Gcg* plasmid. GSIS was evaluated 72hrs. after plasmid transfection. Results represent mean ± S.D from three different experiments.**

### 3.6.6 Immunofluorescence

To investigate the presence of insulin secreting beta cells and glucagon secreting alpha cells in MIN6 cell line immunofluorescence was performed. In this study we were trying to determine the percentage of (i) insulin, (ii) glucagon and (iii) glucagon and insulin expressing cells in the MIN6 cell line. MIN6 low passage cells (passage 35) were cultured over night on slides, fixed and immunofluorescence was performed (See Section: 2.5.8). Immunofluorescence labeling showed the presence of insulin in all most all the cells. However, we were unable to optimise the conditions for immunofluorescence labeling using glucagon antibody (Fig: 3.6.6).

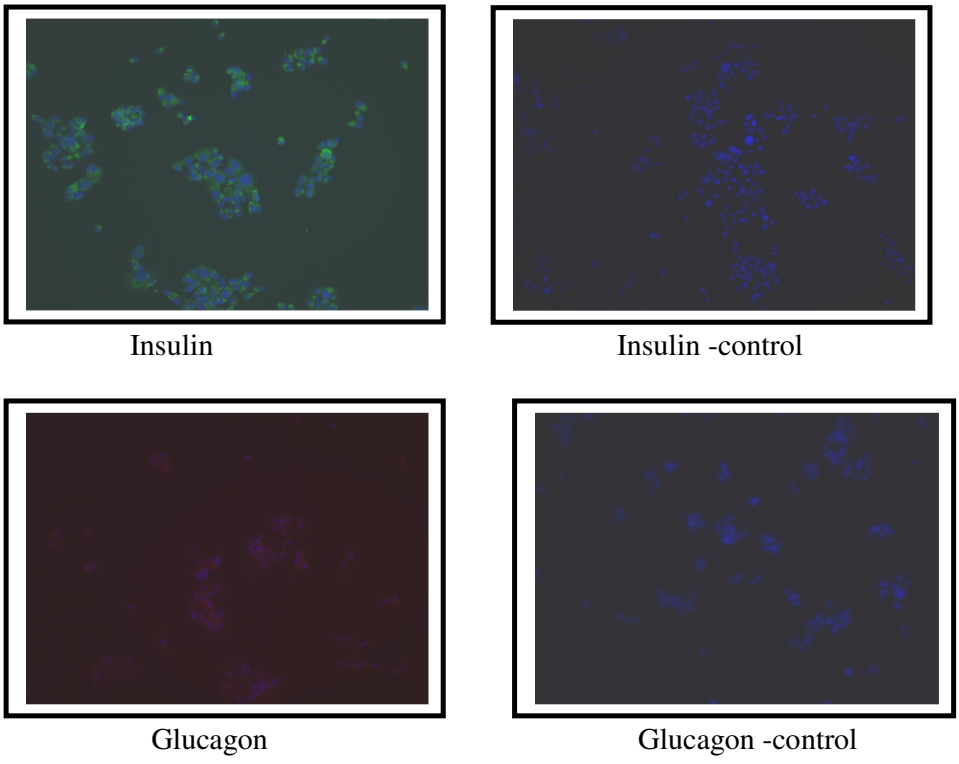


**Fig: 3.6.6 Immunofluorescence using insulin and glucagon on MIN6 low passage cell line using fluorescence microscope. Magnifications 20X. Insulin - green; glucagon – red; nuclear stain – blue.**

### 3.6.7 Summary of results for *Gcg* study on MIN6 cells

Results from proliferation assays showed that the optimum conditions for transfection were used, as a reduction in growth of cells transfected with *kinesin* siRNA was observed in MIN6 low passage cells. This also showed that transfection of *Gcg* siRNA did not have a notable effect on proliferation. After transfection with three separate *Gcg* siRNAs, there was a decrease in *Gcg* mRNA (Gcg-1 and Gcg-2 siRNAs) in *Gcg* siRNA-transfected cells as assessed by qRT-PCR evaluation compared to scrambled siRNA-transfected cells. This was accompanied by a significant decrease in GSIS in *Gcg* siRNA-transfected glucose responsive MIN6 low passage cells compared to scrambled siRNA-transfected cells.

*Gcg* cDNA was then transfected into high passage MIN6 cells to see if GSIS was increased following *Gcg* over-expression. *Gcg* mRNA level was determined using qRT-PCR after DNase-treatment of the transfected cells. There was a 10.9-fold increase in *Gcg* expression in *Gcg* plasmid-transfected cells compared to empty plasmid-transfected cells. *Gcg* cDNA over-expression showed a marked increase in GSIS in MIN6 high passage cells compared to empty plasmid-transfected cells.

Immunofluorescence labeling showed the presence of insulin in all most all the cells but we were unable to optimise the conditions for immunofluorescence labeling using glucagon antibody.

### 3.7 Proprotein convertase subtilisin/kexin type 9 (*Pcsk9*)

*Pcsk9* was down-regulated in the MIN6 B1(Non-GSIS) cells compared to MIN6 B1(GSIS) cells in the microarray study. The microarray study showed a 1.5-fold and qRT-PCR showed 2.59-fold down-regulation of *Pcsk9* in MIN6 B1(Non-GSIS) compared to MIN6 B1(GSIS) cells. Therefore it was planned to knock-down *Pcsk9* in glucose responsive MIN6 cells to determine the role of *Pcsk9* in GSIS.

#### 3.7.1 Proliferation assay

Proliferation assay was done in 96-well plate after 72hrs. of siRNA transfection using the acid phosphatase assay (See Section: 2.3.3). Proliferation assays were carried out on MIN6 low passage cells transfected with three independent *Pcsk9* siRNA, including *Kinesin* siRNA as a positive control. Cellular arrest in the presence of *Kinesin* siRNA was taken as confirmation of efficient transfection conditions. Reduced growth of *Kinesin* siRNA transfected cells compared to scrambled transfected cells was observed. There was no significant effect in growth when transfected with *Pcsk9* siRNA and *Gapdh* siRNA compared to scrambled-transfected cells (Fig: 3.7.1.1).

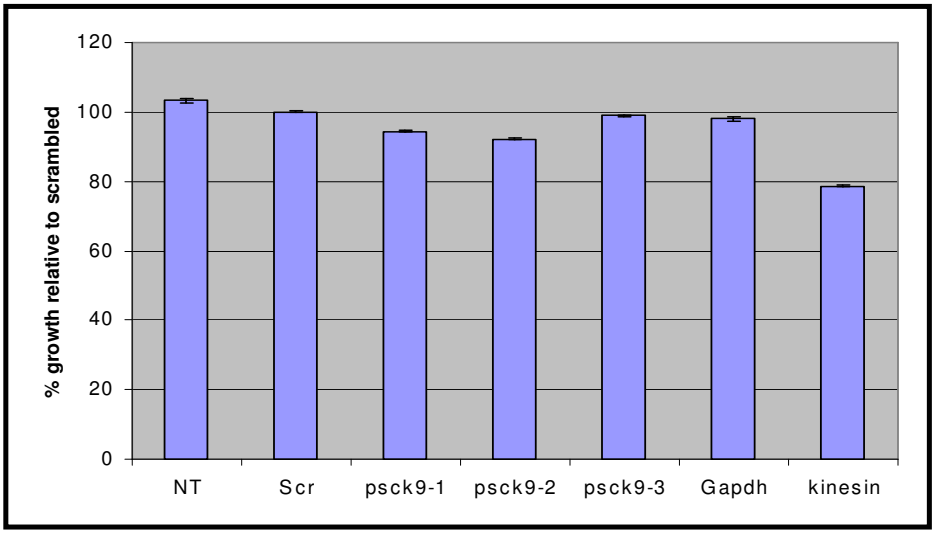


**Fig: 3.7.1.1 Growth rate of MIN6 low passage cells after siRNA transfection using *Pcsk9* (n=3), Scrambled, *Gapdh* and *Kinesin*. NT=non-transfected cells, Scr= scrambled transfected, *Pcsk9*-1, 2, 3= 3 different siRNA.**

There was no change in the morphology of the cells after siRNA transfection except for *Kinesin* transfected cells that showed a rounded morphology indicating cell growth arrest (Fig:3.7.1.2).

**Effect of *Pcsk9* and kinesin siRNA on cell morphology of MIN6 cells**

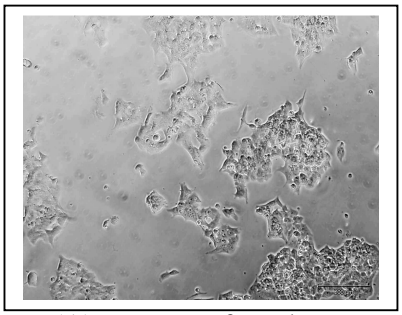

(A) Non-transfected

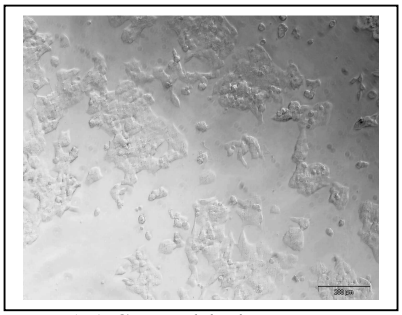

(B) Scrambled

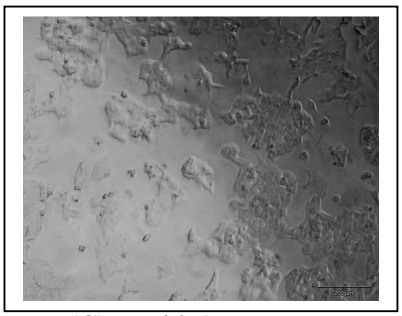

(C) *Pcsk9*-1

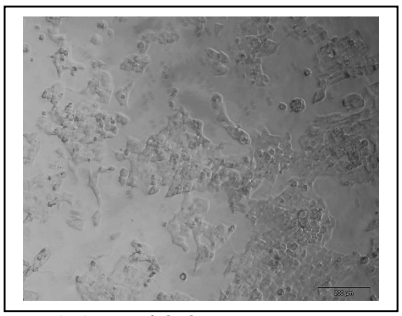

(D) *Pcsk9*-2

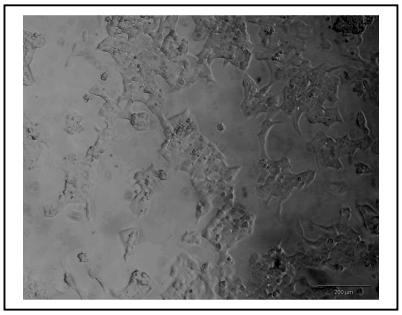

(E) *Pcsk9*-3

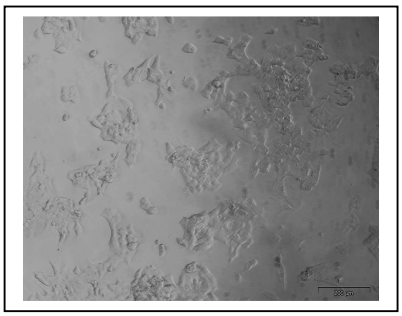

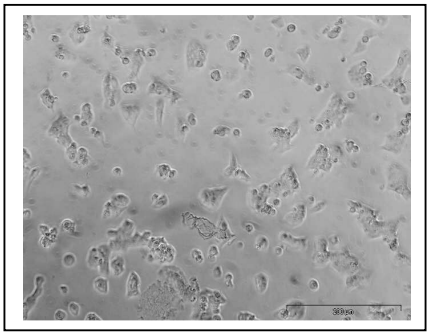

(G) Kinesin

**Fig: 3.7.1.2 Photographs (A) Non-transfected, (B) scrambled, (C) *Pcsk9*-1, (D) *Pcsk9*-2, (E) *Pcsk9*-3, (F) *Gapdh* and (G) *kinesin* siRNA transfected cells. Rounded morphology of cells indicates cell arrest.**

### 3.7.2 qRT-PCR

qRT-PCR was performed on three independent *Pcsk9* siRNA transfected MIN6 low passage cells (passage 35) along with scrambled and non-transfected cells. After 72hrs. of siRNA transfection RNA was isolated (See Section: 2.5.1.2.3) and cDNA was prepared (See Section: 2.5.2.1). Fig: 3.7.2 shows the qRT-PCR results 72hrs. after transfection. qRT-PCR showed a knock-down of approx. 39% in *Pcsk9*-1, 4.3% in *Pcsk9*-2 and 46.6% in *Pcsk9*-3 siRNA-transfected cells compared to scrambled siRNA-transfected cells

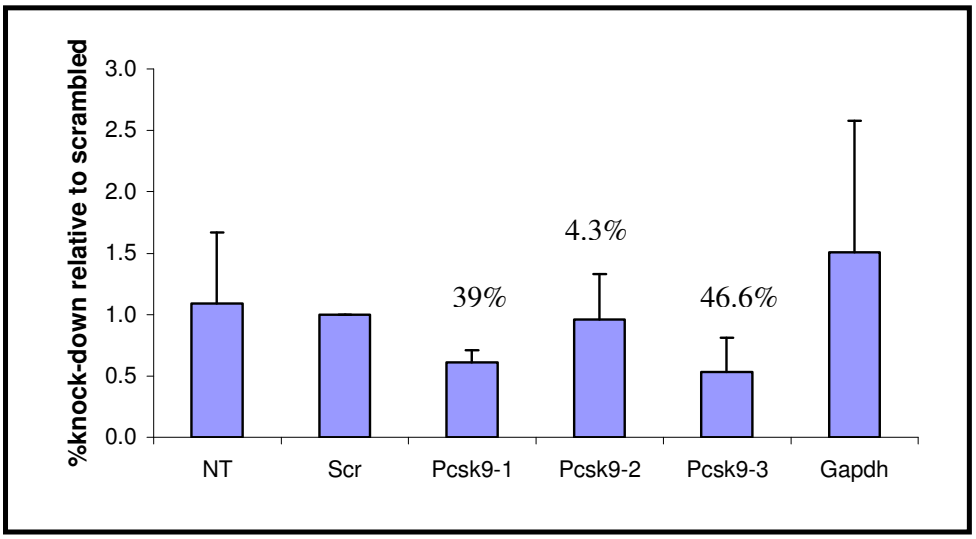


**Fig: 3.7.2 MIN6 low passage cells were transfected with *Pcsk9*, Scr and Gapdh. After 72hrs. of siRNA transfection RNA was isolated and qRT-PCR was performed for *Pcsk9* mRNA level. Pcsk9 -1 induced 39%, Pcsk9 -3 induced 46.6% whereas Pcsk9 -2 showed just 4.3% knock-down in MIN6 low passage cells. NT=non-transfected, Scr= Scrambled, Pcsk9 -1, 2, 3= *Pcsk9* siRNA (n=3) and Gapdh= *Gapdh* siRNA transfected cells. Results represent mean ± S.D from three different experiments.**

### 3.7.3 GSIS after *Pcsk9* siRNA transfection

Three independent *Pcsk9*-specific siRNA was transfected in MIN6 low passage cells to determine if silencing of *Pcsk9* affects GSIS. GSIS assay (See Section: 2.3.2.1) was performed after 72hrs. of siRNA transfection (See Section: 2.5.4.1.2). The three *Pcsk9*-specific siRNA transfected MIN6 low passage cells along with *Gapdh*-transfected cells, scrambled-transfected cells and non-transfected cells were incubated in 3.3 and 16.7mmol/L glucose for 1hr (See Section: 2.3.2.1). Insulin secretion was determined using ELISA (See Section: 2.3.2.4) and normalised to total cellular protein.

There was a significant loss of GSIS in *Pcsk9*-1 (p-value=0.007) and *Pcsk9*-3 (p-value= 0.013) siRNA transfected MIN6 low passage cells whereas *Pcsk9*-2 transfected cells did not show a significant loss of GSIS (*Pcsk9*-2 (p-value=0.058)) compared to scrambled siRNA-transfected cells. *Pcsk9*-1 showed 1.5-fold, *Pcsk9*-2 showed 1.7-fold and *Pcsk9*-3 showed 1.2-fold GSIS whereas non-transfected and scrambled-transfected cells showed 2.2-fold and 2.0-fold GSIS respectively (Fig:3.7.3). Gapdh-transfected cells showed a GSIS of 1.6-fold and were not significantly (0.76) different compared to scrambled siRNA-transfected cells.

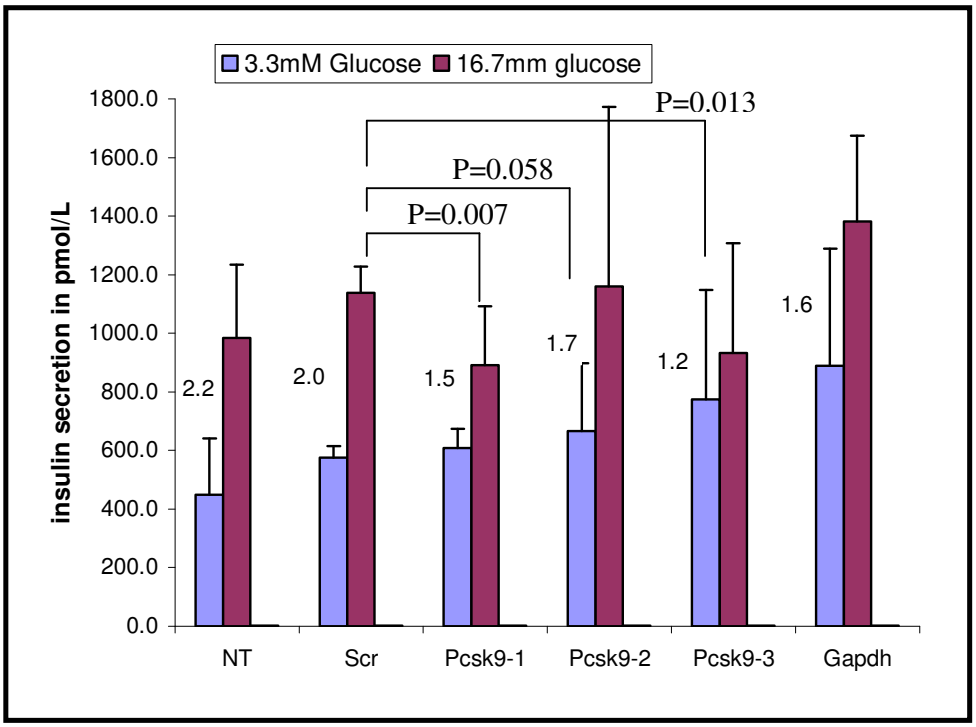


**Fig: 3.7.3 siRNA-mediated knockdown of *Pcsk9* decreases GSIS in MIN6 low passage cells. GSIS was quantitated in non-transfected MIN6 low passage cells and MIN6 cells transfected with either scrambled siRNA, *Pcsk9* siRNA or the *Gapdh* siRNA. GSIS assay was performed 72hrs. after transfection. Insulin secretion was measured by ELISA and normalised to total cellular protein. The other numbers near the bars shows the GSIS fold change. NT= non-transfected, Scr= scrambled transfected, *Pcsk9* -1, 2, 3= *Pcsk9* siRNA (n=3), Gapdh= siRNA transfected cells. Results represent mean ± S.D from three different experiments.**

### 3.7.4 Summary of results for *Pcsk9* siRNA transfection in MIN6 low passage

Results from proliferation assays showed that the optimum conditions for transfection were used, as a reduction in growth of cells transfected with kinesin siRNA was observed in MIN6 low passage cells. This also showed that transfection of *Pcsk9* siRNA did not have a notable effect on proliferation. After transfection with three separate *Pcsk9* siRNAs, there was a decrease in *Pcsk9* mRNA as estimated by qRT-PCR. This was accompanied by a significant decrease in GSIS.

There was no over-expression study performed on this gene transcript as there was no cDNA available to purchase and time did not allow cloning of this product.

### 3.8 Thioredoxin interacting protein (*Txnip*)

*Txnip* was up-regulated in the MIN6 B1(Non-GSIS) cells compared to MIN6 B1(GSIS) cells in the microarray study. The microarray study showed a 5.25-fold and qRT-PCR showed 3.11-fold up-regulation of *Txnip* in MIN6 B1(Non-GSIS) cells compared to MIN6 B1(GSIS). To investigate the relevance of *Txnip* in glucose-stimulated insulin secretion, *Txnip* specific siRNA transfection was performed in high passage MIN6 cells.

#### 3.8.1 Proliferation assay

Cells grown in 96-well plates were assayed for changes in proliferation at 72hrs. using the acid phosphatase assay (See Section: 2.3.3). Proliferation assays were carried out on MIN6 high passage cells transfected with *Txnip* siRNA including *Kinesin* siRNA as a positive control. Cellular growth arrest in the presence of *Kinesin* siRNA was taken as confirmation of efficient transfection conditions. Reduced growth of *Kinesin* siRNA-transfected cells compared to scrambled siRNA-transfected cells was observed. There was no significant effect in growth when transfected with *Txnip* specific siRNA compared to scrambled siRNA-transfected cells (Fig: 3.8.1.1).

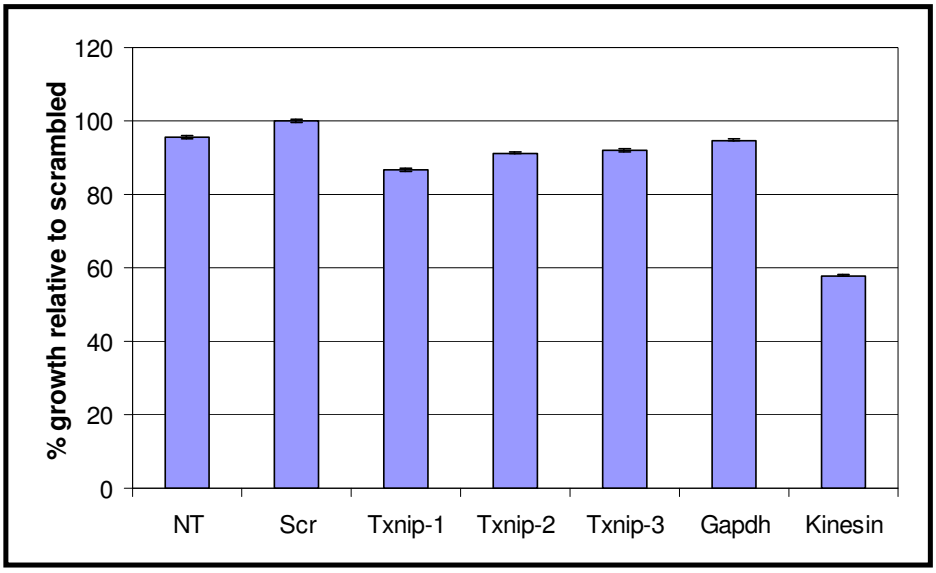


**Fig: 3.8.1.1 Growth rate of MIN6 high passage cells after siRNA transfection using *Txnip* (n=3), Scrambled and *Kinesin*. Scrambled, *Gapdh* and *Kinesin*. NT=non-transfected cells, Scr= scrambled transfected, *Txnip* -1, 2, 3= 3 different siRNA.**

There was no change in the morphology of the cells after siRNA transfection except for kinesin siRNA-transfected cells that showed a rounded morphology indicating cell growth arrest (Fig:3.8.1.2).

**Effect of *Txnip* and kinesin siRNA on cell morphology of MIN6 cells**

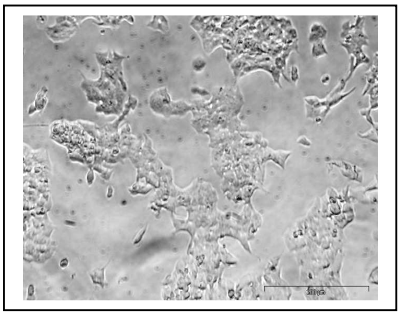

(A) Non-transfected

(B) Scrambled

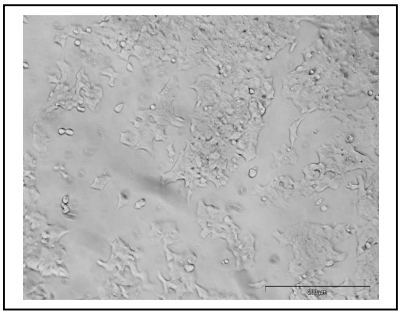

(C) *Txnip*-1

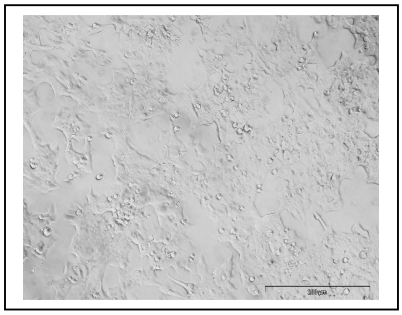

(D) *Txnip*-2

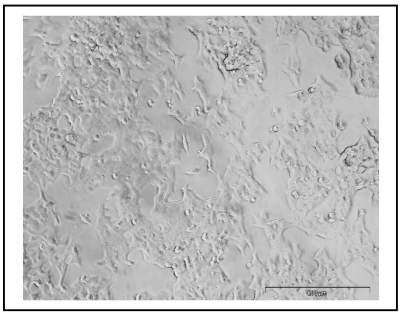

(E) *Txnip*-3

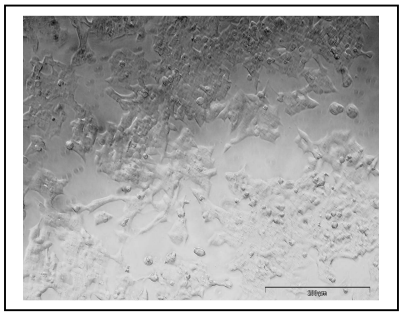

(F) *Gapdh*

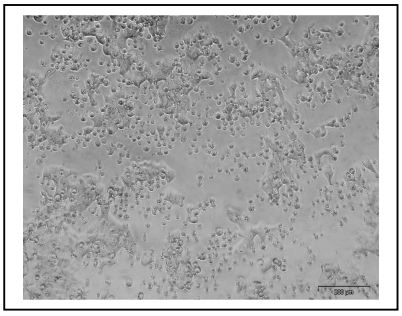

(G) Kinesin

**Fig: 3.8.1.2 Photographs (A) Non-transfected, (B) scrambled, (C) *Txnip*-1, (D) *Txnip*-2, (E) *Txnip*-3, (F) *Gapdh* and (G) *kinesin* siRNA transfected cells. Rounded morphology of cells indicates cell growth arrest.**

### 3.8.2 qRT-PCR after siRNA transfection

qRT-PCR was carried out on MIN6 high passage cells (passage 47) transfected with three independent *Txnip* siRNA. RNA was isolated (See Section: 2.5.1.2.3) from the non-transfected, scrambled siRNA-transfected, *Txnip* siRNA-transfected and *Gapdh* siRNA-transfected cells after 72hrs. of transfection. Fig: 3.8.2 shows a knock-down of *Txnip* mRNA in *Txnip* specific siRNA-transfected cells compared to scrambled siRNA-transfected cells. qRT-PCR showed *Txnip* mRNA knock-down of approx. 43.5% in *Txnip*-1, 42.4% in *Txnip*-2 and 25.3% in *Txnip*-3 siRNA-transfected cells compared to scrambled siRNA-transfected cells (Fig: 3.8.2).

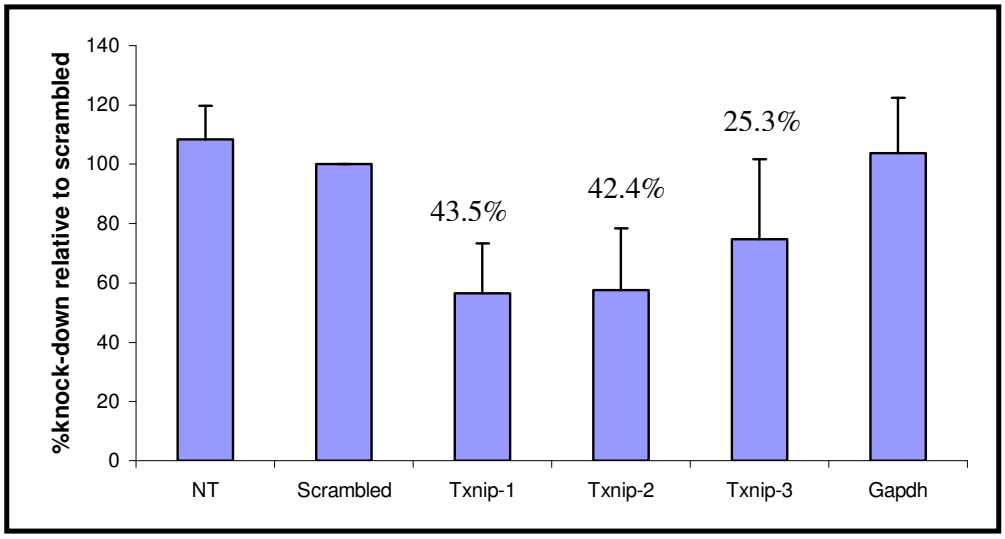


**Fig: 3.8.2 MIN6 high passage cells were transfected with *Txnip*, Scr and *Gapdh*. After 72hrs. of siRNA transfection RNA was isolated and qRT-PCR was performed for *Txnip* mRNA level. Txnip -1 induced 43.5%; Txnip -2 induced 42.4% whereas Txnip -3 induced 25.3% knock-down in MIN6 high passage cells. NT=non-transfected, Scr= Scrambled, Txnip -1, 2, 3= *Txnip* siRNA (n=3) and Gapdh= *Gapdh* siRNA transfected cells. Results represent mean ± S.D from three different experiments.**

### 3.8.3 GSIS after *Txnip* siRNA

Three independent *Txnip*-specific siRNAs were transfected in MIN6 high passage cells (passage 47) to determine if silencing of *Txnip* affects GSIS. GSIS assay (See Section: 2.3.2.1) was performed after 72hrs. of siRNA transfection (See Section: 2.5.4.1.2). The three *Txnip*-specific siRNA transfected MIN6 high passage cells along with *Gapdh* siRNA-transfected cells, scrambled-transfected cells and non-transfected cells were incubated in 3.3 and 16.7mmol/L glucose for 1hr (See Section: 2.3.2.1). Insulin secretion was determined using ELISA (See Section: 2.3.2.4) and normalised to total cellular protein.

There was a significant increase in GSIS in *Txnip* -1 (p-value=0.03) and *Txnip* -2 (p-value=0.019) siRNA transfected MIN6 high passage cells whereas there was no significant increase in GSIS with *Txnip*-3 (p-value=0.93) compared to scrambled siRNA transfected cells (Fig: 3.8.3). *Txnip* -1 showed 1.4-fold, *Txnip* -2 showed 1.6-fold and *Txnip*-3 showed 0.9-fold GSIS whereas non-transfected and scrambled-transfected cells showed 0.9-fold and 0.9-fold GSIS respectively (Fig: 3.8.3).

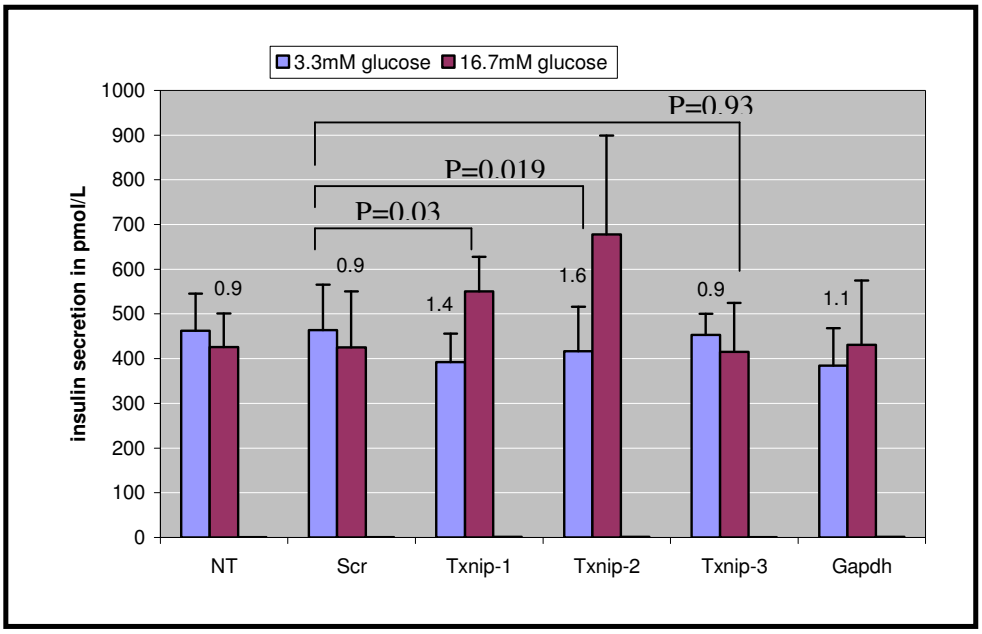


**Fig: 3.8.3 siRNA-mediated knockdown of *Txnip* increases GSIS in MIN6 high passage cells. GSIS was quantitated in non-transfected MIN6 high passage cells and transfected with either scrambled siRNA, *Txnip* siRNA or the *Gapdh* siRNA. GSIS assay was performed 72hrs. after transfection. Insulin secretion was measured by ELISA and normalised to total cellular protein. NT= non-transfected, Scr= scrambled transfected, Txnip -1, 2, 3= *Txnip* siRNA (n=3), Gapdh= *Gapdh* siRNA transfected cells. Results represent mean ± S.D from three different experiments.**

### 3.8.4 qRT-PCR after cDNA over-expression

qRT-PCR was carried out on *Txnip* cDNA over-expressed MIN6 low passage cells (passage 35). RNA was isolated (See Section: 2.5.1.2.3) from the cells 72hrs. after cDNA over-expression. RNA were then treated with DNase enzyme (See Section: 2.5.1.3.1) and cDNA prepared from the treated RNA (See Section: 2.5.2.1). Fig: 3.8.4 shows a 23.7-fold increase of *Txnip* mRNA in *Txnip* plasmid-transfected cells compared to empty plasmid-transfected cells. To exclude any amplification product derived from genomic DNA or any other contaminent that could contaminate the DNase-treated RNA preparation, DNase-treated RNA without reverse transcriptase enzyme and water on its own was amplified as a negative controls (See Section: 2.5.3.1).

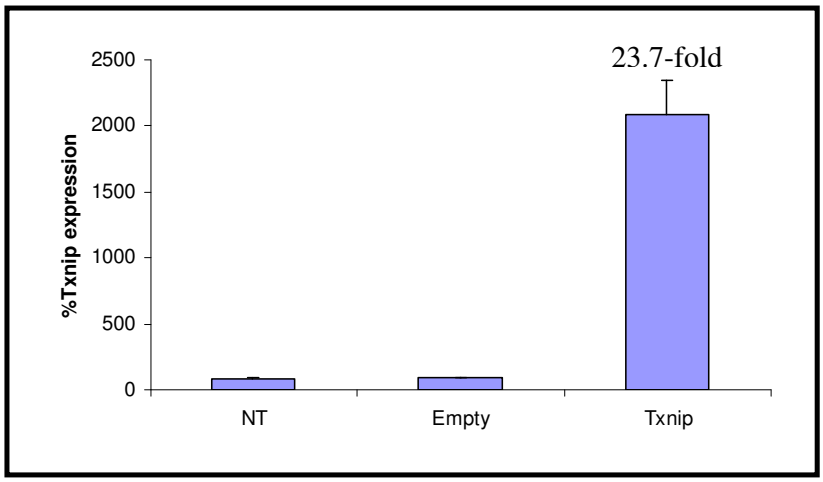


**Fig: 3.8.4 MIN6 low passage cells were transfected with empty plasmid and *Txnip* plasmid. qRT-PCR for *Txnip* mRNA level was performed after 72hrs. of cDNA over-expression in MIN6 low passage cells. A 23.7-fold increased expression of *Txnip* mRNA was observed in *Txnip* plasmid-transfected cells compared to empty plasmid-transfected cells The results represent mean ± S.D from three different experiments.**

### 3.8.5 GSIS after *Txnip* cDNA over-expression

*Txnip* cDNA over-expression was performed on MIN6 low passage cells (passage 35). GSIS assay (See Section: 2.3.2.1) was performed 72hrs. after transfection. *Txnip* cDNA transfected MIN6 low passage cells along with empty-transfected cells and non-transfected cells were incubated in 3.3 and 16.7mmol/L glucose for 1hr (See Section: 2.3.2.1). Insulin secretion was measured using ELISA (See Section: 2.3.2.4) and normalised to total cellular protein.

There was a significant loss (p-value= 0.013) of GSIS in *Txnip* over-expressed cells compared to empty plasmid-transfected cells (Fig: 3.8.5). *Txnip* cDNA transfected cells showed 1.89-fold GSIS whereas non-transfected and empty-transfected cells showed 2.9-fold and 2.67-fold GSIS respectively.

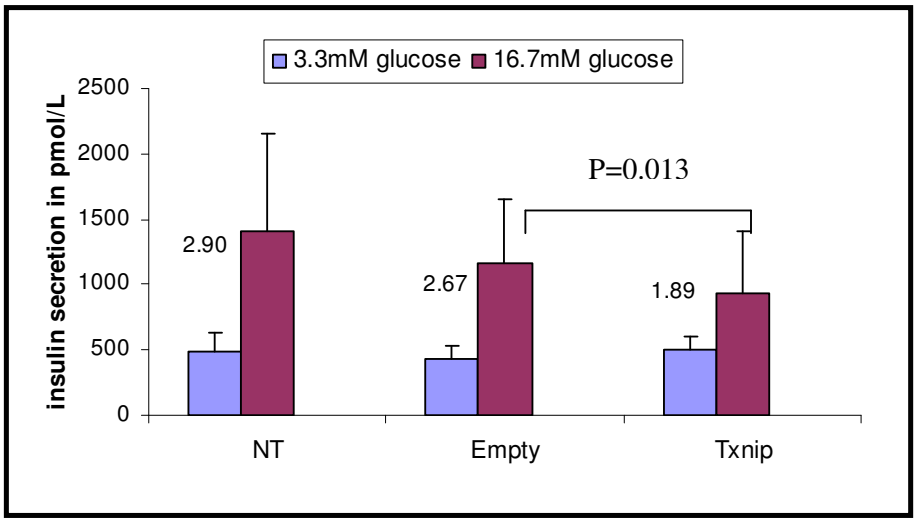


**Fig: 3.8.5 Over-expression of *Txnip* led to a significant (p-value= 0.013) loss of GSIS in MIN6 low passage cells compared to empty-transfected cells. GSIS was quantitated in non-transfected MIN6 low passage cells and MIN6 cells transfected with either empty plasmid or the *Txnip* Plasmid. GSIS was measured 72hrs. after plasmid transfection. *Txnip* cDNA transfected cells showed 1.89-fold GSIS whereas non-transfected and empty-transfected cells showed 2.9-fold and 2.67-fold GSIS respectively. Results represent mean ± S.D from three different experiments.**

### 3.8.6 Western Blot analysis

Western blot analysis was performed using Txnip specific antibody to detect the expression of Txnip protein in MIN6 cells. However there was no band detected for Txnip protein using MIN6 cell lysate. Some cell lines including, MDA-MB-453, MDA-MB-231, BT-474, MCF 7 and MDA-MB-157 were used as positive controls. These cells showed high expression of *Txnip* mRNA in microarray study (publicly available datasets) and was used as positive control. Fig 3.8.6 shows detectable band for Txnip protein at 50 kDa using cell lysate from MDA-MB-453, MDA-MB-231, BT-474, MCF 7 and MDA-MB-157, whereas no band was detected in MIN6 cell lysate. Gapdh was used as a control to show equal loading of cell lysate in all wells. Gapdh was detected at 40 kDA in cell lysate from all the cell lines (Fig: 3.8.6).

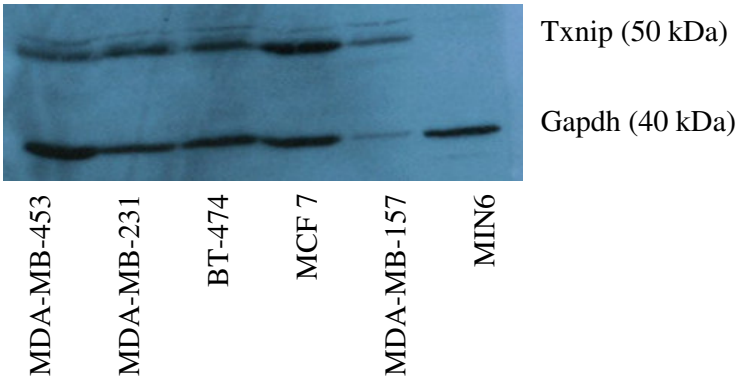


**Fig: 3.8.6 Western blot showing level of expression of Txnip protein in MDA-MB-453, MDA-MB-231, BT-474, MCF 7 and MDA-MB-157 used as positive control and MIN6 cell lysate.**

### 3.8.7 Summary of results for *Txnip* siRNA transfection in MIN6 high passage

Results from proliferation assays showed a reduction in growth of MIN6 high passage cells transfected with *kinesin* siRNA and that transfected with *Txnip* siRNA did not have a major effect on proliferation. After transfection with two out of three separate *Txnip* siRNAs there was a decrease in *Txnip* mRNA as estimated by qRT-PCR. This was accompanied by significant increase in GSIS in *Txnip* specific siRNA-transfected cells compared to scrambled siRNA-transfected cells.

*Txnip* was then over-expressed in low passage MIN6 cells to see if GSIS was lost following over-expression. *Txnip* mRNA level was determined using qRT-PCR after DNase-treatment of the RNA from the transfected cells. There was a 23.7-fold increase in *Txnip* expression in *Txnip* plasmid-transfected cells compared to empty plasmid-transfected cells. *Txnip* cDNA over-expression showed a significant (p-value= 0.013) loss of GSIS in MIN6 low passage cells compared to empty plasmid-transfected cells.

Western blot analysis was performed using Txnip specific antibody but no bands were detected for Txnip protein using MIN6 cell lysate, whereas there was a band detected using Gapdh antibody.

### 3.9 *Txnip* shRNA transfection

A significant increase in GSIS was observed after *Txnip* specific siRNA transfection in MIN6 high passage cells compared to scrambled transfected-cells. siRNA-induced silencing is short-lived so to study long-term effect of silencing a gene shRNA technique is used. Therefore *Txnip* shRNA was transfected in MIN6 high passage cells to establish a stable cell line that hopefully would not loose its GSIS phenotype with passaging. A set of five shRNA (Open biosystems, RMM4534-NM_001009935) were transfected in high passage MIN6 cells.

#### 3.9.1 qRT-PCR on heterogeneous population shRNA-transfected cells

qRT-PCR was performed (See Section: 2.5.3.1) on heterogeneous cell population to check the expression level of *Txnip* mRNA. MIN6 high passage cells were transfected with *Txnip* shRNA and empty plasmid shRNA as control in a 24-well plate. After 72hrs. of transfection cells were fed with puromycin containing media (selection media) for selection of transfected cells. Cells were fed with this selection media every 2-3 days until the cells were confluent. Cells were then trypsinised and transfered to a T25cm$^2$ flask and grown for RNA isolation. RNA was isolated (See Section: 2.5.1.2.3) from empty plasmid transfected cells as well as five independent *Txnip* shRNA transfected cells. qRT-PCR showed *Txnip* mRNA knock-down of approx. 21.8% in *Txnip* shRNA-3 and 25.4% in *Txnip* shRNA-4 transfected cells compared to empty shRNA-transfected cells. Whereas shRNA-1, shRNA-2 and shRNA-5 showed no knock-down of *Txnip* mRNA compared to empty shRNA-transfected cells (Fig: 3.9.1).

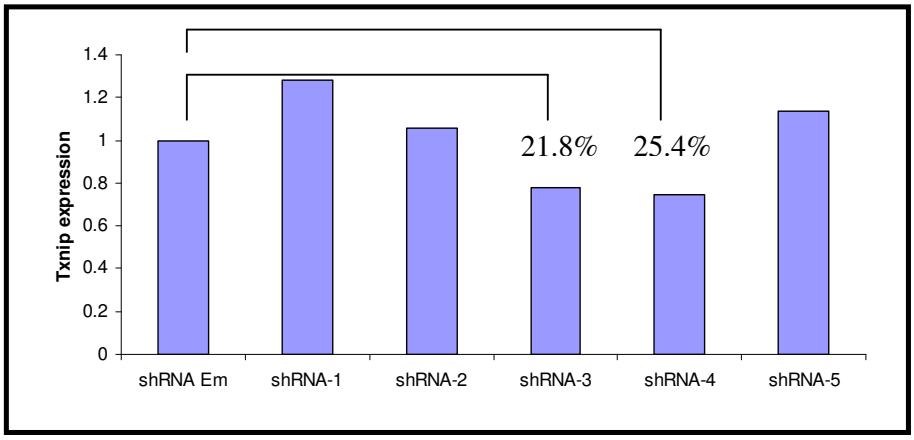


**Fig: 3.9.1 MIN6 high passage cells were transfected with *Txnip* shRNA and empty plasmid (Em) as control. RNA was isolated and qRT-PCR was performed for *Txnip* mRNA level. shRNA-1, shRNA-2 and shRNA-5 did not show any knock-down of *Txnip* mRNA whereas, shRNA-3 induced 21.8% and shRNA-4 induced 25.4% knock-down of *Txnip* mRNA in MIN6 high passage cells.**

### 3.9.2 GSIS on heterogeneous population of shRNA-transfected cells

GSIS assay (See Section: 2.3.2.1) was performed on heterogeneous population of *Txnip* shRNA-transfected and empty shRNA-transfected cells (See Section: 2.5.4.1.2). Insulin secretion was determined using ELISA (See Section: 2.3.2.4) and normalised by protein. There was an increase in GSIS in *Txnip* shRNA-3 (2.16-fold) and shRNA-4 (1.28-fold) transfected cells compare to empty shRNA-transfected cells (1.16-fold) (Fig: 3.9.2).

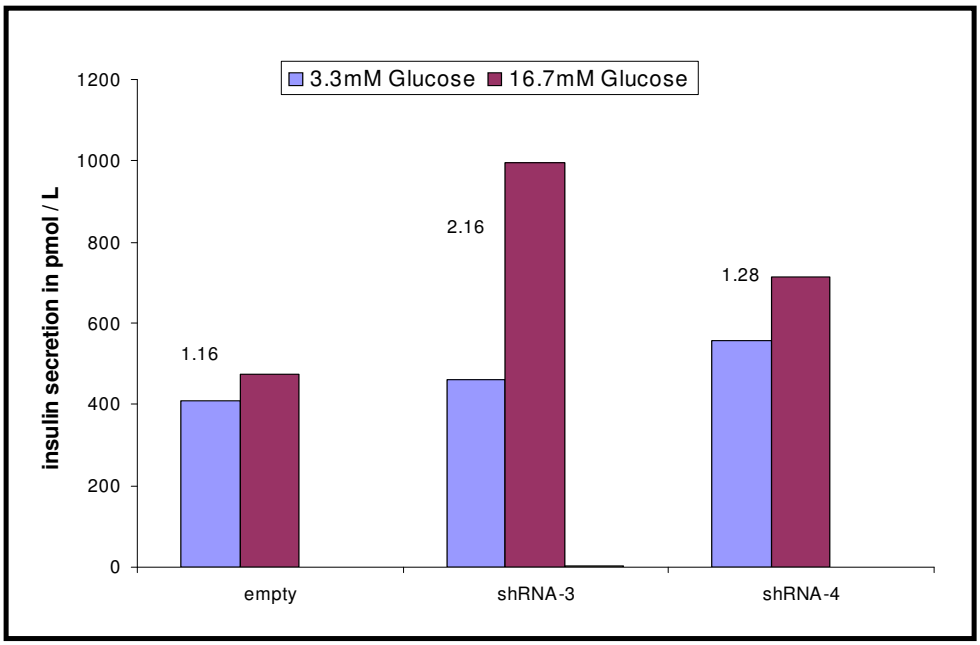


**Fig: 3.9.2 shRNA-mediated knock-down of *Txnip* increased GSIS in MIN6 high passage cells. GSIS was quantitated in empty shRNA-transfected cells and *Txnip* shRNA-3 and shRNA-4 transfected cells. Insulin secretion was measured by ELISA and normalised to total cellular protein. shRNA-3 and shRNA-4 transfected cells showed *Txnip* mRNA knock-down by qRT-PCR.**

### 3.9.3 Cell morphology heterogeneous population of shRNA-transfected cells

Morphological analysis was performed using phase contrast light microscopy. The morphological analysis indicated that *Txnip* shRNA-transfected cells grows as tight, rounded, localised clumps whereas, empty shRNA-transfected cells form a monolayer of "flat", stretched cells (Fig: 3.9.3).

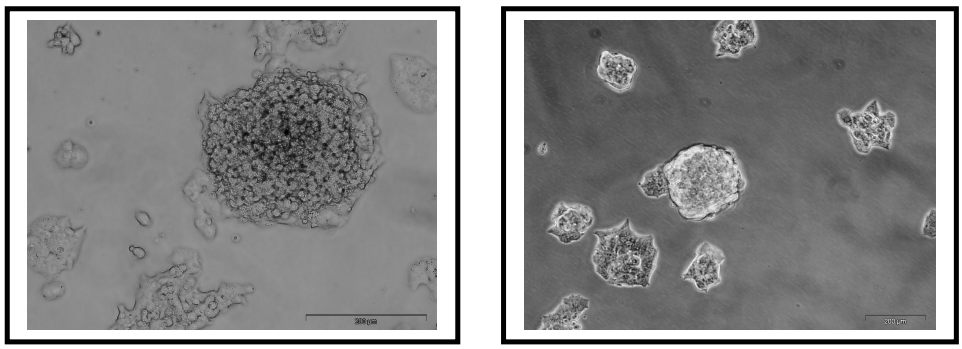

Txnip shRNA-3 transfected cells  Txnip shRNA-4 transfected cells

Empty shRNA transfected cells

**Fig: 3.9.3 MIN6 cells transfected with *Txnip* shRNA and empty shRNA plasmid and grown in T75cm$^2$ vented flask. These cells were photographed using phase-contrast microscope. (Magnification = 20X; scale bar = 200 µM)**

### 3.9.4 Establishing single cell colonies

Heterogeneous population of *Txnip* shRNA-transfected cells and empty shRNA-transfected cells were plated in 96-well plate for establishing single cell colonies (See Section: 2.5.4.3). When confluent enough these colonies were trypsinised and transferred to a 24-well plate and then to T25cm$^2$ flask. Single cell colonies were developed from heterogeneous population of 2 different sets of *Txnip* shRNA-transfected cells (shRNA-3 and shRNA-4) that showed maximum knock-down of *Txnip* mRNA.

### 3.9.4.1 qRT-PCR on clones

Empty shRNA plasmid-transfected cells were harvested to check the *Txnip* mRNA level using qRT-PCR (See Section: 2.5.3.1). Empty shRNA plasmid-transfected cells were used as controls in this study. In order to select the clones that showed high level of *Txnip* expression, RNA was isolated (See Section: 2.5.1.2.3) from each cell colony and was screened for *Txnip* mRNA level (Fig: 3.9.4.1.1).

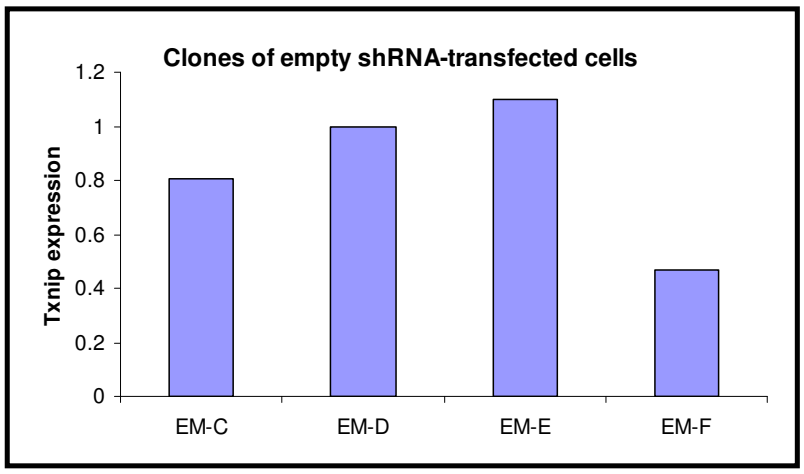


**Fig: 3.9.4.1.1 Level of *Txnip* expression as determined by qRT-PCR in clones of empty shRNA-transfected cells. EM-C, EM-D, EM-E and EM-F represent different clones from heterogeneous population of empty shRNA-transfected cells.**

*Txnip* specific shRNA transfected colonies were used to study the effect of *Txnip* knock-down on GSIS. To verify the levels of *Txnip* mRNA in *Txnip* shRNA transfected cells, clones were harvested to check for low *Txnip* expressing colonies. RNA was isolated (See Section: 2.5.1.2.3) from each cell colony of *Txnip* shRNA-transfected cells and was screened for *Txnip* mRNA knock-down (Fig: 3.9.4.1.2). The *Txnip* mRNA knock-down was calculated compared to empty shRNA plasmid-

transfected clone (Em-D). *Txnip* shRNA-transfected clones sh-16, sh-1 and sh-9 showed 74.7%, 81.4% and 78.5% *Txnip* mRNA knock-down respectively. The other clones showed the *Txnip* expression of 50% or less. For further study clones sh-1 and sh-9 was used as they showed a maximum knock-down of *Txnip*.

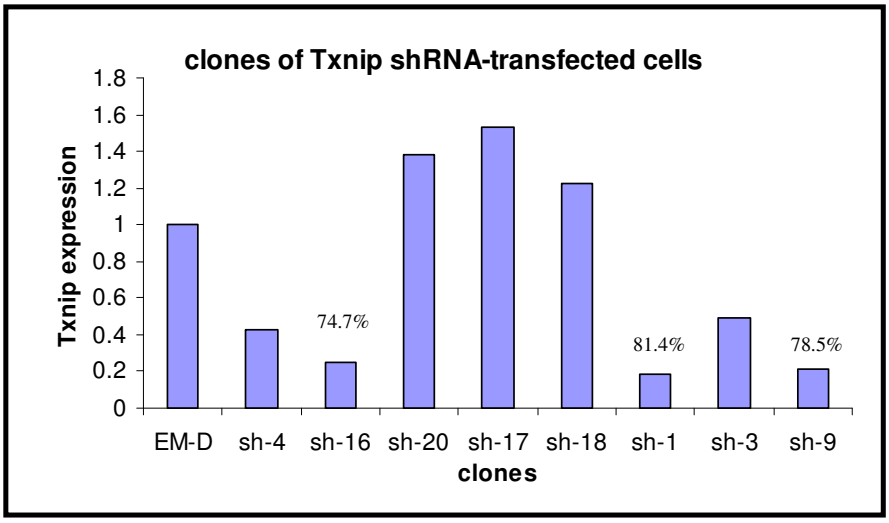


**Fig: 3.9.4.1.2 Level of *Txnip* expression as determined by qRT-PCR on clones of *Txnip* shRNA-transfected cells. Sh-4, sh-16, sh-20, sh-17, sh-18, sh-1, sh-3 and sh-9 represent different clones from heterogeneous population of *Txnip* shRNA-transfected cells. Clone sh-1 and sh-9 were chosen for further studies as they showed the maximum knock-down of *Txnip* mRNA.**

### 3.9.4.2 ELISA on clones

*Txnip* was up-regulated in the microarray study (5.25-fold) and qRT-PCR study (3.11-fold) in MIN6 B1(Non-GSIS) cells compared to MIN6 B1(GSIS) cells. Clone sh-1 (*Txnip* shRNA transfected clone#1) showed a significant increase in GSIS (p-value=0.024) and a moderate but not significant (p-value=0.23) increase in sh-9 clone (*Txnip* shRNA-transfected clone#9) compared to empty shRNA-transfected cells.

*Txnip* shRNA-transfected clones were incubated in 3.3 and 16.7mmol/L glucose for 1hr (See Section: 2.3.2.1). Insulin secretion was determined using ELISA (See Section: 2.3.2.4) and normalised to total cellular protein. sh-1 showed 2.96-fold, sh-9 showed 1.82-fold, sh-3 showed 1.08-fold and Em-F (empty shRNA-transfected cells) showed 1.58-fold GSIS (Fig: 3.9.4.2).

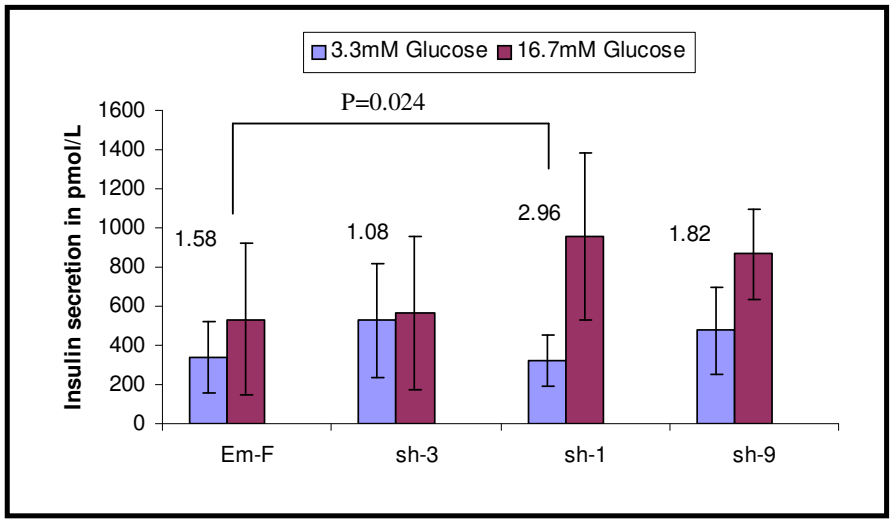


**Fig: 3.9.4.2 shRNA-mediated knock-down of *Txnip* led to a significant increase in GSIS in sh-1 clone (*Txnip* shRNA-transfected cells clone#1 (p-value= 0.024)) and a mild increase in sh-9 clone but not significant (p-value=0.23) (*Txnip* shRNA-transfected cells clone#9) compared to empty shRNA transfected cells. GSIS was quantitated in Em-F, sh-3, sh-1 and sh-9 clones. Insulin secretion was measured by ELISA and normalised to total cellular protein. Em-F (empty shRNA transfected clone), sh-3 (*Txnip* shRNA transfected clone with no *Txnip* mRNA knock-down) and sh-1 and sh-9 (clone showing *Txnip* mRNA knock-down). Results represent mean ± S.D from three different experiments.**

### 3.9.4.3 ROS levels in clones

In order to assess whether *Txnip* knock-down exerted any effect in regulating ROS (reactive oxygen species) as an indicator of oxidative stress, the ROS level was detected by 2′,7′-dichlorodihydrofluorescein diacetate (DCFHDA) and expressed as percentage relative to empty shRNA-transfected cells (Em-F) (See Section: 2.5.9).

*Txnip* shRNA transfected clone sh-1 and sh-9 showed a reduced ROS level of 40.5% and 35.6% respectively compared to empty shRNA transfected clone Em-F. Whereas, *Txnip* shRNA-transfected clone sh-3 (which showed no *Txnip* mRNA knock-down) showed 3.4% more ROS compared to empty shRNA transfected clone Em-F (Fig: 3.9.4.3).

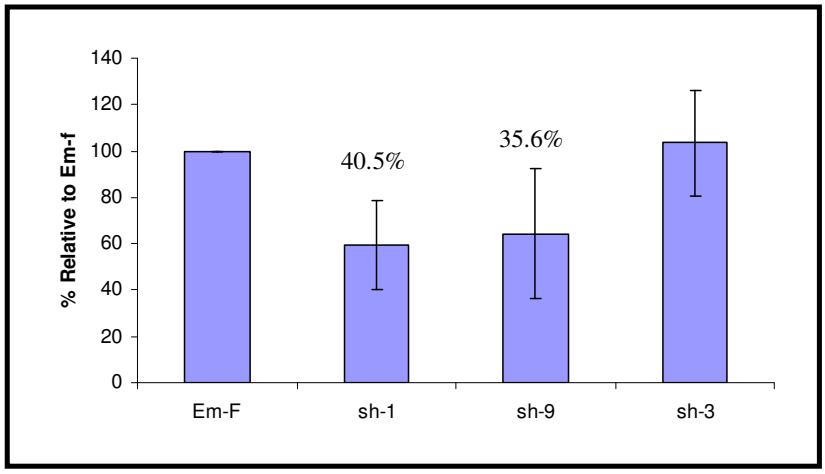


**Fig: 3.9.4.3 Cells were assessed for ROS levels by DCFHDA fluorescence staining. *Txnip* shRNA transfected clone sh-1 and sh-9 showed a ROS % of 40.5% and 35.6% respectively. sh-3 (with no *Txnip* mRNA knock-down) showed a 3.4% more ROS level compared to Em-F. Results represent mean ± S.D from three different experiments.**

### 3.9.4.4 Proliferation assay on clones

Proliferation assay was performed on shRNA transfected cells using acid phosphatase assay (See Section: 2.3.3). Growth curves were plotted over 7 days following seeding at a density of 1 X $10^4$ cells/well (96-well plate). An increased proliferation rate was observed in *Txnip* shRNA transfected sh-3 clone (Fig: 3.9.4.4).

Clone sh-3 (*Txnip* shRNA transfected clone#3) showed no *Txnip* mRNA knock-down compared to empty shRNA transfected cells. Clone sh-3 showed 1.5-fold increased proliferation compared to Em-F whereas, clone sh-1 showed 1.3-fold reduced proliferation compared to Em-F (Fig: 3.9.4.4).

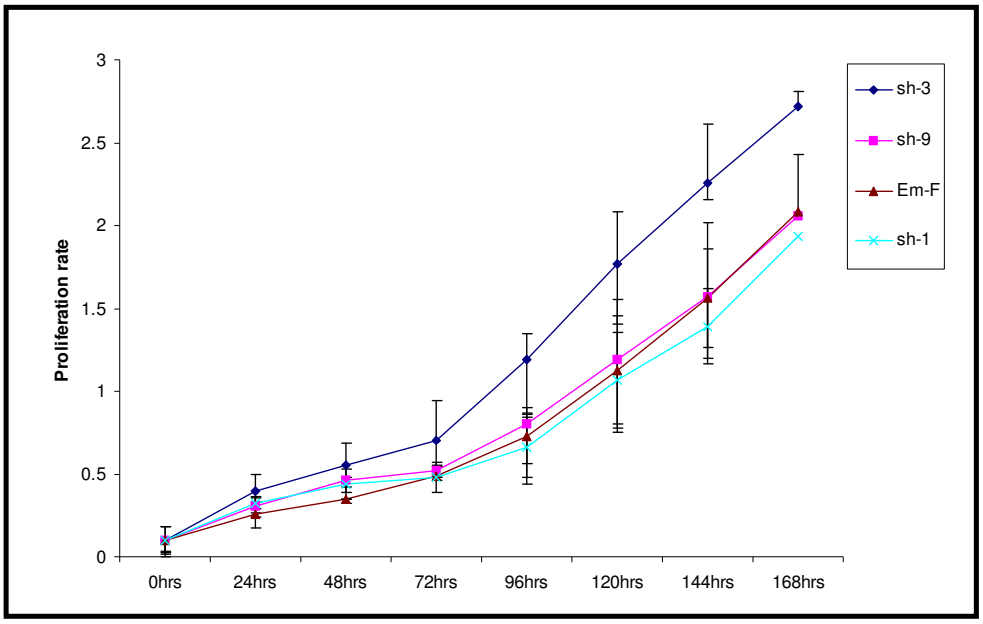


**Fig: 3.9.4.4 Graph showing comparison of proliferation assay performed on MIN6 *Txnip* shRNA-transfected and empty shRNA transfected cells. Empty shRNA transfected cells are shown as (—▲—), Txnip shRNA transfected cells clone#9 (sh-9) (—■—), clone#1 (sh-1) (—✕—) and clone#3 (sh-3) (—◆—). Txnip shRNA transfected clone#3 did not show any knock-down of *Txnip* mRNA. Mean = ± S.D and n=3.**

### 3.9.4.5 Gene transcripts affected by *Txnip* knock-down

#### *Txnip* knock-down decreases *Egr1* expression

*Egr1* was up-regulated in MIN6 B1(Non-GSIS) compared to MIN6 B1(GSIS) in the microarray (1.98-fold) and qRT-PCR (4.64-fold) study. The expression level of *Egr1* was determined by qRT-PCR in the single cell colonies of the *Txnip* shRNA transfected cells. *Txnip* knock-down clones showed a decreased expression of *Egr1* in sh-1 (52.7%) and sh-9 clones (56.2%) compared to empty vector-transfected Em-F clone. There was 54.8% increased expression of *Egr1* in sh-3 clones (with no *Txnip* knock-down) compared to empty vector-transfected Em-F clone (Fig: 3.9.4.5.1).

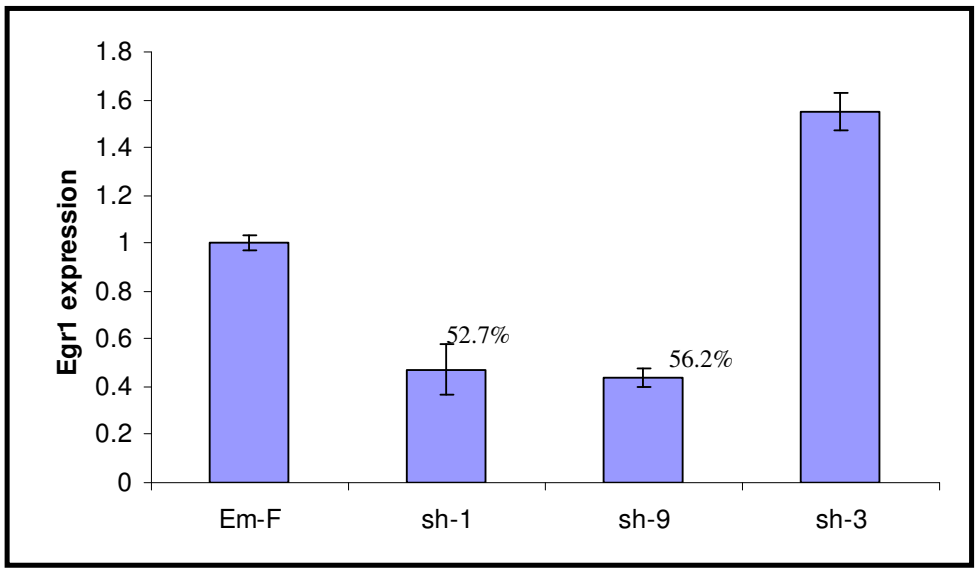


**Fig: 3.9.4.5.1 *Egr1* expression as determined by qRT-PCR in sh-1, sh-9 and sh-3 *Txnip* shRNA-transfected clone and Em-F empty shRNA transfected clone. sh-1 clone showed 52.7% and sh-9 clone showed 56.2% knock-down of *Egr1* compared to Em-F. sh-3 (*Txnip* shRNA transfected clone with no *Txnip* mRNA knock-down) and sh-1 and sh-9 (clone showing *Txnip* mRNA knock-down). Results represent mean ± S.D.**

***Txnip* knock-down decreases *Fos* expression**

The microarray (2.12-fold) and qRT-PCR (6.49-fold) study showed an up-regulation of *Fos* gene transcript in MIN6 B1(Non-GSIS) compared to MIN6 B1(GSIS). *Fos* expression level was determined by qRT-PCR in the single cell colony of the *Txnip* shRNA transfected cells. *Fos* expression was decreased in *Txnip* knock-down sh-1 clone (80.5%) and sh-9 clones (73.8%) compared to empty vector-transfected Em-F clone. Whereas, there was no knock-down of *Fos* in sh-3 clones (with no *Txnip* knock-down) compared to empty shRNA-transfected Em-F clone (Fig: 3.9.4.5.2).

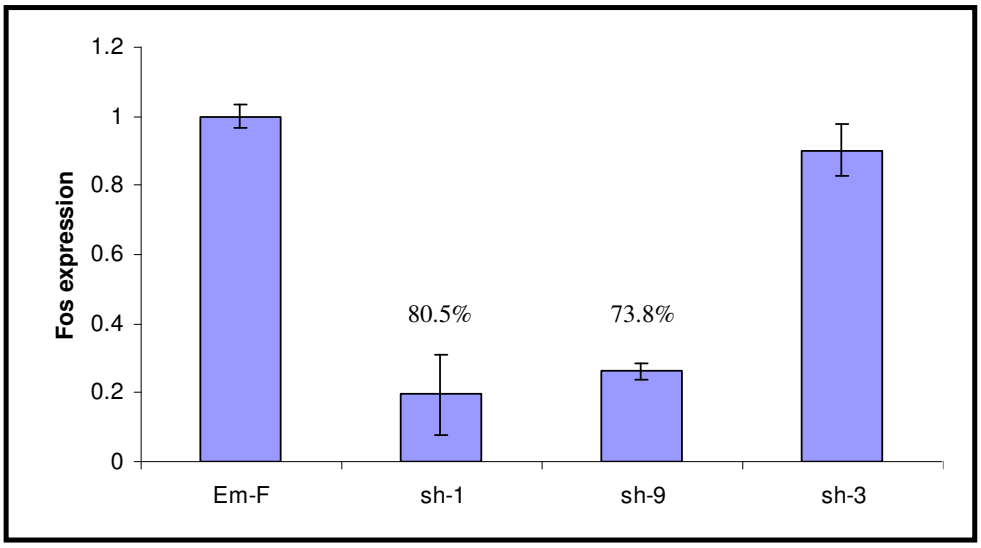


**Fig: 3.9.4.5.2 *Fos* expression as determined by qRT-PCR in sh-1, sh-9 and sh-3 *Txnip* shRNA-transfected clones and Em-F empty shRNA transfected clone. Sh-1 clone showed 80.5% and sh-9 clone showed 73.8% knock-down of *Fos* compared to Em-F. sh-3 (*Txnip* shRNA transfected clone with no *Txnip* mRNA knock-down) and sh-1 and sh-9 (clone showing *Txnip* mRNA knock-down). Results represent mean ± S.D.**

***Txnip* knock-down decreases *Gadd45g* expression**

An up-regulation of *Gadd45g* gene transcript was observed in MIN6 B1(Non-GSIS) compared to MIN6 B1(GSIS) following microarray (1.59-fold) and qRT-PCR (1.59-fold) study. The expression level of *Gadd45g* was determined by qRT-PCR in the single cell colony of the *Txnip* shRNA transfected cells. *Txnip* knock-down decreased the expression of *Gadd45g* in sh-1 (43.7%) and sh-9 clones (29.2%) compared to empty shRNA-transfected Em-F clone. Whereas, 16% knock-down of *Gadd45g* was observed in sh-3 clones (with no *Txnip* knock-down) compared to empty shRNA-transfected Em-F clone (Fig: 3.9.4.5.3).

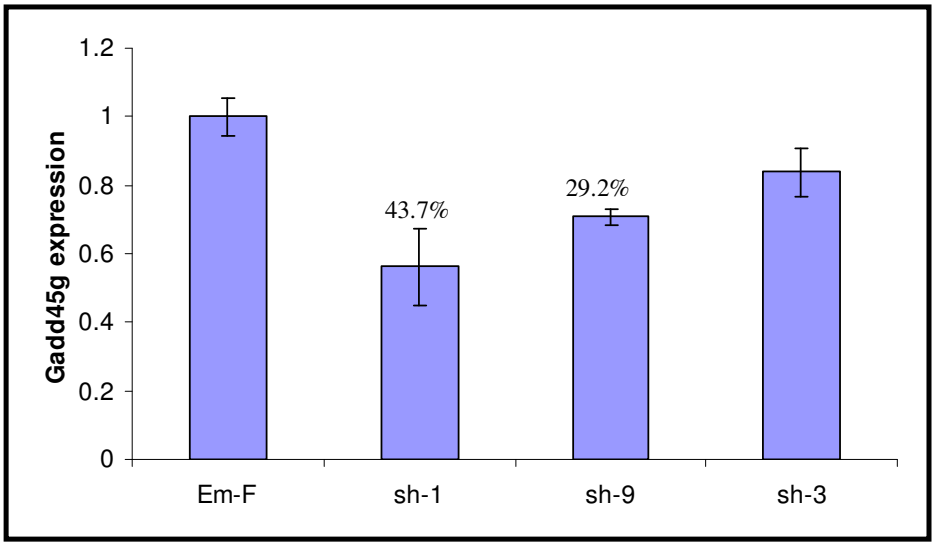


**Fig: 3.9.4.5.3 *Gadd45g* expression as determined by qRT-PCR in sh-1, sh-9 and sh-3 *Txnip* shRNA-transfected clones and Em-F empty shRNA transfected clone. Sh-1 clone showed 43.7% and sh-9 clone showed 29.2% knock-down of *Gadd45g* compared to Em-F. sh-3 (*Txnip* shRNA transfected clone with no *Txnip* mRNA knock-down) and sh-1 and sh-9 (clone showing *Txnip* mRNA knock-down). Results represent mean ± S.D.**

***Txnip* knock-down decreases *Jun* expression**

Up-regulation of *Jun* gene transcript was observed in MIN6 B1(Non-GSIS) compared to MIN6 B1(GSIS) following microarray (2.73-fold) and qRT-PCR (2.93-fold) study. qRT-PCR was performed to check the expression level of *Jun* in the single cell colony of the *Txnip* shRNA transfected cells. Expression of *Jun* was decreased in *Txnip* knock-down sh-1 clones (44.5%) and sh-9 clones (16.5%) compared to empty shRNA-transfected Em-F clone. There was 23% increased expression of *Jun* in sh-3 clones (with no *Txnip* knock-down) compared to empty shRNA-transfected Em-F clone (Fig: 3.9.4.5.4).

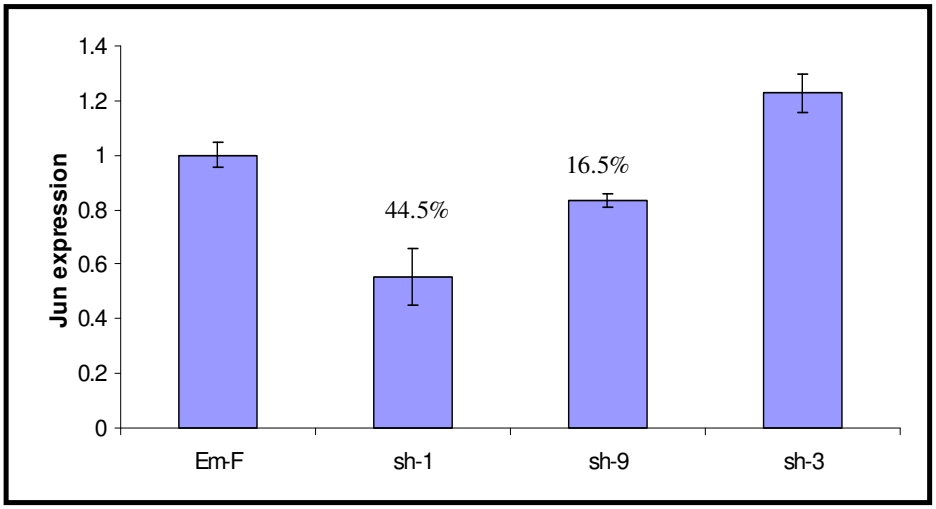


**Fig: 3.9.4.5.4 *Jun* expression as determined by qRT-PCR in sh-1, sh-9 and sh-3 *Txnip* shRNA-transfected clones and Em-F empty shRNA transfected clone. Sh-1 clone showed 44.5% and sh-9 clone showed 16.5% knock-down of *Jun* compared to Em-F. sh-3 (*Txnip* shRNA transfected clone with no *Txnip* mRNA knock-down) and sh-1 and sh-9 (clone showing *Txnip* mRNA knock-down). Results represent mean ± S.D.**

***Txnip* knock-down increases *Mapk3* expression**

Up-regulation of *Mapk3* gene transcript was observed in MIN6 B1(Non-GSIS) compared to MIN6 B1(GSIS) following microarray (1.27-fold) and qRT-PCR (1.17-fold) study. qRT-PCR was performed to check the expression level of *Mapk3* in the single cell colony of the *Txnip* shRNA transfected cells. *Txnip* knock-down increased the expression of *Mapk3* in sh-1 (14.8%) and sh-9 clones (66.9%) whereas, there is no effect on *Mapk3* in sh-3 clones (with no *Txnip* knock-down) compared to empty shRNA-transfected Em-F clone (Fig: 3.9.4.5.5).

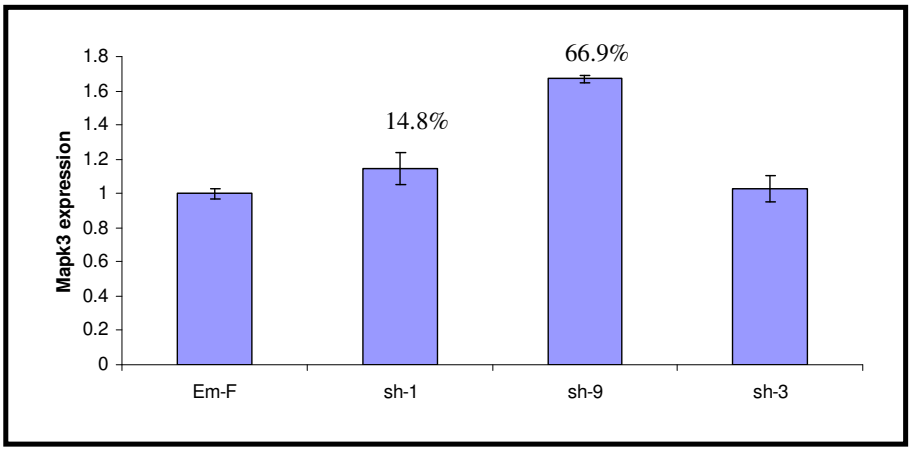


**Fig: 3.9.4.5.5 *Mapk3* expression as determined by qRT-PCR in sh-1, sh-9 and sh-3 *Txnip* shRNA-transfected clone and Em-F empty shRNA transfected clone. Sh-1 (14.8%) and sh-9 clone (66.9%) showed an increase in expression of *Mapk3* compared to Em-F. sh-3 (*Txnip* shRNA transfected clone with no *Txnip* mRNA knock-down) and sh-1 and sh-9 (clone showing *Txnip* mRNA knock-down). Results represent mean ± S.D.**

### 3.10 Analysis of conditioned media for amplifiable Gene Transcripts

Extracellular RNA has been detected in plasma and serum of patients presenting with various forms of cancer (Wieczorek *et al*., 1987; Kopreski *et al*., 1999; Hasselmann *et al*., 2001); DNA and mRNA from foetal origin have been discovered in the plasma of pregnant women (Bianchi *et al*., 1997; Poon *et al*., 2000; Tsui *et al*., 2006); and significantly higher levels of *rhodopsin* mRNA have been reported in peripheral blood from diabetic individuals compared to healthy controls (Hamaoui *et al*., 2004). While the possibility exists that there may be circulating RNA biomarkers indicative of beta cell mass and function in diabetes patients, no studies have yet investigated this.

Insulin-producing cells were grown and conditioned media (CM) collected at different time points to analyze the suitable time-point for CM collection and analysis. Once a suitable time-point was established, we extracted and amplified mRNA from CM to determine if extracellular mRNAs are reproducibly detectable in CM from insulin-producing cell lines. Secondly this study aimed to identify if the presence and amounts of CM are indicative of beta cell number and/or function.

All transcript underwent 45 PCR cycles, while 30 cycles of PCR was found to be adequate for analysis of transcripts using RNA isolated from cell lines, amplified products often did not results from CM RNA at this stage. For this reason, 45 cycles was used for all subsequent experiments to analyse gene transcripts from both cells and CM.

### 3.10.1 Identifying suitable time-point for CM collection and analysis from insulin-producing cell lines

Conditioned media (CM) samples were collected at 4 time-points (24, 48, 72 and 96 hrs.) after seeding cells in T75cm$^2$ flask, to identify a suitable time-point at which amplifiable mRNA could be routinely isolated for analysis. After samples were collected and they were stored at -80°C until required, RNA was extracted from the samples and reverse- transcribed. PCR was then carried out. In the case of relatively highly expressed gene transcripts such as *Beta-actin*, mRNA could be isolated and amplified at all time points evaluated. However, for gene transcripts where levels expressed by the cell populations were lower (e.g. *Egr1*) amplified product was undetected after 24hrs., but was present when analysed after 48hrs., or more, of culture. To ensure that all CM analysed was from healthy, proliferating cells, all subsequent analysis was performed using 48hrs. CM.

### 3.10.2 Analysis of CM and cells MIN6 for amplifiable Gene Transcripts

After identifying a suitable time point for CM collection and analysis, cells were seeded in T75cm$^2$ flask at 2x10$^6$ cells with 8 mls culture medium. Conditioned media was removed after 48hrs. and filtered with 0.45 µm filter. Aliquots of 250 µl filtered CM were added to 750 µl of TriReagent. RNA was isolated, quantified and RT-PCR analysis was done. RT-PCR analysis of the CM taken from MIN6 (L) & (H) passage showed the presence of amplifiable mRNA.

### 3.10.3 mRNA Detection in CM: Identifying Suitable PCR Cycle Number

mRNA transcripts were detected in medium conditioned by all cell types included in this study i.e. MIN6 (L), (H), MIN6 B1 and Vero-PPI cell lines.

While 30 cycles of PCR was found to be adequate for analysis of transcripts using RNA isolated from cell lines, amplified products often did not results from CM RNA at this stage. In the case of CM the bands were undetectable or very low in intensity following 30 cycles of PCR (Fig: 3.10.3 (A): *pancreatic and duodenal homeobox gene-1* (*Pdx1*)). Forty-five cycles of PCR, however, was found to be adequate to produce a detectable band from CM RNA (Fig: 3.10.3 (B)). There were no bands detected in negative controls including water instead of RNA as control and water instead of cDNA as a control. For this reason, 45 cycles was used for all subsequent experiments to analyse gene transcripts from both cells and CM.

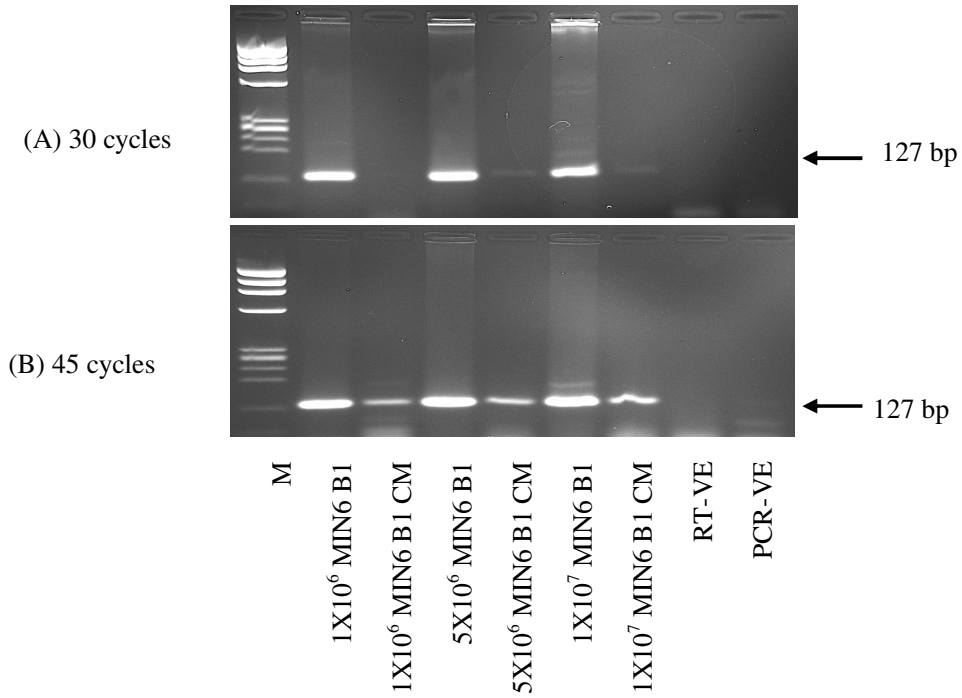


**Fig: 3.10.3 *Pdx1* mRNA analysis of MIN6 B1 cells, grown at a range of densities, and their corresponding CM using (A) 30 PCR cycles and (B) 45 PCR cycles. RT-VE = reaction with $H_2O$ instead of RNA as control; PCR-VE = PCR reaction with $H_2O$ instead of cDNA as a control. M = molecular weight marker: ΦX174 DNA HaeIII digest. Results are representative of n = 3 biological repeats.**

### 3.10.4 RNase- and DNase-treated RNA Samples

To ensure that any products detected following RT-PCR analysis of isolates from cells and/or CM were of mRNA, not DNA, origin, aliquots of isolates were treated with DNase enzyme (to destroy any contaminating DNA), with RNase enzyme (to destroy RNA, as control) or were untreated (See Section: 2.5.1.3).

#### 3.10.4.1 Bioanalyzer on RNase- and DNase-treated RNA Samples

The quality of the RNA after treating the RNA samples with RNase, DNase and untreated were analysed using Bioanalyzer (See Section: 2.5.1.5). For the RNA standard, the electropherograms obtained from the Agilent Bioanalyzer 2100 gave clear and well-defined 28S and 18S RNA peaks, with high 28S/18S RNA ratio for the untreated cell RNA.

1. Untreated samples showed a distinct peak of 28s and 18s RNA (Fig: 3.10.4.1 (A)).
2. RNase treated samples showed a complete degradation of cell and CM RNA. CM sample showed 2 peaks but were not at the right place and when the values of y axis were compared it was of very low value. The RNase-treated cell RNA showed a complete degradation of the RNA (Fig: 3.10.4.1 (B)).

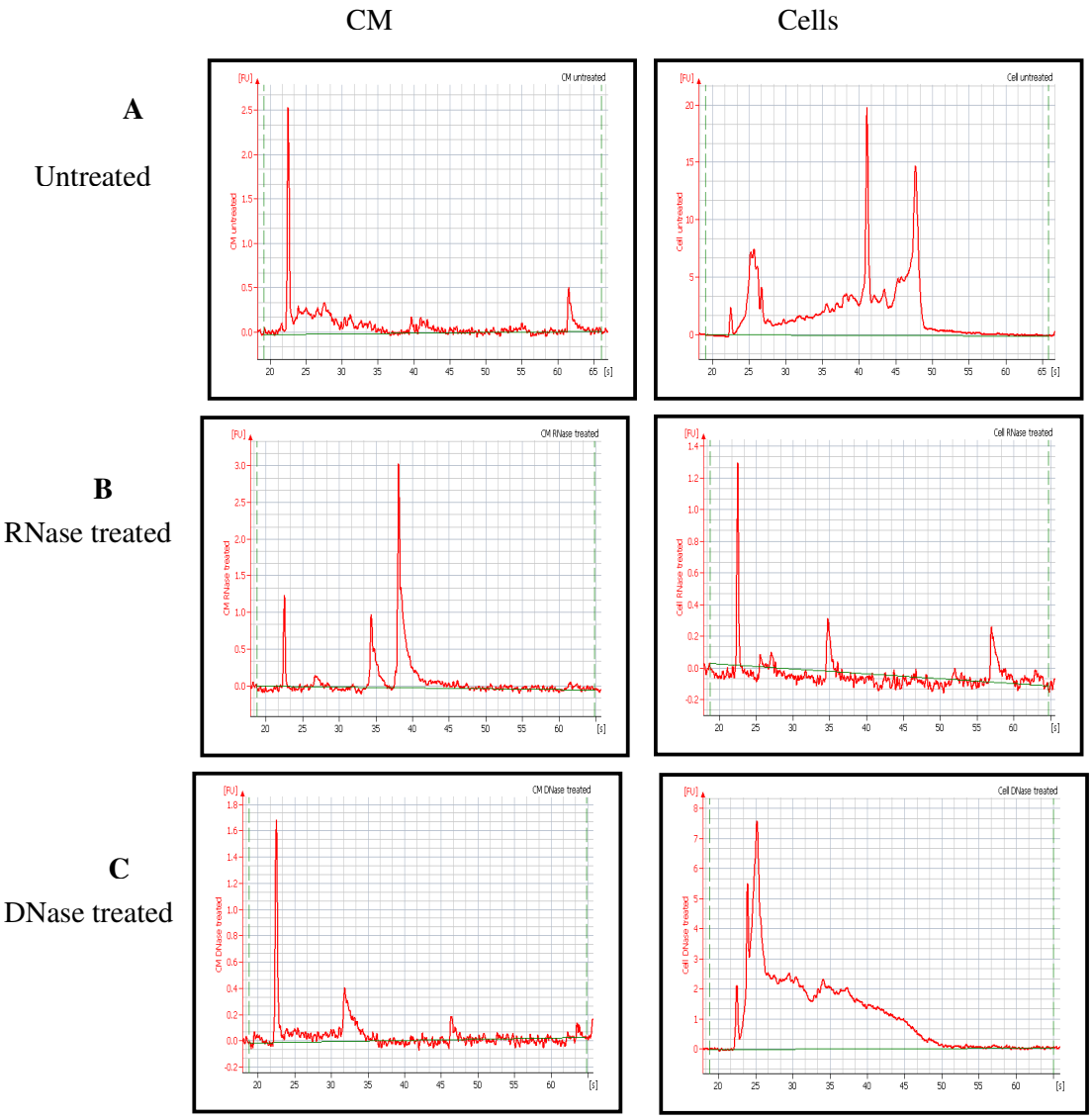


**Fig: 3.10.4.1 MIN6 B1 cell and CM RNA samples showing 18S and 28S ribosomal bands after (A) untreated, (B) RNase-treated and (C) DNase-treated.**

3. However DNase-treatment has also caused some degradation to the RNA samples as 28S and 18S RNA peaks are not so well-defined (Fig: 3.10.4.1 (C)).

### 3.10.4.2 RT-PCR on RNase- and DNase-treated RNA Samples

Reverse-transcriptase (RT) reactions were subsequently performed prior to PCR. In parallel, RT reactions were set up with and without reverse transcriptase enzyme (MMLV-RT) – an enzyme which is necessary for the formation of cDNA on an mRNA template.

The absence of reverse transcriptase enzyme resulted in no amplified PCR products, regardless of whether the cell and CM isolates were untreated, treated with RNase or treated with DNase (Fig: 3.10.4.2.1 (A)). This was found to be the cases for all products investigated. The presence of MMLV-RT enzyme in the RT reaction did, however, result in amplified products from cell and CM isolates that were untreated with a digestive enzyme or that were treated with DNase enzyme. However, no bands were detected where samples had been treated with RNase enzyme (Fig: 3.10.4.2.1 (B). These results indicate that the amplified products detected in cell and CM isolates are of mRNA, not DNA, origin.

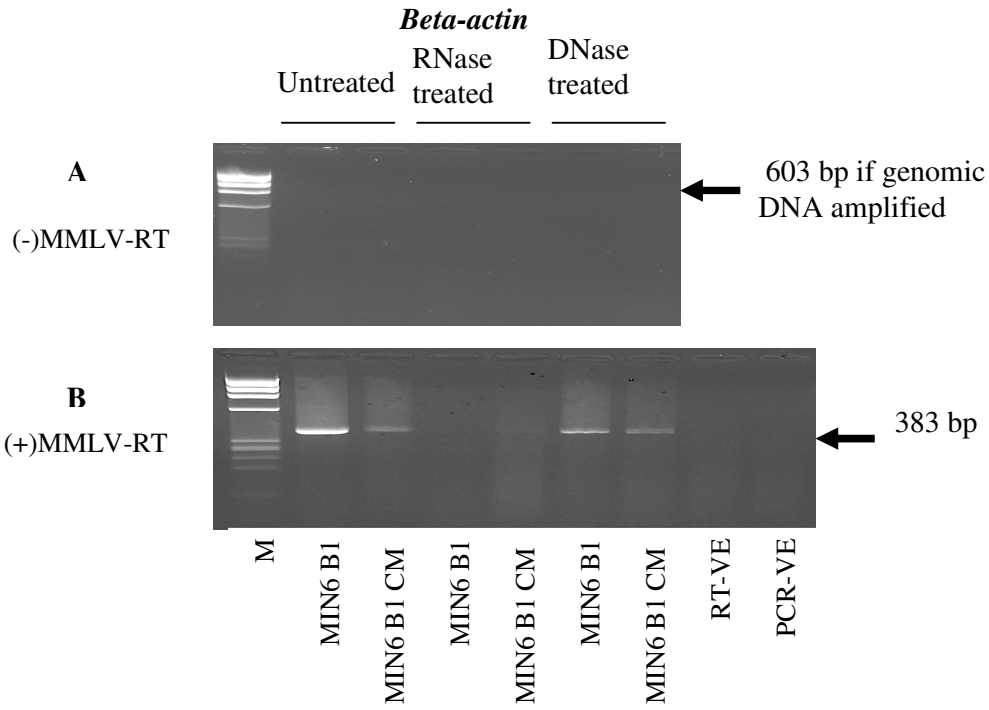


**Fig: 3.10.4.2.1 Cell and CM RNA isolates treated with RNase or DNase prior to cDNA formation, using MMLV-RT enzyme, and amplification using *Beta-actin* primers. (+) MMLV-RT (B) represents reverse transcriptase (RT) reaction performed with necessary RT enzyme, MMLV-RT; (A) (–) MMLV = represent RT cycle performed in the absence of MMLV-RT enzyme, as control. RT-VE = reaction with $H_2O$ instead of RNA as control; PCR-VE = PCR reaction with $H_2O$ instead of cDNA as a control. M = molecular weight marker: ΦX174 DNA Hae III digest.**

***Pdx1***

Contaminating genomic DNA can lead to false-positive signals, reduced specificity, or overestimation of specific RNA amounts in RT-PCR. RT-PCR primers for *Pdx1* were designed to flank a region within a single exon. The primers were aligned against mRNA and DNA sequence from PubMed to check the fragment size of the products that would be amplified from mRNA and genomic DNA (Fig: 3.10.4.2.2). There were no size difference of the products to detect the presence of contaminating DNA (125 bp) or mRNA (125 bp) amplified product.

So the reverse transcriptase reaction was carried with or without reverse transcriptase enzyme MMLV. The absence of reverse transcriptase enzyme resulted in no amplified PCR products, regardless of whether the cell and CM isolates were untreated, treated with RNase or treated with DNase (Fig: 3.10.4.2.3 (A)). The presence of MMLV-RT enzyme in the RT reaction did, however, result in amplified products from cell and CM isolates that were untreated with a digestive enzyme or that were treated with DNase enzyme. However, no bands were detected where samples had been treated with RNase enzyme (Fig: 3.10.4.2.3 (B)). These results indicate that the amplified products detected in cell and CM isolates are of mRNA, not DNA, origin.

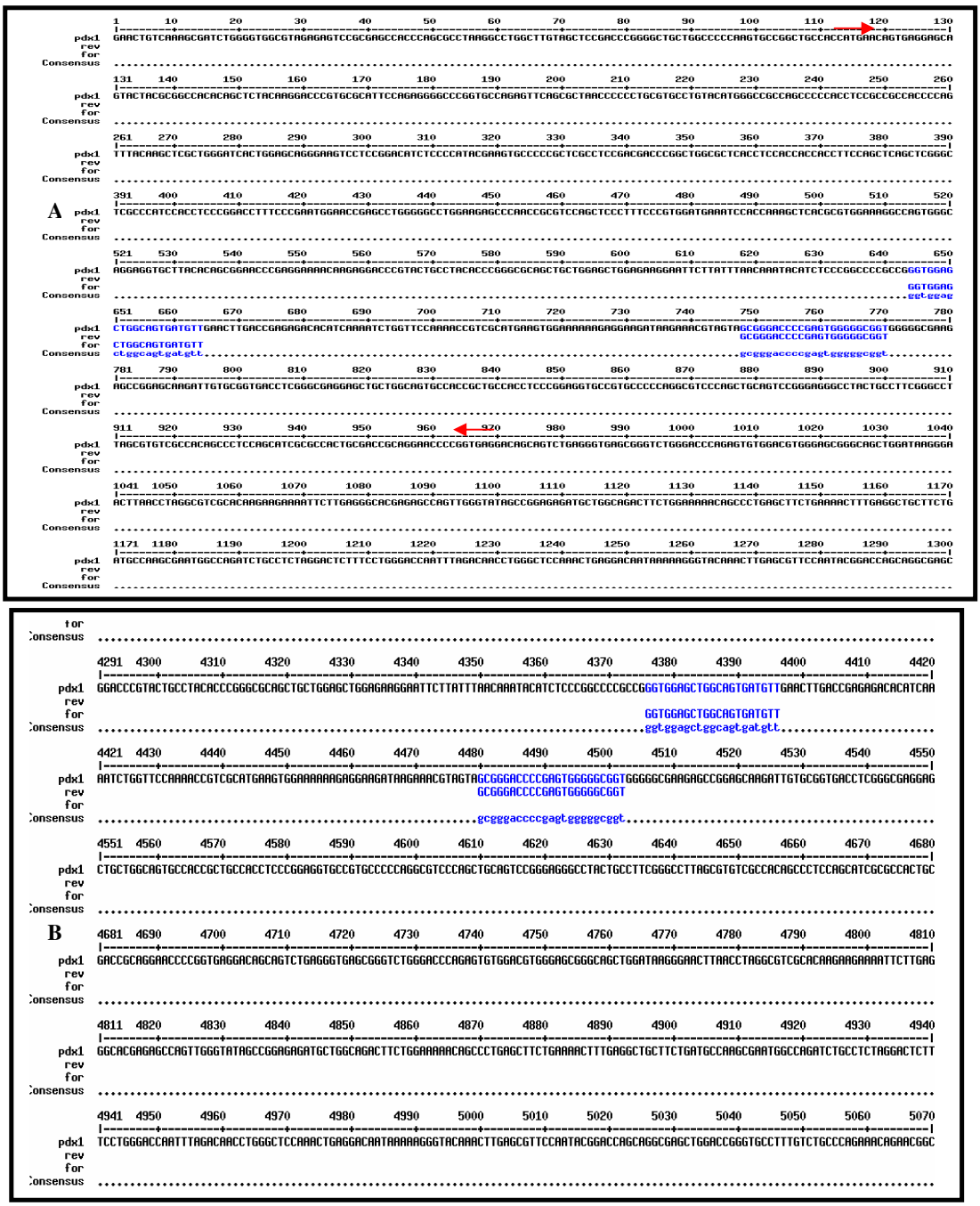


**Fig: 3.10.4.2.2 Multalin results for *Pdx1* mRNA (A) and DNA (B) sequence (black letters) with forward and reverse RT-PCR primers (blue letters) (→) showing the coding sequence 114-968.**

***Pdx1***

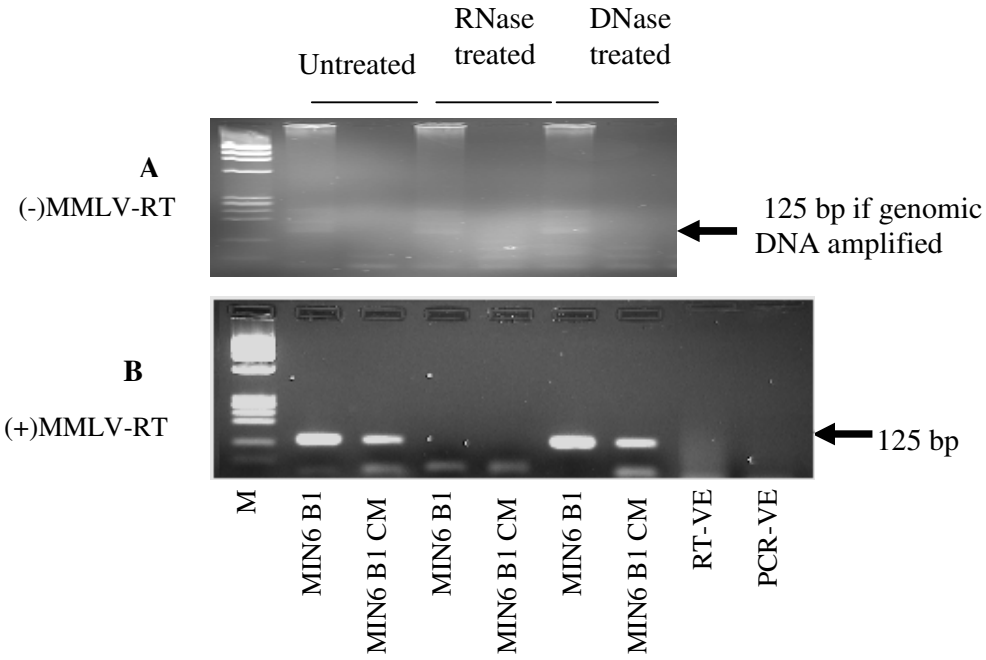


**Fig: 3.10.4.2.3 Cell and CM RNA isolates treated with RNase or DNase prior to cDNA formation, using MMLV-RT enzyme, and amplification using *Pdx1* primers. (+) MMLV-RT represents reverse transcriptase (RT) reaction performed with necessary RT enzyme, MMLV-RT; (–) MMLV = represent RT cycle performed in the absence of MMLV-RT enzyme, as control. RT-VE = reaction with $H_2O$ instead of RNA as control; PCR-VE = PCR reaction with $H_2O$ instead of cDNA as a control. M = molecular weight marker: ΦX174 DNA Hae III digest.**

### *Insulin I* (*Ins1*)

*Ins1* (Fig: 3.10.4.2.4) has only one exon so the RT-PCR primers were designed through the coding region. The primers were aligned using multialin software against mRNA and DNA sequence from PubMed to check the fragment size of the products that would be amplified from mRNA and genomic DNA. Products that were amplified from mRNA (288 bp) were smaller than those amplified from genomic DNA (407 bp). The size difference of the products was used to detect the presence of RNA or contaminating DNA.

Reverse transcriptase reaction was carried out with or without reverse transcriptase enzyme MMLV. No amplified PCR products were obtained in the absence of reverse transcriptase enzyme, regardless of whether the cell and CM isolates were untreated, treated with RNase or treated with DNase (*Ins1* (Fig: 3.10.4.2.5 (A)). Amplified products were obtained from cell and CM isolates that were untreated or that were treated with DNase enzyme. However, no bands were detected where samples had been treated with RNase enzyme (*Ins1* (Fig: 3.10.4.2.5 (B)).

*Ins1*

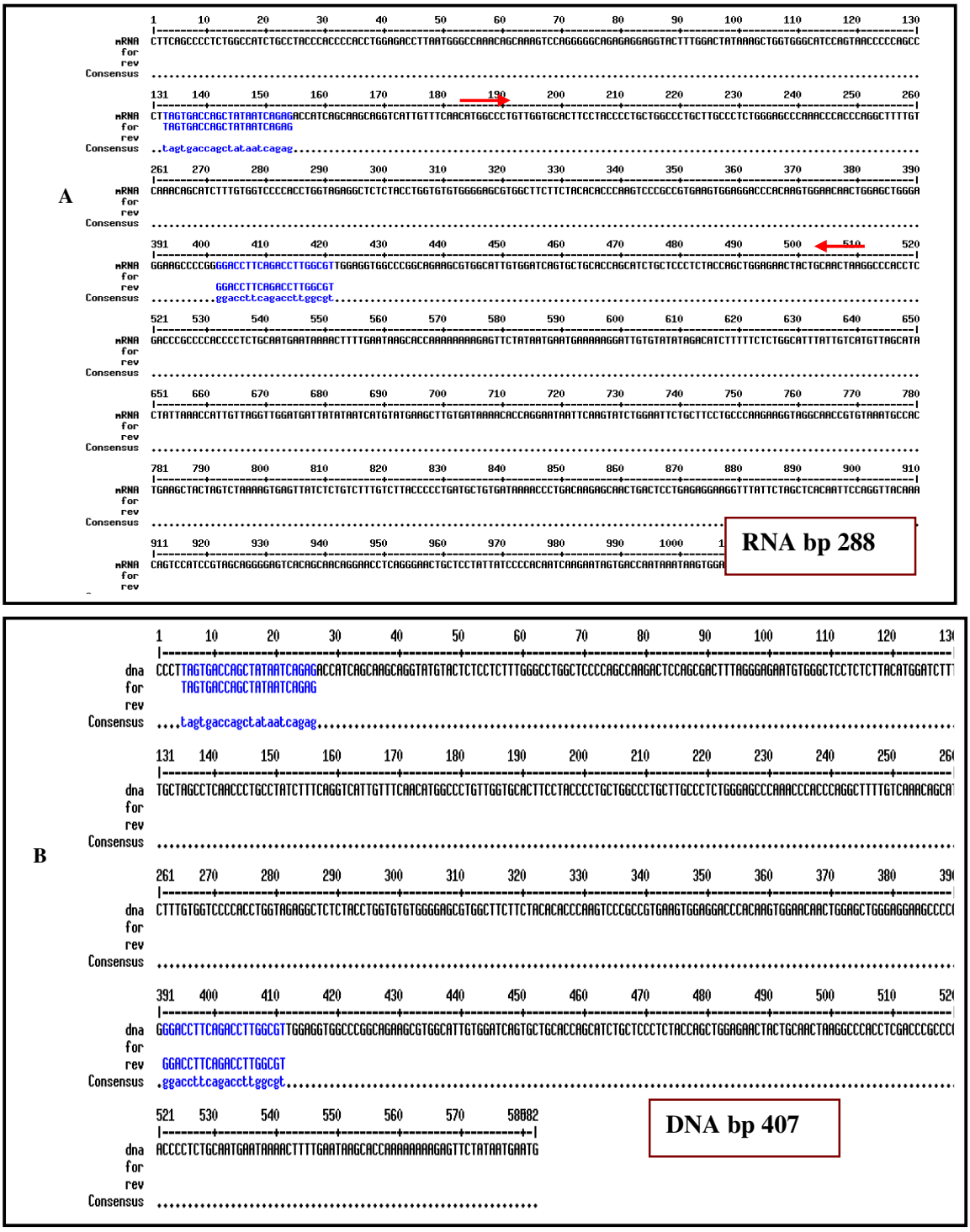


**Fig: 3.10.4.2.4 Multalin results for *Ins1* mRNA (A) and DNA (B) sequence (black letters) with forward and reverse RT-PCR primers (blue letters) ( → ) showing the coding sequence 184-510.**

***Ins1***

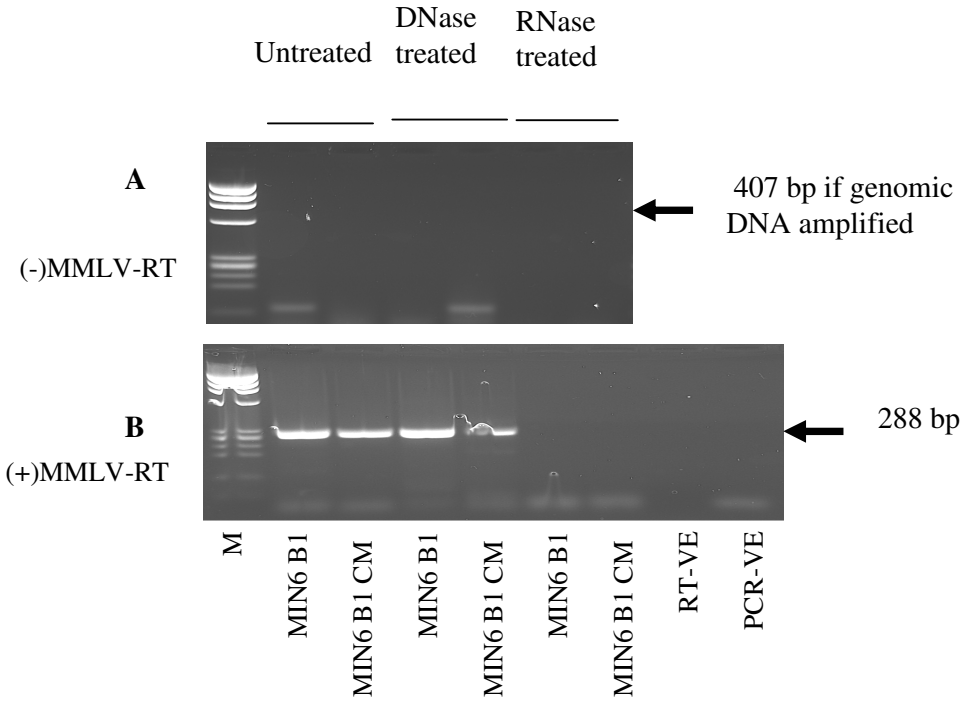


**Fig: 3.10.4.2.5 Cell and CM RNA isolates treated with RNase or DNase prior to cDNA formation, using MMLV-RT enzyme, and amplification using *Ins1* primers. (B)(+) MMLV-RT represents reverse transcriptase (RT) reaction performed with necessary RT enzyme, MMLV-RT; (A) (–) MMLV = represent RT cycle performed in the absence of MMLV-RT enzyme, as control. RT-VE = reaction with $H_2O$ instead of RNA as control; PCR-VE = PCR reaction with $H_2O$ instead of cDNA as a control. M = molecular weight marker: ΦX174 DNA Hae III digest.**

### *Insulin II (Ins2)*

*Ins2* has only one exon so the RT-PCR primers were designed through the coding region. The primers were aligned using multialin software against mRNA and DNA sequence from PubMed to check the fragment size of the products that would be amplified from mRNA and genomic DNA. Products that were amplified from mRNA (212 bp) were smaller than those amplified from genomic DNA (701 bp) (Fig: 3.10.4.2.6). The size difference of the products was used to detect the presence of RNA or contaminating DNA.

Reverse transcriptase reaction was carried out with or without reverse transcriptase enzyme MMLV. No amplified PCR products were obtained in the absence of reverse transcriptase enzyme, regardless of whether the cell and CM isolates were untreated, treated with RNase or treated with DNase (*Ins2* (Fig: 3.10.4.2.7 (A)). Amplified products were obtained from cell and CM isolates that were untreated or that were treated with DNase enzyme. However, no bands were detected where samples had been treated with RNase enzyme (*Ins2* (Fig: 3.10.4.2.7 (B)).

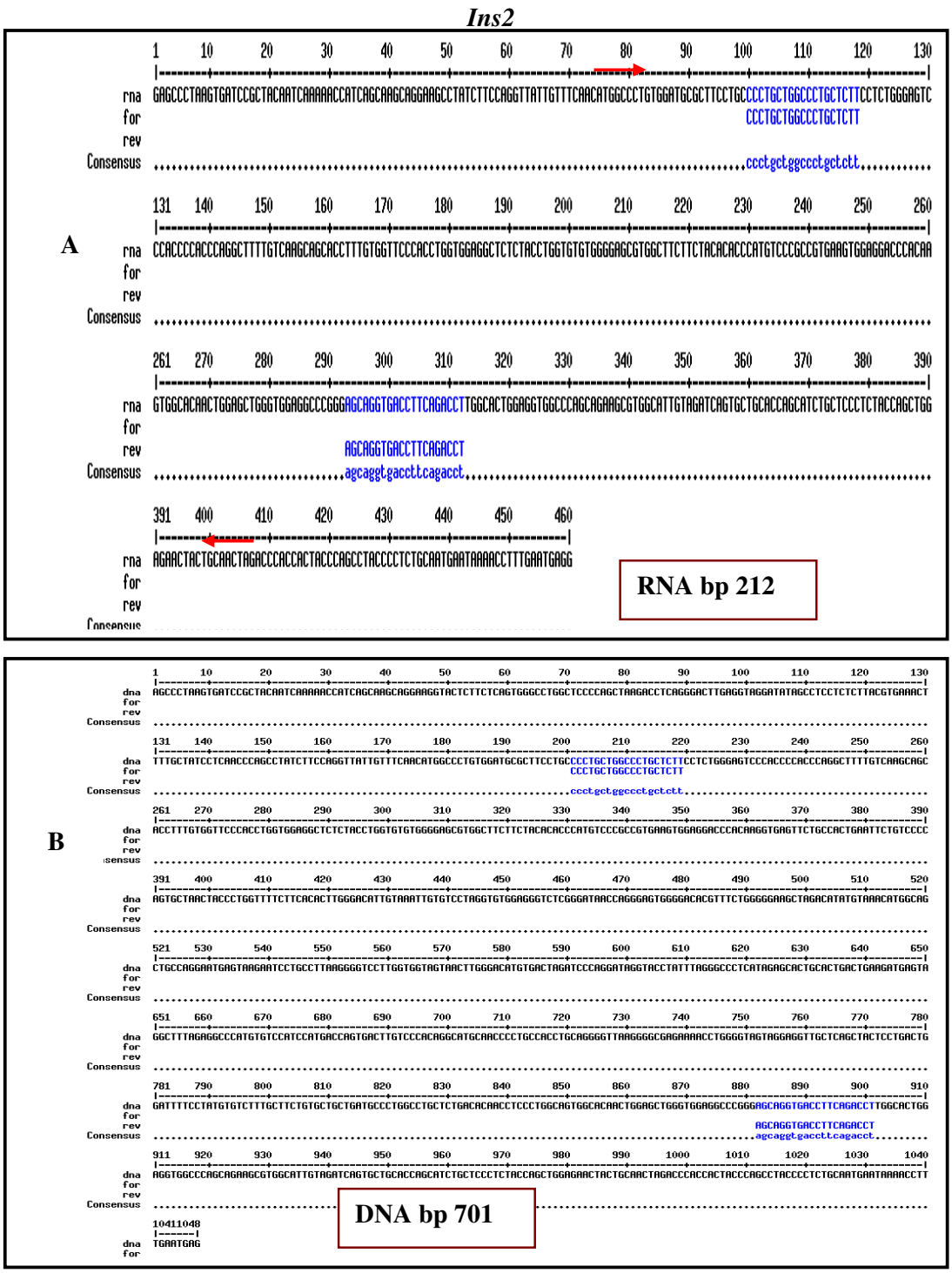


**Fig: 3.10.4.2.6 Multalin results for *Ins2* mRNA (A) and DNA (B) sequence (black letters) with forward and reverse RT-PCR primers (blue letters) ( ) showing the exon region 75-407.**

***Ins2***

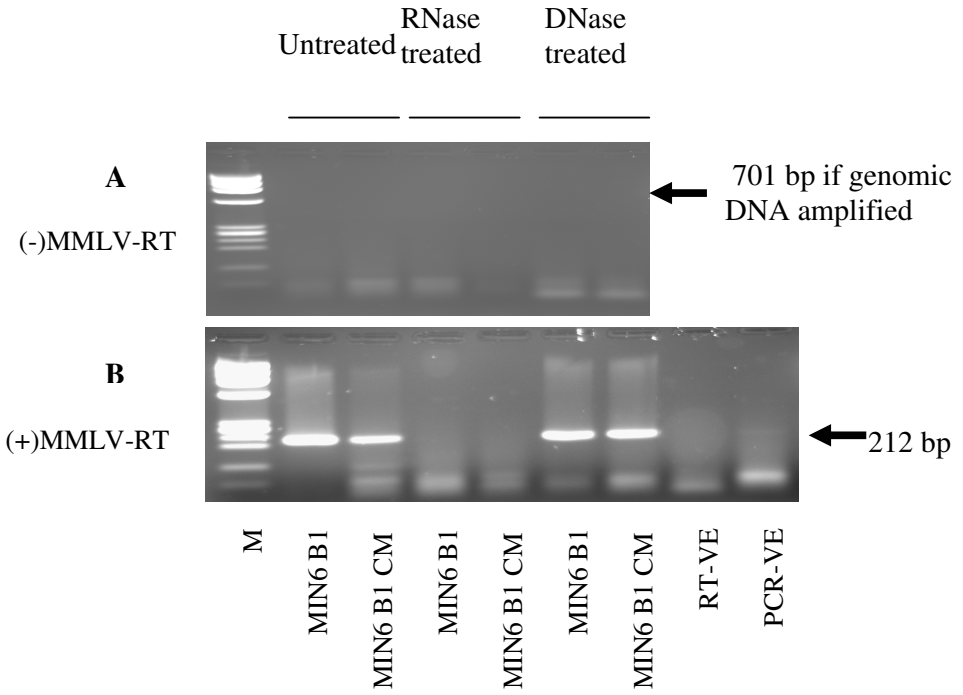


**Fig: 3.10.4.2.7 Cell and CM RNA isolates treated with RNase or DNase prior to cDNA formation, using MMLV-RT enzyme, and amplification using *Ins2* primers. (B)(+) MMLV-RT represents reverse transcriptase (RT) reaction performed with necessary RT enzyme, MMLV-RT; (A) (–) MMLV = represent RT cycle performed in the absence of MMLV-RT enzyme, as control. RT-VE = reaction with $H_2O$ instead of RNA as control; PCR-VE = PCR reaction with $H_2O$ instead of cDNA as a control. M = molecular weight marker: ΦX174 DNA Hae III digest.**

### *Neuropeptide Y* (*Npy)*

As *Npy* gene transcripts has only one exon so the RT-PCR primers were designed through the coding region. The primers were aligned using multialin software against mRNA and DNA sequence from PubMed to check the fragment size of the products that would be amplified from mRNA and genomic DNA. Products that were amplified from mRNA (249 bp) were smaller than those amplified from genomic DNA (5679 bp) (Fig: 3.10.4.2.8). The size difference of the products was used to detect the presence of RNA or contaminating DNA.

Reverse transcriptase reaction was carried out with or without reverse transcriptase enzyme MMLV. No amplified PCR products were obtained in the absence of reverse transcriptase enzyme, regardless of whether the cell and CM isolates were untreated, treated with RNase or treated with DNase enzyme (*Npy* (Fig: 3.10.4.2.9 (A)). Amplified products were obtained from cell and CM isolates that were untreated or that were treated with DNase enzyme. However, no bands were detected where samples had been treated with RNase enzyme (*Npy* (Fig: 3.10.4.2.9 (B)).

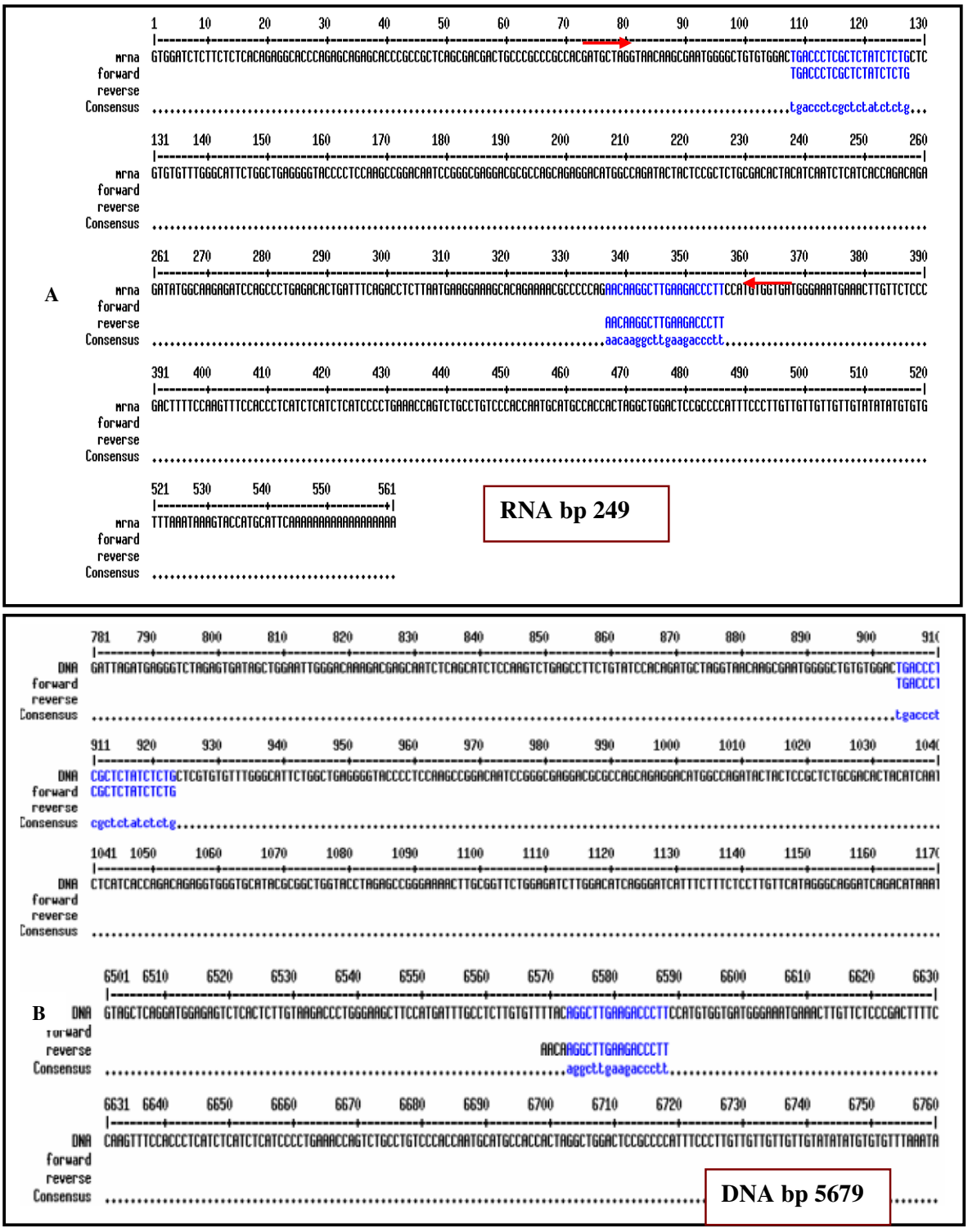


**Fig: 3.10.4.2.8 Multalin results for *Neuropeptide Y* mRNA (A) and DNA (B) sequence (black letters) with forward and reverse RT-PCR primers (blue letters) (⟶) showing the exon region 74-367.**

***Npy***

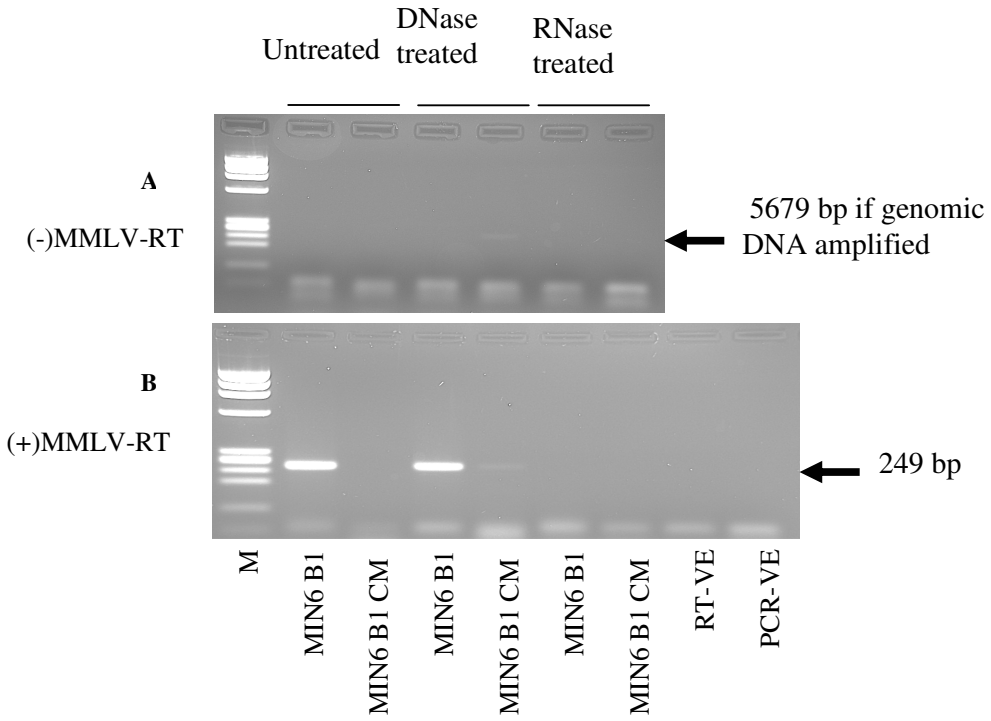


**Fig: 3.10.4.2.9 Cell and CM RNA isolates treated with RNase or DNase prior to cDNA formation, using MMLV-RT enzyme, and amplification using *Npy* primers. (B)(+) MMLV-RT represents reverse transcriptase (RT) reaction performed with necessary RT enzyme, MMLV-RT; (A) (–) MMLV = represent RT cycle performed in the absence of MMLV-RT enzyme, as control. RT-VE = reaction with $H_2O$ instead of RNA as control; PCR-VE = PCR reaction with $H_2O$ instead of cDNA as a control. M = molecular weight marker: ΦX174 DNA Hae III digest.**

Reverse-transcriptase (RT) reactions were subsequently performed prior to PCR with and without reverse transcriptase enzyme (MMLV-RT) – an enzyme which is necessary for the formation of cDNA on an mRNA template.

The absence of reverse transcriptase enzyme resulted in no amplified PCR products, regardless of whether the cell and CM isolates were untreated, treated with RNase or treated with DNase (*Pld1* (Fig: 3.10.4.2.10 (A)), *Chgb* (Fig: 3.10.4.2.11 (A)), *Egr1* (Fig: 3.10.4.2.12 (A))**.** This was found to be the cases for all products investigated. The presence of MMLV-RT enzyme in the RT reaction did, however, result in amplified products from cell and CM isolates that were untreated with a digestive enzyme or that were treated with DNase enzyme. However, no bands were detected where samples had been treated with RNase enzyme (*Pld1* (Fig: 3.10.4.2.10 (B)), *Chgb* (Fig: 3.10.4.2.11 (B)), *Egr1* (Fig: 3.10.4.2.12 (B)). These results indicate that the amplified products detected in cell and CM isolates are of mRNA, not DNA, origin.

***Pld1***

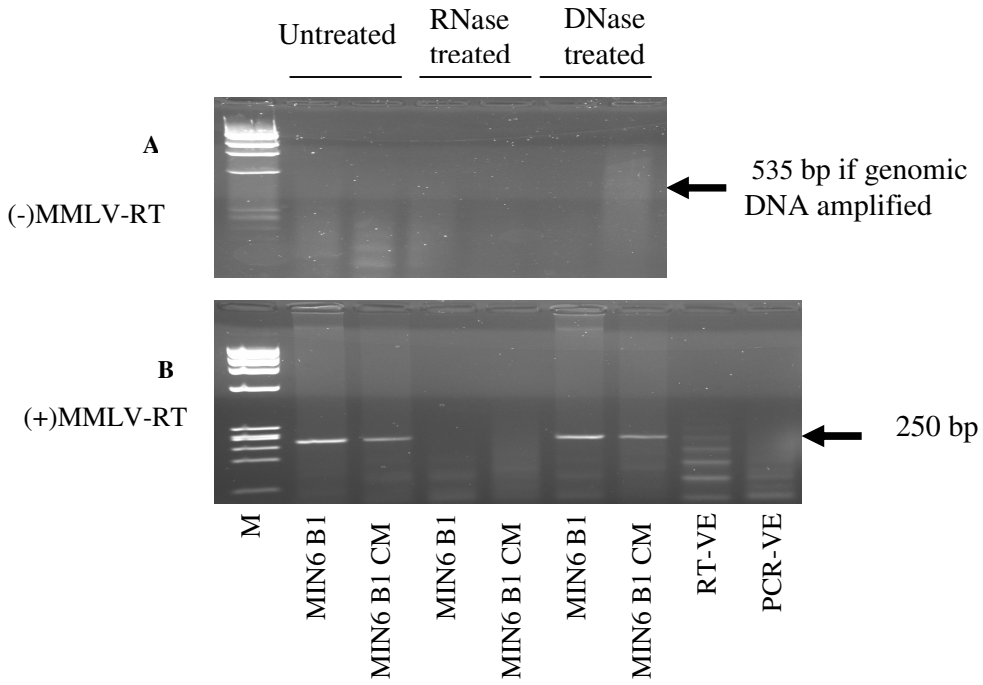


**Fig: 3.10.4.2.10 Cell and CM RNA isolates treated with RNase or DNase prior to cDNA formation, using MMLV-RT enzyme, and amplification using *Pld1* primers. (B)(+) MMLV-RT represents reverse transcriptase (RT) reaction performed with necessary RT enzyme, MMLV-RT; (A) (–) MMLV = represent RT cycle performed in the absence of MMLV-RT enzyme, as control. RT-VE = reaction with $H_2O$ instead of RNA as control; PCR-VE = PCR reaction with $H_2O$ instead of cDNA as a control. M = molecular weight marker: ΦX174 DNA Hae III digest.**

***Chgb***

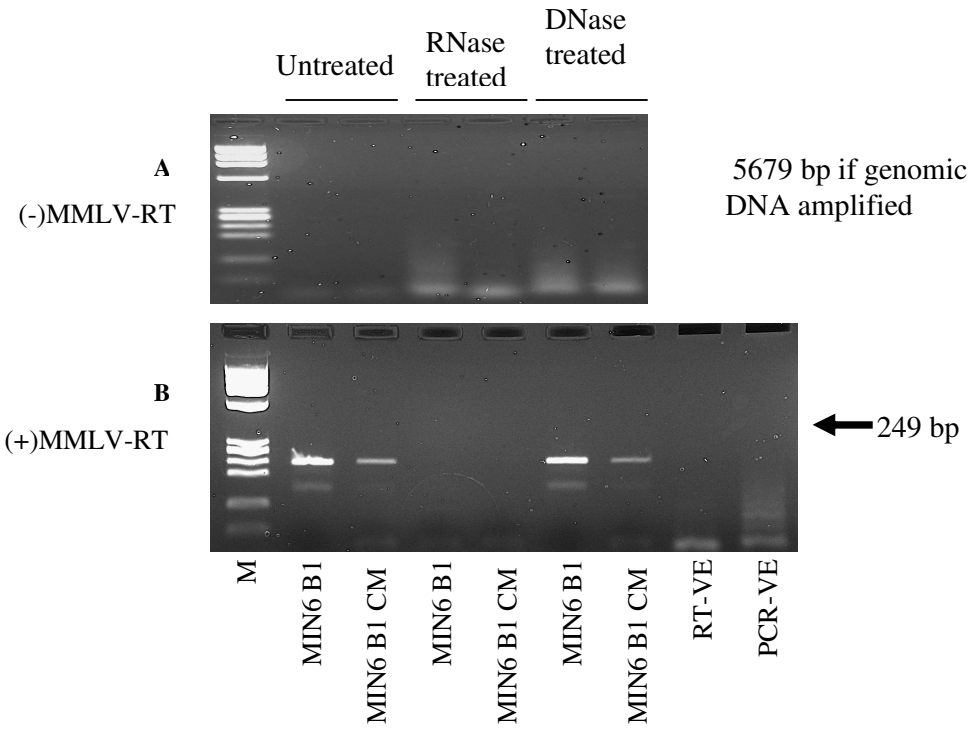


**Fig: 3.10.4.2.11 Cell and CM RNA isolates treated with RNase or DNase prior to cDNA formation, using MMLV-RT enzyme, and amplification using *Chgb* primers. (B)(+) MMLV-RT represents reverse transcriptase (RT) reaction performed with necessary RT enzyme, MMLV-RT; (A) (–) MMLV = represent RT cycle performed in the absence of MMLV-RT enzyme, as control. RT-VE = reaction with $H_2O$ instead of RNA as control; PCR-VE = PCR reaction with $H_2O$ instead of cDNA as a control. M = molecular weight marker: ΦX174 DNA Hae III digest.**

***Egr1***

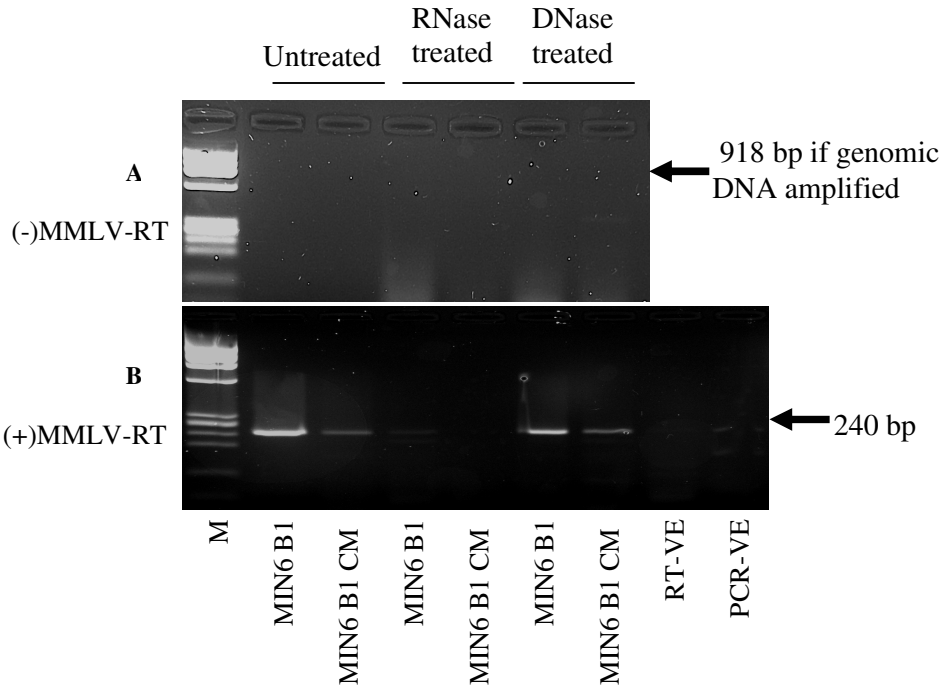


**Fig: 3.10.4.2.12 Cell and CM RNA isolates treated with RNase or DNase prior to cDNA formation, using MMLV-RT enzyme, and amplification using *Egr1* primers. (B) (+) MMLV-RT represents reverse transcriptase (RT) reaction performed with necessary RT enzyme, MMLV-RT; (A) (–) MMLV = represent RT cycle performed in the absence of MMLV-RT enzyme, as control. RT-VE = reaction with $H_2O$ instead of RNA as control; PCR-VE = PCR reaction with $H_2O$ instead of cDNA as a control. M = molecular weight marker: ΦX174 DNA Hae III digest.**

### 3.10.5 Glucose-Responsiveness and corresponding mRNA Levels in CM

CM collected from glucose-responsive MIN6 (L) and glucose non-responsive MIN6 (H) cells were collected and filtered as described in Section 2.4.3.2. RNA was isolated (See Section: 2.5.1.2.1) and cDNA was prepared as in section 2.5.2.1. CM collected from glucose-responsive MIN6 (L) and glucose non-responsive MIN6 (H) cells was analyzed for the presence of a range of transcripts, including *phospholipase D1* (*Pld1*), *Egr1*, *Chgb* and *InsI*. *Pld1*, *Egr1* and *Chgb* were reproducibly detected in the triplicate biological repeat analysis of MIN6 (L) CM samples, but were undetected in MIN6 (H) CM. *Beta-actin* (Fig: 3.10.5.1), *Ins1* (Fig: 3.9.5.2) *Ins2* (Fig: 3.10.5.3) and *Pdx1* (Fig: 3.10.5.4) however, were detected, at similar levels, in MIN6 (L) and (H) CM.

### *Beta-Actin (actb)*

*Beta-actin* was detected in all triplicate samples of CM from MIN6 (L) and (H). Densitometry analysis of the PCR product from medium conditioned by MIN6 (L) and (H) cells showed no significant difference (p-value = 0.686) (Fig: 3.10.5.1). RNA from MIN6 (L) cells was taken as control.

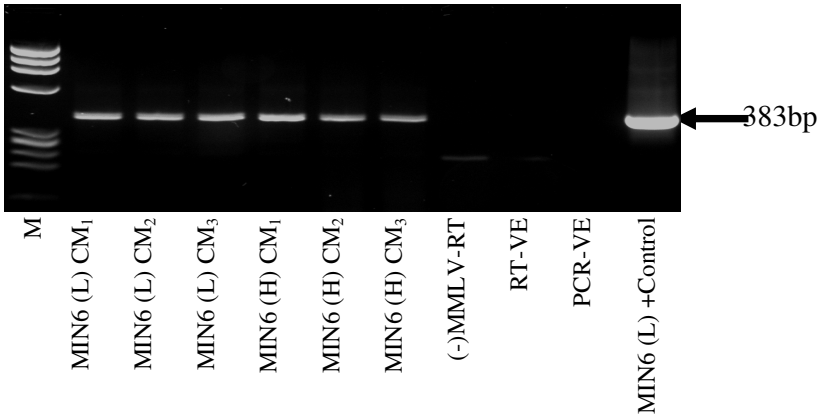


**Fig: 3.10.5.1 *Beta-actin* amplification of cDNA prepared from MIN6 (L) & (H) CM RNA. (-)MMLV-RT = RT-PCR reaction carried out without reverse transcriptase enzyme; RT-VE = reaction with $H_2O$ instead of RNA as control; PCR-VE = PCR reaction with $H_2O$ instead of cDNA as a control; M = molecular weight marker: ΦX174 DNA Hae III digest. 1, 2 & 3 represent biological repeat experiments. Densitometry analysis indicates that the levels of RNA detectable in CM from MIN6 (L) and (H) did not differ significantly (T-test: P = 0.686).**

### *Insulin I* (*Ins1*)

CM obtained from MIN6 (L) and (H) passage cells after 48 hrs. was amplified at 45 PCR cycles for *Ins1*. RNA from MIN6 (L) cells were taken as positive control. Densitometry analysis showed no significant difference in the PCR band between MIN6 (L) and (H) CM (p-value = 0.543) (Fig: 3.10.5.2).

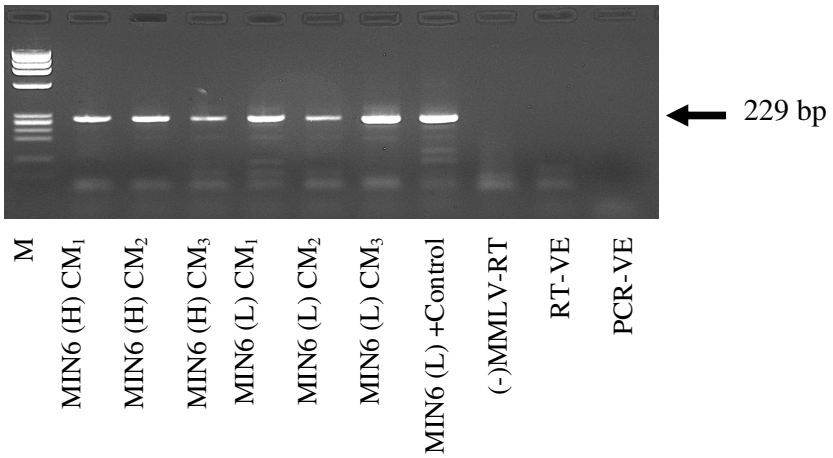


**Fig: 3.10.5.2 *Ins1* analysis in CM from MIN6 (L) and (H). RT-VE = reaction with $H_2O$ instead of RNA as control; PCR-VE = PCR reaction with $H_2O$ instead of cDNA as a control; (-) MMLV-RT = RT-PCR reaction carried out without reverse transcriptase enzyme. M = molecular weight marker: ΦX174 DNA Hae III digest. 1, 2 & 3 represent biological repeat experiments. Densitometry analysis indicates that the levels of detected in CM from MIN6 (L) and (H) did not differ significantly (T-test: P = 0.543).**

### *Insulin II* (*Ins2*)

*Ins2* gene transcript was detected in all triplicate samples of medium conditioned by MIN6 (L) and (H) passage cells. MIN6 (L) cell RNA was taken as positive control. There was no significant change in expression between MIN6 (L) and (H) CM as analysed by densitometer (p-value = 0.092) (Fig: 3.10.5.3).

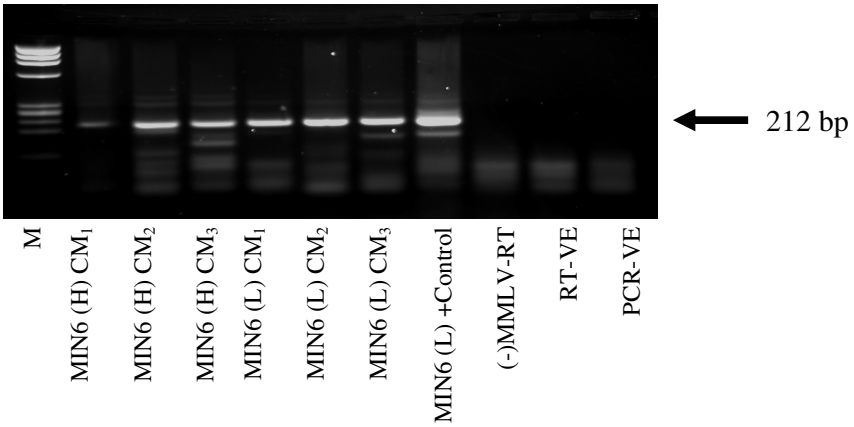


**Fig: 3.10.5.3 *Ins2* analysis in CM from MIN6 (L) and (H). RT-VE = reaction with $H_2O$ instead of RNA as control; PCR-VE = PCR reaction with $H_2O$ instead of cDNA as a control; (-) MMLV-RT = RT-PCR reaction carried out without reverse transcriptase enzyme. M = molecular weight marker: ΦX174 DNA Hae III digest. 1, 2 & 3 represent biological repeat experiments. Densitometry analysis indicates that the levels of detected in CM from MIN6 (L) and (H) did not differ significantly (T-test: P = 0.092).**

### *Pancreatic and duodenal homeobox gene 1 (Pdx1)*

*Pdx1* was amplified using CM RNA from all MIN6 (L) and (H) passage cells. Densitometry analysis showed no significant difference in expression of *Pdx1* in CM RNA from MIN6 (L) and (H) passage cells (Fig: 3.10.5.4).

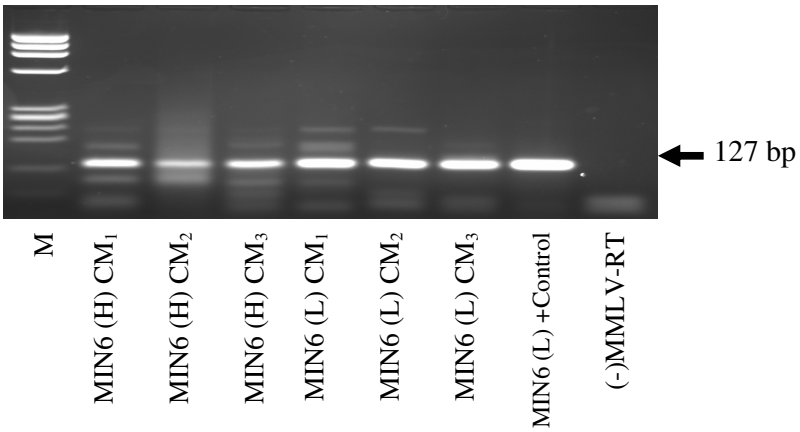


**Fig: 3.10.5.4 *Pancreatic and duodenal homeobox gene 1* (*Pdx1*) analysis in CM from MIN6 (L) and (H). (-) MMLV-RT = RT-PCR reaction carried out without reverse transcriptase enzyme. M = molecular weight marker: ΦX174 DNA Hae III digest. 1, 2 & 3 represent biological repeat experiments.**

### *Neuropeptide Y* (*Npy*)

RNA from CM collected from glucose responsive MIN6 (L) and glucose non-responsive MIN6 (H) were analysed for *Npy*. *Npy* (Fig: 3.10.5.5) were amplified using RNA from media conditioned by MIN6 (L) cells but were undetected in media conditioned by MIN6 (H) cells.

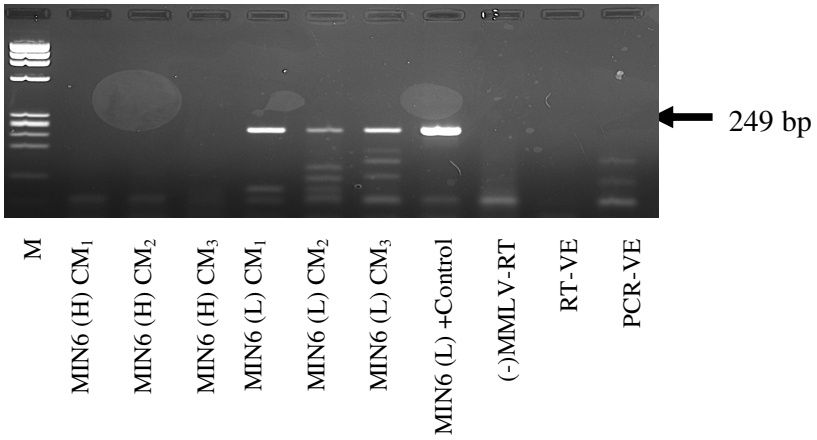


**Fig: 3.10.5.5 *Neuropeptide Y* analysis in CM from MIN6 (L) and (H). RT-VE = reaction with $H_2O$ instead of RNA as control; PCR-VE = PCR reaction with $H_2O$ instead of cDNA as a control; (-) MMLV-RT = RT-PCR reaction carried out without reverse transcriptase enzyme. M = molecular weight marker: ΦX174 DNA Hae III digest. 1, 2 & 3 represent biological repeat experiments.**

### *Chromogranin B* (*Chgb*)

Fig 3.10.5.6 shows that *Chgb* was amplified using MIN6 (L) CM RNA whereas no amplification was detected using CM RNA from MIN6 (H). RNA from MIN6 (L) was taken as positive control.

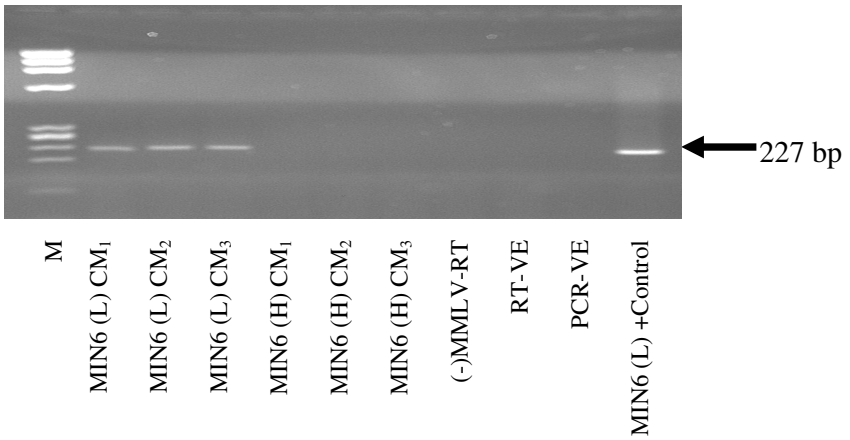


**Fig: 3.10.5.6 *Chromogranin B* (*Chgb*) analysis in CM from MIN6 (L) and (H). RT-VE = reaction with $H_2O$ instead of RNA as control; PCR-VE = PCR reaction with $H_2O$ instead of cDNA as a control; (-) MMLV-RT = RT-PCR reaction carried out without reverse transcriptase enzyme. M = molecular weight marker: ΦX174 DNA Hae III digest. 1, 2 & 3 represent biological repeat experiments.**

***Prohormone convertase 2 (PC2)***

RNA from CM collected from glucose responsive MIN6 (L) and glucose non-responsive MIN6 (H) were analysed for PC2. PC2 (Fig: 3.10.5.7) were amplified using RNA from media conditioned by MIN6 (L) cells but were undetected in media conditioned by MIN6 (H) cells.

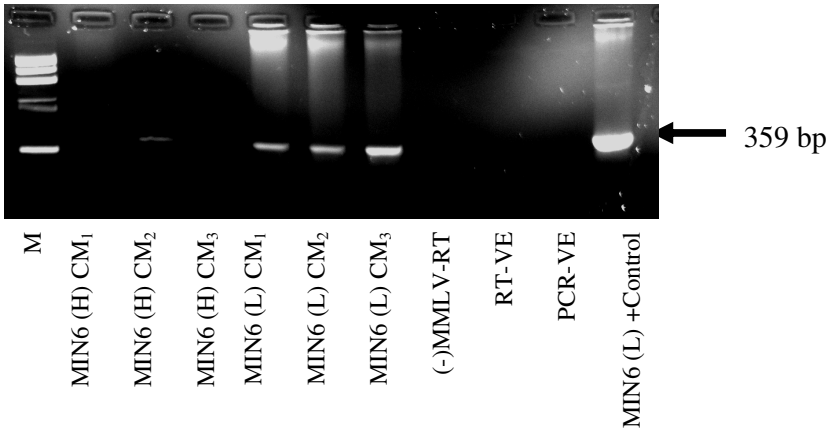


**Fig: 3.10.5.7 *Prohormone convertase 2 (PC2)* analysis in CM from MIN6 (L) and (H). RT-VE = reaction with $H_2O$ instead of RNA as control; PCR-VE = PCR reaction with $H_2O$ instead of cDNA as a control; (-) MMLV-RT = RT-PCR reaction carried out without reverse transcriptase enzyme. M = molecular weight marker: ΦX174 DNA Hae III digest. 1, 2 & 3 represent biological repeat experiments.**

### *Phospholipase D1 (Pld1)*

*Pld1* was amplified using RNA from media conditioned by MIN6 (L) cells but was undetected in media conditioned by MIN6 (H) cells (Fig: 3.10.5.8). RNA from MIN6 (L) was used as control.

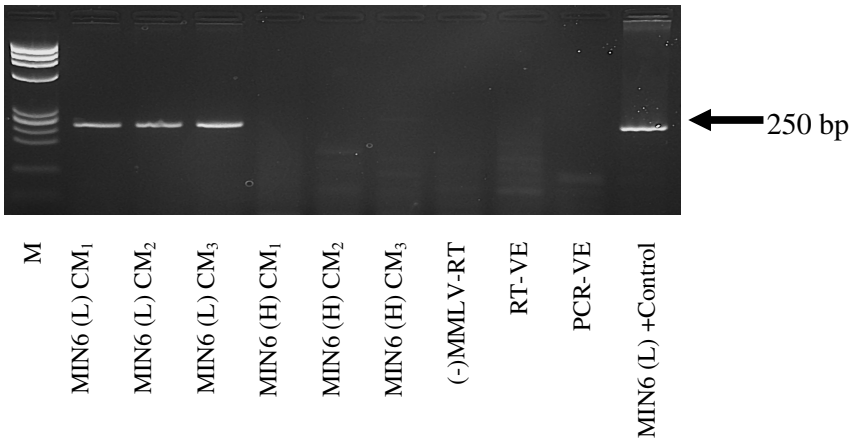


**Fig: 3.10.5.8 *Phospholipase D1 (Pld1)* analysis in CM from MIN6 (L) and (H). RT-VE = reaction with $H_2O$ instead of RNA as control; PCR-VE = PCR reaction with $H_2O$ instead of cDNA as a control; (-) MMLV-RT = RT-PCR reaction carried out without reverse transcriptase enzyme. M = molecular weight marker: ΦX174 DNA Hae III digest. 1, 2 & 3 represent biological repeat experiments.**

***Early growth response 1 (Egr1)***

Fig 3.10.5.9 shows that *Egr1* was amplified using MIN6 (L) CM RNA whereas no amplification was detected using CM RNA from MIN6 (H). RNA from MIN6 (L) was taken as positive control.

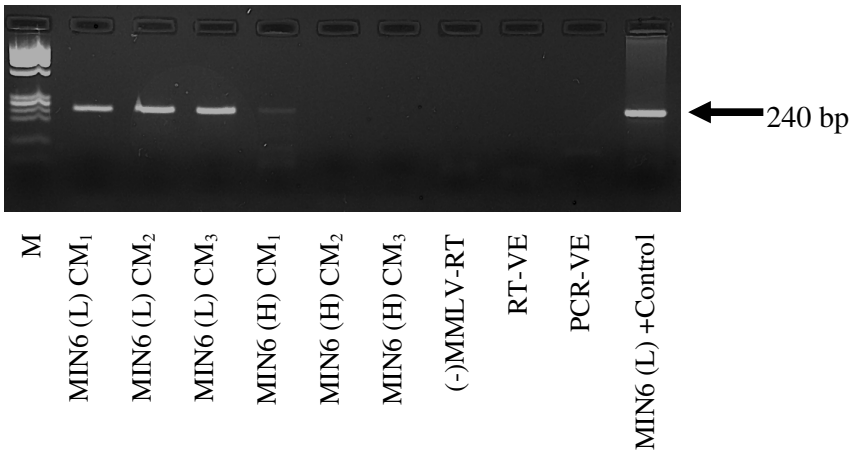


**Fig: 3.10.5.9 *Early growth response 1 (Egr1)* analysis in CM from MIN6 (L) and (H). RT-VE = reaction with $H_2O$ instead of RNA as control; PCR-VE = PCR reaction with $H_2O$ instead of cDNA as a control; (-) MMLV-RT = RT-PCR reaction carried out without reverse transcriptase enzyme. M = molecular weight marker: ΦX174 DNA Hae III digest. 1, 2 & 3 represent biological repeat experiments.**

### *Glutamate decarboxylase 1 (Gad1)*

Conditioned media RNA isolated from MIN6 (L), glucose responsive and MIN6 (H), glucose non-responsive were amplified for *Gad1*. *Gad1* was amplified using MIN6 (H) CM RNA (Fig: 3.10.5.10), whereas it was undetected in MIN6 (L) CM RNA. This result shows that the expression of this gene was up-regulated in MIN6 (H) cells compared to MIN6 (L) cells.

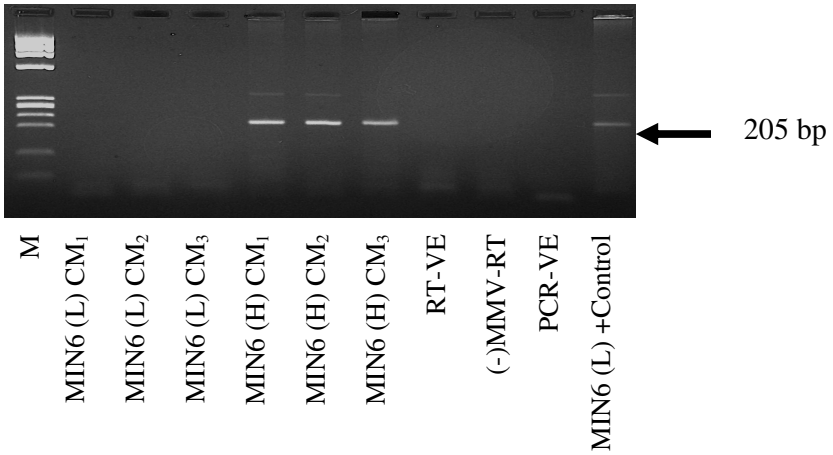


**Fig: 3.10.5.10 *Glutamate decarboxylase 1* analysis in CM from MIN6 (L) and (H). RT-VE = reaction with $H_2O$ instead of RNA as control; PCR-VE = PCR reaction with $H_2O$ instead of cDNA as a control; (-) MMLV-RT = RT-PCR reaction carried out without reverse transcriptase enzyme. M = molecular weight marker: ΦX174 DNA Hae III digest. 1, 2 & 3 represent biological repeat experiments.**

### 3.10.6 Analysis of mRNA from cells and conditioned media at different cell density

#### 3.10.6.1 Analysis of mRNA from cells and conditioned media of MIN6 B1 cell line

To investigate if the abundance of specific mRNAs detectable in CM reflected the cell numbers conditioning the medium, MIN6 B1 cells were seeded at a range of densities. Insulin-producing MIN6 B1 were seeded at different densities i.e. 1x $10^6$ cells, 5x$10^6$ cells and 1x$10^7$ cells per T25cm$^2$ flask along with a total of 4 mls of culture media. Cells were allowed to grow for 48 hrs. Conditioned media was taken off and sterile filtered using 0.45 μm to make sure that there are no cells (See Section: 2.4.3.1).

*Beta-actin* (Fig: 3.10.6.1) was amplified using all cell and CM RNA from MIN6 B1 cells. The presence and amounts of a number of transcripts including *Pdx1* (Fig: 3.10.6.5), *early growth response gene 1* (*Egr1*) (Fig: 3.10.6.3), *chromagranin B* (*Chgb*) (Fig: 3.9.6.2), *insulin I* (*Ins1*) (Fig: 3.10.6.7), *Glucokinase (Gck) (*Fig: 3.10.6.4), and *paired box transcription factor 4* (*Pax4*) (Fig: 3.10.2.1) were investigated. As shown, all 5 transcripts analysed were detected in MIN6 B1 cell RNA isolates and all – with the exception of *Pax4* – were detected in the corresponding CM samples.

*Beta-Actin (actb)*

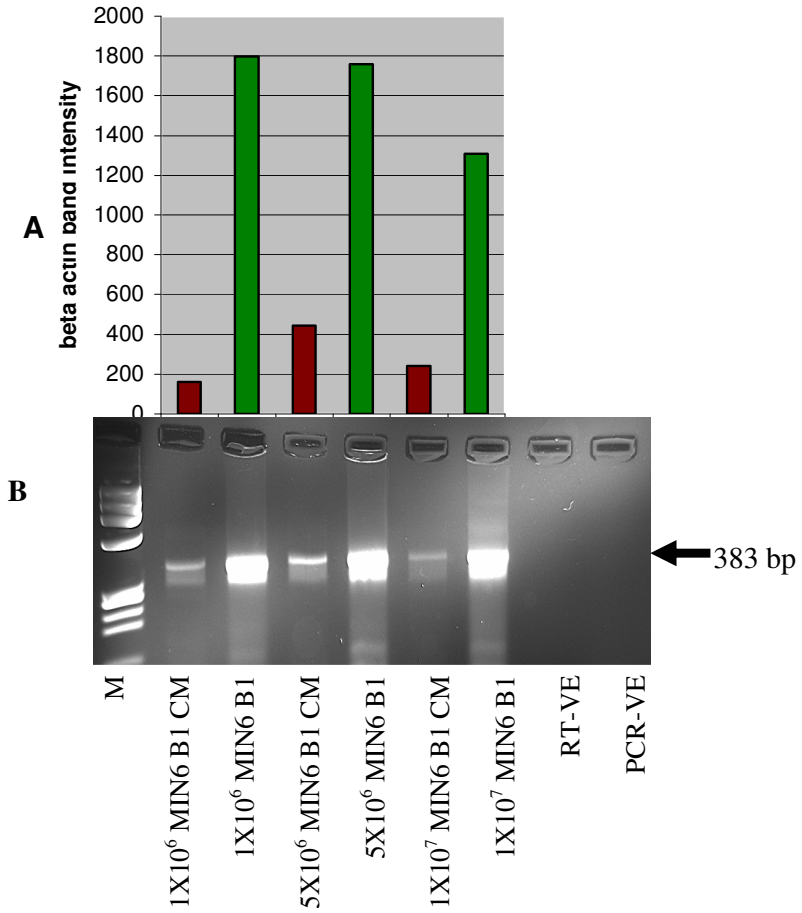


**Fig: 3.10.6.1** ***Beta-Actin*** **mRNA analysis of MIN6 B1 cells, grown at a range of densities, and their corresponding CM. RT-VE = reaction with $H_2O$ instead of RNA as control; PCR-VE = PCR reaction with $H_2O$ instead of cDNA as control. (A) Densitometry analysis of amplified gene products shown above image of gel. M = molecular weight marker: ΦX174 DNA Hae III digest. Results are representative of n = 3 biological repeats.**

### *Chromogranin B (Chgb)*

Chgb was amplified in all cell RNA from different cell densities and their corresponding CM. The intensity of the *Chgb* band produced following 45 cycles of PCR was directly associated with the numbers of cells conditioning the medium *i.e.* increased number of cells resulted in increased levels of these transcripts detectable in a fixed volume of CM (Fig: 3.10.6.2).

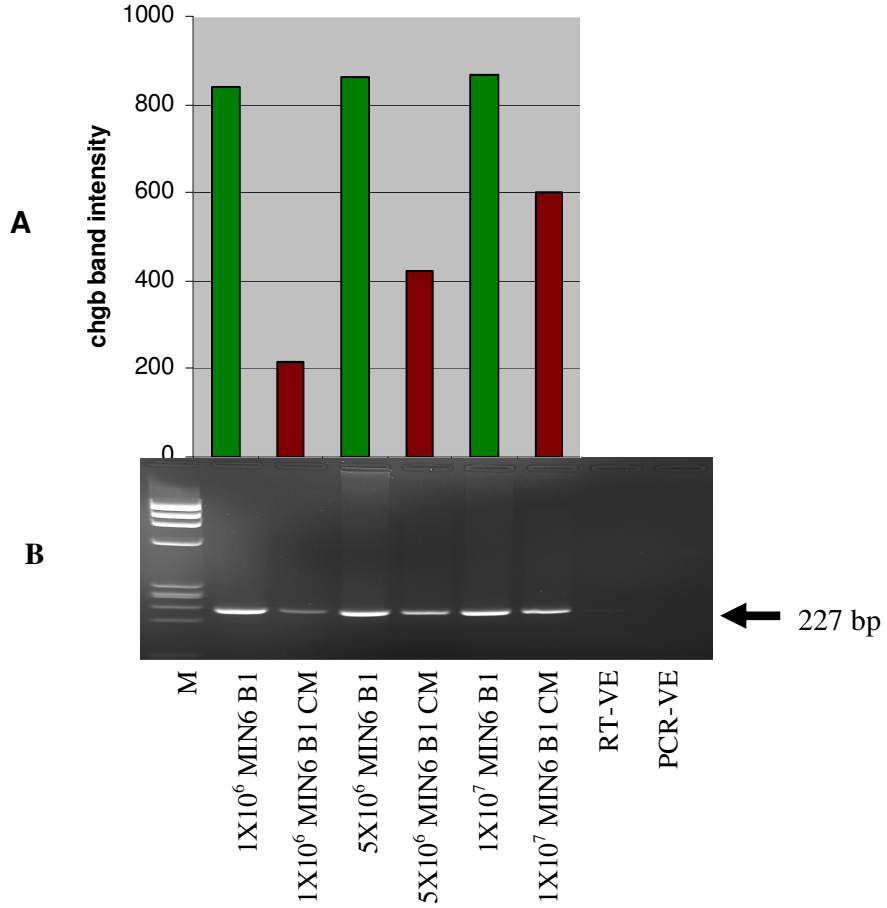


**Fig: 3.10.6.2** ***Chromogranin B*** **mRNA analysis of MIN6 B1 cells, grown at a range of densities, and their corresponding CM. RT-VE = reaction with $H_2O$ instead of RNA as control; PCR-VE = PCR reaction with $H_2O$ instead of cDNA as control. (A) Densitometry analysis of amplified gene products shown above image of gel. M = molecular weight marker: ΦX174 DNA Hae III digest. Results are representative of n = 3 biological repeats.**

### *Early growth response 1* (*Egr1*)

*Egr1* was amplified in RNA from range of different cell densities and their corresponding CM. Increased number of cells resulted in increased levels of *Egr1* transcript detectable in a fixed volume of CM. Fig: 3.10.6.3 shows that the intensity of *Egr1* band produced following 45 cycles of PCR was directly associated with the numbers of cells conditioning the medium.

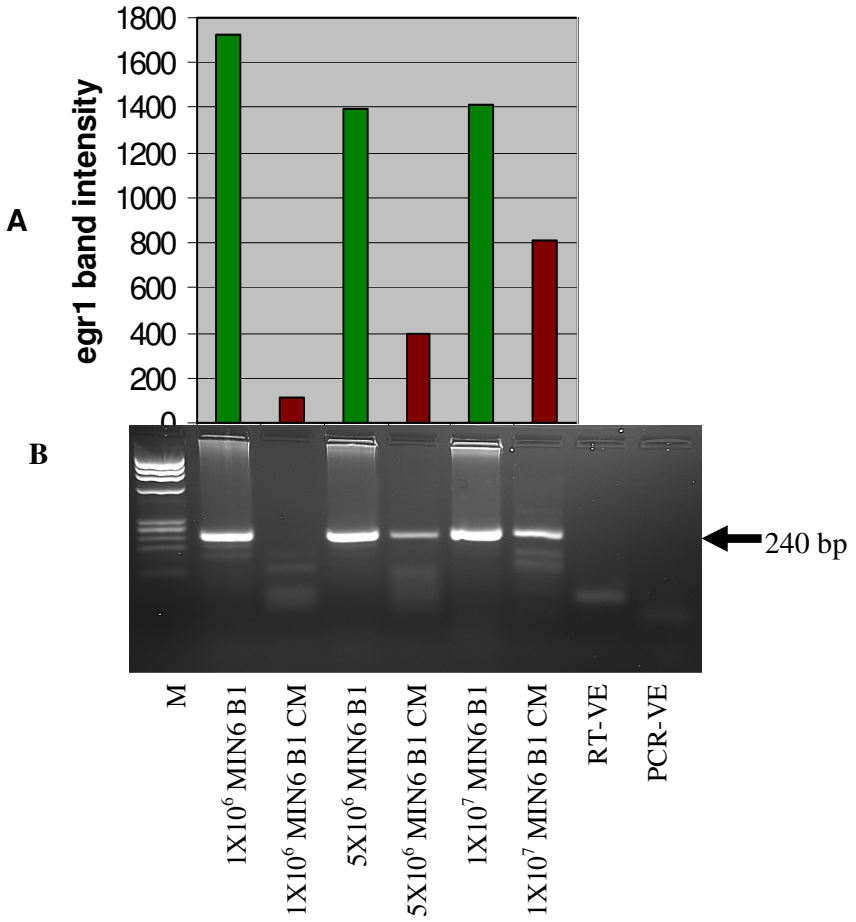


**Fig: 3.10.6.3** ***Early growth response 1*** **mRNA analysis of MIN6 B1 cells, grown at a range of densities, and their corresponding CM. RT-VE = reaction with $H_2O$ instead of RNA as control; PCR-VE = PCR reaction with $H_2O$ instead of cDNA as control. (A) Densitometry analysis of amplified gene products shown above image of gel. M = molecular weight marker: ΦX174 DNA Hae III digest. Results are representative of n = 3 biological repeats.**

*Glucokinase (Gck)*

Amplification of cell RNA from different cell densities using 45 cycles of PCR showed increased levels of transcript corresponding with increased number of cells analysed.

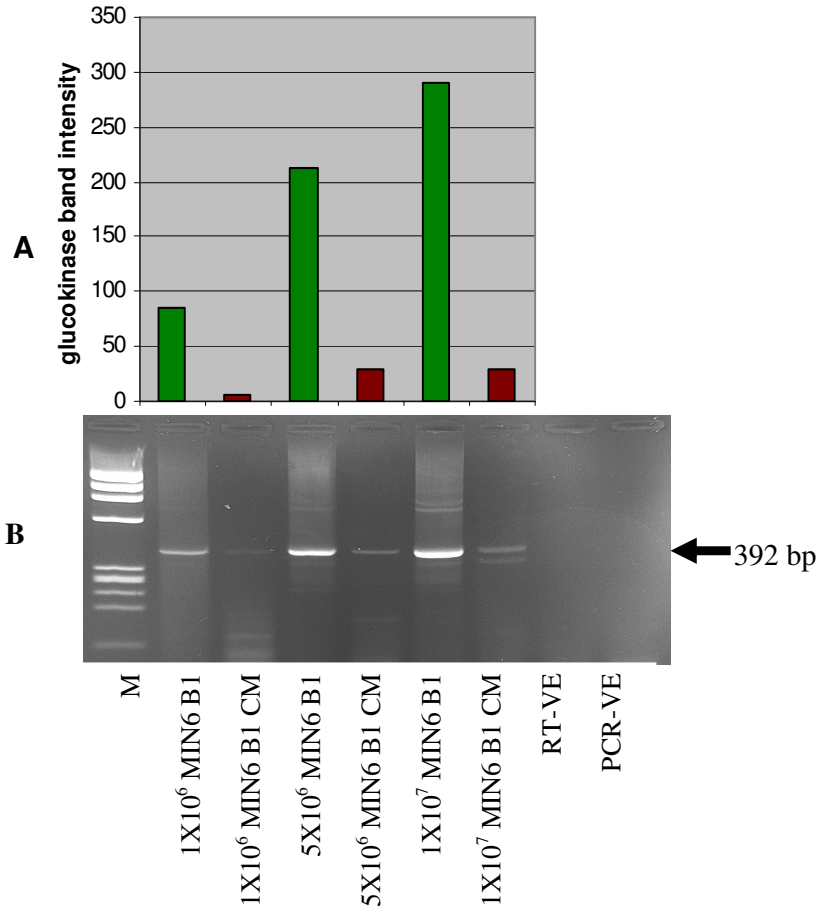


**Fig: 3.10.6.4** ***Glucokinase*** **mRNA analysis of MIN6 B1 cells, grown at a range of densities, and their corresponding CM. RT-VE = reaction with $H_2O$ instead of RNA as control; PCR-VE = PCR reaction with $H_2O$ instead of cDNA as control. (A) Densitometry analysis of amplified gene products shown above image of gel. M = molecular weight marker: ΦX174 DNA Hae III digest. Results are representative of n = 3 biological repeats.**

Similar result was seen with the media conditioned by these cells. Fig: 3.10.6.4 shows that the intensity of *Egr1* band produced following 45 cycles of PCR was directly associated with the numbers of cells conditioning the medium.

***Pancreatic and duodenal homeobox gene 1(Pdx1)***

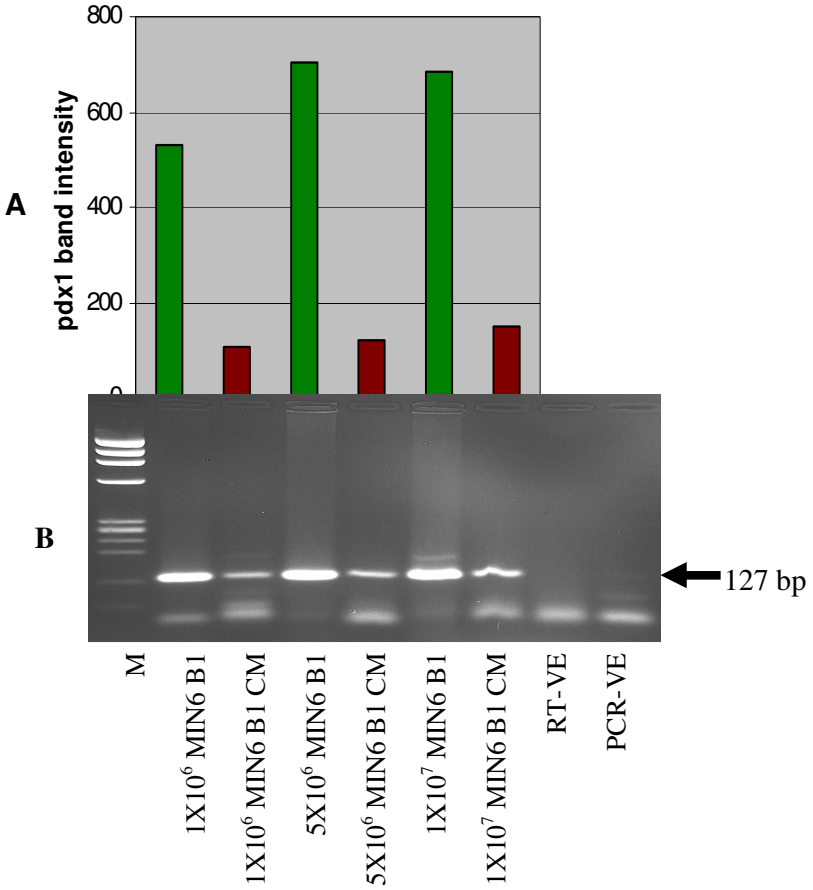


**Fig: 3.10.6.5** ***Pancreatic and duodenal homeobox gene 1*** **mRNA analysis of MIN6 B1 cells, grown at a range of densities, and their corresponding CM. RT-VE = reaction with $H_2O$ instead of RNA as control; PCR-VE = PCR reaction with $H_2O$ instead of cDNA as control. (A) Densitometry analysis of amplified gene products shown above image of gel. M = molecular weight marker: ΦX174 DNA Hae III digest. Results are representative of n = 3 biological repeats.**

CM and cell RNA from MIN6 B1 cells seeded at range of different densities were amplified for *Glutamate decarboxylase1*, *Insulin II* and *Phospholipase D1*. *Gad1* (Fig: 3.10.6.6) was amplified using cell RNA from $10^6$ cells and $5x10^6$ cells however there was no further increase in band size/intensity upon analysis of $1x10^7$ cells RNA. This may be due to the high levels of *Gad1* present in the cells, which are reaching plateau phase for PCR analysis at the higher cell densities. *Gad1* was amplified only in CM RNA isolated from $1x10^7$ cells.

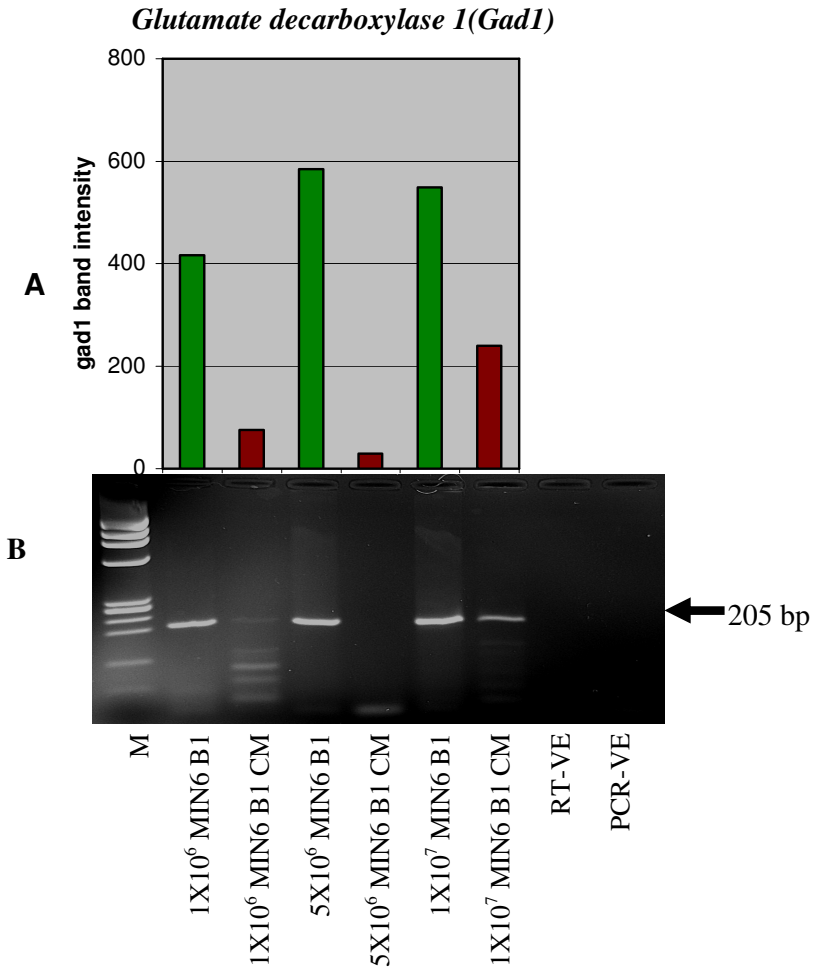


**Fig: 3.10.6.6 *Glutamate decarboxylase 1* mRNA analysis of MIN6 B1 cells, grown at a range of densities, and their corresponding CM. RT-VE = reaction with $H_2O$ instead of RNA as control; PCR-VE = PCR reaction with $H_2O$ instead of cDNA as control. (A) Densitometry analysis of amplified gene products shown above image of gel. M = molecular weight marker: ΦX174 DNA Hae III digest. Results are representative of n = 3 biological repeats.**

### *Insulin II (Ins2)*

*Ins2* (Fig: 3.10.6.7) was amplified using cell RNA from $10^6$ cells and $5x10^6$ cells however there was no further increase in band size/intensity upon analysis of $1x10^7$ cells RNA which seemed to reach plateau phase of PCR analysis.

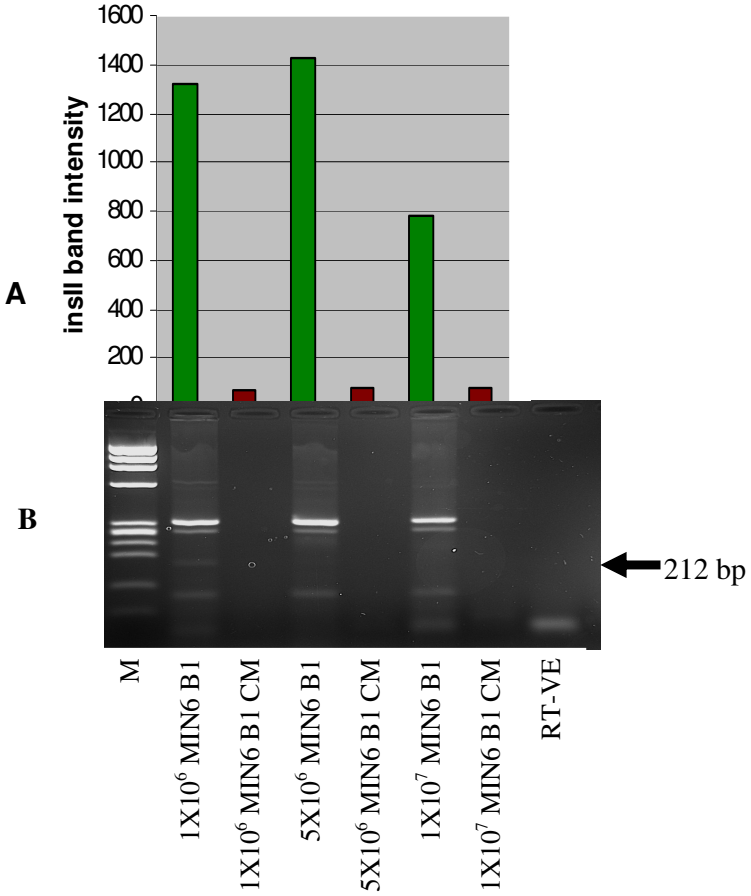


**Fig: 3.10.6.7** ***Insulin II*** **mRNA analysis of MIN6 B1 cells, grown at a range of densities, and their corresponding CM. RT-VE = reaction with $H_2O$ instead of RNA as control; PCR-VE = PCR reaction with $H_2O$ instead of cDNA as control. (A) Densitometry analysis of amplified gene products shown above image of gel. M = molecular weight marker: ΦX174 DNA Hae III digest. Results are representative of n = 3 biological repeats.**

***Phospholipase D1 (Pld1)***

*Pld1* (Fig: 3.10.6.8) was amplified in RNA isolated from $10^6$ cells, $5x10^6$ cells and $1x10^7$ cells following 45 cycles of PCR, however very low level of this transcript was detectable in a fixed volume of CM.

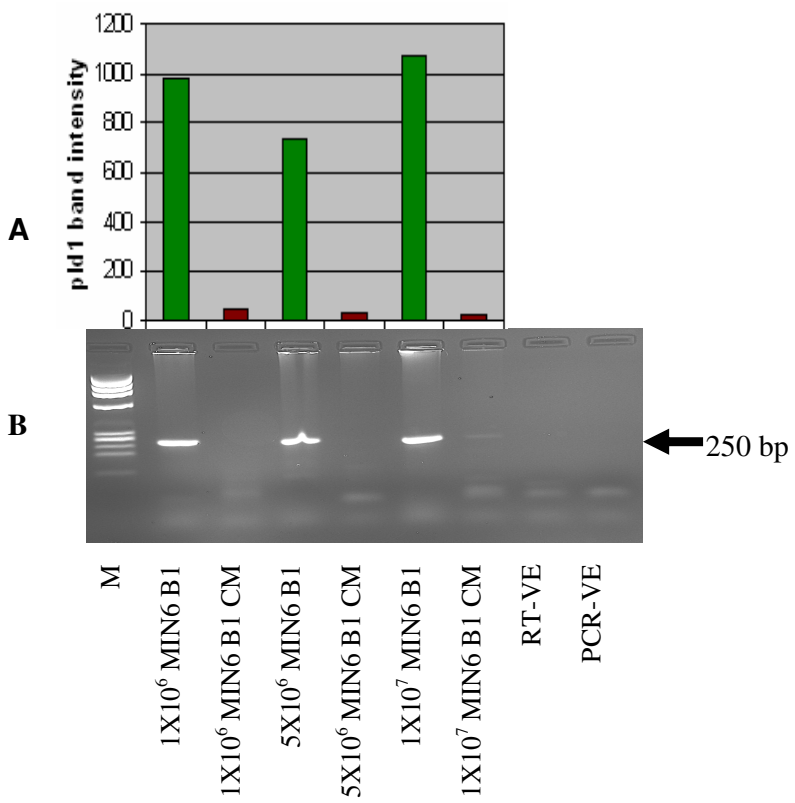


**Fig: 3.10.6.8** ***Phospholipase D1*** **mRNA analysis of MIN6 B1 cells, grown at a range of densities, and their corresponding CM. RT-VE = reaction with $H_2O$ instead of RNA as control; PCR-VE = PCR reaction with $H_2O$ instead of cDNA as control. (A) Densitometry analysis of amplified gene products shown above image of gel. M = molecular weight marker: ΦX174 DNA Hae III digest. Results are representative of n = 3 biological repeats.**

### *Insulin I (Ins1)*

In the case of *Ins1* (Fig: 3.10.6.9 ) increased amounts of amplified product resulted for RNA isolated from medium conditioned by $5X10^6$ cells compared to medium conditioned by $1X10^6$ cells.

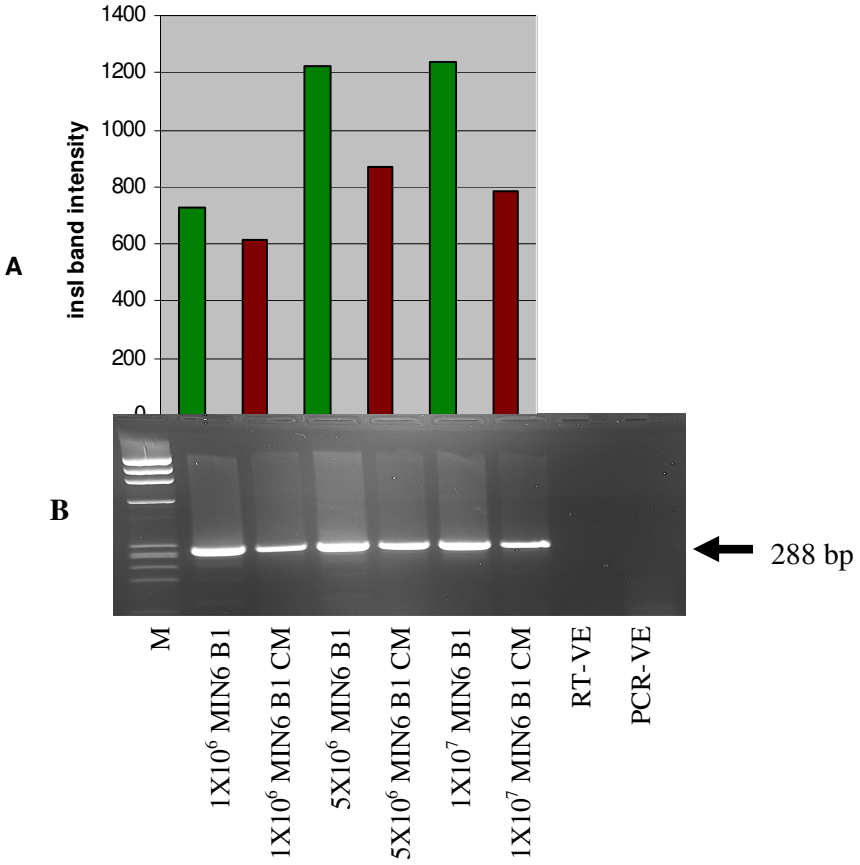


**Fig: 3.10.6.9** ***Insulin I*** **mRNA analysis of MIN6 B1 cells, grown at a range of densities, and their corresponding CM. RT-VE = reaction with $H_2O$ instead of RNA as control; PCR-VE = PCR reaction with $H_2O$ instead of cDNA as control. (A) Densitometry analysis of amplified gene products shown above image of gel. M = molecular weight marker: ΦX174 DNA Hae III digest. Results are representative of n = 3 biological repeats.**

However, a further increase in band size/intensity was not found upon analysis of medium conditioned by $1X10^7$ cells. This is likely to be due to the high levels of *Ins1* present in CM, which are reaching plateau phase for PCR analysis at the higher cell densities.

### 3.10.7 Selective release of gene transcript

*Pax4* (Fig: 3.10.7) was expressed by MIN6 B1 cells and on amplification of cell RNA using 45 cycles of PCR increased levels of transcript were found to correspond with increased number of cells analysed. However, using RT-PCR methods, this gene transcript was not detected in medium conditioned by these cells.

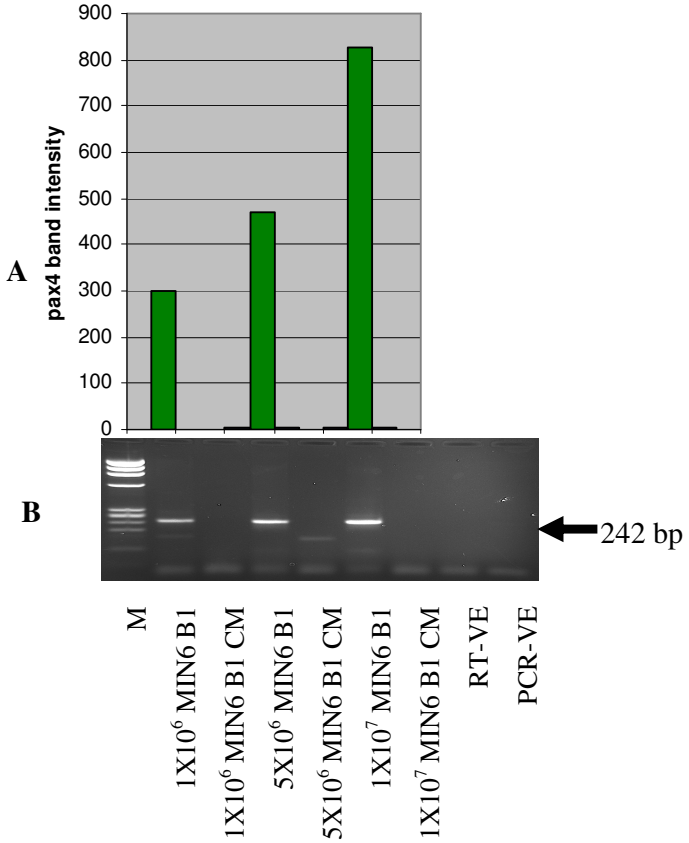


**Fig: 3.10.7** ***Paired box gene 4*** **mRNA analysis of MIN6 B1 cells, grown at a range of densities, and their corresponding CM. RT-VE = reaction with $H_2O$ instead of RNA as control; PCR-VE = PCR reaction with $H_2O$ instead of cDNA as control. (A) Densitometry analysis of amplified gene products shown above image of gel. M = molecular weight marker: ΦX174 DNA Hae III digest. Results are representative of n = 3 biological repeats.**

### 3.10.8 Analysis of mRNA from cells and conditioned media from Vero-PPI cell line

After investigating specific mRNAs detectable in CM reflected the cell numbers conditioning the medium in MIN6 B1 cells, Vero-PPI cells were investigated. Insulin-producing Vero-PPI cells were seeded at a range of densities i.e. 1x $10^6$ cells, 5x$10^6$ cells and 1x$10^7$ cells per T25cm$^2$ flask along with a total of 4 mls of culture media. Cells were allowed to grow for 48hrs. Conditioned media was taken off and sterile filtered using 0.45 μm to make sure that there are no cells (See Section: 2.4.3.1). The presence and amounts of *preproinsulin* was investigated.

Analysis of human *preproinsulin* mRNA (Fig: 3.10.8), transcribed by Vero-PPI cells, showed increasing levels of *preproinsulin* mRNA in 1x $10^6$ cells and 5x$10^6$ cells; however, the amounts of *preproinsulin* detected in 1x$10^7$ cells seemed to reach plateau phase and PCR was no longer exponential beyond analysis of RNA from 5X$10^6$ cells. Similarly the amounts of *preproinsulin* detected in CM seemed to reach plateau phase and PCR was no longer exponential beyond analysis of CM from 5X$10^6$ cells.

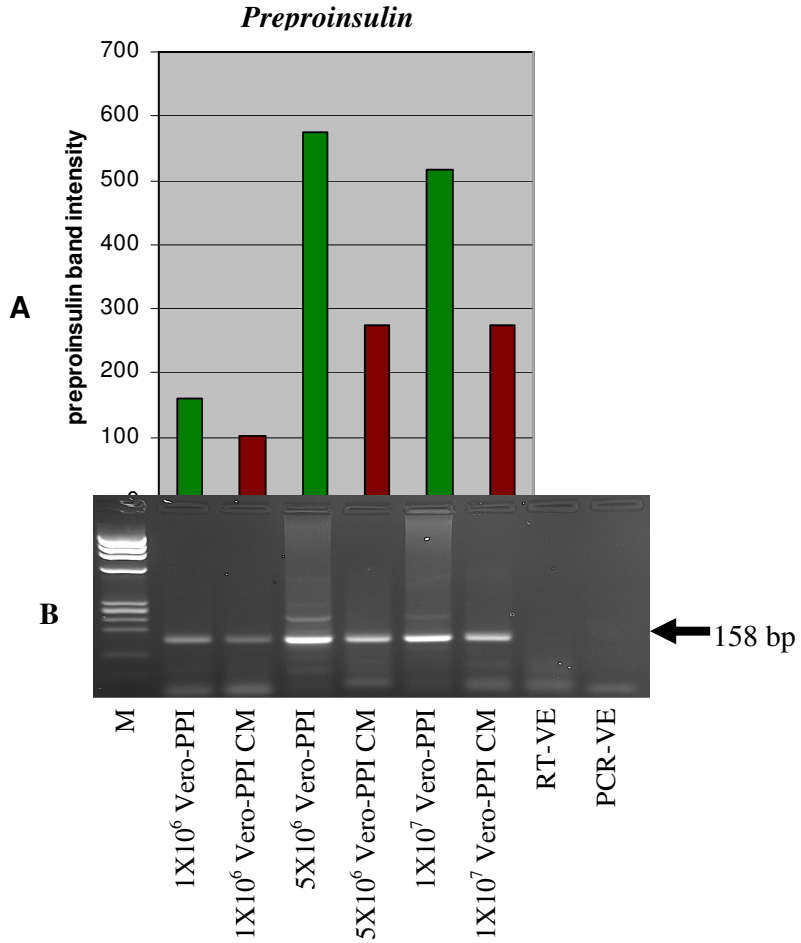


**Fig: 3.10.8 Human *preproinsulin* mRNA analysis of Vero-PPI cells, grown at a range of densities, and their corresponding CM. RT-VE = reaction with $H_2O$ instead of RNA as control; PCR-VE = PCR reaction with $H_2O$ instead of cDNA as a control. M = molecular weight marker: ΦX174 DNA Hae III digest. Results are representative of n = 3 biological repeats.**

### 3.11 Analysis of serum for amplifiable Gene Transcripts

In the study of media conditioned by insulin-producing cell lines we were able to reproducibly amplify extracellular mRNAs. Building on these findings we advanced our study to serum from people with diabetes and those without this condition as control.

#### 3.11.1 Patient information

The study involved patients with newly diagnosed Type 2 diabetes (4.36 +/- 2.33 months mean duration) (6 male and 5 female) with a mean age of 56 ± 9 (male 53 ± 8 years, female 59 ± 11 years; mean ± S.D.). This study also included control group with a mean age of 52 ± 8 (male 49 ± 9 years, female 56 ± 5; mean ± S.D.). All the controls had normal oral glucose tolerance test. The oral glucose tolerance for non-diabetic controls used were cut-off values less than 5.6 fasting glucose and less than 7.8 two hours postprandial blood glucose. Table 3.11.1 shows the details of controls and Type 2 diabetes subjects.

Haemoglobin A1C (HbA1C) level were significantly higher in Type 2 diabetes subject compared to controls (p-value=0.00036). Fasting glucose was significantly higher in Type 2 diabetes subject compared to controls (p-value=0.005) with no significant change in insulin secretion or fasting insulin levels. Controls showed a significantly higher cholesterol (p-value=0.001) and LDL-cholesterol level (p-value=0.006) compared to Type 2 diabetes subjects whereas, there was no significant difference in HDL-cholesterol.

**Table: 3.11.1 General characteristics of the study population**

| | **Controls** | **Type 2 Diabetes subject** | **p-value** |
|---|---|---|---|
| Age (years) | 52 ± 8 | 56 ± 9.8 | 0.387 |
| BMI (kg/m$^2$) | 29.31 ± 4.8 | 31.9 ± 4 | 0.187 |
| Waist/hip ratio | 0.93±0.05 | 0.98±0.09 | 0.27 |
| Fasting glucose (mmol/L) | 5.15 ± 0.4 | 7.62 ± 2.6 | 0.005 |
| Insulin (pmmol/L) | 50.24 ± 32.6 | 52.36 ± 28.4 | 0.872 |
| Cholesterol (mmol/L) | 5.9 ± 1.0 | 4.24 ± 1.0 | 0.001 |
| 2hPP Glc | 5.17 ± 0.9 | NA | NA |
| HOMA IR | 1.08 ± 0.7 | 1.24 ± 0.6 | 0.591 |
| HOMA %S | 112.8 ± 45.8 | 94.05 ± 59.1 | 0.415 |
| HOMA %B | 97.9 ± 55.0 | 67.15 ± 43.6 | 0.162 |
| Diastolic BP (mmHg) | 82 ± 8.1 | 83.45 ± 7.0 | 0.658 |
| Systolic BP (mmHg) | 138.45 ± 17.4 | 139.45 ± 17.4 | 0.894 |
| HDL-cholesterol (mmol/L) | 1.46 ± 0.5 | 1.14 ± 0.3 | 0.100 |
| LDL-cholesterol (mmol/L) | 3.78 ± 0.8 | 2.5 ± 1.0 | 0.006 |
| HbA1C | 5.4 ± 0.3 | 7.43 ± 1.53 | 0.000 |
| Triglyceride (mmol/L) | 1.96 ± 1.6 | 1.28 ± 0.4 | 0.186 |

BMI, body mass index; HOMA IR, homeostasis model assessment-insulin resistance; HbA1C, haemoglobin A1C; 2hPP Glc, 2 hours postprandial blood glucose

### 3.11.2 *Txnip* expression in Type 2 diabetes and controls

There was 1.8-fold increase in *Txnip* expression but was not significant (p-value=0.12) in Type 2 diabetes subjects compared to controls. To exclude any amplification product derived from genomic DNA that could contaminate the RNA preparation, total RNA from Type 2 diabetes subjects and controls were amplified without reverse transcriptase enzyme as a negative control. Water on its own was amplified as a negative control to rule out presence of any contaminating RNA or DNA in it.

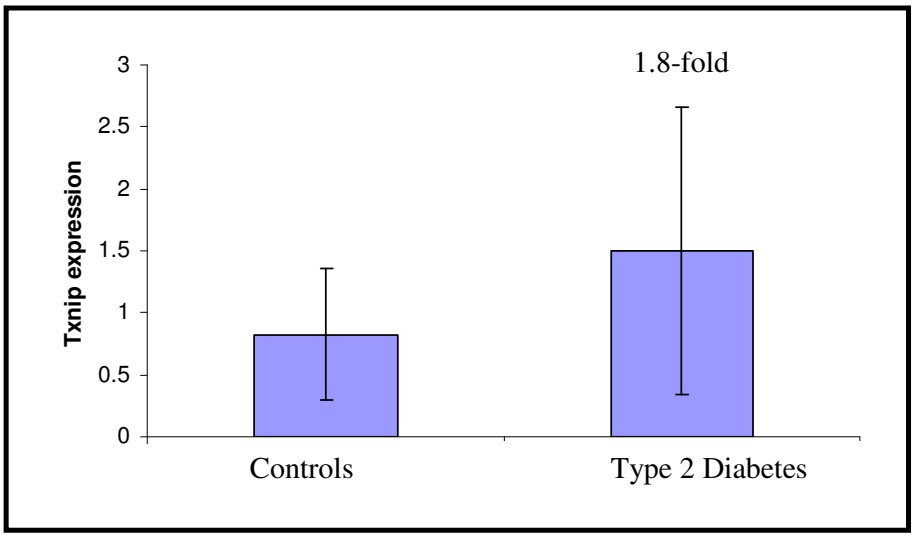


**Fig: 3.11.2.1 *Txnip* expression as determined by qRT-PCR in controls and Type 2 diabetes subjects. Type 2 diabetes subject showed 1.8-fold increase in *Txnip* expression compared to controls. *Beta-actin* was taken as endogenous control. Results represent mean ± S.D from 11 Type 2 diabetes and controls. –RT was used as control to prove that amplification was RNA specific and not from contaminating-DNA**

The *Txnip* was amplified at 31.6 cycle threshold (ct) in Type 2 diabetes subject and 30.2 ct in controls (Fig: 3.11.2.2).

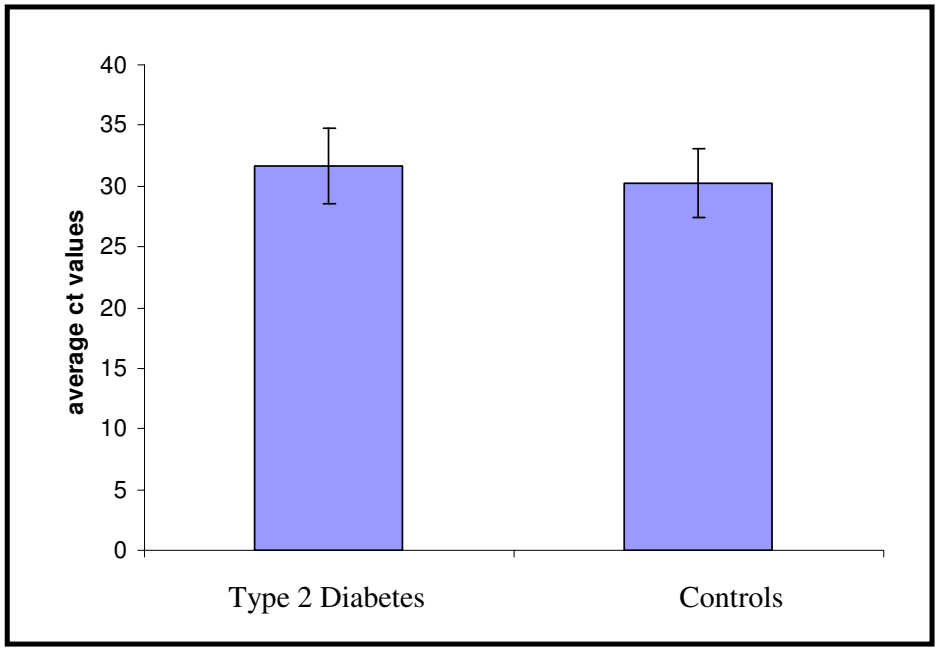


**Fig: 3.11.2.2 Average cycle threshold (ct) at which *Txnip* mRNA was amplified in controls and Type 2 diabetes subjects. The graph shows the mean ct values of 11 controls and Type 2 diabetes subjects. Results represent mean ± S.D.**

*Txnip* expression and insulin levels (fasting) (correlation= -0.46) as well as insulin secretion in Type 2 diabetes subjects was negatively correlated (correlation= -0.50). Comparison of *Txnip* expression and insulin levels (fasting) in 11 Type 2 diabetes (Fig: 3.11.2.3) and controls (Fig: 3.11.2.4).

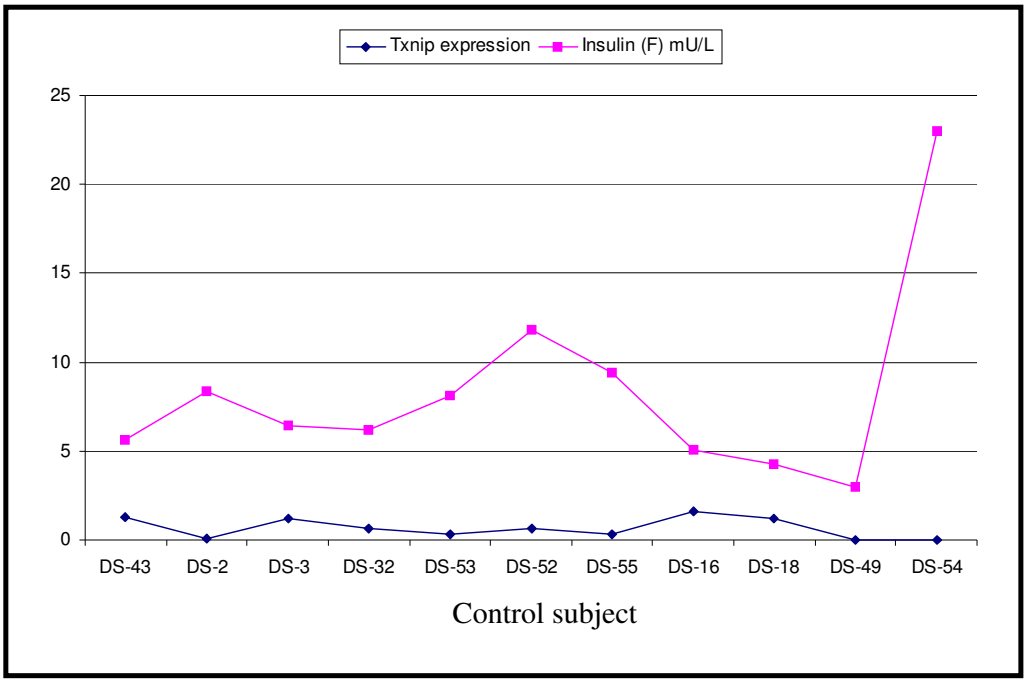


**Fig: 3.11.2.3 *Txnip* expression and insulin levels (fasting) in different controls.**

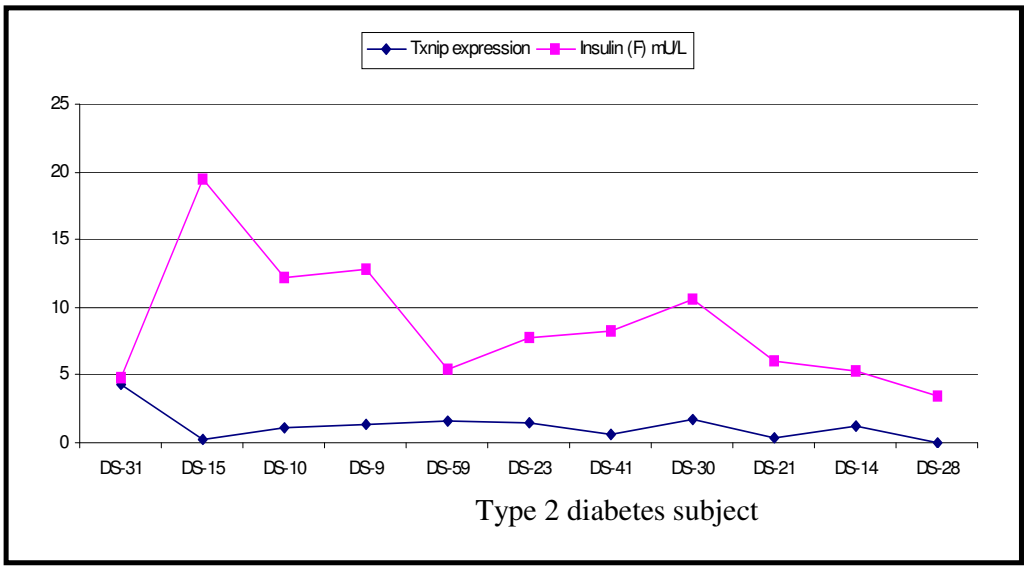


**Fig: 3.11.2.4 *Txnip* expression and insulin levels (fasting) in different Type 2 diabetes subjects.**

### 3.11.3 *Egr1* expression in Type 2 diabetes subjects and controls

*Egr1* expression was significantly (p-value=0.017) down-regulated in Type 2 diabetes subjects compared to controls. *Egr1* expression was down-regulated 2.21-fold in Type 2 diabetes subject (Fig: 3.11.3.1). In order to exclude any amplification product derived from genomic DNA that could contaminate the RNA preparation, total RNA from Type 2 diabetes subjects and controls were amplified without reverse transcriptase enzyme as a negative control. Water on its own was amplified as a negative control to rule out presence of any contaminating RNA or DNA in it.

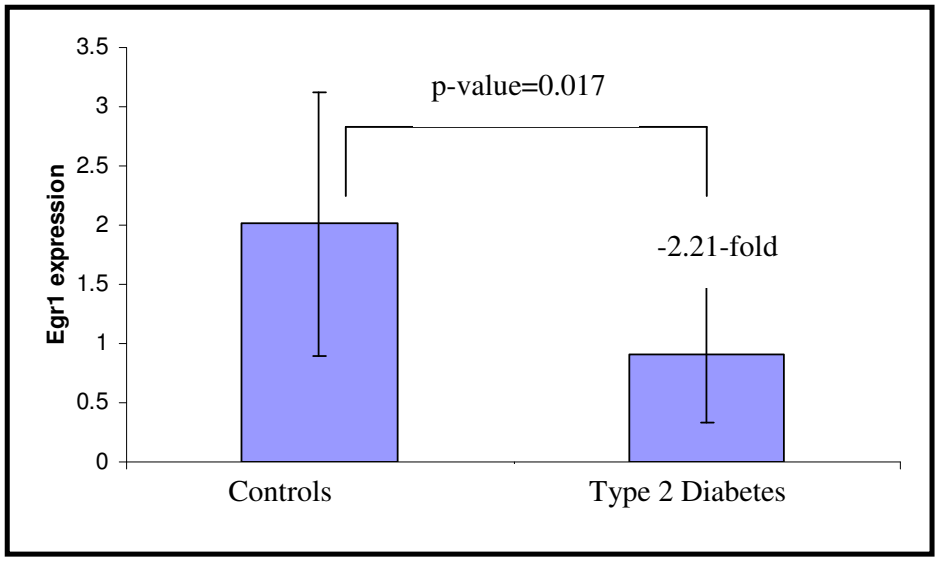


**Fig: 3.11.3.1 *Egr1* expression as determined by qRT-PCR in Type 2 diabetes and controls. Type 2 diabetes subjects showed -2.21-fold down-regulation of *Egr1* expression compared to controls. *Beta-actin* was taken as endogenous control. Results represent mean ± S.D form 11 Type 2 diabetes and controls.**

The *Egr1* was amplified at 37.5 ct in Type 2 diabetes subject and 35.5 ct in controls (Fig: 3.11.3.2).

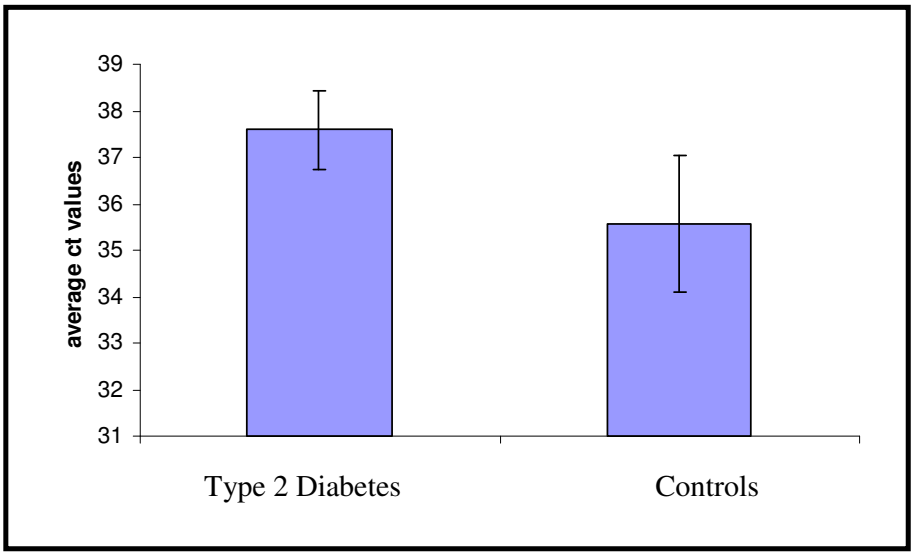


**Fig: 3.11.3.2 Average cycle threshold (ct) at which *Egr1* mRNA was amplified in Type 2 diabetes and controls. The graph shows the mean ct values of 11 Type 2 diabetes and controls. Results represent mean ± S.D.**

*Egr1* expression and insulin fasting (correlation= 0.53) was positively correlated in Type 2 diabetes subject and was negatively correlated (correlation= -0.12) in controls.

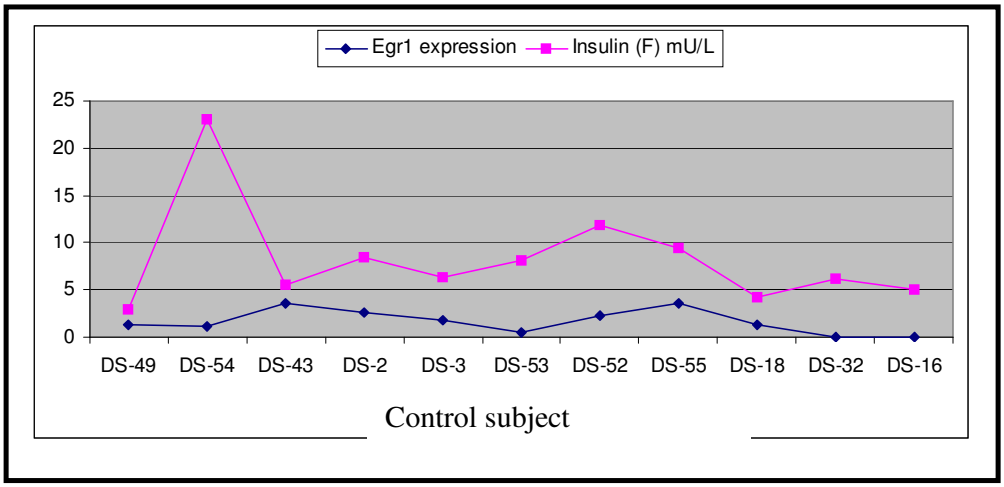


**Fig: 3.11.3.3 *Egr1* expression and insulin fasting in different controls.**

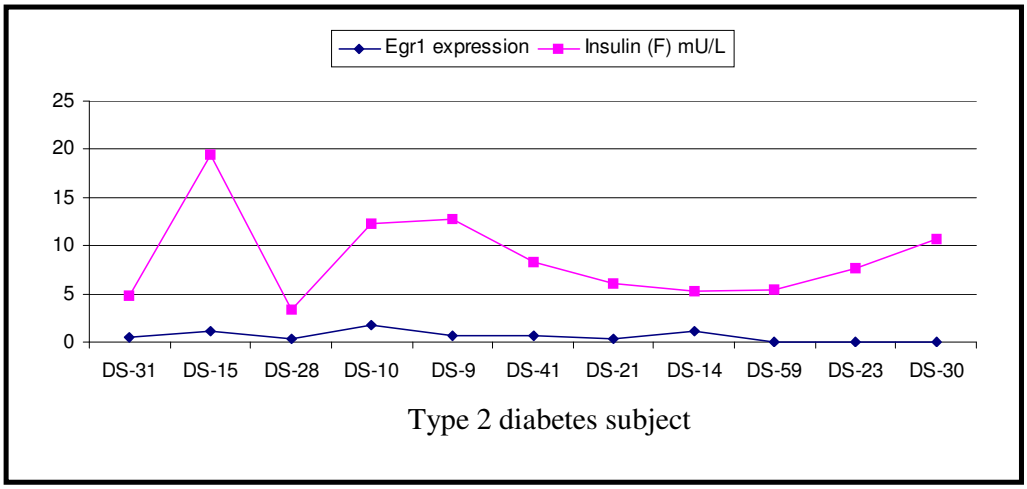


**Fig: 3.11.3.4 *Egr1* expression and insulin fasting in different Type 2 diabetes subjects.**

### 3.11.4 *Beta-actin* expression in Type 2 diabetes subjects and controls

*Beta-actin* was amplified at 34.4 ct in Type 2 diabetes subjects and at 33.9 in controls with no significant difference (p-value=0.5). To exclude any amplification product derived from genomic DNA that could contaminate the RNA preparation, total RNA from Type 2 diabetes subjects and controls were amplified without reverse transcriptase enzyme as a negative control. Water on its own was amplified as a negative control to rule out presence of any contaminating RNA or DNA in it.

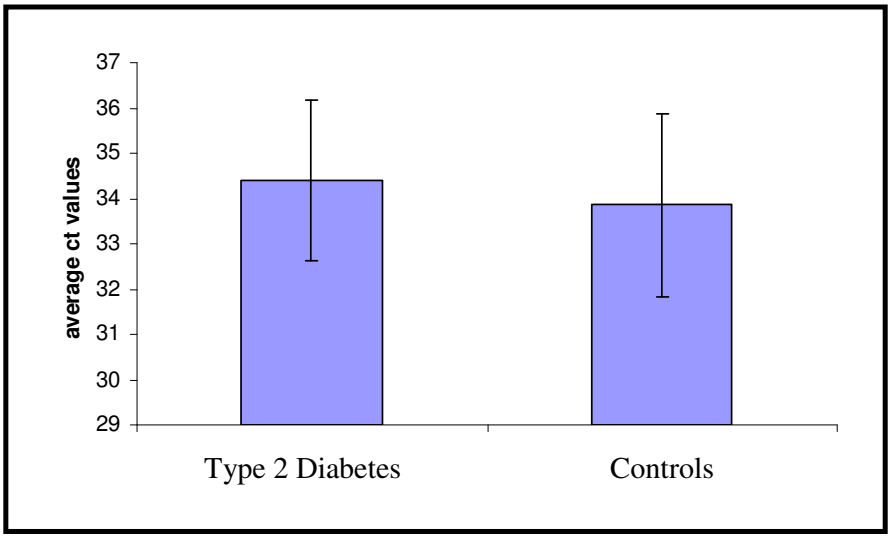


**Fig: 3.11.4 Average cycle threshold (ct) at which *Beta-actin* mRNA was amplified in Type 2 diabetes subjects and controls. The graph shows the mean ct values of 11 Type 2 diabetes subjects and controls. Results represent mean ± S.D.**

### 3.11.5 Validating qRT-PCR assay on demand

cDNA from different cancerous cell lines (Table: 3.11.5.1) were used to make a pool as positive control for validating qRT-PCR assay on demand in Table: 2.5.3.1.3.

| Cell line | Origin |
|---|---|
| HCC1954 | Breast cancer |
| HCC1419 | Breast cancer |
| HCC1937 | Breast cancer |
| BT20 | Breast cancer |
| SK-Mel28 | Melanoma |
| MCF7 | Breast cancer |
| MDA-MB-231 | Breast cancer |
| Mel5 | Melanoma |
| MDA-MB-435S | Breast cancer |
| MALME-3M | Melanoma |
| HT144 | Melanoma |
| M14 | Melanoma |
| MDA-MB-468 | Breast cancer |
| LOX | Melanoma |
| SKBR3 | Breast cancer |

**Table: 3.11.5.1 cell lines and their origin used to make cDNA pool as positive control for validating qRT-PCR assay on demand.**

*Chgb*, *Npy*, *Pdx1*, *Pld1* and *INS* were amplified using cDNA pool from different cancerous cell lines (Table: 3.11.5.1) showing that the assays were working but was just not amplified in the serum samples. *Pax4* was not amplified in the cDNA pool. Fig 3.11.5.2 shows the ct values of different gene transcripts amplified in the cDNA pool.

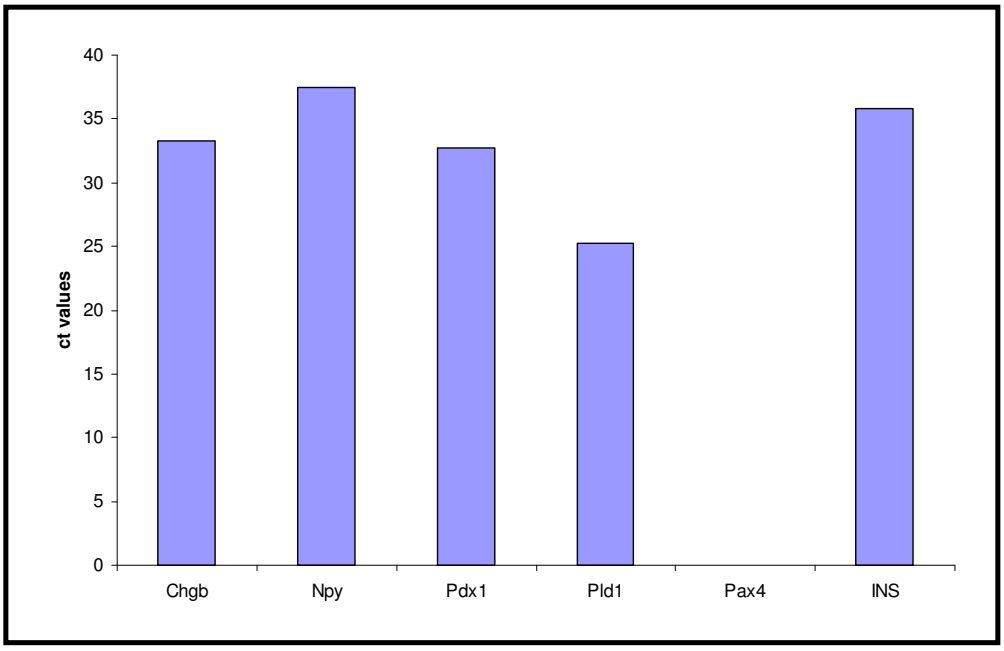


**Fig: 3.11.5.2 ct values at which the different assay on demand was amplified in cDNA pool from cancer cell line.**

# Section 4.0 DISCUSSION

## 4.1 Introductions

There is currently 246 million people worldwide suffering from diabetes making it fourth or fifth leading cause of death in most developed countries. Diabetes is now one of the most common non-communicable diseases globally and there is substantial evidence that it is epidemic in many developing and newly industrialized nations (http://www.eatlas.idf.org/).

Complications from diabetes, such as coronary artery and peripheral vascular disease, stroke, diabetic neuropathy, amputations, renal failure and blindness are resulting in increasing disability, reduced life expectancy and enormous health costs for virtually every society. Diabetes is certain to be one of the most challenging health problems in the 21st century. Careful control is needed to regulate glucose homeostasis and reduce the risk of long-term complications. This could be achieved with combinations of diet, exercise and weight loss (Type 2 diabetes) (Hainer *et al*., 2008), various oral diabetic drugs (Type 2 diabetes only) and insulin use (Type 1 and for Type 2 not responding to oral medications, mostly those with extended duration diabetes). In Type 1 diabetes only realistic method of achieving normoglycaemia is by replacing the patients' destroyed beta cells by beta cell/islet replacement (White *et al.*, 2001). Annual Report published by CITR (2008) summarizes information on 325 islet transplant recipients and 649 islet infusion procedures. According to CITR, at 3 years post-first infusion, about 23% are insulin independent, 29% are insulin dependent with detectable C-peptide, 26% have no detectable C-peptide (lost function) and 22% have missing data (required but not yet reported) (Collaborative islet transplant registry coordinating center, 2008).

Type 2 diabetes is characterized by progressive deterioration in the function of the pancreatic beta cells. In this present study we found that the MIN6 B1 cells lose their function of insulin secretion in long-term culture. Gene transcripts including *Txnip*, *Pcsk9* and *Gcg* manipulation using siRNA, shRNA and cDNA transfection the GSIS function was improved in non glucose-responsive cells. This work could be clinically relevant in maintaining beta cell function in patients suffering from Type 2 diabetes.

In this project we also investigated circulating extracellular mRNA in CM and serum specimens. Study on extracellular mRNA in CM was directed towards identifying biomarkers indicative of cell number and function, which could be clinically relevant to identifying loss of beta cells in patients suffering from Type 1 diabetes. Studies on serum specimens were performed to identify differentially-regulated gene transcripts that could be indicative of loss of beta cell function in Type 2 diabetes. However, studies on large numbers of Type 2 diabetes and controls would be required to establish the relevance, of these mRNAs as biomarkers.

**4.2 MIN6 cell line- model for studying GSIS**

Insulin is secreted from the beta cells in response to glucose. Studies on MIN6 cell line have shown a loss of glucose-stimulated insulin secretion (GSIS) phenotype in continuous culture (O'Driscoll *et al.*, 2004 and 2006). One way to identify the genes associated with impaired GSIS would be to compare the genes expressed in the beta cell of normal subjects with those of Type 2 diabetes patients who have impaired secretion. However, this is not practical, as pancreatic islets from human subjects are difficult to obtain. Alternatively, islets

from model animals such as the Goto-Kakizaki (GK) rat can be used for this purpose (Ihara *et al.*, 1996). Another approach is to compare gene expression between two different beta cell lines (or variants of the same cell line) that exhibit different insulin secretory profiles, i.e. between a cell line showing normal insulin response to glucose and one showing impaired response (Minami *et al.*, 2000).

One of the most commonly studied beta cell lines is MIN6 (See Section: 1.10.1). This insulinoma cell line MIN6, was derived from a transgenic mouse expressing the large T-antigen of SV40 in pancreatic beta cells (Miyazaki *et al.*, 1990). Glucose-stimulated insulin secretion, glucose transport, glucose phosphorylation and glucose utilization have been characterized in MIN6 cell line. Glucose utilization quantitatively and qualitatively reflected glucose phosphorylation in MIN6 cells, a characteristic very similar to those of isolated islets, indicating that this cell line is an appropriate model for studying the mechanism of GSIS in pancreatic beta cells (Ishihara *et al.*, 1993).

The MIN6 cell line maintains a substantial component of beta cell function at early passages *i.e.* the cells respond synchronously and physiologically to changes in glucose concentration (Webb *et al.*, 2000). Previous MIN6 studies, by ourselves and others, have indicated that the GSIS phenotype is relatively unstable in long-term culture. This loss in functional GSIS correlated with changes in morphology and increased proliferation, suggesting that the loss of GSIS may be due to de-differentiation of the high passage MIN6 cells (Kayo *et al.*, 1996; O' Driscoll *et al.*, 2004; O' Driscoll *et al.*, 2006)

It is very important to identify means of preserving beta cell function *i.e.* GSIS, while in culture for possible future applications involving the use of cultured replacement tissue for diabetes. The MIN6 system, *i.e.* glucose responsive low passage cells versus glucose non-responsive high passage cells, has the potential to facilitate discovery of crucial pathways in beta cell development and function.

### 4.2.1 Loss of GSIS in MIN6/MIN6 B1 cells following prolonged sub-culture

Differing levels of GSIS, ranging from 1.2 to 30-fold, have been reported for MIN6 cells. Following the initial establishment of MIN6 as a cell line, exposure to 25mmol/L glucose (compared to 0.7mmol/L) resulted in an approximately 30-fold GSIS, with similar results reported to be achieved after 30 passages (Miyazaki *et al.*, 1990). Results from studies of MIN6 cells at passage 16 indicated a 2-fold GSIS that was reduced to approximately 1.2-fold by passage 35 when stimulated with 5mmol/L compared to 25mmol/L glucose (Kayo *et al.*, 1996). Other reported glucose-stimulated insulin secretion results for these cells include a 7.3-fold GSIS (Ishihara *et al.*, 1993) and an approximately 4.8-fold GSIS from MIN6 cells analyzed between passages 12 to 15 when stimulated with 5mmol/L compared to 25mmol/L glucose (Kinoshita *et al.*, 2001).

Studies carried out previously in our laboratory on MIN6 cells demonstrated that low passage MIN6 (p 18) cells responded to changes in glucose concentrations, producing an approximately four- to five-fold GSIS in response to 26.7mmol/L, compared to 3.3mmol/L glucose. After continuous culture of MIN6 cells to passage 40 to 49, this GSIS was no longer present (O'Driscoll *et al.*, 2004; O'Driscoll *et al.*, 2006).

As described in section 1.10.2 MIN6 B1 subline was derived from the mouse pancreatic beta cell line MIN6. In this study we report that MIN6 B1, like MIN6 heterogeneous population, show a gradual loss of GSIS in continuous passage. To analyze insulin secretion from MIN6 B1(GSIS) (low passage glucose responsive MIN6 B1 cells) and MIN6 B1(Non-GSIS) (high passage non-glucose responsive MIN6 B1 cells) cells, response to glucose at different concentration (3.3mmol/L and 16.7mmol/L) were tested. Our present study on MIN6 B1 cells showed a 2.9-fold insulin secretion at passage 17, and was lost to 1.35-fold at passage 23 when stimulated with 3.3mmol/L was compared with 16.7mmol/L glucose.

### 4.3 Phenotypic changes in MIN6 / MIN6 B1 cells following prolonged sub-culture

Low passage glucose-responsive MIN6 and MIN6 B1 cells grow in multilayered clumps (Fig: 3.1.2) facilitating cell-to-cell interactions and formation of gap-junctions. The integrated secretory response of intact islets of Langerhans is greater than that of dispersed islet cells (Hauge-Evans *et al.*, 1999). This reaggregation improves secretory responsiveness, suggesting that intra-islet interactions are essential for normal secretory responses (Hauge-Evans *et al.*, 1999). High passage glucose non-responsive MIN6 and MIN6 B1 cells grow in a monolayer pattern. Previous studies have reported disruptions in GSIS when MIN6 cells are unable to interact and form gap junctions (Hauge-Evans *et al.*, 1999).

The earlier study in our laboratory indicated that continuous sub-culturing of MIN6 cells resulted in an increase in proliferation rate exhibiting approximately

two-fold increased proliferation in MIN6 (H) than that of MIN6 (L) (O'Driscoll *et al.*, 2006). Growth curves plotted over 7 days following seeding for this study showed rate of proliferation in MIN6 (H) cells was approximately 2.4-fold greater than that of MIN6 (L). The MIN6 (H) population demonstrated greater proliferation potential than MIN6 (L) (Fig: 3.2.2). Zimmer *et al.* (1999) stated in their study that growth arrest of the proliferating beta cell line stimulated the expression of genes associated with beta cell function and resulted in a phenotype that more closely resembled to that of the mature terminally differentiated beta cell. A study on MIN6 passage 17 and passage 41, Sawada *et al*. (2001) found that on the eighth day, the growth rate of passage 41 was nearly twice that of passage 17.

Like MIN6 cells, MIN6 B1(GSIS) (low passage) cells grow in clumps whereas MIN6 B1(Non-GSIS) (high passage) cells spread out to grow as monolayer (Fig: 3.1.1). Increase in the proliferation rate was observed as the MIN6 B1(Non-GSIS) cells when compared to MIN6 B1(GSIS) cells. The rate of proliferation in MIN6 B1(Non-GSIS) was approximately 2-fold greater than that of MIN6 B1(GSIS) (Fig: 3.2.1). MIN6 B1 proliferation result is in collaboration with the MIN6 proliferation study that described an increased rate of proliferation in high passage cells (O'Driscoll *et al.*, 2006).

**4.4 Microarray profiling of MIN6 B1(GSIS) and MIN6 B1(Non-GSIS) cells**

Whole genome microarray experiment was performed on triplicates of glucose responsive MIN6 B1(GSIS) and non-glucose responsive MIN6 B1(Non-GSIS) cells (See Section: 2.6). In this study GeneChip® Mouse Genome 430 2.0 Array was used that represented 45,101 transcripts. Continuous culture of MIN6 B1

cells caused changes in gene expression resulting in both up-regulation and down-regulation of gene transcripts associated with transcription factor, protein kinase activity, response to stress, secretory pathway and intracellular protein transport (Table: 3.4.5.1 and Table: 3.4.5.2) in MIN6 B1(Non-GSIS) compared to MIN6 B1(GSIS) cells. Whereas in the MIN6 study, 1000 genes were significantly differentially-expressed that was involved in regulated insulin secretion, proliferation, adhesion and development (O'Driscoll *et al.*, 2006).

### 4.4.1 Effect of continuous passaging on expression of gene transcripts and GSIS

#### 4.4.1.1 Endoplasmic reticulum related genes

The largest cluster of genes that were differentially-regulated was related to Endoplasmic Reticulum (ER), an important cellular organelle for proper functioning of pancreatic beta cells by correct folding of proinsulin into mature insulin and, subsequent insulin secretion.

It has been reported that *Copb2* and *Mcfd2* are associated with protein transport and their down-regulation fails to transport protein from ER to Golgi apparatus (Barlowe 2003; Nyfeler *et al*., 2006). *Copb2* and *Mcfd2,* were found to be down-regulated in association with loss of GSIS in MIN6 B1(Non-GSIS) cells. Cargo receptor protein *Mcfd2* helps in quality control of protein folding in the ER involving in homeostasis of the intermediate compartment and Golgi complex (Renna *et al*., 2006).

*Hspa5*, *Heat shock 70kD protein 5 (glucose-regulated protein)* (*Dnajb1*) and *WFS1* are localised in ER and were found to be down-regulated in MIN6

B1(Non-GSIS) cells. *Hspa5* reportedly helps in protein folding activity, reducing the load of new protein synthesis and degradation of misfolded proteins in ER (Oyadomari *et al*., 2002; Wang *et al*., 2008). *Wolfram syndrome 1 homolog (human)* (*WFS1*) is found to be associated with ER stress signalling component and helps in maintaining ER homeostasis in beta cell (Fonseca *et al.*, 2005). Although *WFS1* is found to be present in rat pancreatic beta cells and acts as a regulator of ER calcium channel activity, it is not yet definitively established if it plays a role in secretion and membrane trafficking (Ueda *et al*., 2005). Recently, single nucleotide polymorphisms (SNPs) in *WFS1* have been associated with Type 2 diabetes (Florez *et al*., 2008). Florez *et al*., (2008) concluded *WFS1* polymorphisms to be modest contributors to diabetes risk and suggested that they may do so by conferring impairment in insulin secretion. *WFS1* was down-regulated in MIN6 B1(Non-GSIS) compared to MIN6 B1(GSIS) and therefore may be responsible for its loss of its function of insulin secretion.

#### 4.4.1.2 Oxidative stress related genes

The strongest effect of continuous passaging was seen on the expression of *thioredoxin interacting protein* (*Txnip*) with the microarray data showing five-fold increase in its expression in high passage cells. The beta cell is particularly vulnerable to oxidative stress, probably due to its low anti-oxidative enzyme activity, which makes it difficult to inactivate reactive oxygen species (Grankvist *et al.*, 1981; Lenzen *et al.*, 1996; Tiedge *et al.*, 1997).

Activation of stress-sensitive pathways like the MAPK leads to insulin resistance, beta cell dysfunction and eventual development of late complications of diabetes (Evans *et al.*, 2002). The activation of MAPK signal processing

pathways are controlled via multiple mechanisms, including change in expression of effector members by upstream kinase components of the pathway (Sung *et al.*, 2007). *Gadd45g* is an ubiquitously expressed mammalian gene and is induced by genotoxic stresses (Vairapandi *et al.*, 2002). DNA damage leads to the over-expression of *Gadd45g* gene which in turn induces the activation of MAPK pathways (Takekawa *et al.*, 1998). Tribbles are identified as regulators of signal processing system and their involvement in diabetes. *Trib1* increases the expression of *Cdkn1a* and leads to the MAPK phosphorylation /activation (Devgan *et al.*, 2006; Kiss-Toth *et al.*, 2004; Hegedus *et al.*, 2006; Eder *et al*., 2008). *Cdkn1a* and *Gadd45g* are nuclear proteins and have been implicated in induction of growth arrest, apoptosis, excision repair and DNA stability (Dotto, 2000). Devgan *et al.* (2006) therefore speculated that the direct interaction between *Cdkn1a* and *Gadd45* may have a direct bearing on modulation of MAPK and its related proteins. *Trib1*, a modulator of MAPK, has been associated with proliferation of vascular smooth muscle (Sung *et al*., 2007; Hermanto *et al*., 2000; Xu *et al*., 1999). Interestingly, Hermanto *et al*. (2000) reported reduced proliferation in breast cancer cells following blocking of MAPK pathway. The up-regulation of genes associated with MAPK pathway which we observed in MIN6 B1(Non-GSIS) cells may potentially contribute to their increased proliferation rate.

There is evidence that *regulator of G-protein signaling 4* (*Rgs4*) suppresses G-protein signalling (Berman *et al.*, 1996), which is critically important for regulation of $Ca^{2+}$ channels (Béguin *et al*., 2001). Furthermore, *Rgs4* inhibits $Ca^{2+}$ signalling in rat pancreatic acinar cells, thereby affecting the exocytotic release of digestive enzymes (Xu et al., 1999). Here we report *Rgs4* to be up-

regulated in MIN6 B1(Non-GSIS) cells, which may inhibit the $Ca^{2+}$ signalling necessary for insulin exocytosis.

*Dusp1*, identified as a stress-responsive immediate-early gene expressed following oxidative stress in a diabetic rat model (Wu *et al*., 2006), was found to be up-regulated in MIN6 B1(Non-GSIS) cells. Over-expression of this gene has previously been shown to induce insulin expression through its dephosphorylation reaction of the JNK/c-jun pathway (Zhang *et al.*, 2003). *Dusp1* is also up-regulated during MAPK activation and plays a negative feedback role by directly inactivating multiple MAP kinases in insulin-producing cells (McMorran *et al.*, 2003; Wu *et al.*, 2006). *Txnip* is reported to be a pro-apoptotic beta cell gene that is found to be elevated in insulin resistance (Minn *et al*., 2005). It is known as endogenous inhibitor of thioredoxin, inhibiting thioredoxin antioxidative function by binding to its redox-active cysteine residues resulting in a shift of the cellular redox balance that promotes increased intracellular oxidative stress (Schulze *et al.*, 2004). Oxidative stress associated with over-expression of *Txnip* (5.25-fold higher in MIN6 B1(Non-GSIS)) may contribute to the impaired insulin secretion observed in these cells.

#### 4.4.1.3 Transcription factors

Transcriptional factors are modulated by up-stream signalling activity and influence gene regulation (Vukkadapu *et al.*, 2005). *Klf4* is a zinc-finger transcription factor and *in vitro* studies have suggested that it plays an important role in cell proliferation and/or differentiation (Katz *et al.*, 2002). Gary *et al.,* (2002) in their over-expression study of *Klf4* reported that it reduces the expression of *GLUT4* in 3T3-L1 cells. The over-expression of *Klf4* observed here

in beta cells, in association with loss of glucose-responsiveness, may similarly affect GLUT2 (another member of the GLUT transporters; well established as an important component of beta cell glucose sensing). ROS-induced over-expression of redox-sensitive *Klf4* gene may cause proliferation and over-expression of *Cdkn1a* (Nickenig *et al.*, 2002). The role of *Atf5* in islet function or maintenance is not known and is associated with neuroendocrine as well as pancreatic endocrine development and function (Vukkadapu *et al.*, 2005). High expression of *Atf4*, *Atf5*, and *Hspa5* during insulitis in BDC2.5/N mice suggests ER stress (Vukkadapu *et al.*, 2005). Insulitis is an inflammation of the islets of Langerhans caused by lymphocyte infiltration. This lymphocyte infiltration results in destruction of the insulin producing beta cells of the islets and clinical diabetes (Rossini *et al*., 1977).

*AP-1* has been reported to be a redox-sensitive transcription factor constituted from Jun, FOS and ATF family protein (Kunsch *et al.*, 1999). Here *c-jun*, *c-fos* and *fosB* were all found to be expressed at higher levels in MIN6 B1(Non-GSIS) cells. qRT-PCR results were in agreement to microarray study with a dramatic 59-fold up-regulation of *fosB* gene (See Section: 3.4.8). It has been reported that *c-jun* and *c-fos* represses the basal activities of the insulin promoter in hamster beta (HIT) cells (Inagaki *et al.*, 1992). *c-jun* is also found to be associated with increased proliferation (Shaulian *et al*., 2002) and was up-regulated in rapidly proliferating MIN6 B1(Non-GSIS) cells.

#### 4.4.1.4 Secretory pathway

*Mcfd2* forms a cargo receptor complex in the early secretory pathway on interaction with different proteins (Renna *et al.*, 2006). The secretory granules of

pancreatic beta cell contain four *Rab3* isoforms with similar roles in the regulation of insulin secretion (Iezzi *et al.*, 1999). In fact, Riedel *et al.* (2002) reported presences of *Rab3D* in several secretory cells including pancreatic cells and are not involved in exocytosis but plays role in granule maturation. The loss of *Rab3d* expression found in MIN6 B1(Non-GSIS) is in keeping with this role.

Secretory and membrane proteins are transported across, or integrated into, the membrane of the ER by a multi-protein assembly, termed the translocon. *Tram*, *Srpr* and *Sec61p* complex are essential component of the translocon component (Webb *et al.*, 2000). Interestingly, our microarray study showed a down-regulation (by 1.2-fold) of *Tram1* and *Srpr* in MIN6 B1(Non-GSIS) compared to MIN6 B1(GSIS) cells. In a study of early-passage (passages 17-19) MIN6 cells exposed to high (25mM) or low (5.5mM) glucose, Webb *et al.* (2000) reported that the secretory pathway genes including *Trapα*, *SRP receptor* and *tram protein* are up-regulated in glucose-responsive MIN6 cells. In their study, an increased rate of proinsulin biosynthesis at the ER in glucose-responsive MIN6 cells was observed, suggesting a role of secretory pathway genes in glucose-responsive beta cell function (Webb *et al.*, 2000). Again, in agreement with this, our study on MIN6 B1 cells showed down-regulation of *Ssr1*, *Tram1* and *Srpr* genes in non glucose-responsive cells.

Furthermore, our previous study on heterogeneous MIN6 cells (passages 18-40) reported reduced expression of genes associated with vesicle formation, transportation and secretion in MIN6 (H) cells (passage 40) (O'Driscoll *et al.*, 2006). O'Driscoll *et al.* (2006) reported gene transcripts associated with secretion including nucleobindin, PC2, secretogranin V, synaptotagmin 1 etc to be

significantly lower in MIN6 (H) compared with MIN6 (L) cells. *Egr1* has been specifically associated with insulin secretion (Josefsen *et al*., 1999). O'Driscoll *et al.* (2006) reported down-regulation of *Egr1* by 5.5-fold in high passage MIN6 cells, whereas our present microarray study showed a 1.98-fold and qRT-PCR showed 4.64-fold up-regulation of *Egr1* in MIN6 B1(Non-GSIS) compared to MIN6 B1(GSIS) cells. Here we report a different set of gene transcripts associated with secretion, including *Ssr1*, *Tram1* and *Srpr*, to be significantly down-regulated in MIN6 B1(Non-GSIS) compared to MIN6 B1(GSIS) cells.

### 4.5 Glucagon (*Gcg*)

The pancreatic islets are comprised of different type of cells, predominant beta cells (approximately 70%) with alpha cells constituting approximately 20% of the islets (Baetens *et al*., 1979). Type 2 diabetes is associated with a defect in beta cell function and mass, insulin secretion and resistance, as well as abnormalities in glucagon secretion (Diao *et al*., 2005). The key regulatory hormones for glucose homeostasis are insulin and glucagon. Glucagon acts as counter-regulatory hormone of insulin by raising plasma glucose levels in response to insulin-induced hypoglycaemia (Jiang *et al*., 2003). Glucagon contributes to the maintenance of the glucose-induced insulin secretion phenotype of beta cells, a key feature commonly impaired in Type 2 diabetes (Huypens *et al*., 2000). It also helps in differentiation of precursor cells into insulin-secreting beta cells in the embryonic pancreas (Kumagai *et al*., 2002).

Glucagon is a 29 amino acid peptide hormone secreted by alpha cells (Bromer *et al*., 1957). RIN, HIT, beta TC, MIN6 and INS-1 cells are the most commonly used and studied insulin-secreting cell lines. These cell lines represent a good

model of beta cells but are also known to secrete glucagon and somatostatin (Poitout *et al*., 1996; Hohmeier *et al*., 2004). There has been evidence of loss of GSIS along with down-regulation of glucagon mRNA expression with increased passage in MIN6 cells (O'Driscoll *et al*., 2004). Here we report the down-regulation of glucagon mRNA expression in MIN6 B1(Non-GSIS) compared to MIN6 B1(GSIS) in a microarray study which was validated by qRT-PCR.

Impaired glucagon secretion is observed in Type 1 Diabetes mellitus (T1DM) (Fanelli *et al*., 2006). The physiological decrease in endogenous insulin secretion from the beta cell in response to hypoglycaemia is a mechanism believed to be necessary in order for glucagon to be released by the alpha cell. The intra-islet insulin hypothesis suggests that a decrease in beta cell insulin secretion leads to a decreased intra-islet alpha cell inhibition by insulin and is a signal for increased glucagon secretion in response to hypoglycemia. This mechanism is altered in diabetes because of the loss of beta cell mass and function, which is thought to blunt the response of glucagon to hypoglycaemia (Fanelli *et al*., 2003). Various *in vitro* studies have suggested a role of intra-islet insulin or beta cell product in the glucagon response (Taborsky *et al*., 1998; Banarer *et al*., 2002). A tight co-regulation has been observed between loss of the glucagon response and loss of the endogenous insulin secretion (Banarer *et al*., 2002). The distorted biphasic insulin secretion in diabetes is known to cause altered docking and fusion of insulin granules (Ohara-Imaizumi *et al*., 2004). During the process of exocytosis the secretory organelles containing pre-formed material fuse with the plasma membrane releasing their contents through a resulting connection between the lumen of the organelle and the extracellular space called the fusion pore (Scepek *et al*., 1998). Diabetes could also distort this fusion pore opening dynamics of

both alpha and beta cells, thereby perturbing paracrine and autocrine control (Gaisano *et al*., 2008).

Glucagon has the ability to induce GSIS from the beta cell (Moens *et al*., 2002). Glucagon secretion, in conjunction with changes in glucose levels, stimulates insulin secretion and separation of beta cells from alpha cells shows lower secretory activity of purified beta cell as compared with isolated islets (Pipeleerset *et al*., 1985). Endogenous glucagon secretion was found to amplify glucose-induced insulin release from isolated islet cell preparations (Pipeleers *et al*., 1985; Moens *et al*., 2002). Insulin release from perifused purified beta cells is greatly enhanced in the presence of added glucagon or co-culture with alpha cells (Pipeleers *et al*., 1982). These earlier reported results shows that glucagon helps in insulin secretion and the knock-down of glucagon by *Gcg*-specific siRNA, as performed in this study reported here (See Section: 3.6.3), could have contributed to the significant loss of GSIS in MIN6 low passage cells.

Cell composition and distribution in the pancreatic islet varies in different part of the pancreas. Dorsal islets contained 10 times more glucagon than ventral islets, whereas insulin and total protein contents are similar (Baetens *et al*., 1979). The basal rates of insulin secretion and proinsulin biosynthesis were similar in dorsal and ventral islets but, under conditions of glucose stimulation, both insulin secretion and proinsulin biosynthesis were significantly greater in the alpha cell rich dorsal islets. Similarly, glucose utilization rates and ATP levels were greater in dorsal islets. These observations reported by Trimble *et al*., (1982) indicated that a greater alpha cell number and glucagon content is associated with higher rates of GSIS and biosynthesis. Purified flow-sorted rat beta cells separated from

glucagon-producing alpha cells show poor insulin secretory response to glucose (Huypens *et al*., 2000). Here, down-regulation of glucagon by 1.5-fold in MIN6 B1(GSIS) was associated with a significant loss of GSIS compared to scrambled transfected cells (See Section: 3.6.3), suggesting that in this cell model paracrine glucagon plays a role in glucose-responsiveness of MIN6 B1(GSIS).

A number of *in vitro* studies using purified islet cells have supported the idea that the glucose stimulation of insulin release is strongly influenced by the intracellular cAMP level which, in turn, is found to potentiate $Ca^{2+}$-dependent exocytosis (Renström *et al*., 1997). cAMP is regulated by various hormones and neurotransmitters (Moens *et al*., 2002). Endogenously released glucagon apparently determines the cAMP production in beta cells and thus participates in the nutrient-induced secretory process (Pipeleers *et al*., 1985). cAMP induces glycogenolysis increasing the intracellular ATP level for translocation, docking and fusion of secretory granules (He *et al*., 1998). Dalle *et al*., (1999 and 2004) in their study of beta cell models, they reported that glucagon increases cAMP level thereby activating protein kinase A (PKA) which, in turn, phosphorylates the L-type voltage-dependent calcium channel (VDCC). This leads to an increased glucose-induced calcium entry causing membrane depolarization and thus potentiating insulin secretion (Dalle *et al*., 1999; Dalle *et al*., 2004). Glucagon also acts in a paracrine fashion as a modulator of glucose induced calcium oscillations in mouse pancreatic islets. GSIS is also mediated by an increase in the intracellular free $Ca^{2+}$ concentration (Baltrusch *et al*., 2007). In our experiments (See Section: 3.6.5) glucagon over-expression in MIN6 high passage cells resulted in a marked increase in the GSIS.

In this study we report that glucagon plays an important role in regulating GSIS in MIN6 cells. Using *Gcg*-specific siRNA, here we report a significant loss of GSIS in MIN6 low passage cells (passage 35). cDNA over-expression of *Gcg* in MIN6 high passage cells (passage 47) resulted an increase in GSIS. Therefore we can conclude that glucagon is a regulator of GSIS in MIN6 cells and any abnormality in its secretion would result in an impaired insulin secretion.

### 4.6 Proprotein convertase subtilisin/kexin type 9 (*Pcsk9*)

In the study reported in the thesis, *Pcsk9* was down-regulated by a 1.5-fold in the microarray study and 2.59-fold in qRT-PCR study in MIN6 B1(Non-GSIS) cells compared to MIN6 B1(GSIS) cells. *Pcsk9* knock-down, using three independent siRNAs, resulted in a significant loss of GSIS (*Pcsk9*-1 (p-value=0.007) and *Pcsk9*-3 (p-value=0.013)) in MIN6 B1(GSIS) cells compared to scrambled siRNA transfected cells (See Section: 3.7.3). *Pcsk9* is found to be responsive to insulin but not glucose (Costet *et al*., 2006). In an *in vitro* study in primary cultures of hepatocytes and *in vivo* study during hyperinsulinemic-euglycemic clamps *Pcsk9* was found to be up-regulated by insulin via sterol regulatory element-binding protein-1c (SREBP-1c). Insulin increases the expression of *Pcsk9* mRNA suggesting that *Pcsk9* might play a role in insulin-related pathologies including Type 2 diabetes and the metabolic syndrome (Costet *et al*., 2006). Niesen *et al*., (2008) reported that streptozotocin-induced diabetic rats showed a significant reduction in *Pcsk9* protein expression.

*Pcsk9* is thought to be involved in liver regeneration and neuronal differentiation (Ouguerram *et al*., 2004). Type 2 diabetes is associated with hepatic fat accumulation (hepatic steatosis) and dyslipidemia, a major risk factor for the

development of diabetes-associated coronary heart disease (Seppälä-Lindroos *et al*., 2002). The causative factor of diabetic dyslipidemia are elevated plasma triglyceride (TG) levels, low concentrations of high density lipoprotein (HDL) cholesterol and the presence of small, low density lipoprotein (LDL) particles (Taskinen, 2003). The major cause of diabetic dyslipidemia is an increased production of TG-rich very low density lipoprotein (VLDL) (Ginsberg *et al*., 2005). As VLDL is an attribute of insulin resistance and Type 2 diabetes in humans, Costet *et al*. (2006) proposed the possibility that *Pcsk9* function might be altered in the metabolic syndrome and/or diabetes. Adenoviral mediated *Pcsk9* over-expression in fasting mice resulted in massive hypertriglyceridemia, associated with a striking increase in VLDL hepatic output (Naoumova *et al*., 2005).

Oxidized LDL reduces GSIS in the clonal hamster beta cell line, HIT-T15 (Abderrahmani *et al*., 2007), as well as reduces both insulin content and preproinsulin mRNA expression in isolated islets (Hao *et al*., 2007). It also increases beta cell apoptosis (Brunham *et al*., 2008). The level of cell-surface LDL receptor (LDLR) is indirectly proportional to the level of *Pcsk9* in the liver and small intestine (Rashid *et al*., 2005). In an *in vivo* study of *Pcsk9* knockout mice, Rashid *et al*. (2005) reported an increase in LDLR protein causing increased clearance of circulating lipoproteins and decreased plasma cholesterol levels. Increased levels of circulating LDL cholesterol have been observed in mice over-expressing *Pcsk9* following recombinant adenoviral infections (Benjannet *et al*., 2006). In the *Pcsk9*-specific siRNA study, here we propose that *Pcsk9* is associated with the loss of GSIS in MIN6 low passage cells.

### 4.7 Thioredoxin interacting protein (*Txnip*)

*Thioredoxin-interacting protein* (*Txnip*) was first isolated from a 1,25-dihydroxyvitamin D3-treated HL-60 human promyelocytic cell line and therefore is also known as vitamin D3-up-regulated gene 1 (VDUP1) (Chen *et al*., 1994). *Txnip* was found to be up-regulated in an oligonucleotide microarray study assessing glucose effects on isolated human pancreatic islets (Shalev *et al*., 2002) as well as in islets of insulin-resistant and diabetic mice (Minn *et al*., 2005). *Txnip* has been identified as a potential diabetogenic signal in human skeletal muscle (Muoio, 2007). Diabetes leads to glucose toxicity affecting different organ systems including pancreatic islets leading to beta cell apoptosis. *Txnip* is induced by glucose and up-regulated in diabetes in the cardiovascular system (Schulze *et al*., 2004) as well as in pancreatic beta cells. This suggests its involvement in glucose toxicity, beta cell loss and diabetes complications (Minn *et al*., 2005; Chen *et al*., 2008). In our microarray study, we identified *Txnip* to be up-regulated in non-glucose responsive MIN6 B1(Non-GSIS) compared to MIN6 B1(GSIS). The exact role of *Txnip* in glucose homeostasis is not known, but the up-regulation of *Txnip* in high passage cells may have contributed to glucose toxicity, stress and loss of GSIS function.

*Txnip* has been studied in various cancer forms and is associated with increased tumour cell growth and metastatic potential in human breast cancer, colon cancer, and malignant pheochromocytomas (Goldberg *et al*., 2003; Butler *et al*., 2003; Ohta *et al*., 2005). *Txnip* is also associated with cell cycle arrest at the G0/G1 phase and has been shown to inhibit proliferation in a variety of cell types including human aortic smooth muscle cells (Schulze *et al*., 2002; Han *et al*.,

2003). Over-expression of *Txnip* renders cells more susceptible to oxidative stress and it induces apoptosis (Wang *et al*., 2002; Minn *et al*., 2005).

Chen *et al*. (2008) reported that the beta cell-specific knockout of *Txnip* in bTKO mice enhanced beta cell mass and protected against diabetes. They also proposed that down-regulation of *Txnip* induces Akt/Bcl-xL signaling which in turn inhibits mitochondrial beta cell death, suggesting that these mechanisms may mediate the beta cell protective effects of *Txnip* deficiency (Chen *et al*., 2008). Our study of *Txnip*-specific siRNA in MIN6 high passage cells resulted in a significant increase in GSIS in high passage cells (See Section: 3.8.3). These results suggest that lowering beta cell *Txnip* mRNA expression levels could serve as a novel strategy for the treatment of Type 2 diabetes by promoting endogenous beta cell survival (Chen *et al*., 2008).

*Txnip* expression has been found to govern glucose uptake in insulin-responsive cells. In an over-expression study of *Txnip* using lentiviral transduction in adipocyte differentiated 3T3-L1, Parikh *et al*. (2007) reported a diminished basal and insulin-stimulated glucose uptake, whereas *Txnip* siRNA enhanced both basal and insulin-stimulated glucose uptake (Parikh *et al*., 2007). In our *Txnip* siRNA study on MIN6 high passage cells we found a significant increase in GSIS (*Txnip* -1 (p-value=0.03) and *Txnip* -2 (p-value=0.019)), whereas over-expression of *Txnip* significantly reduced (p-value= 0.013) the GSIS in MIN6 low passage cells (See Section: 3.8.3). A significant increase (p-value=0.024) in GSIS was also observed in *Txnip* shRNA transfected MIN6 clones (See Section: 3.9.4.2).

Elevated glucose concentration in beta cells may trigger the mechanism of beta cell toxicity by generating free radicals in beta cells during oxidative metabolism of glucose *via* production of proinflammatory cytokines such as interleukin-1 and by the induction of ER stress in beta cells (Corbett, 2008). Chen *et al*. (2008) have also proposed that the loss of beta cell mass in response to elevated concentrations of glucose is the result of enhanced expression of a single protein, Txnip which has been found to negatively regulate thioredoxin. Over-expression of thioredoxin in streptozotocin-induced diabetic mice protected pancreatic beta cells from autoimmune destruction by reducing apoptosis (Hotta *et al*., 1998). *Txnip* may be causing pro-apoptotic effects on beta cells by inhibiting thioredoxin and inducing oxidative stress (Junn *et al*., 2000), leading to beta cell glucotoxicity and apoptosis (Robertson *et al*., 2003; Kajimoto *et al*., 2004). Vascular *Txnip* expression is also found to be elevated in streptozotocin-induced diabetic rats where it induces vascular oxidative stress (Schulze *et al*., 2004). Reactive oxygen species (ROS) have been suggested to have a role in insulin resistance. It has been proposed that cells may interpret elevated ROS levels as a signal to limit the input to the electron transport chain by decreasing glucose uptake causing insulin resistance (Houstis *et al*., 2006). Varying *Txnip* mRNA level has been associated with differences in ROS levels and thioredoxin activity. Low *Txnip* mRNA level in MCF10A/MCF-7/T47D cells has been associated with significantly lower fold increase of ROS levels compared with the high *Txnip* mRNA level in MDA-MB-435s/MDA-MB-231 cells (Turturro *et al*., 2007). Our study of ROS level in *Txnip* shRNA-transfected clones have shown reduced ROS level by 40.5% and 35.6% in sh-1 and sh-9 clones respectively

compared to empty shRNA-transfected clone (See Section: 3.9.4.3), suggesting that *Txnip* is associated with increasing levels of ROS.

*Txnip* has shown to possess tumour-suppressive activity in breast, gastrointestinal and lung cancers, suppressing cell proliferation *via* cell cycle arrest at the G1 phase (Filby *et al*., 2006; Yu *et al*., 2007). Over-expression of *Txnip* was found to inhibit the proliferation of stomach cancer and promyelocytic leukemia cells (Han *et al*., 2003). Suppressed tumour growth and metastasis was also reported in a *Txnip* over-expression study of tumour transplant in nude mice model (Goldberg *et al*., 2003). However, in their study of pretumorous livers from *Txnip*-deficient mice, Sheth *et al*. (2006) found that there was no increase in cellular proliferation suggesting that loss of *Txnip* itself is not sufficient to induce proliferation. In the studies reported in this thesis, the proliferation rate of *Txnip* shRNA-transfected clone#1 (sh-1) were reduced by 1.3-fold compared to empty shRNA-transfected cells and reduced by 2-fold compared to sh-3 clone (i.e. a clone with no *Txnip* knock-down) (See Section: 3.9.4.4). Beta cell-specific *Txnip* deletion in HcB-19 mice has been found to enhance beta cell mass and protect against diabetes (Chen *et al*., 2008). In a study of INS-1 beta cells and primary mouse islet, Chen *et al*. (2008) suggested that inhibition of *Txnip* could be a novel approach to reduce glucotoxic beta cell loss (Chen *et al*., 2008).

Pancreatic islets express *Egr1* mRNA and its reduced expression may inhibit beta cell proliferation (Garnett *et al*., 2005). Garnett *et al*. (2005) in their *Egr1* siRNA study on INS-1 cells found that it had no effect on GSIS but did inhibit proliferation. Our study showed a 52.7% and 56.2% knock-down by qRT-PCR of *Egr1* gene transcript in *Txnip* shRNA-transfected clones sh-1 and sh-9

respectively. Studies performed on tissue culture models such as rodent and avian fibroblasts suggested that c-Jun and the Fos proteins positively regulate cell proliferation (Shaulian *et al*., 2002). In the study reported in this thesis (See Section: 3.9.4.5), qRT-PCR on *Txnip* shRNA-transfected clones showed a 80.5% and 73.8% knock-down of *Fos* gene transcript in sh-1 and sh-9 clones respectively. qRT-PCR showed a knock-down of 44.5% and 16.5% of *Jun* gene transcript transcript in sh-1 and sh-9 clones respectively. Reduced expression of *Egr1*, *Fos* and *Jun* suggests that *Txnip* knock-down alone may not be responsible for reduced proliferation in *Txnip* knock-down clones but they might act in harmony possibly with other intracellular molecules to reduce proliferation.

Our findings in this study suggest that *Txnip* is associated with insulin secretion in MIN6 cells. *Txnip*-specific siRNA and cDNA transfection study showed that *Txnip* expression was inversely related to insulin secretion in MIN6 cells. *Txnip* shRNA transfected clones showed a reduced ROS levels suggesting reduced oxidative stress and increased insulin secretion compared to empty shRNA transfected clone. Increased ROS levels also suggest increased oxidative stress in MIN6 high passage cells that may lead to an increased expression of *Txnip* and insulin resistance.

### 4.8 Extracellular nucleic acid

Presence of extracellular nucleic acids was first reported by Mandel and Métais (Mandel *et al.*, 1948). Circulating mRNAs have more recently been detected in plasma and serum from people with cancer, as well as people with no history of cancer (El-Hefnawy *et al.*, 2004). These RNAs are apparently not only able to escape from cells, but are also protected from degradation by the serum ribonucleases (Ng *et al.*, 2002; Tsui *et al.*, 2002). Wiecozorek *et al*. (1985 and 1987) reported that tumour cells secrete RNA-proteolipid complexes into the serum of the cancer patients, which may protect the RNA from the plasma ribonucleases. Normal cells in culture have been found to release RNA-DNA nucleoprotein complexes (Stroun *et al.*, 1978) and it has been shown in our laboratory that mRNAs can be detected in culture medium conditioned by a broad range of cultured cancer cell types (O'Driscoll *et al.*, 2005). However, although there is increasing evidence to suggest the existence of extracellular mRNAs that may be clinically-relevant as biomarkers, extracellular mRNAs associated with pancreatic beta cells have not previously been investigated. Here we analysed a range of gene transcripts in media conditioned by insulin-producing cell lines, investigating if their presence is in any way indicative of beta cell mass/density and/or function, and assessing the reproducibility of the procedures employed.

#### 4.8.1 Identifying a suitable time point for CM collection and analysis

As described in section 2.4.1 and 2.4.2 conditioned media (CM) samples were collected at 4 time-points after cell seeding to identify a suitable time-point at which amplifiable mRNA could be routinely isolated for analysis. In the case of

*Beta-actin*, mRNA could be isolated and amplified at all time points evaluated. The increasing intensity of the PCR bands in the samples over the 24hrs. intervals may be due to the increasing amounts of *Beta-actin* transcripts secreted into the CM, assuming that the transcripts are stable in CM for that length of time. As the cells were in a healthy, proliferating state at the 48hrs. time-point with no dead cells floating in the media, this time-point was chosen for all further studies using the RNA extraction protocol as described in section: 2.5.1.2.1.

### 4.8.2 Identifying Suitable PCR Cycle Number

Studying medium conditioned by a range of insulin-producing cell types, including glucose-responsive and non-responsive murine beta cells, MIN6 (L) and (H), respectively, the glucose-responsive clonal population of MIN6 (MIN6 B1), and monkey fibroblast cells engineered to produce human insulin (Vero-PPI), here we have shown, for the first time, that a range of mRNAs are detectable extracellularly to insulin-producing cells. The amplified products detected range in size from 125-288 bp and the results obtained were highly reproducible between triplicate biological repeat experiments.

Although 30 cycles of PCR were sufficient for amplification of RNA from cultured cells, 45 cycles was generally found to be necessary for CM studies. However, use of nested or semi-nested primers and large number of PCR cycles, as reported for some of the serum studies (Wieczorek *et al.*, 1987; Chen *et al.*, 2000), were found not to be necessary in our analyses.

### 4.8.3 RT-PCR on RNase- and DNase-treated RNA Samples

It had been suggested (Kumar *et al.*, 2006) that expression microarray and qRT-PCR analysis of saliva specimens might be detecting genomic DNA, rather than mRNA. This assumption was based on the analysis of "no-RT" (i.e. no reverse transcriptase enzyme included in cDNA reaction: RT (-)) and "+RT" (RT (+)) conditions yielding similar amounts of PCR product; microarrays signals, unaffected by RNase-treatment; and the absence of RT-PCR products following DNase-treatment. In order to investigate if the extracellular nucleic acids detected in CM were either wholly or partly DNA in origin and not from mRNA as controls, we included analysis following DNase treatment, RNase treatment, and in the absence of RT enzyme. The presence of amplified products following DNase treatment of samples, and the complete lack of product following RNase treatment and in the absence of RT enzyme, and the fact that the amplified products detected are of the sizes expected for cDNA, but not genomic DNA, supports the assumption that the nucleic acids that we detected throughout the course of these studies are of RNA, not DNA, origin.

### 4.8.4 Cell Density and corresponding mRNA Levels

In order to investigate if levels of specific mRNAs in CM correlate with numbers of cells conditioning the medium, MIN6 B1 and Vero-PPI cells were grown at a range of densities in fixed volumes of medium and RT-PCR was performed on both cells and their CM. Our results from the amplification of a number of beta cell gene transcripts (including *Pdx1*, *Egr1* and *Chgb*) indicated that levels of expression reflected the numbers of MIN6 B1 cells conditioning the medium. Although previous beta cell studies have not been performed to which these

findings can be compared, it is interesting to note that a correlation has been reported between increased amount of circulating tumour-specific mRNA and tumour stage (Stroun *et al.*, 1978; Morozkin *et al.*, 2004). Increased extracellular DNA is also detected in the plasma of the patients after trauma correlating with the severity of injury and it is also found to be predictive of late post-traumatic complications, such as organ failure (Wong *et al.*, 2004). From our analysis of MIN6 B1 and Vero-PPI CM, we can speculate that by quantification of the level of circulating mRNA, assessment of surviving beta cell as in Type 1 diabetes patient could be possible.

### 4.8.5 Glucose-Responsiveness and corresponding mRNA Levels

To establish if the presence of extracellular mRNAs may reflect beta cell function *i.e.* specifically the ability of beta cells to secrete insulin in a glucose-regulated manner, analysis of mRNA in medium conditioned by glucose-responsive MIN6 (L) and glucose non-responsive MIN6 (H) was performed. Choice of transcripts to study were based on our previously reported analysis of MIN6 (L) and (H) where we identified a number of mRNAs to be differentially expressed between these cells (O'Driscoll *et al.*, 2006). Using both microarray and quantitative RT-PCR, we found *Egr1*, *Pld1*, and *Chgb* to be significantly down-regulated in MIN6 (H) cells compared to MIN6 (L). In agreement with our previous analysis of cells, in studies of CM reported here, we detected these 3 gene transcripts in biological repeat analysis of MIN6 (L); however, these mRNAs were not detectable in MIN6 (H) CM. Our microarray analysis indicated no significant difference in expression levels *Ins I*, *Ins II* or *Beta-actin* mRNAs between MIN6 (L) and (H) cells. Similarly, all 3 of these transcripts were

detected in MIN6 (L) and (H) CM, but the amounts present in CM from these cell populations did not differ significantly.

### 4.8.6 Possible selective release of gene transcript into CM

Furthermore, results from this study suggest that the secretion of mRNA by pancreatic beta cells may be somewhat selective, and not just be a general "dumping" mechanism. This is supported by the fact that although *Pdx1*, *Egr1*, *Chgb*, *Pax4* and *Beta-actin* are expressed by MIN6 B1 and *Pdx1*, *Egr1*, *Chgb*, and *Beta-actin* are detectable in corresponding CM, *Pax4* is not. It should, however, be considered that alternative explanations to selective secretion of the gene transcripts may be insensitivity of RT-PCR as a methods of detection very low levels of mRNA or, alternatively, differing stabilities of mRNAs secreted into the extracellular environment.

## 4.10 Serum study

Serum and plasma has been the subject of extensive research for years. Circulating RNA in plasma and serum has emerged as an upcoming field for non-invasive diagnostic applications (Ng *et al*., 2002). Quantitative real-time RT-PCR (qRT-PCR) is a very sensitive assay which makes serum/plasma RNA detection assays more informative and sensitive (Tsui *et al*., 2002). Currently all the routinely used serum markers are proteins and the conventional methods used for measuring them are labor-intensive (Chen *et al*., 2008). Some of the examples of the serum protein include adipocyte fatty acid-binding protein. Serum Adipocyte fatty acid-binding protein has been associated with glucose

dysregulation and predicting the development of Type 2 diabetes in Chinese population (Tso *et al*., 2007).

In order to investigate if the amplified signal was of RNA origin and not from contaminated DNA, as controls, we included analysis following DNase treatment, RNase treatment and in the absence of RT enzyme. In the case of serum RNA treated with RNase enzyme there was no amplification observed. Amplified products were observed in few samples following DNase treatment of serum RNA. The reason for this could be that the DNase treatment could have lead to the degradation of RNA resulting in amplification at later cycle that is beyond the detection limit of the qRT-PCR machine. Therefore in the case of serum RNA study only –RT (reverse transcription carried out in the absence of reverse transcriptase enzyme) was taken as control.

All the gene transcripts chosen for the serum RNA study were selected from previously reported microarray analysis of MIN6 (L) and (H) cells and were validated using qRT-PCR (Table: 2.5.3.1.3). These gene transcripts were also amplified in our study of medium conditioned by insulin secreting cell lines (See Section: 3.10).

Glucose and hyperglycemia induces *Txnip* expression in breast-cancer derived cells, MDA-MB-231 (Turturro *et al*., 2007), along with the islets of different mouse models of diabetes and insulin resistance. This suggests that *Txnip* contributes to the pathogenesis and secondary complications of diabetes (Minn *et al*., 2005). The 1q21-1q23 chromosomal area has been involved in Type 2 diabetes in several human populations (van Greevenbroek *et al*., 2007). Several lines of evidence and functional data on the roles of *Txnip* and thioredoxin,

combined with its chromosomal localization on 1q21-23 leads to the hypothesis that variations in the *Txnip* gene may affect susceptibility to Type 2 diabetes or to hyper-triglyceridaemia in Type 2 diabetes (van Greevenbroek *et al*., 2007).

*Txnip* mRNA expression was found to be suppressed by insulin in healthy subjects, but this relationship was lost in diabetes subjects (Muoio, 2007). Muscle expression of *Txnip* was also found to be higher in patients with diabetes or pre-diabetes, as compared to those with normal glucose tolerance (Muoio, 2007).

In the present study, we have detected increased amount of *Txnip* in Type 2 diabetes serum compared to controls. Since *Txnip* has been associated with oxidative stress and inhibits the function of thioredoxin, our result suggests that the diabetic condition enhance the expression of *Txnip*. In the cell line model reported in this thesis we have also found that increased expression of *Txnip*, in microarray and qRT-PCR study, is associated with loss of function of insulin secretion in MIN6 B1(Non-GSIS) cells.

Stronger induction of *Egr1* mRNA was found in glucose-responsive cell lines including, MIN6, βTC3 and INS-1 cells, compared to weakly glucose-responsive RINm5F cells (Josefsen *et al*., 1999). *Egr1* was undetected in beta cell lines including, HIT-T15 cells, that do not secrete insulin in response to glucose (Josefsen *et al*., 1999). *Egr1* mRNA is also expressed in pancreatic beta cells and primary rat islets (Garnett *et al*., 2005). Eto *et al*. (2006) proposed that *Egr1* contributes to the function of pancreatic beta cells by regulation of *Pdx1* expression and activation of insulin gene transcript and glucose responsiveness. In our present study we observed that *Egr1* mRNA expression was significantly

(p-value=0.017) down-regulated in Type 2 diabetes subjects compared to controls.

Serum is supposed to contain large amounts of RNA that is derived from various tissues and organs. The serum RNA expression profile could be used as a novel serum-based biomarker and potentially is more sensitive and specific tests for early diagnosis of diabetes and other related diseases. Studies on large number of Type 2 diabetes and controls are required to determine the diagnostic and prognostic value of this measurement.

# Section 5.0 Summary

# AND

# Conclusion

### 5.1 Studies on MIN6 / MIN6 B1

- MIN6 B1 at p19 showed a glucose concentration-dependent increase in insulin secretion producing a 2.15-fold increased insulin secretion when glucose stimulation was increased from 3.3 mmol/L to 16.7 mmol/L for 1 hr and so these cells were subsequently termed MIN6 B1(GSIS). By contrast, the same increase in glucose concentration when added to MIN6 B1 at p23 cells resulted in 1.35-fold increase in insulin secretion only *i.e.* MIN6 B1(Non-GSIS) cells.
- Gradual loss of GSIS was observed in continuously cultured MIN6 B1 cell.
- The loss in functional GSIS after continuous culture correlated with phenotypic changes, including an increased proliferation and change in cell morphology. MIN6 B1 cells grow in clumps at low passages (MIN6 B1(GSIS), passage 19) whereas, at high passages (MIN6 B1(Non-GSIS), passage 23), it formed a monolayer of "flat", stretched, cells

### 5.2 Whole genome microarray studies on MIN6 B1 cell

- Of the 45,101 transcripts represented on the Mouse Whole Genome 430 2.0 Array, 111 genes were differentially regulated with 53 genes found to be up-regulated and 58 genes down-regulated in MIN6 B1(Non-GSIS) compared to MIN6 B1(GSIS) cells.
- To validate the microarray results, twelve up-regulated genes and four down-regulated genes were selected for qRT-PCR analysis based on fold change >1.2 and p-value <0.05. qRT-PCR validation was performed on the following differentially-regulated genes *Anxa A2*, *Dusp1*, *Egr1*, *Fos*,

*FosB*, *Gadd45g*, *Ier-5*, *Jun*, *Klf4*, *Mapk3*, *Sox4*, *Txnip*, *Gcg*, *Pcsk9, Slc38a4* and *Txndc5*. Comparison of qRT-PCR data with microarray data demonstrated matching trends in expression change for both methods.

- Up-regulated gene transcripts including *Gadd45g*, *Cdkn1a*, *Rgs4* and *Trib1* are known, from the literature, to be associated with regulation of protein kinase activity.
- *Txnip*, *Dusp1*, *Dnajb1*, *Anxa2*, *Gadd45g* and *Mapk3* are known, from the literature, to be associated with response to stress were up-regulated in MIN6 B1(Non-GSIS) compared to MIN6 B1(GSIS).
- mRNAs, including *Ssr1*, *Tram1, and Srpr* are known from the literature to be associated with protein targeting to endoplasmic reticulum and were down-regulated in MIN6 B1(Non-GSIS).
- Down-regulated gene transcripts including *Copb2*, *Mcfd2* and *Rab3d* are known from the literature to be associated with secretory pathway.

### 5.3 *Gcg* siRNA and Over-expression on MIN6 cells

- *Gcg* was down-regulated in the MIN6 B1 high passage cells compared to low passage cells in the microarray study and validated by qRT-PCR.
- *Gcg*-1 and *Gcg*-2 siRNA transfection showed a knock-down of approx. 32% and 27% respectively in qRT-PCR study, compared to scrambled-siRNA transfected control cells.
- There was no change in cell proliferation or cell morphology following *Gcg* siRNA transfection.
- Significant loss of GSIS (*Gcg*-1 (p-value=0.00009), *Gcg*-2 (p-value=0.015) and *Gcg*-3 (p-value= 0.032)) was observed in low passage

MIN6 cells following *Gcg* (*Gcg*-1, *Gcg*-2 and *Gcg*-3) siRNA transfection.

- 10.9-fold increase of *Gcg* mRNA in MIN6 high passage cells was observed by qRT-PCR after 72hrs. of *Gcg* cDNA over-expression compared to empty plasmid transfected cells.
- Increase in GSIS in *Gcg* over-expressing cells (1.43-fold) was observed compared to empty plasmid transfected cells (1.16) (p-value= 0.14).
- *Gcg* expression was directly related to insulin secretion in MIN6 B1 cells. Therefore we can conclude that by regulating glucagon secretion in Type 2 diabetes we can increase the insulin secretion.

### 5.4 *Pcsk9* siRNA on MIN6 low passage cells

- *Pcsk9* was down-regulated in the MIN6 B1 high passage cells compared to low passage cells in the microarray study and validated by qRT-PCR.
- qRT-PCR showed a knock-down of approx 39% in *Pcsk9*-1, 4.3% in *Pcsk9*-2, and 46% in *Pcsk9*-3 siRNA transfected cells.
- There was no change in cell proliferation or cell morphology followed by *Pcsk9* siRNA transfection.
- Significant loss of GSIS (*Pcsk9*-1 (p-value=0.007) and *Pcsk9*-3 (p-value= 0.013)) was observed in low passage MIN6 cells following *Pcsk9* (*Pcsk9* -1 and *Pcsk9* -3) siRNA transfection.
- Reduced expression of *Pcsk9* was associated with reduced insulin secretion in MIN6(L) cells. In this study for the first time we have reported association of *Pcsk9* with beta cell and loss of GSIS.

### 5.5 Study of *Txnip*

- *Txnip* was up-regulated in the MIN6 B1 high passage cells compared to low passage cells in the microarray study and validated by qRT-PCR.
- qRT-PCR showed *Txnip* mRNA knock-down of approx. 43% in *Txnip*-1, 42% in *Txnip*-2 and 25% in *Txnip*-3 siRNA transfected cells.
- There was no change in cell proliferation or cell morphology followed by *Txnip* siRNA transfection.
- Significant increase in GSIS was observed in high passage MIN6 cells following *Txnip* (*Txnip*-1 (p-value=0.03) and *Txnip*-2 (p-value=0.019)) siRNA transfection.
- 23.7-fold increase of *Txnip* mRNA in MIN6 low passage cells was observed by qRT-PCR after 72hrs. of *Txnip* cDNA over-expression, compared to empty plasmid transfected cells.
- There was a significant loss (p-value= 0.013) of GSIS in MIN6 low passage cells following *Txnip* cDNA over-expression.
- qRT-PCR was performed on clones to select the clones with lowest expression of *Txnip*
- *Txnip* shRNA transfected clone#1 (sh-1) showed a significant increase in GSIS (p-value=0.024) with (2.96-fold) and a moderate increase in clone#9 (sh-9) (p-value=0.23) (1.82-fold) compared to empty shRNA-transfected cells (Em-F).
- *Txnip* shRNA transfected clones sh-1 and sh-9 showed reduced ROS levels of 40.5% and 35.6%, respectively, compared to empty shRNA transfected clone Em-F.

- Clone sh-3 showed 1.5-fold increased proliferation compared to Em-F, whereas clone sh-1 showed 1.3-fold reduced proliferation compared to Em-F.
- Reduced expression of *Egr1* was observed in Sh-1 clone (52.7%) and sh-9 clone (56.2%), compared to Em-F.
- Sh-1 clone showed 80.5% and sh-9 clone showed 73.8% knock-down of *Fos*, compared to Em-F.
- Sh-1 clone showed 43.7% and sh-9 clone showed 29.2% knock-down of *Gadd45g*, compared to Em-F.
- Sh-1 clone showed 44.5% and sh-9 clone showed 16.5% knock-down of *Jun*, compared to Em-F.
- Increased expression of *Mapk3* in Sh-1 (14.8%) and sh-9 clones (66.9%) was observed, compared to Em-F.
- Reduced expression of *Egr1*, *Fos* and *Jun* in *Txnip* shRNA transfected clones may contribute to its reduced proliferation.
- Expression of *Txnip* is inversely related to insulin secretion in MIN6 cells. So we can conclude that by beta cell specific deletion of *Txnip* mRNA GSIS function of beta cells could be preserved.

**5.6 Study on medium conditioned by insulin-producing cells**

- A range of healthy, proliferating, insulin-producing cell lines in culture apparently pass many gene transcripts out into their media, which can be reproducibly detected extracellularly.
- Forty-five cycles of PCR was found to be adequate to produce a detectable band from CM (conditioned media) RNA.

- Gene transcripts including *Beta-actin*, *Ins1*, *Ins2* and *Pdx1* were detected at similar levels in MIN6 low passage (L) and high passage (H) CM.
- Gene transcripts including *Npy*, *Chgb*, *Pld1*, *Egr1* and *PC2* were amplified using RNA from medium conditioned by MIN6 (L) cells but were undetected in medium conditioned by MIN6 (H) cells.
- *Gad1* was amplified using MIN6 (H) CM RNA, whereas it was undetected in MIN6 (L) CM RNA.
- In case of *Chgb*, *Egr1*, *Gck* and *Pdx1*, the intensity of the band produced following 45 cycles of PCR was directly associated with the numbers of cells conditioning the medium i.e. increased number of cells resulted in increased levels of these transcripts detectable in a fixed volume of CM.
- *Ins1*, *Ins2* and *Pld1* was amplified using cell RNA from $10^6$ cells and $5x10^6$ cells, however, there was no further increase in band size/intensity upon analysis of $1x10^7$ cells RNA which seemed to reach plateau phase of PCR analysis.
- Human *preproinsulin* transcribed by Vero-PPI cells showed increased levels of mRNA in medium conditioned by increasing number of cells; however, amounts of preproinsulin detected in CM seemed to reach plateau phase and PCR was no longer exponential beyond analysis of CM from $5X10^6$ cells.
- mRNAs is detected in the extracellular environment and these mRNAs may have potential as extracellular biomarkers for assessing beta cell mass and function.

### 5.7 Study on serum

- A 1.8-fold increase in *Txnip* mRNA expression was observed in Type 2 diabetes compared to controls.
- A negative correlation was observed between *Txnip* mRNA expression and insulin fasting (correlation= -0.46) as well as insulin secretion (correlation= -0.50) in Type 2 diabetes subjects.
- *Egr1* mRNA expression was significantly (p-value=0.017) down-regulated in Type 2 diabetes subjects compared to controls.
- *Egr1* mRNA expression and insulin fasting (correlation= 0.53) was positively correlated in Type 2 diabetes subjects and was negatively correlated (correlation= -0.12) in controls.
- Amplification of *Beta-actin* was not significantly different in Type 2 diabetes compared to controls.
- *Egr1* mRNA expression was significantly (p-value=0.017) down-regulated whereas, *Txnip* mRNA expression was up-regulated in Type 2 diabetes compared to controls. Studies on large number of serum specimens from Type 2 diabetes and controls are required to determine the diagnostic and prognostic value of this measurement.

# Section 6 Future Work

**Future work**

- siRNA, shRNA and cDNA transfection for other gene transcripts (*Egr1*, *Fos*, *FosB* and *Jun*) that were up-regulated in MIN6 B1 microarray study. Transfection study of these gene transcripts would possibly help to understand their role in GSIS.
- *Txnip* shRNA-transfected clones showed an increase in GSIS. Microarray study on *Txnip* shRNA-transfected clone and empty shRNA-transfected clone would help to identify differentially-regulated gene transcripts in *Txnip* knock-down clone that would possibly be associated with GSIS.
- Knock-down of *Txnip* mRNA in MIN6 high passage cells resulted in significantly increase in GSIS. It could be possible that *Txnip* could be interacting with some other gene to restore insulin secretion in MIN6 cells. LC-mass spectrometry could be performed to identify other proteins that interact with *Txnip* to increase GSIS.
- *Txnip* knock-down mouse models to better understand the role of this protein in insulin secretion. Plasmid vector containing the *Txnip* gene could be electroporated into ES cell. Chimeric mice could be generated by injecting of clones into blastocysts. These could then be implanted into pseudopregnant female recipients to produce chimeras. *Txnip* knock-down mouse model would also enable the analysis of other genes regulated by Txnip protein.

- Microarray on serum from Type 2 diabetes and controls to find any potential biomarker.

- Detection of amplifiable mRNA extracellular to isolated pancreatic islets cells.
- Detection of amplifiable gene transcript in isolated pancreatic islets seeded at range of densities and corresponding mRNA levels in their CM.
- Identify gene transcripts extracellular to isolated islet cells showing the functional status of the isolated islet cells. Glucose responsive and glucose non-responsive islets could be identified by determining the glucose-stimulated insulin secretion (GSIS) in freshly isolated islet cells and then growing them in culture for few days when GSIS is lost.

**References:**

Abderrahmani A, Niederhauser G, Favre D, Abdelli S, Ferdaoussi M, Yang J.Y, Regazzi R, Widmann C and Waeber G: (2007): Human high-density lipoprotein particles prevent activation of the JNK pathway induced by human oxidised low-density lipoprotein particles in pancreatic beta cell: Diabetologia.;50(6):1304-14

Aggarwal B.B, Shishodia S, Takada Y, Jackson-Bernitsas D, Ahn K.S, Sethi G and Ichikawa H: (2006): TNF blockade: an inflammatory issue: Ernst Schering Res Found Workshop.;(56):161-86.

Anker P, Mulcahy H, Chen X.Q and Stroun M: (1999): Detection of circulating tumour DNA in the blood (plasma/serum) of cancer patients: Cancer Metastasis Rev.; 18(1):65-73.

Antinozzi P.A, Segall L, Prentki M, McGarry J.D and Newgard C.B: (1998): Molecular or pharmacologic perturbation of the link between glucose and lipid metabolism is without effect on glucose-stimulated insulin secretion. A re-evaluation of the long-chain acyl-CoA hypothesis: J Biol Chem.; 273(26):16146-54.

Araki E, Oyadomari S and Mori M: (2003): Impact of endoplasmic reticulum stress pathway on pancreatic beta-cells and diabetes mellitus: Exp Biol Med (Maywood).; 228(10):1213-7

Asfari M, Janjic D, Meda P, Li G, Halban P.A and Wollheim C.B: (1992): Establishment of 2-mercaptoethanol-dependent differentiated insulin-secreting cell lines: Endocrinology.;130(1):167-78.

Assady S, Maor G, Amit M, Itskovitz-Eldor J, Skorecki KL, Tzukerman M: (2001): Insulin production by human embryonic stem cells: Diabetes.; 50(8):1691-7.

Atkinson M.A: (2005): Thirty Years of Investigating the Autoimmune Basis for Type 1 Diabetes, Why Can't We Prevent or Reverse This Disease?: Diabetes 54:1253-1263.

Baetens D, Malaisse-Lagae F, Perrelet A and Orci L: (1979): Endocrine pancreas: three-dimensional reconstruction shows two types of islets of langerhans: Science.; 14;206(4424):1323-5

Baltrusch S and Lenzen S: (2007): Regulation of [Ca2+]i oscillations in mouse pancreatic islets by adrenergic agonists: Biochem Biophys Res Commun.;363(4):1038-43

Barlowe C: (2003): Signals for COPII-dependent export from the ER: What's the ticket out? Trends Cell Biol.; 13: 295-300.

Beattie G.M, Montgomery A.M, Lopez A.D, Hao E, Perez B, Just M.L, Lakey J.R, Hart M.E and Hayek A: (2002): A novel approach to increase human islet cell mass while preserving beta-cell function: Diabetes.; 51(12):3435-9.

Béguin P, Nagashima K, Gonoi T, Shibasaki T, Takahashi K, Kashima Y, Ozaki N, Geering K, Iwanaga T and Seino S: (2001): Regulation of Ca2+ channel expression at the cell surface by the small G-protein kir/Gem: Nature;411(6838):701-6.

Bell G.I, Pictet R.L, Rutter W.J, Cordell B, Tischer E and Goodman H.M: (1980): Sequence of the human insulin gene: Nature.;284(5751):26-32.

Bender K, Newsholme P, Brennan L and Maechler P: (2006): The importance of redox shuttles to pancreatic beta-cell energy metabolism and function: Biochem Soc Trans.; 34(Pt 5):811-4.

Benjannet S, Rhainds D, Hamelin J, Nassoury N and Seidah N.G: (2006): The proprotein convertase (PC) PCSK9 is inactivated by furin and/or PC5/6A: functional consequences of natural mutations and post-translational modifications: J Biol Chem.; 281(41):30561-72

Berman D.M, Wilkie T.M and Gilman A.G: (1996): GAIP and RGS4 are GTPase-activating proteins for the Gi subfamily of G protein alpha subunits: Cell.; 86(3):445-52.

Berney T, Mamin A, James Shapiro A.M, Ritz-Laser B, Brulhart M.C, Toso C, Demuylder-Mischler S, Armanet M, Baertschiger R, Wojtusciszyn A, Benhamou P.Y, Bosco D, Morel P and Philippe J: (2006): Detection of insulin mRNA in the peripheral blood after human islet transplantion predicts deterioration of metabolic control : Am J Transplant.;6(7):1704-11

Berts A, Ball A, Dryselius G, Gylfe E and Hellman B: (1996): Glucose stimulation of somatostatin-producing islet cells involves oscillatory Ca2+ signalling: Endocrinology.; 137(2):693-7

Bertuzzi F, Berra C, Socci C, Davalli A.M, Calori G, Freschi M, Piemonti L, De Nittis P, Pozza G and Pontiroli A.E : (1995) : Glucagon improves insulin secretion from pig islets in vitro: J Endocrinol.;147(1):87-93

Bhathena S.J, Voyles N.R, Oie H.K, Smith S.S, Gazdar A.F and Recant L: (1980): Glucagon secreting clones of rat islet cell tumor: Horm Metab Res.; 12(11):632-3

Bianchi D.W, Williams J.M, Sullivan L.M, Hanson F.W, Klinger K.W, and Shuber A.P: (1997): PCR Quantitation of Fetal Cells in Maternal Blood in Normal and Aneuploid Pregnancies: Am. J. Hum. Genet.; 61:822–829.

Blancou P, Mallone R, Martinuzzi E, Sévère S, Pogu S, Novelli G, Bruno G, Charbonnel B, Dolz M, Chaillous L, van Endert P and Bach J.M: (2007): Immunization of HLA class I transgenic mice identifies autoantigenic epitopes eliciting dominant responses in type 1 diabetes patients: J Immunol.; 178(11):7458-66.

Blaszczyk J, Tropea J.E, Bubunenko M, Routzahn K.M, Waugh D.S, Court D.L and Ji X : (2001): Crystallographic and modeling studies of RNase III suggest a mechanism for double-stranded RNA cleavage: Structure.; 9(12):1225-36.

Brange J and Langkjoer L: (1993): Insulin structure and stability: Pharm Biotechnol.; 5:315-50

Bretzel R.G, Eckhard M and Brendel M.D: (2004): Pancreatic islet and stem cell transplantation: new strategies in cell therapy of diabetes mellitus: Panminerva Med.; 46(1): 25-42.

Bretzel R.G, Jahr H, Eckhard M, Martin I, Winter D and Brendel M.D: (2007): Islet cell transplantation today: Langenbecks Arch Surg.; 392(3):239-53.

Brissova M, Fowler M.J, Nicholson W.E, Chu A, Hirshberg B, Harlan D.M and Powers A.C: (2005): Assessment of human pancreatic islet architecture and composition by laser scanning confocal microscopy: J Histochem Cytochem.; 53(9):1087-97

Bromer W.W, Sinn L.G, Staub A and Beheens O.K: (1957): The amino acid sequence of glucagon: Diabetes.; 6(3):234-8.

Bromer W.W, Sinn L.G, Staub A and Behrens O.K: (1957): The amino acid sequence of glucagons: Diabetes.; 6(3):234-8.

Brummelkamp T.R, Bernards R and Agami R: (2002): A system for stable expression of short interfering RNAs in mammalian cells: Science.; 296(5567):550-3.

Brunham L.R, Kruit J.K, Verchere C.B and Hayden M.R: (2008): Cholesterol in islet dysfunction and type 2 diabetes: J Clin Invest.; 118(2):403-8

Brunton S.A: (2008): The changing shape of type 2 diabetes: Medscape J Med.; 10(6):143.

Bryzgunova O.E, Skvortsova T.E, Kolesnikova E.V, Starikov A.V, Rykova E.Y, Vlassov V.V and Laktionov P.P: (2006): Isolation and comparative study of cell-free nucleic acids from human urine: Ann N Y Acad Sci.; 1075: 334-340.

Buchanan T.A and Xiang A.H: (2005): Gestational diabetes mellitus: J Clin Invest.; 115(3):485-91.

Butler L.M, Zhou X, Xu W.S, Scher H.I, Rifkind R.A, Marks P.A and Richon V.M: (2002): The histone deacetylase inhibitor SAHA arrests cancer cell growth, up-regulates thioredoxin-binding protein-2, and down-regulates thioredoxin: Proc. Natl. Acad. Sci. USA; 99: 11700–11705.

Butt A.N, Shalchi Z, Hamaoui K, Samadhan A, Powrie J, Smith S, Janikoun S and Swaminathan R: (2006): Circulating nucleic acids and diabetic complications: Ann N Y Acad Sci; 1075:258-70

Camastra S, Bonora E, Del Prato S, Rett K, Weck M and Ferrannini E: (1999): Effect of obesity and insulin resistance on resting and glucose-induced thermogenesis in man. EGIR (European Group for the Study of Insulin Resistance): Int J Obes Relat Metab Disord.; 23(12):1307-13.

Centers for Disease Control and Prevention. National diabetes fact sheet: general information and national estimates on diabetes in the United States, (2005): Atlanta, GA: U.S. Department of Health and Human Services, Centers for Disease Control and Prevention.

Chen J, Couto F.M, Minn A.H and Shalev A: (2006): Exenatide inhibits beta-cell apoptosis by decreasing thioredoxin-interacting protein: Biochem Biophys Res Commun.; 346(3):1067-74

Chen J, Hui S.T, Couto F.M, Mungrue I.N, Davis D.B, Attie A.D, Lusis A.J, Davis R.A and Shalev A: (2008): Thioredoxin-interacting protein deficiency

induces Akt/Bcl-xL signaling and pancreatic beta-cell mass and protects against diabetes: FASEB J; [Epub ahead of print]

Chen J, Saxena G, Mungrue I.N, Lusis A.J and Shalev A: (2008): Thioredoxin-interacting protein: a critical link between glucose toxicity and beta-cell apoptosis: Diabetes.; 57(4):938-44

Chen K.S and DeLuca H.F: (1994): Isolation and characterization of a novel cDNA from HL-60 cells treated with 1,25-dihydroxyvitamin D-3: Biochim Biophys Acta.;1219(1):26-32

Chen L.M, Yang X.W and Tang J.G: (2002): Acidic residues on the N-terminus of proinsulin C-Peptide are important for the folding of insulin precursor.J Biochem.; 131(6):855-9.

Chen X, Ba Y, Ma L, Cai X, Yin Y, Wang K, Guo J, Zhang Y, Chen J, Guo X, Li Q, Li X, Wang W, Zhang Y, Wang J, Jiang X, Xiang Y, Xu C, Zheng P, Zhang J, Li R, Zhang H, Shang X, Gong T, Ning G, Wang J, Zen K, Zhang J and Zhang C.Y: (2008): Characterization of microRNAs in serum: a novel class of biomarkers for diagnosis of cancer and other diseases: Cell Res. [Epub ahead of print]

Chen X.Q, Bonnefoi H, Pelte M.F, Lyautey J, Lederrey C, Movarekhi S, Schaeffer P, Mulcahy H.E, Meyer P, Stroun M and Anker P: (2000): Telomerase RNA as a detection marker in the serum of breast cancer patients: Clin Cancer Res; 6:3823-6.

Chiasson J.L, Liljenquist J.E, Sinclair-Smith B.C and Lacy W.W: (1975): Gluconeogenesis from alanine in normal postabsorptive man. Intrahepatic stimulatory effect of glucagon: Diabetes.; 24:574–584.

Chick W.L, Warren S, Chute R.N, Like A.A, Lauris V and Kitchen K.C: (1977): A transplantable insulinoma in the rat: Proc Natl Acad Sci U S A.; 74(2):628-32.

Cho J.H, Hong S.K, Kim E.Y, Park S.Y, Park C.H, Kim J.M, Kwon O.J, Kwon S.J, Lee K.S and Han J.S: (2008): Overexpression of phospholipase D suppresses taxotere-induced cell death in stomach cancer cells: Biochim Biophys Acta.;1783(5):912-23

Chutkow W.A, Patwari P, Yoshioka J and Lee R.T: (2008): Thioredoxin-interacting protein (Txnip) is a critical regulator of hepatic glucose production: J Biol Chem.; 283(4):2397-406

Claiborn K.C and Stoffers D.A: (2008): Toward a cell-based cure for diabetes: advances in production and transplant of beta cells: Mt Sinai J Med.; 75(4):362-71.

Collaborative islet transplant registry coordinating center, 2008 http://www.citregistry.org/

Corbett J.A: (2008): Thioredoxin-interacting protein is killing my beta-cells!: Diabetes.;57(4):797-8.

Costet P, Cariou B, Lambert G, Lalanne F, Lardeux B, Jarnoux A.L, Grefhorst A, Staels B and Krempf M: (2006): Hepatic PCSK9 expression is regulated by

nutritional status via insulin and sterol regulatory element-binding protein 1c: J Biol Chem.;281(10):6211-8.

Dalle S, Longuet C, Costes S, Broca C, Faruque O, Fontés G, Hani E.H and Bataille D : (2004) : Glucagon promotes cAMP-response element-binding protein phosphorylation via activation of ERK1/2 in MIN6 cell line and isolated islets of Langerhans: J Biol Chem.;279(19):20345-55

Dalle S, Smith P, Blache P, Le-Nguyen D, Le Brigand L, Bergeron F, Ashcroft F.M and Bataille D: (1999): Miniglucagon (glucagon 19-29), a potent and efficient inhibitor of secretagogue-induced insulin release through a Ca2+ pathway: J Biol Chem.; 274(16):10869-76

Damholt A.B, Buchan A.M, Holst J.J and Kofod H: (1999): Proglucagon processing profile in canine L cells expressing endogenous prohormone convertase 1/3 and prohormone convertase 2: Endocrinology.; 140(10):4800-8.

D'Amour K.A, Bang A.G, Eliazer S, Kelly O.G, Agulnick A.D, Smart N.G, Moorman M.A, Kroon E, Carpenter M.K and Baetge E.E: (2006): Production of pancreatic hormone-expressing endocrine cells from human embryonic stem cells: Nat Biotechnol.;24(11):1392-401.

de la Tour D, Halvorsen T, Demeterco C, Tyrberg B, Itkin-Ansari P, Loy M, Yoo S.J, Hao E, Bossie S and Levine F: (2001): Beta-cell differentiation from a human pancreatic cell line in vitro and in vivo: Mol Endocrinol.; 15(3):476-83.

DeFronzo R.A and Ferrannini E: (1991): Insulin resistance. A multifaceted syndrome responsible for NIDDM, obesity, hypertension, dyslipidemia, and atherosclerotic cardiovascular disease: Diabetes Care.; 14(3):173-94.

Dembiński A, Warzecha Z, Ceranowicz P, Pawlik M, Dembiński M, Kabat K, Konturek S.J, Kownacki P, Hładki W and Pawlik W.W: (2004): Influence of central and peripheral administration of pancreatic polypeptide on gastric mucosa growth: J Physiol Pharmacol.; 55:223-37

Dennis G, Sherman B.T, Hosack D.A, Yang J, Gao W, Lane H.C and Lempicki R.A: (2003): DAVID: Database for Annotation, Visualization, and Integrated Discovery: Genome Biol.; 4(5):P3.

Devendra D, Liu E and Eisenbarth G.S: (2004): Type 1 diabetes: recent developments: BMJ.; 328(7442):750-4.

Devgan V, Nguyen B.C, Oh H and Dotto G.P: (2006): p21WAF1/Cip1 suppresses keratinocyte differentiation independently of the cell cycle through transcriptional up-regulation of the IGF-I gene: J Biol Chem.; 281(41):30463-70.

Diabetes Mellitus Classification & Pathogenesis. Diabetes Mellitus & Hypoglycemia. Armenian Medical Network (2006).

Diao J, Asghar Z, Chan C.B and Wheeler M.B: (2005): Glucose-regulated glucagon secretion requires insulin receptor expression in pancreatic alpha-cells: J Biol Chem.; 280(39):33487-96.

Do H, Falcone D, Lin J, Andrews D.W and Johnson A.E: (1996): The cotranslational integration of membrane proteins into the phospholipid bilayer is a multistep process: Cell.; 85(3):369-78

Dodson G and Steiner D: (1998): The role of assembly in insulin's biosynthesis: Curr Opin Struct Biol.; 8(2):189-94

Dong Z.Z, Yao D.F, Yao M, Qiu L.W, Zong L, Wu W, Wu X.H, Yao D.B and Meng X.Y: (2008): Clinical impact of plasma TGF-beta1 and circulating TGF-beta1 mRNA in diagnosis of hepatocellular carcinoma: Hepatobiliary Pancreat Dis Int.;7(3):288-95

Donley V.R, Hiskett E.K, Kidder A.C and Schermerhorn T: (2005): ATP-sensitive potassium channel (KATP channel) expression in the normal canine pancreas and in canine insulinomas: BMC Vet Res.; 1:8

Dotto G.P: (2000): p21(WAF1/Cip1): More than a break to the cell cycle? Biochim. Biophys. Acta; 1471: M43-56.

Dowling P, O'Driscoll L, O'Sullivan F, Dowd A, Henry M, Jeppesen P.B, Meleady P and Clynes M: (2006): Proteomic screening of glucose-responsive and glucose non-responsive MIN-6 beta cells reveals differential expression of proteins involved in protein folding, secretion and oxidative stress: Proteomics.; 6(24):6578-87.

Draghici S, Khatri P, Bhavsar P, Shah A, Krawetz S.A and Tainsky M.A: (2003): Onto-Tools, the toolkit of the modern biologist: Onto-Express, Onto-Compare, Onto-Design and Onto-Translate: Nucleic Acids Res.; 31(13):3775-81

Drucker D.J: (2006): The biology of incretin hormones: Cell Metab.; 3(3):153-65

Du G, Altshuller Y.M, Vitale N, Huang P, Chasserot-Golaz S, Morris A.J, Bader M.F and Frohman M.A: (2003): Regulation of phospholipase D1 subcellular cycling through coordination of multiple membrane association motifs: J Cell Biol.; 162(2):305-15

Dunning B.E and Gerich J.E: (2007): The role of alpha-cell dysregulation in fasting and postprandial hyperglycemia in type 2 diabetes and therapeutic implications: Endocr Rev.; 28(3):253-83.

Dunning B.E and Gerich J.E: (2007): The role of alpha-cell dysregulation in fasting and postprandial hyperglycemia in type 2 diabetes and therapeutic implications: Endocr Rev.; 28(3):253-83.

Eaton R.P, Allen R.C, Schade D.S, Erickson K.M and Standefer J: (1980): Prehepatic insulin production in man: kinetic analysis using peripheral connecting peptide behaviour: J Clin Endocrinol Metab.; 51(3):520-8.

Eder K, Guan H, Sung H.Y, Francis S.E, Crossman D.C and Kiss-Toth E: (2008): LDL uptake by monocytes in response to inflammation is MAPK dependent but independent of tribbles protein expression: Immunol Lett.;116(2):178-83

Efrat S, Linde S, Kofod H, Spector D, Delannoy M, Grant S, Hanahan D and Baekkeskov S: (1988): Beta-cell lines derived from transgenic mice expressing a hybrid insulin gene-oncogene: Proc Natl Acad Sci U S A.;85(23):9037-41.

Elbashir S.M, Harborth J, Lendeckel W, Yalcin A, Weber K and Tuschl T: (2001): Duplexes of 21-nucleotide RNAs mediate RNA interference in cultured mammalian cells: Nature.;411(6836):494-8

Elbein S.C, Hoffman M.D, Teng K, Leppert M.F and Hasstedt S.J: (1999): A genome-wide search for type 2 diabetes susceptibility genes in Utah Caucasians: Diabetes; 48: 1175–1182.

Eledrisi M.S, Alshanti M.S, Shah M.F, Brolosy B and Jaha N: (2006): Overview of the diagnosis and management of diabetic ketoacidosis: Am J Med Sci.; 331(5):243-51.

Eto K, Kaur V and Thomas M.K: (2006): Regulation of insulin gene transcription by the immediate-early growth response gene Egr-1: Endocrinology.; 147(6):2923-35

Evans J.L, Goldfine I.D, Maddux B.A and Grodsky G.M: (2002): Oxidative Stress and Stress-Activated Signaling Pathways: A Unifying Hypothesis of Type 2 Diabetes: Endocrine Reviews.; 23 (5): 599-622:

Fanelli C.G, Porcellati F, Rossetti P and Bolli G.B: (2006): Glucagon: the effects of its excess and deficiency on insulin action: Nutr Metab Cardiovasc Dis.; 16 Suppl 1:S28-34

Farina A, Sekizawa A, Sugito Y, Iwasaki M, Jimbo M, Saito H and Okai T: (2004): Fetal DNA in maternal plasma as a screening variable for preeclampsia. A preliminary nonparametric analysis of detection rate in low-risk nonsymptomatic patients: Prenat Diagn.; 24(2):83-6

Fernandes L.C, Kim S.B and Matos D: (2005) Cytokeratins and carcinoembryonic antigen in diagnosis, staging and prognosis of colorectal adenocarcinoma: World J Gastroenterol; 11: 645–8.

Filby C.E, Hooper S.B, Sozo F, Zahra V.A, Flecknoe S.J and Wallace M.J: (2006): VDUP1: a potential mediator of expansion-induced lung growth and epithelial cell differentiation in the ovine fetus: Am J Physiol Lung Cell Mol Physiol.; 290(2):L250-8.

Florez J.C, Jablonski K.A, McAteer J, Sandhu M.S, Wareham N.J, Barroso I, Franks P.W, Altshuler D and Knowler W.C: (2008): Testing of diabetes-associated WFS1 polymorphisms in the Diabetes Prevention Program: Diabetologia.;51(3):451-7

Fonseca S.G, Fukuma M, Lipson K.L, Nguyen L.X, Allen J.R, Oka Y and Urano F: (2005): WFS1 is a novel component of the unfolded protein response and maintains homeostasis of the endoplasmic reticulum in pancreatic beta-cells: J Biol Chem.; 280(47):39609-15

Foulis A.K, McGill M and Farquharson M.A: (1991) : Insulitis in type 1 (insulin-dependent) diabetes mellitus in man--macrophages, lymphocytes, and interferon-gamma containing cells: J Pathol.; 165(2):97-103.

Fox A, Gal S, Fisher N, Smythe J, Wainscoat J, Tyler M.P, Watt S.M and Harris A.L: (2008): Quantification of circulating cell-free plasma DNA and endothelial gene RNA in patients with burns and relation to acute thermal injury: Burns. [Epub ahead of print]

Fricker L.D: (1991): Peptide Biosynthesis and Processing: CRC Press

Fridlyand L.E and Philipson L.H: (2004): Does the glucose-dependent insulin secretion mechanism itself cause oxidative stress in pancreatic beta-cells?: Diabetes.;53(8):1942-8

Funckes C.L, Minth C.D, Deschenes R., Magazin M, Tavianini M.A, Sheets M, Collier K, Weith H.L, Aron D.C, Roos B.A and Dixon J.C: (1983): Cloning and characterisation of a mRNA encoding rat preprosomatostatin: J. Biol. Chem. 258, 18781–18787.

Furuta M, Zhou A, Webb G, Carroll R, Ravazzola M, Orci L and Steiner D.F: (2001): Severe defect in proglucagon processing in islet A-cells of prohormone convertase 2 null mice: J Biol Chem.;276(29):27197-202

Gahan P.B: (2008): Circulating nucleic acids in plasma and serum: roles in diagnosis and prognosis in diabetes and cancer: Infect Disord Drug Targets.; 8(2):100-8

Gaisano H.Y and Leung Y.M: (2008): Pancreatic islet alpha cell commands itself: secrete more glucagon!: Cell Metab.;7(6):474-5

Gale E.A: (1996): Theory and practice of nicotinamide trials in pre-type 1 diabetes: J Pediatr Endocrinol Metab.; 9(3): 375-9.

Ganda O.P and Arkin C.F: (1992): Hyperfibrinogenemia. An important risk factor for vascular complications in diabetes: Diabetes Care.; 15(10):1245-50

Gannon M, Ables E.T, Crawford L, Lowe D, Offield M.F, Magnuson M.A and Wright C.V: (2008): pdx-1 function is specifically required in embryonic β cells to generate appropriate numbers of endocrine cell types and maintain glucose homeostasis: Dev Biol.;314(2):406-17.

Garnett K.E, Chapman P, Chambers J.A, Waddell I.D and Boam D.S: (2005): Differential gene expression between Zucker Fatty rats and Zucker Diabetic Fatty rats: a potential role for the immediate-early gene Egr-1 in regulation of beta cell proliferation: J Mol Endocrinol.; 35(1):13-25

Gazdar A.F, Chick W.L, Oie H.K, Sims H.L, King D.L, Weir G.C and Lauris V: (1980): Continuous, clonal, insulin- and somatostatin-secreting cell lines established from a transplantable rat islet cell tumor: Proc Natl Acad Sci U S A.; 77(6):3519-23

Gerich J.E, Langlois M, Noacco C, Karam J.H and Forsham P.H: (1973): Lack of glucagon response to hypoglycemia in diabetes: evidence for an intrinsic pancreatic alpha cell defect: Science.; 182:171–173.

Ghosh A, Ronner P, Cheong E, Khalid P and Matschinsky F.M: (1991): The role of ATP and free ADP in metabolic coupling during fuel-stimulated insulin release from islet beta-cells in the isolated perfused rat pancreas: J. Biol. Chem.; 266, 22887–22892

Giannoukakis N and Robbins P.D: (2002): Gene and cell therapies for diabetes mellitus: strategies and clinical potential: BioDrugs.; 16(3):149-73.

Gibson D.M, Harris R.A and Roach P: (2002): Metabolic Regulation in Mammals: CRC Press

Gillespie K.M: (2006): Type 1 diabetes: pathogenesis and prevention: CMAJ.; 175(2):165-70.

Gilmore R, Walter P and Blobel G: (1982): Protein translocation across the endoplasmic reticulum. II. Isolation and characterization of the signal recognition particle receptor: J Cell Biol.; 95(2 Pt 1):470-7

Ginsberg H.N, Zhang Y.L and Hernandez-Ono A: (2005): Regulation of plasma triglycerides in insulin resistance and diabetes: Arch Med Res.; 36(3):232-40

Ginsberg-Fellner F, Witt M.E, Yagihashi S, Dobersen M.J, Taub F, Fedun B, McEvoy R.C, Roman S.H, Davies R.G, Cooper L.Z, et al.: (1984): Congenital rubella syndrome as a model for type 1 (insulin-dependent) diabetes mellitus: increased prevalence of islet cell surface antibodies: Diabetologia.; 27 Suppl:87-9.

Giordano T, Brigatti C, Podini P, Bonifacio E, Meldolesi J and Malosio M.L : (2008) : Beta cell chromogranin B is partially segregated in distinct granules and can be released separately from insulin in response to stimulation: Diabetologia.;51(6):997-1007

Glover I.D, Barlow D.J, Pitts J.E, Wood S.P, Tickle I.J, Blundell T.L, Tatemoto K, Kimmel J.R, Wollmer A and Strassburger W: (1984): Conformational studies on the pancreatic polypeptide hormone family: Eur J Biochem; 142: 379-385.

Goldberg S.F, Miele M.E, Hatta N, Takata M, Paquette-Straub C, Freedman L.P and Welch D.R: (2003): Melanoma metastasis suppression by chromosome 6: evidence for a pathway regulated by CRSP3 and TXNIP, Cancer Res.; 63:432–440.

Goodge K.A and Hutton J.C: (2000): Translational regulation of proinsulin biosynthesis and proinsulin conversion in the pancreatic beta-cell: Semin Cell Dev Biol.; 11(4):235-42

Goodman H.M: (2003): Basic Medical Endocrinology: Academic Press

Gosmanov N.R, Szoke E, Israelian Z, Smith T, Cryer P.E, Gerich J.E and Meyer C: (2005): Role of the decrement in intraislet insulin for the glucagon response to hypoglycemia in humans: Diabetes Care.; 28:1124–1131

Grankvist K, Marklund S.L and Täljedal I.B: (1981): CuZn-superoxide dismutase, Mn-superoxide dismutase, catalase and glutathione peroxidase in pancreatic islets and other tissues in the mouse: Biochem J.; 199(2):393-8

Gray S, Feinberg M.W, Hull S, Kuo C.T, Watanabe M, Sen-Banerjee S, DePina A, Haspel R and Jain M.K: (2002): The Krüppel-like factor KLF15 regulates the insulin-sensitive glucose transporter GLUT4: J Biol Chem.; 277(37):34322-8.

Grishok A, Pasquinelli A.E, Conte D, Li N, Parrish S, Ha I, Baillie D.L, Fire A, Ruvkun G and Mello C.C: (2001): Genes and mechanisms related to RNA interference regulate expression of the small temporal RNAs that control C. elegans developmental timing: Cell.;106(1):23-34.

Gromada J and Dissing S: (1996): Membrane potential and cytosolic free calcium levels modulate acetylcholine-induced inositol phosphate production in insulin-secreting BTC3 cells: Biochim Biophys Acta.; 1310(1):145-8

Gromada J, Franklin I and Wollheim C.B: (2007): Alpha-cells of the endocrine pancreas: 35 years of research but the enigma remains: Endocr Rev.; 28(1):84-116.

Gromada J, Ma X, Høy M, Bokvist K, Salehi A, Berggren PO, Rorsman P: (2004): ATP-sensitive K+ channel-dependent regulation of glucagon release and electrical activity by glucose in wild-type and SUR1-/- mouse alpha-cells Diabetes.;53 Suppl 3:S181-9.

Gruden G, Bruno G, Chaturvedi N, Burt D, Schalkwijk C, Pinach S, Stehouwer C.D, Witte D.R, Fuller J.H and Cavallo Perin P: (2008): Serum HSP27 and diabetic complications in the Eurodiab prospective complications study: A novel circulating marker for diabetic neuropathy : Diabetes. [Epub ahead of print]

Guz Y, Montminy M, Stein R, Leonard J, Gamer L, Wright C and Teitelman G: (1995): Expression of murine STF-1, a putative insulin gene transcription factor, in b cells of pancreas, duodenal epithelium and pancreatic exocrine and endocrine progenitors during ontogeny: Development.; 121:11–18.

Hainer V, Toplak H, Mitrakou A: (2008): Treatment modalities of obesity: what fits whom?:Diabetes Care.;31 Suppl 2:S269-77.

Halban P.A and Irminger J.C: (1994): Sorting and processing of secretory proteins: Biochem J.; 299 (Pt 1):1-18.

Halvorsen T.L, Beattie G.M, Lopez A.D, Hayek A and Levine F: (2000): Accelerated telomere shortening and senescence in human pancreatic islet cells stimulated to divide in vitro: J Endocrinol.; 166(1):103-9.

Hamaoui K, Butt A, Powrie J and Swaminathan R: (2004): Concentration of Circulating Rhodopsin mRNA in Diabetic Retinopathy: Clin Chem.; 50:2152-2155.

Hamilton A, Voinnet O, Chappell L and Baulcombe D: (2002): Two classes of short interfering RNA in RNA silencing: EMBO J.; 21(17):4671-9.

Hamilton A.J and Baulcombe D.C: (1999): A species of small antisense RNA in posttranscriptional gene silencing in plants: Science.; 286(5441):950-2.

Hammond S.M, Bernstein E, Beach D and Hannon G.J: (2000): An RNA-directed nuclease mediates post-transcriptional gene silencing in Drosophila cells: Nature.; 404(6775):293-6.

Han S.H, Jeon J.H, Ju H.R, Jung U, Kim K.Y, Yoo H.S, Lee Y.H, Song K.S, Hwang H.M, Na Y.S, Yang Y, Lee K.N and Choi I: (2003): VDUP1 upregulated by TGF-beta1 and 1,25-dihydorxyvitamin D3 inhibits tumor cell growth by blocking cell-cycle progression, Oncogene; 22: 4035–4046.

Hao M, Head W.S, Gunawardana S.C, Hasty A.H and Piston D.W: (2007): Direct effect of cholesterol on insulin secretion: a novel mechanism for pancreatic beta-cell dysfunction: Diabetes.; 56(9):2328-38

Harmon J.S, Gleason C.E, Tanaka Y, Oseid E.A, Hunter-Berger K.K and Robertson R.P: (1999): In vivo prevention of hyperglycemia also prevents

glucotoxic effects on PDX-1 and insulin gene expression: Diabetes: 48(10): 1995-2000.

Harris E.D: (1992): Regulation of antioxidant enzymes: FASEB J.; 6(9): 2675-83.

Hasselmann D.O, Rappl G, Rossler M, Ugurel S, Tilgen W and Reinhold U: (2001): Detection of tumor-associated circulating mRNA in serum, plasma and blood cells from patients with disseminated malignant melanoma: Oncol Rep.; 8:115-118.

Hauge-Evans A.C, Squires P.E, Persaud S.J and Jones P.M: (1999): Pancreatic beta-cell-to-beta-cell interactions are required for integrated responses to nutrient stimuli: enhanced Ca2+ and insulin secretory responses of MIN6 pseudoislets: Diabetes.; 48(7):1402-8

Hayek A, Beattie G.M, Cirulli V, Lopez A.D, Ricordi C and Rubin J.S: (1995): Growth factor/matrix-induced proliferation of human adult beta-cells: Diabetes.; 44(12):1458-60.

He L.P, Mears D, Atwater I and Kitasato H: (1998): Glucagon induces suppression of ATP-sensitive K+ channel activity through a Ca2+/calmodulin-dependent pathway in mouse pancreatic beta-cells: J Membr Biol.;166(3):237-44

Hegedus Z, Czibula A and Kiss-Toth E: (2007): Tribbles: a family of kinase-like proteins with potent signalling regulatory function: Cell Signal.; 19(2):238-50.

Henquin J.C, Ishiyama N, Nenquin M, Ravier M.A and Jonas J.C: (2000): Signals and pools underlying biphasic insulin secretion: Diabetes.; 51 Suppl 1:S60-7

Hermanto U, Zong C.S and Wang L.H: (2000): Inhibition of mitogen-activated protein kinase kinase selectively inhibits cell proliferation in human breast cancer cells displaying enhanced insulin-like growth factor I-mediated mitogen-activated protein kinase activation: Cell Growth Differ.; 11: 655-664.

High S, Martoglio B, Görlich D, Andersen S.S, Ashford A.J, Giner A, Hartmann E, Prehn S, Rapoport T.A, Dobberstein B, et al.: (1993): Site-specific photocross-linking reveals that Sec61p and TRAM contact different regions of a membrane-inserted signal sequence: J Biol Chem.; 268(35):26745-51

Hirai H, Miura J, Hu Y, Larsson H, Larsson K, Lernmark A, Ivarsson S.A, Wu T, Kingman A, Tzioufas A.G and Notkins A.L: (2008): Selective screening of secretory vesicle-associated proteins for autoantigens in type 1 diabetes: VAMP2 and NPY are new minor autoantigens: Clin Immunol.;127(3):366-74

Hohmeier H.E and Newgard C.B: (2004): Cell lines derived from pancreatic islets: Mol Cell Endocrinol.; 228(1-2):121-8

Holt R.I: (2004): Diagnosis, epidemiology and pathogenesis of diabetes mellitus: an update for psychiatrists.Br J Psychiatry Suppl.; 47:S55-63.

Honeyman M: (2005): How robust is the evidence for viruses in the induction of type 1 diabetes?: Curr Opin Immunol.;17(6):616-23.

Hotta M, Tashiro F, Ikegami H, Niwa H, Ogihara T, Yodoi J and Miyazaki J: (1998): Pancreatic ß-cell-specific expression of thioredoxin, an antioxidative and antiapoptotic protein, prevents autoimmune and streptozotocin-induced diabetes: J Exp Med.; 188:1445–1451

Houstis N, Rosen E.D and Lander E.S: (2006): Reactive oxygen species have a causal role in multiple forms of insulin resistance: Nature.; 440(7086):944-8

http://health.howstuffworks.com/diabetes1.htm : 14 Apr. 08

http://www.eatlas.idf.org/

http://www.iptr.umn.edu/IPTR/annual_reports/2004_annual_report/total.html

http://www.vivo.colostate.edu/hbooks/pathphys/endocrine/pancreas/insulin.html

Huang da W, Sherman BT, Tan Q, Kir J, Liu D, Bryant D, Guo Y, Stephens R, Baseler M.W, Lane H.C and Lempicki R.A: (2007): DAVID Bioinformatics Resources: expanded annotation database and novel algorithms to better extract biology from large gene lists: Nucleic Acids Res.;35(Web Server issue):W169-75

Hughes W.E, Elgundi Z, Huang P, Frohman M.A and Biden T.J: (2004): Phospholipase D1 regulates secretagogue-stimulated insulin release in pancreatic beta-cells: J Biol Chem.; 279(26): 27534-41.

Hui H and Perfetti R: (2002): Pancreas duodenum homeobox-1 regulates pancreas development during embryogenesis and islet cell function in adulthood: Eur J Endocrinol.; 146(2):129-41

Hui T.Y, Sheth S.S, Diffley J.M, Potter D.W, Lusis A.J, Attie A.D and Davis R.A: (2004): Mice lacking thioredoxin-interacting protein provide evidence linking cellular redox state to appropriate response to nutritional signals: J Biol Chem.;279(23):24387-93

Hunter T, Hunt T, Jackson R.J and Robertson H.D: (1975): The characteristics of inhibition of protein synthesis by double-stranded ribonucleic acid in reticulocyte lysates: J Biol Chem.; 250(2):409-17.

Hurteau G.J and Spivack S.D: (2002) mRNA-specific reverse transcription-polymerase chain reaction from human tissue extracts: Anal Biochem; 307:304–15

Hutchison C.A, Cockwell P, Harding S, Mead G.P, Bradwell A.R and Barnett A.H: (2008): Quantitative assessment of serum and urinary polyclonal free light chains in patients with type II diabetes: an early marker of diabetic kidney disease?: Expert Opin Ther Targets.;12(6):667-76

Huypens P, Ling Z, Pipeleers D and Schuit F: (2000): Glucagon receptors on human islet cells contribute to glucose competence of insulin release: Diabetologia.; 43(8):1012-9

Hyöty H, Leinikki P, Reunanen A, Ilonen J, Surcel H.M, Rilva A, Käär M.L, Huupponen T, Hakulinen A, Mäkelä A.L, et al.:(1988): Mumps infections in the etiology of type 1 (insulin-dependent) diabetes: Diabetes Res.; 9(3):111-6.

Iezzi M, Escher G, Meda P, Charollais A, Baldini G, Darchen F, Wollheim C.B and Regazzi R: (1999): Subcellular distribution and function of Rab3A, B, C, and D isoforms in insulin-secreting cells: Mol Endocrinol.;13(2):202-12.

Ihara Y, Yamada Y, Yasuda K and Seino Y: (1996): Analysis of novel cDNAs in pancreatic islets of GK rats by fluorescent differential display procedure: Diabetes.; 45, Suppl2: 312.

Imagawa A, Hanafusa T, Itoh N, Waguri M, Yamamoto K, Miyagawa J, Moriwaki M, Yamagata K, Iwahashi H, Sada M, Tsuji T, Tamura S, Kawata S, Kuwajima M, Nakajima H, Namba M and Matsuzawa Y: (1999): Immunological abnormalities in islets at diagnosis paralleled further deterioration of glycaemic control in patients with recent-onset Type I (insulin-dependent) diabetes mellitus: Diabetologia.; 42(5):574-8.

Inagaki N, Maekawa T, Sudo T, Ishii S, Seino Y and Imura H : (1992) : c-Jun represses the human insulin promoter activity that depends on multiple cAMP response elements: Proc Natl Acad Sci U S A.;89(3):1045-9

International Diabetes Federation http://www.idf.org/home/index.cfm?node=37

Ishihara H, Asano T, Tsukuda K, Katagiri H, Inukai K, Anai M, Kikuchi M, Yazaki Y, Miyazaki J.I and Oka Y: (1993): Pancreatic beta cell line MIN6 exhibits characteristics of glucose metabolism and glucose-stimulated insulin secretion similar to those of normal islets: Diabetologia.;36(11):1139-45

Jamal H, Jones P.M and Byrne J: (1991) Peptide contents of neuropeptide Y, vasoactive intestinal polypeptide, and p-calcitonin gene-related peptide and their

messenger ribonucleic acids after dexamethasone treatment m the isolated rat islets of Langerhans: Endocrinology. 129:3372-3380.

Jauch-Chara K, Hallschmid M, Schmid S.M, Oltmanns K.M, Peters A, Born J and Schultes B: (2007): Plasma glucagon decreases during night-time sleep in Type 1 diabetic patients and healthy control subjects: Diabet Med.;24(6):684-7.

Jenkins N.A, Mattei M.G, Gilbert D.J, Linard C.G, Mbikay M, Chretien M and Copeland N.G: (1991) : Assignment of secretogranin I locus to mouse chromosome 2 by in situ hybridization and interspecific backcross analysis: Genomics.;11(2):479-80

Jiang G and Zhang B.B: (2003): Glucagon and regulation of glucose metabolism: Am J Physiol Endocrinol Metab.; 284(4):E671-8

Josefsen K, Sørensen L.R, Buschard K and Birkenbach M: (1999): Glucose induces early growth response gene (Egr-1) expression in pancreatic beta cells: Diabetologia.; 42(2):195-203

Jun H.S and Yoon J.W: (2003): A new look at viruses in type 1 diabetes: Diabetes Metab Res Rev.; 19(1):8-31.

Junn E, Han S.H, Im J.Y, Yang Y, Cho E.W, Um H.D, Kim D.K, Lee K.W, Han P.L, Rhee S.G and Choi I: (2000): Vitamin D3 up-regulated protein 1 mediates oxidative stress via suppressing the thioredoxin function, J. Immunol.; 164:6287–6295.

Kado S, Nagase T and Nagata N: (1999): Circulating levels of interleukin-6, its soluble receptor and interleukin-6/interleukin-6 receptor complexes in patients with type 2 diabetes mellitus: Acta Diabetol.; 36(1-2):67-72

Kajimoto Y and Kaneto H: (2004): Role of oxidative stress in pancreatic beta-cell dysfunction: Ann N Y Acad Sci.: 1011:168-76

Katz J.P, Perreault N, Goldstein B.G, Lee C.S, Labosky P.A, Yang V.W and Kaestner K.H: (2002): The zinc-finger transcription factor Klf4 is required for terminal differentiation of goblet cells in the colon: Development.;129(11):2619-28.

Kayo T, Sawada Y, Suzuki Y, Suda M, Tanaka S, Konda Y, Miyazaki J and Takeuchi T: (1996): Proprotein-processing endoprotease furin decreases regulated secretory pathway-specific proteins in the pancreatic beta cell line MIN6: J Biol Chem.; 271(18):10731-7

Kelly C.D, Edwards Y, Johnstone A.P, Harfst E, Nógrádi A, Nussey S.S, Povey S and Carter N.D: (1992) : Nucleotide sequence and chromosomal assignment of a cDNA encoding the large isoform of human glutamate decarboxylase: Ann Hum Genet.;56(Pt 3):255-65

Khatri P and Drăghici S: (2005): Ontological analysis of gene expression data: current tools, limitations, and open problems: Bioinformatics.;21(18):3587-95

Khatri P, Sellamuthu S, Malhotra P, Amin K, Done A and Draghici S: (2005): Recent additions and improvements to the onto-tools: Nucleic Acids Res.;33(Web Server issue):W762-5

Kim D.H, Behlke M.A, Rose S.D, Chang M.S, Choi S and Rossi J.J: (2005): Synthetic dsRNA Dicer substrates enhance RNAi potency and efficacy: Nat Biotechnol.; 23(2):222-6.

Kinoshita N, Echigo Y, Shinohara S, Gu Y, Miyazaki J, Inoue K and Imamura M: (2001): Regulation of cell proliferation using tissue engineering in MIN6 cells: Cell Transplant.;10(4-5):473-7

Kiss-Toth E, Bagstaff S.M, Sung H.Y, Jozsa V, Dempsey C, Caunt J.C, Oxley K.M, Wyllie D.H, Polgar T, Harte M, O'neill LA, Qwarnstrom E.E and Dower S.K: (2004): Human tribbles, a protein family controlling mitogen-activated protein kinase cascades: J Biol Chem.;279(41):42703-8.

Klöppel G, Löhr M, Habich K, Oberholzer M and Heitz P.U: (1985): Islet pathology and the pathogenesis of type 1 and type 2 diabetes mellitus revisited: Surv Synth Pathol Res.; 4(2):110-25.

Knight B.C and High S: (1998): Membrane integration of Sec61alpha: a core component of the endoplasmic reticulum translocation complex: Biochem J.; 331 (Pt 1):161-7

Kobayashi N, Okitsu T, Lakey J.R and Tanaka N: (2004): The current situation in human pancreatic islet transplantation: problems and prospects: J Artif Organs.; 7(1):1-8

Koffler D, Agnello V, Winchester R and Kunkel H.G: (1973): The occurrence of single-stranded DNA in the serum of patients with systemic lupus erythematosus and other diseases: J Clin Invest.; 52:198-204.

Kopreski M.S, Benko F.A, Kwak L.W and Gocke C.D: (1999): Detection of Tumor Messenger RNA in the Serum of Patients with Malignant Melanoma: Clin Cancer Res.; 5, 1961-1965.

Korsgren O, Buhler L.H and Groth C.G: (2003): Toward clinical trials of islet xenotransplantation: Xenotransplantation.; 10(4):289-92.

Kozak J.A, Misler S and Logothetis D.E: (1998): Characterization of a Ca2+-activated K+ current in insulin-secreting murine betaTC-3 cells: J Physiol.; 509 (Pt 2):355-70

Kroon E, Martinson L.A, Kadoya K, Bang A.G, Kelly O.G, Eliazer S, Young H, Richardson M, Smart N.G, Cunningham J, Agulnick A.D, D'Amour K.A, Carpenter M.K and Baetge E.E: (2008): Pancreatic endoderm derived from human embryonic stem cells generates glucose-responsive insulin-secreting cells in vivo: Nat Biotechnol.; 26(4):443-52.

Kumagai N, LaMattina J.C, Kamano C, Vagefi P.A, Barth R.N, O'Neil J.J, Yamamoto S, Moran S.G, Utsugi R, Sachs D.H and Yamada K: (2002): Vascularized islet cell transplantation in miniature Swine: islet-kidney allografts correct the diabetic hyperglycemia induced by total pancreatectomy: Diabetes.; 51(11):3220-8

Kumar S.V, Hurteau G.J and Spivack S.D: (2006): Validity of messenger RNA expression analyses of human saliva: Clin Cancer Res.; 12:5033-9.

Kunsch C and Medford R.M: (1999): Oxidative stress as a regulator of gene expression in the vasculature: Circ Res.; 85(8):753-66.

Kuzuya T: (2000): Early diagnosis, early treatment and the new diagnostic criteria of diabetes mellitus: Br J Nutr.; 84 Suppl 2:S177-81.

Labrie F, Candas B, Cusan L, Gomez J.L, Bélanger A, Brousseau G, Chevrette E and Lévesque J: (2004): Screening decreases prostate cancer mortality: 11-year follow-up of the 1988 Quebec prospective randomized controlled trial: Prostate; 59: 311–8.

Lam N.Y.L, Rainer T.H, Chan L.Y.S, Joynt G.M and Lo Y.M.D: (2003): Time course of early and late changes in plasma DNA in trauma patients: Clin Chem.; 49:1286-91.

Lambert G, Krempf M and Costet P: (2006): *PCSK9*: a promising therapeutic target for dyslipidemias? Trends Endocrinol Metab.; 17(3):79-81.

Langin D: (2001): Diabetes, insulin secretion, and the pancreatic beta-cell mitochondrion: N Engl J Med.; 345(24):1772-4

Larsson L.I, Sundler F and Hakanson R: (1976): Pancreatic polypeptide - a postulated new hormone:identification of its cellular storage site by light and electron microscopic immunocytochemistry: Diabetologia.; 12: 211-226.

Leahy J. L: (1996): Impaired β-cell function with chronic hyperglycemia: "Overworked β-cell" hypothesis: Diabetes Rev.; 4, 298–319.

Lenzen S, Drinkgern J and Tiedge M: (1996): Low antioxidant enzyme gene expression in pancreatic islets compared with various other mouse tissues: Free Radic Biol Med.; 20(3):463-6

Leon S.A, Shapiro B, Sklaroff D.M and Yaros M.J: (1977): Free DNA in the serum of cancer patients and the effect of therapy: Cancer Res.; 37: 646-650.

Leung Y.M, Ahmed I, Sheu L, Tsushima R.G, Diamant N.E, Hara M and Gaisano H.Y: (2005): Electrophysiological characterization of pancreatic islet cells in the mouse insulin promoter-green fluorescent protein mouse: Endocrinology.; 146(11):4766-75.

Li C and Wong W.H: (2001): Model-based analysis of oligonucleotide arrays: Expression index computation and outlier detection: PNAS.; 98: 31-36

Li X.C, Liao T.D and Zhuo J.L: (2008): Long-term hyperglucagonaemia induces early metabolic and renal phenotypes of Type 2 diabetes in mice: Clin Sci (Lond).; 114(9):591-601.

Li Y, St John M.A, Zhou X, Kim Y, Sinha U, Jordan R.C, Eisele D, Abemayor E, Elashoff D, Park N.H and Wong D.T: (2004): Salivary transcriptome diagnostics for oral cancer detection: Clin Cancer Res.; 10: 8442-8450.

Li Y, Zhou X, St John M.A and Wong D.T: (2004): RNA profiling of cell-free saliva using microarray technology: J Dent Res.; 83: 199-203.

Lilla V, Webb G, Rickenbach K, Maturana A, Steiner D, Halban P and Irminger J-C: (2003): Differential Gene Expression in Well-Regulated and Dysregulated Pancreatic ß-Cell (MIN6) Sublines: Endocrinology.; 144, 4 (1368-1379).

Limbert C, Päth G, Jakob F and Seufert J: (2008): Beta-cell replacement and regeneration: Strategies of cell-based therapy for type 1 diabetes mellitus: Diabetes Res Clin Pract.; 79(3):389-99

Linn F, Heidmann I, Saedler H and Meyer P: (1990): Epigenetic changes in the expression of the maize A1 gene in Petunia hybrida: role of numbers of integrated gene copies and state of methylation: Mol Gen Genet.; 222(2-3):329-36.

Liu Y.J, Hellman B and Gylfe E: (1999): Ca2+ signaling in mouse pancreatic polypeptide cells: Endocrinology.; 140(12):5524-9

Lomedico P, Rosenthal N, Efstratidadis A, Gilbert W, Kolodner R and Tizard R: (1979) : The structure and evolution of the two nonallelic rat preproinsulin genes: Cell.;18(2):545-58

Lönnrot M, Korpela K, Knip M, Ilonen J, Simell O, Korhonen S, Savola K, Muona P, Simell T, Koskela P and Hyöty H: (2000): Enterovirus infection as a risk factor for beta-cell autoimmunity in a prospectively observed birth cohort: the Finnish Diabetes Prediction and Prevention Study: Diabetes.; 49(8):1314-8.

Lopez D: (2008): PCSK9: an enigmatic protease: Biochim Biophys Acta.; 1781(4):184-91.

Lorenzi M, Bohannon N, Tsalikian E and Karam J.H: (1984): Duration of type I diabetes affects glucagon and glucose responses to insulin-induced hypoglycaemia: West J Med.; 141(4):467-71.

Ludvigsson J, Faresjö M, Hjorth M, Axelsson S, Chéramy M, Pihl M, Vaarala O, Forsander G, Ivarsson S, Johansson C, Lindh A, Nilsson N.O, Aman J, Ortqvist E, Zerhouni P and Casas R: (2008): GAD treatment and insulin secretion in recent-onset type 1 diabetes: N Engl J Med.; 359(18):1909-20.

Ludwig D.L, Kotanides H, Le T, Chavkin D, Bohlen P and Witte L : (2001) : Cloning, genetic characterization, and chromosomal mapping of the mouse VDUP1 gene: Gene.; 269(1-2):103-12

MacDonald P.E, De Marinis Y.Z, Ramracheya R, Salehi A, Ma X, Johnson P.R, Cox R, Eliasson L and Rorsman P: (2007): A K ATP channel-dependent pathway within alpha cells regulates glucagon release from both rodent and human islets of Langerhans: PLoS Biol.; 5(6):e143.

Magnusson I, Rothman D.L, Gerard D.P, Katz L.D and Shulman G.I: (1995): Contribution of hepatic glycogenolysis to glucose production in humans in response to a physiological increase in plasma glucagon concentration: Diabetes.; 44:185–189

Malik R.A, Li C, Aziz W, Olson J.A, Vohra A, McHardy K.C, Forrester J.V, Boulton A.J, Wilson P.B, Liu D, McLeod D and Kumar S: (2005): Elevated plasma CD105 and vitreous VEGF levels in diabetic retinopathy: J Cell Mol Med.; 9(3):692-7

Mandel P and Métais P: (1948): Les acides nucléiques du plasma sanguin chez l'homme : C. R. Acad. Sci. Paris.; 142: 241-243.

Margraf S, Lögters T, Reipen J, Altrichter J, Scholz M and Windolf J: (2008): NEUTROPHIL-DERIVED CIRCULATING FREE DNA (cf-DNA/NETs), A POTENTIAL PROGNOSTIC MARKER FOR POSTTRAUMATIC DEVELOPMENT OF INFLAMMATORY SECOND HIT AND SEPSIS: Shock. [Epub ahead of print]

Martinez J, Patkaniowska A, Urlaub H, Lührmann R and Tuschl T: (2002): Single-stranded antisense siRNAs guide target RNA cleavage in RNAi: Cell.; 110(5):563-74.

Masella R, Cantafora A, Guidoni L, Luciani A.M, Mariutti G, Rosi A and Viti V: (1989): Characterization of vesicles, containing an acylated oligopeptide, released by human colon adenocarcinoma cells. NMR and biochemical studies: FEBS Lett.; 246: 25-29.

Matzke M.A, Primig M, Trnovsky J and Matzke A.J: (1989): Reversible methylation and inactivation of marker genes in sequentially transformed tobacco plants: EMBO J.; 8(3):643-649.

McCormick P.J, Miao Y, Shao Y, Lin J and Johnson A.E: (2003): Cotranslational protein integration into the ER membrane is mediated by the binding of nascent chains to translocon proteins: Mol Cell.; 12(2):329-41

McMorran B, Town L, Costelloe E, Palmer J, Engel J, Hume D and Wainwright B: (2003): Effector ExoU from the type III secretion system is an important modulator of gene expression in lung epithelial cells in response to Pseudomonas aeruginosa infection: Infect Immun.;71(10):6035-44.

McPhee S.J and Ganong W.F: (2006): Pathophysiology of Disease: An Introduction to Clinical Medicine: Published by McGraw-Hill Professional

Meier J.J, Kjems L.L, Veldhuis J.D, Lefebvre P and Butler P.C: (2006): Postprandial suppression of glucagon secretion depends on intact pulsatile

insulin secretion: further evidence for the intraislet insulin hypothesis: Diabetes.; 55:1051–1056

Minami K, Yano H, Miki T, Nagashima K, Wang C.Z, Tanaka H, Miyazaki J.I and Seino S: (2000): Insulin secretion and differential gene expression in glucose-responsive and -unresponsive MIN6 sublines: Am J Physiol Endocrinol Metab.;279(4):E773-81

Minn A.H, Hafele C and Shalev A: (2005): Thioredoxin-interacting protein is stimulated by glucose through a carbohydrate response element and induces beta-cell apoptosis: Endocrinology.; 146(5):2397-405

Minn A.H, Pise-Masison C.A, Radonovich M, Brady J.N, Wang P, Kendziorski C and Shalev A: (2005): Gene expression profiling in INS-1 cells overexpressing thioredoxin-interacting protein: Biochem Biophys Res Commun.;336(3):770-8.

Miyazaki J, Araki K, Yamato E, Ikegami H, Asano T, Shibasaki Y, Oka Y and Yamamura K: (1990): Establishment of a pancreatic beta cell line that retains glucose-inducible insulin secretion: special reference to expression of glucose transporter isoforms: Endocrinology, 126-132

Moens K, Berger V, Ahn J.M, Van Schravendijk C, Hruby V.J, Pipeleers D and Schuit F: (2002): Assessment of the role of interstitial glucagon in the acute glucose secretory responsiveness of in situ pancreatic beta-cells: Diabetes.;51(3):669-75.

Moller D.E and Flier J.S: (1991): Insulin resistance--mechanisms, syndromes, and implications: N Engl J Med.; 325(13):938-48.

Montminy M.R, Goodman R.H, Horovitch S.J and Habener J.F: (1984): Primary structure of the gene encoding rat preprosomatostatin: In: Proc. Nad. Acad. Sci. (USA).; 81, 3337–3340

Moody A.J, Holst J.J, Thim L and Jensen S.L: (1981): Relationship of glicentin to proglucagon and glucagon in the porcine pancreas: Nature.; 289(5797):514-6.

Mor A, Chartrel N, Vaudry H and Nicolas P: (1994): Skin peptide tyrosine-tyrosine, a member of the pancreatic polypeptide family: isolation, structure, synthesis, and endocrine activity: Proc Natl Acad Sci U S A.; 91(22):10295-9

Moritoh Y, Yamato E, Yasui Y, Miyazaki S, Miyazaki J: (2003): Analysis of insulin-producing cells during in vitro differentiation from feeder-free embryonic stem cells: Diabetes.;52(5):1163-8.

Morozkin E.S, Laktionov P.P, Rykova E.Y and Vlassov V.V: (2004): Extracellular nucleic acids in cultures of long-term cultivated eukaryotic cells: Ann N Y Acad Sci.; 1022: 244-249.

Muñoz A, Hu M, Hussain K, Bryan J, Aguilar-Bryan L and Rajan A.S: (2005): Regulation of glucagon secretion at low glucose concentrations: evidence for adenosine triphosphate-sensitive potassium channel involvement: Endocrinology.; 146(12):5514-21.

Muoio D.M: (2007): TXNIP Links Redox Circuitry to Glucose Control: Cell Metab.; 5(6):412-4.

Murlin J.R, Clough H.D, Gibbs C.B.F and Stokes A.M: (1923): Aqueous extracts of pancreas. I. Influence on the carbohydrate metabolism of depancreatized animals: J Biol Chem.; 56:253–296

Nancy B.Y, Tsui Y. M and Dennis LO: (2006): Placental RNA in Maternal Plasma toward Non-invasive Fetal Gene Expression Profiling: Ann NY Acad Sci: 1075: 96.

Naoumova R.P, Tosi I, Patel D, Neuwirth C, Horswell S.D, Marais A.D, van Heyningen C and Soutar A.K: (2005): Severe hypercholesterolemia in four British families with the D374Y mutation in the PCSK9 gene: long-term follow-up and treatment response: Arterioscler Thromb Vasc Biol.;25(12):2654-60.

Napoli C, Lemieux C and Jorgensen R: (1990): Introduction of a Chimeric Chalcone Synthase Gene into Petunia Results in Reversible Co-Suppression of Homologous Genes in trans: Plant Cell.; 2(4):279-289.

Nathan D.M, Cleary P.A, Backlund J.Y, Genuth S.M, Lachin J.M, Orchard T.J, Raskin P and Zinman B: (2005): Diabetes Control and Complications Trial/Epidemiology of Diabetes Interventions and Complications (DCCT/EDIC) Study Research Group: Intensive diabetes treatment and cardiovascular disease in patients with type 1 diabetes: N Engl J Med.; 353(25): 2643-53.

National Diabetes Fact Sheet: (2007): http://www.cdc.gov/diabetes/pubs/pdf/ndfs_2007.pdf

Neerman-Arbez M, Cirulli V and Halban P.A: (1994): Levels of the conversion endoproteases PC1 (PC3) and PC2 distinguish between insulin-producing pancreatic islet beta cells and non-beta cells: Biochem J.; 300 (Pt 1):57-61

Ng E.K, Tsui N.B, Lam N.Y, Chiu R.W, Yu S.C, Wong S.C, Lo E.S, Rainer T.H, Johnson P.J and Lo Y.M: (2002): Presence of filterable and nonfilterable mRNA in the plasma of cancer patients and healthy individuals: Clin Chem.; 48(8):1212-7.

Nicholson A.W: (1999): Function, mechanism and regulation of bacterial ribonucleases: FEMS Microbiol Rev.; 23(3):371-90.

Nickenig G, Baudler S, Müller C, Werner C, Werner N, Welzel H, Strehlow K, Böhm M: (2002): Redox-sensitive vascular smooth muscle cell proliferation is mediated by GKLF and Id3 in vitro and in vivo: FASEB J.;16(9):1077-86.

Nie Y, Nakashima M, Brubaker P.L, Li Q.L, Perfetti R, Jansen E, Zambre Y, Pipeleers D and Friedman T.C: (2000): Regulation of pancreatic PC1 and PC2 associated with increased glucagon-like peptide 1 in diabetic rats: J Clin Invest.; 105(7):955-65

Niesen M, Bedi M and Lopez D: (2008): Diabetes alters LDL receptor and PCSK9 expression in rat liver: Arch Biochem Biophys.; 470(2):111-5.

Nilsson T, Schultz V, Berggren P.O, Corkey B.E and Tornheim K: (1996): Temporal patterns of changes in ATP/ADP ratio, glucose 6-phosphate and cytoplasmic free Ca2+ in glucose-stimulated pancreatic beta-cells: Biochem J.; 314 (Pt 1):91-4

Nishiyama A, Masutani H, Nakamura H, Nishinaka Y and Yodoi J: (2001): Redox regulation by thioredoxin and thioredoxin-binding proteins: IUBMB Life.; 52:29–33

Noe B.D, Milgram S.L, Balasubramaniam A, Andrews P.C, Calka J and McDonald J.K: (1989): Localization and characterization of neuropeptide Y-like peptides in the brain and islet organ of the anglerfish (Lophius americanus): Cell Tissue Res.; 257(2),303-311.

Novina C.D and Sharp P.A: (2004): The RNAi revolution: Nature.; 430(6996):161-4.

Nussey S.S and Whitehead S.A: (2001): Endocrinology, An integrated approach: Taylor & Francis

Nyfeler B, Zhang B, Ginsburg D, Kaufman R.J and Hauri H.P: (2006): Cargo selectivity of the ERGIC-53/MCFD2 transport receptor complex: Traffic.; 7: 1473-1481.

O'Driscoll L, Gammell P and Clynes M: (2002): Engineering Vero cells to secrete human insulin: In Vitro Cell Dev Biol Anim.; 38:146-53.

O'Driscoll L, Gammell P, McKiernan E, Ryan E, Jeppesen P.B, Rani S and Clynes M: (2006): Phenotypic and global gene expression profile changes between low passage and high passage MIN-6 cells: Journal of Endocrinology.; 191, 665-676

O'Driscoll L, Kenny E, Villarreal M.P.D and Clynes M: (2005): Detection of specific mRNAs in culture medium conditioned by human tumour cells:

Potential for new class of cancer biomarkers in serum: Cancer genomics & proteomics.; 2: 43-52.

O'Driscoll L: (2007): Extracellular nucleic acids and their potential as diagnostic, prognostic and predictive biomarkers: Anticancer Res.; 27:3

O'Driscoll L, Gammell P and Clynes M: (2004): Mechanisms associated with loss of glucose responsiveness in beta cells: Pancreas physiology.; 1159-1162

O'Driscoll L, Gammell P and Clynes M: (2004): Mechanisms associated with loss of glucose responsiveness in beta cells: Transplant Proc.; 36(4):1159-62

O'Driscoll L, Kenny E, Mehta J.P, Doolan P, Joyce H, Gammell P, Hill A, O'Daly B, O'Gorman D and Clynes M: (2008): Feasibility and relevance of global expression profiling of gene transcripts in serum from breast cancer patients using whole genome microarrays and quantitative rt-PCR: Cancer Genomics Proteomics.; 5(2):94-104

Ohara-Imaizumi M and Nagamatsu S: (2006): Insulin exocytotic mechanism by imaging technique: J Biochem (Tokyo).; 140(1): 1-5.

Ohara-Imaizumi M, Nishiwaki C, Kikuta T, Nagai S, Nakamichi Y and Nagamatsu S: (2004): TIRF imaging of docking and fusion of single insulin granule motion in primary rat pancreatic beta-cells: different behaviour of granule motion between normal and Goto-Kakizaki diabetic rat beta-cells: Biochem J.; 381(Pt 1):13-8

Ohta S, Lai E.W, Pang A.L, Brouwers F.M, Chan W.Y, Eisenhofer G, de Krijger R, Ksinantova L, Breza J, Blazicek P, Kvetnansky R, Wesley R.A and Pacak K:

(2005): Downregulation of metastasis suppressor genes in malignant pheochromocytoma: Int. J. Cancer.; 114:139–143.

Okamoto H: (1990): Molecular Biology of the Islets of Langerhans: Cambridge University Press.

Oliveira H.R, Curi R and Carpinelli A.R: (1999): Glucose induces an acute increase of superoxide dismutase activity in incubated rat pancreatic islets: Am J Physiol.; 276(2 Pt 1): C507-10.

Onaca N, Naziruddin B, Matsumoto S, Noguchi H, Klintmalm G.B and Levy M.F: (2007): Pancreatic islet cell transplantation: update and new developments: Nutr Clin Pract.; 22(5):485-93

Ouguerram K, Chetiveaux M, Zair Y, Costet P, Abifadel M, Varret M, Boileau C, Magot T and Krempf M: (2004): Apolipoprotein B100 metabolism in autosomal-dominant hypercholesterolemia related to mutations in PCSK9: Arterioscler Thromb Vasc Biol.;24(8):1448-53

Oyadomari S, Koizumi A, Takeda K., Gotoh T, Akira S, Araki E and Mori M: (2002): Targeted disruption of the chop gene delays endoplasmic reticulum stress-mediated diabetes: J. Clin. Invest.; 109: 525-532.

Pak C.Y, Eun H.M, McArthur R.G and Yoon J.W: (1988): Association of cytomegalovirus infection with autoimmune type 1 diabetes: Lancet.; 2(8601):1-4.

Pal-Bhadra M, Bhadra U and Birchler J.A: (2002): RNAi related mechanisms affect both transcriptional and posttranscriptional transgene silencing in Drosophila: Mol Cell.; 9(2):315-27.

Palmer J.P, Fleming G.A, Greenbaum C.J, Herold K.C, Jansa L.D, Kolb H, Lachin J.M, Polonsky K.S, Pozzilli P, Skyler J.S and Steffes M.W: (2004): C-peptide is the appropriate outcome measure for type 1 diabetes clinical trials to preserve beta-cell function: report of an ADA workshop, 21-22 October 2001: Diabetes.;53(1):250-64.

Parikh H, Carlsson E, Chutkow W.A, Johansson L.E, Storgaard H, Poulsen P, Saxena R, Ladd C, Schulze P.C, Mazzini M.J, Jensen C.B, Krook A, Björnholm M, Tornqvist H, Zierath J.R, Ridderstråle M, Altshuler D, Lee R.T, Vaag A, Groop L.C and Mootha V.K: (2007): TXNIP regulates peripheral glucose metabolism in humans: PLoS Med.; 4(5):e158

Park H, Yu L, Kim T, Cho B, Kang J and Park Y: (2006): Antigenic determinants to GAD autoantibodies in patients with type 1 diabetes with and without autoimmune thyroid disease: Ann N Y Acad Sci.;1079:213-9

Paronen J, Moriyama H, Abiru N, Sikora K, Melanitou E, Babu S, Bao F, Liu E, Miao D and Eisenbarth G.S: (2003): Establishing insulin 1 and insulin 2 knockout congenic strains on NOD genetic background: Ann N Y Acad Sci.; 1005:205-10.

Philippe J, Mojsov S, Drucker D.J and Habener J.F: (1986): Proglucagon processing in a rat islet cell line resembles phenotype of intestine rather than pancreas: Endocrinology.; 119(6):2833-9

Pineda M.H: (2003): McDonald's Veterinary Endocrinology and Reproduction: Blackwell Publishing.

Pipeleers D, in't Veld P.I, Maes E and Van De Winkel M: (1982): Glucose-induced insulin release depends on functional cooperation between islet cells: Proc Natl Acad Sci U S A.; 79(23):7322-5

Pipeleers D.G, Schuit F.C, in't Veld P.A, Maes E, Hooghe-Peters E.L, Van de Winkel M and Gepts W: (1985): Interplay of nutrients and hormones in the regulation of insulin release: Endocrinology.; 117(3):824-33

Poitout V, Olson L.K and Robertson R.P: (1996): Insulin-secreting cell lines: classification, characteristics and potential applications: Diabetes Metab.; 22(1):7-14.

Polonsky K, Frank B, Pugh W, Addis A, Karrison T, Meier P, Tager H and Rubenstein A: (1986): The limitations to and valid use of C-peptide as a marker of the secretion of insulin: Diabetes.; 35(4):379-86.

Polonsky K.S, Licinio-Paixao J, Given B.D, Pugh W, Rue P, Galloway J, Karrison T and Frank B: (1986): Use of biosynthetic human C-peptide in the measurement of insulin secretion rates in normal volunteers and type I diabetic patients: J Clin Invest.;77(1):98-105.

Poon L.M, Leung T.N, Lau T.K and Dennis Lo. Y.M: (2000): Presence of Fetal RNA in Maternal Plasma: Clin Chem.; 46: 1832-1834.

Porte D, Sherwin S.R, Baron A, Ellenberg M, Rifkin H: (2003): Ellenberg and Rifkin's Diabetes Mellitus: Theory and Practice: Published by McGraw-Hill Professional.

Proud C.G: (2006): Regulation of protein synthesis by insulin: Biochem Soc Trans.; 34(Pt 2):213-6

Quesada I, Todorova MG, Alonso-Magdalena P, Beltrá M, Carneiro EM, Martin F, Nadal A, Soria B: (2006): Glucose induces opposite intracellular Ca2+ concentration oscillatory patterns in identified alpha- and beta-cells within intact human islets of Langerhans: Diabetes.;55(9):2463-9.

Quesada I, Tudurí E, Ripoll C and Nadal A: (2008): Physiology of the pancreatic alpha-cell and glucagon secretion: role in glucose homeostasis and diabetes: J Endocrinol.; 199(1):5-19.

Quetglas S, Leveque C, Miquelis R, Sato K and Seagar M: (2000): Ca2+-dependent regulation of synaptic SNARE complex assembly via a calmodulin- and phospholipid-binding domain of synaptobrevin: Proc Natl Acad Sci U S A.; 97(17):9695-700

Rajan A.S: (2002): Regulation of Insulin Secretion: 62nd Scientific Sessions of the American Diabetes Association

Raju B and Cryer P.E: (2005): Loss of the decrement in intraislet insulin plausibly explains loss of the glucagon response to hypoglycemia in insulin-deficient diabetes: documentation of the intraislet insulin hypothesis in humans: Diabetes.; 54:757–764

Rashid S, Curtis D.E, Garuti R, Anderson N.N, Bashmakov Y, Ho Y.K, Hammer R.E, Moon Y.A and Horton J.D: (2005): Decreased plasma cholesterol and hypersensitivity to statins in mice lacking Pcsk9: Proc Natl Acad Sci U S A.;102(15):5374-9

Redondo M.J, Fain P.R and Eisenbarth G.S: (2001): Genetics of type 1A diabetes: Recent Prog Horm Res.; 56:69-89.

Ren F.Y, Piao X.X and Jin A.L: (2006) Efficacy of ultrasonography and alphafetoprotein on early detection of hepatocellular carcinoma: World J Gastroenterol.; 12: 4656–9.

Ren J, Jin P, Wang E, Liu E, Harlan D.M, Li X and Stroncek D.F: (2007): Pancreatic islet cell therapy for type I diabetes: understanding the effects of glucose stimulation on islets in order to produce better islets for transplantation: J Transl Med.; 5:1

Rendell M: (1983): The expanding clinical use of C-peptide radioimmunoassay: Acta Diabetol Lat.; 20(2):105-13.

Renna M, Faraonio R, Bonatti S, De Stefano D, Carnuccio R, Tajana G and Remondelli P: (2006): Nitric oxide-induced endoplasmic reticulum stress activates the expression of cargo receptor proteins and alters the glycoprotein transport to the Golgi complex: Int J Biochem Cell Biol.;38(12):2040-8.

Renström E, Eliasson L and Rorsman P: (1997): Protein kinase A-dependent and -independent stimulation of exocytosis by cAMP in mouse pancreatic B-cells: J Physiol.; 502 ( Pt 1):105-18

Rhodes C.J: (2000): Introduction: The molecular cell biology of insulin production: Seminars in Cell & Developmental Biology: 11, 4(223-225).

Richard C, Kamm and Smith A.G: (1972): Nucleic acid concentrations in normal human plasma: Clin Chem.; 18:519-522.

Riedel D, Antonin W, Fernandez-Chacon R, Alvarez de Toledo G, Jo T, Geppert M, Valentijn J.A, Valentijn K, Jamieson J.D, Südhof T.C and Jahn R: (2002): Rab3D is not required for exocrine exocytosis but for maintenance of normally sized secretory granules: Mol Cell Biol.; 22(18):6487-97.

Robertson R.P, Harmon J, Tran P.O, Tanaka Y and Takahashi H: (2003): Glucose Toxicity in ß-Cells: Type 2 Diabetes, Good Radicals Gone Bad, and the Glutathione Connection: Diabetes.; 52:581-587.

Roderigo-Milne H, Hauge-Evans H.C, Persaud S.J and Jones P.M: (2002): Differential expression of insulin genes 1 and 2 in MIN6 cells and pseudoislets: Biochem Biophys Res Commun.; 296, 589-595.

Roe M.W, Philipson L.H, Frangakis C.J, Kuznetsov A, Mertz R.J, Lancaster M.E, Spencer B, Worley J.F and Dukes I.D: (1994): Defective glucose-dependent endoplasmic reticulum Ca2+ sequestration in diabetic mouse islets of Langerhans: J Biol Chem.; 269(28):18279-82.

Rosi A, Guidoni L, Luciani A.M, Mariutti G and Viti V: (1988): RNA-lipid complexes released from the plasma membrane of human colon carcinoma cells: Cancer Lett.; 39: 153-60.

Rossini A.A, Like A.A, Chick W.L, Appel M.C and Cahill G.F Jr: (1977): Studies of streptozotocin-induced insulitis and diabetes: Proc Natl Acad Sci U S A.; 74(6):2485-9.

Rubenstein A. H, Clark J. L, Melani F and Steiner D. F: (1969): Secretion of proinsulin C-peptide by pancreatic beta cells and its circulation in blood: Nature (Lond.); 224:697-699.

Ryan E.A, Paty B.W, Senior P.A, Bigam D, Alfadhli E, Kneteman N.M, Lakey J.R and Shapiro A.M: (2005): Five-year follow-up after clinical islet transplantation: Diabetes.;54(7):2060-9.

Rykova E.Y, Wunsche W, Brizgunova O.E, Skvortsova T.E, Tamkovich S.N, Senin I.S, Laktionov P.P, Sczakiel G and Vlassov V.V: (2006): Concentrations of circulating RNA from healthy donors and cancer patients estimated by different methods: Ann N Y Acad Sci.; 1075: 328-333.

Rykova EIu, Skvortsova T.E, Hoffmann A.I, Tamkovich S.N, Starikov A.V, Bryzgunova O.E, Permiakova V.I, Warnecke J.M, Sczakiel G, Vlasov V.V, Laktionov P.P: (2008): Breast cancer diagnostics based on extracellular DNA and RNA circulating in blood: Biomed Khim.;54(1):94-103

Sabbah E: (2000): Role of antibodies to glutamic acid decarboxylase in type 1 diabetes.Relation to other autoantibodies, HLA risk markers and clinical characteristics: Academic Dissertation. University of Oulu.

Salminen K, Sadeharju K, Lönnrot M, Vähäsalo P, Kupila A, Korhonen S, Ilonen J, Simell O, Knip M and Hyöty H: (2003): Enterovirus infections are associated

with the induction of beta-cell autoimmunity in a prospective birth cohort study: J Med Virol.; 69(1):91-8.

Santerre R.F, Cook R.A, Crisel R.M, Sharp J.D, Schmidt R.J, Williams D.C and Wilson C.P: (1981): Insulin synthesis in a clonal cell line of simian virus 40-transformed hamster pancreatic beta cells: Proc Natl Acad Sci U S A.; 78(7):4339-43

Sawada Y, Zhang B, Okajima F, Izumi T and Takeuchi T: (2001): PTHrP increases pancreatic beta-cell-specific functions in well-differentiated cells: Mol Cell Endocrinol.; 182(2):265-75.

Scepek S, Coorssen J.R and Lindau M: (1998): Fusion pore expansion in horse eosinophils is modulated by Ca2+ and protein kinase C via distinct mechanisms: EMBO J.; 17(15):4340-5.

Schmidt B, Engel E, Carstensen T, Weickmann S, John M, Witt C and Fleischhacker M: (2005): Quantification of free RNA in serum and bronchial lavage: a new diagnostic tool in lung cancer detection?: Lung Cancer.; 48: 145-147.

Schulze P.C, De Keulenaer G.W, Yoshioka J, Kassik K.A and Lee R.T: (2002): Vitamin D3-upregulated protein-1 (VDUP-1) regulates redox-dependent vascular smooth muscle cell proliferation through interaction with thioredoxin: Circ. Res.; 91: 689–695.

Schulze P.C, Yoshioka J, Takahashi T, He Z, King G.L and Lee R.T: (2004): Hyperglycemia promotes oxidative stress through inhibition of thioredoxin function by thioredoxin-interacting protein: J. Biol. Chem.; 279(29):30369-74.

Seidah N. G, Benjannet S, Wickham L, Marcinkiewicz J, Jasmin S. B, Stifani S, Basak A, Prat A and Chretien M : (2003): The secretory proprotein convertase neural apoptosis-regulated convertase 1 (NARC-1): liver regeneration and neuronal differentiation: Proc. Nat. Acad. Sci.; 100: 928-933.

Semenov D.V, Kuligina E.V, Shevyrina O.N, Richter V.A and Vlassov V.V: (2004): Extracellular ribonucleic acids of human milk: Ann N Y Acad Sci 1022: 190-194.

Seppälä-Lindroos A, Vehkavaara S, Häkkinen AM, Goto T, Westerbacka J, Sovijärvi A, Halavaara J, Yki-Järvinen H: (2002): Fat accumulation in the liver is associated with defects in insulin suppression of glucose production and serum free fatty acids independent of obesity in normal men: J Clin Endocrinol Metab.; 87(7):3023-8

Setji T.L, Brown A.J, and Feinglos M.N: (2005): Gestational Diabetes Mellitus: Clinical Diabetes.; 23:17-24.

Shah P, Vella A, Basu A, Basu R, Schwenk W.F and Rizza R.A: (2000): Lack of suppression of glucagon contributes to postprandial hyperglycemia in subjects with type 2 diabetes mellitus: J Clin Endocrinol Metab.; 85(11):4053-9.

Shalev A, Pise-Masison C.A, Radonovich M, Hoffmann S.C, Hirshberg B, Brady J.N and Harlan D.M: (2002): Oligonucleotide microarray analysis of intact

human pancreatic islets: identification of glucose-responsive genes and a highly regulated TGFbeta signaling pathway: Endocrinology.; 143(9):3695-8

Shapiro A.M, Lakey J.R, Ryan E.A., Korbett G.S, Toth E, Warnock G.L, Kneteman N.M and Rajotte R.V: (2000): Islet transplantation in seven patients with type 1 diabetes mellitus using a glucocorticoid free immunosuppressive regimens: N Engl J Med.; 343: 230-238.

Sharma S, Jhala U. S, Johnson T, Ferreri K, Leonard J and Montminy M: (1997): Hormonal regulation of an islet-specific enhancer in the pancreatic homeobox gene STF-1: Molec. Cell. Biol.; 17: 2598-2604.

Shaulian E and Karin M: (2002): AP-1 as a regulator of cell life and death: Nat. Cell Biol.; 4: E131-6.

Sheth S.S, Bodnar J.S, Ghazalpour A, Thipphavong C.K, Tsutsumi S, Tward A.D, Demant P, Kodama T, Aburatani H and Lusis A.J: (2006): Hepatocellular carcinoma in Txnip-deficient mice: Oncogene.; 25(25):3528-36

Shi J and Kandror K.V: (2008): Study of glucose uptake in adipose cells: Methods Mol Biol.; 456:307-15

Sia C: (2004): Autoimmune diabetes: ongoing development of immunological intervention strategies targeted directly against autoreactive T cells: Rev Diabet Stud.; 1:9–17.

Siolas D, Lerner C, Burchard J, Ge W, Linsley P.S, Paddison P.J, Hannon G.J and Cleary M.A: (2005): Synthetic shRNAs as potent RNAi triggers: Nat Biotechnol.; 23(2):227-31.

Sisco K.L: (2001): Is RNA in serum bound to nucleoprotein complexes?: Clin Chem.; 47: 1744-1745.

Skvortsova T.E, Rykova E.Y, Tamkovich S.N, Bryzgunova O.E, Starikov A.V, Kuznetsova N.P, Vlassov V.V and Laktionov P.P: (2006): Cell-free and cell-bound circulating DNA in breast tumours: DNA quantification and analysis of tumour-related gene methylation: Br J Cancer.;94(10):1492-5

Slavin B.G, Ong J.M and Kern P.A: (1994): Hormonal regulation of hormone-sensitive lipase activity and mRNA levels in isolated rat adipocytes: J Lipid Res.; 35(9):1535-41.

Smith C.J, Watson C.F, Bird C.R, Ray J, Schuch W and Grierson D: (1990): Expression of a truncated tomato polygalacturonase gene inhibits expression of the endogenous gene in transgenic plants: Mol Gen Genet.; 224(3):477-81.

Soares M.B, Schon E, Henderson A, Karathanasis S.K, Cate R, Zeitlin S, Chirgwin J and Efstratiadis A: (1985): RNA-mediated gene duplication: the rat preproinsulin I gene is a functional retroposon: Mol Cell Biol.;5(8):2090-103.

Song D.K, Ahn Y.H, Bae J.H, Park W.K, Hong Y.S, Ho W.K and Earm Y.E: (2000): Evidence of enhancement of malate-aspartate shuttle activity in beta cells of streptozotocin-induced non-insulin-dependent diabetic rats: Metabolism.;49(1):92-6.

Spurlin B.A and Thurmond D.C: (2006): Syntaxin 4 facilitates biphasic glucose-stimulated insulin secretion from pancreatic beta-cells: Mol Endocrinol.; 20(1):183-93

Srikant B.C: (2004): Somatostatin/ analogs & derivatives: Published by Springer

Stanley E.G and Elefanty A.G: (2008): Building better beta cells: Cell Stem Cell.; 2(4):300-1.

Stanley S, Wynne K and Bloom S: (2004): Gastrointestinal satiety signals III. Glucagon-like peptide 1, oxyntomodulin, peptide YY, and pancreatic polypeptide: Am J Physiol Gastrointest Liver Physiol.; 286(5):G693-7

Stark G.R, Kerr I.M, Williams B.R, Silverman R.H and Schreiber R.D: (1998): How cells respond to interferons: Annu Rev Biochem.; 67:227-64.

Staub A, Sinn L and Behrens O.K: (1955): Purification and crystallization of glucagon: J Biol Chem.; 214(2):619-32.

Steiner D.F: (2004): The proinsulin C-peptide--a multirole model: Exp Diabesity Res.; 5(1):7-14.

Straub S.G and Sharp G.W: (2002): Glucose-stimulated signaling pathways in biphasic insulin secretion: Diabetes Metab Res Rev.; 18(6):451-63

Stroun M, Anker P, Beljanski M, Henri J, Lederrey C, Ojha M and Maurice P.A: (1978): Presence of RNA in the nucleoprotein complex spontaneously released by human lymphocytes and frog auricles in culture: Cancer Res.; 38: 3546-3554.

Stroun M, Lyautey J, Lederrey C, Olson-Sand A and Anker P: (2001): About the possible origin and mechanism of circulating DNA apoptosis and active DNA release: Clin Chim Acta.; 313(1-2):139-42

Suckale J and Solimena M: (2008): Pancreas islets in metabolic signaling - focus on the beta-cell: Front Biosci.; 13:7156-71

Sundar Rajan S, Srinivasan V, Balasubramanyam M and Tatu U: (2007): Endoplasmic reticulum (ER) stress & diabetes: Indian J Med Res.; 125(3):411-24

Sung H.Y, Guan H, Czibula A, King A.R, Eder K, Heath E, Suvarna S.K, Dower S.K, Wilson A.G, Francis S.E, Crossman D.C and Kiss-Toth E: (2007): Human tribbles-1 controls proliferation and chemotaxis of smooth muscle cells via MAPK signaling pathways: J. Biol. Chem.; 282: 18379-18387.

Susini S, Roche E, Prentki M and Schlegel W: (1998): Glucose and glucoincretin peptides synergize to induce c-fos, c-jun, junB, zif-268, and nur-77 gene expression in pancreatic beta (INS-1) cells: FASEB J.; 12(12):1173-82

Suzuki R, Yoshioka Y, Kitano E, Yoshioka T, Oka H, Okamoto T, Okada N, Tsutsumi Y, Nakagawa S and Miyazaki J: (2003): Development of a novel cytomedical treatment that can protect entrapped cells from host humoral immunity: Cell Transplantation 11 787–797.

Takekawa M and Saito H: (1998): A family of stress-inducible GADD45-like proteins mediate activation of the stress-responsive MTK1/MEKK4 MAPKKK: Cell.; 95(4):521-30.

Tan C, Tuch B.E, Tu J and Brown S.A: (2002): Role of NADH shuttles in glucose-induced insulin secretion from fetal beta-cells: Diabetes.; 51(10):2989-96.

Tan E.M, Schur P.H, Carr R.I and Kunkel H.G: (1966): Deoxybonucleic acid (DNA) and antibodies to DNA in the serum of patients with systemic lupus erythematosus: J Clin Invest.; 45: 1732-1740.

Tanaka T, Akatsuka S, Ozeki M, Shirase T, Hiai H and Toyokuni S: (2004): Redox regulation of annexin 2 and its implications for oxidative stress-induced renal carcinogenesis and metastasis: Oncogene. ; 23(22): 3980-9

Taniguchi C.M, Emanuelli B and Kahn C.R: (2006): Critical nodes in signalling pathways: insights into insulin action: Nat Rev Mol Cell Biol.; 7(2):85-96

Tarasov A, Dusonchet J and Ashcroft F: (2004): Metabolic regulation of the pancreatic beta-cell ATP-sensitive K+ channel: a pas de deux: Diabetes; 53 Suppl 3:S113-22.

Taskinen M.R: (2003): Diabetic dyslipidaemia: from basic research to clinical practice: Diabetologia.; 46(6):733-49

Teitelman G, Alpert S, Polak J.M, Martinez A and Hanahan D: (1993): Precursor cells of mouse endocrine pancreas coexpress insulin, glucagon and the neural proteins tyrosine hydroxylase and neuropeptide Y, but not pancreatic polypeptide: Development.; 118:1031-1039.

Terenghi G, Polak J. M, Hamid Q, O'Brien E, Denny P, Legon S, Dixon J, Minth C. D, Palay S. L, Yasargil G and Chan-Palay V: (1987): Localization of neuropeptide Y mRNA in neurons of human cerebral cortex by means of in situ hybridization with a complementary RNA probe: Proc. Nat. Acad. Sci. 84: 7315-7318.

The CITR Coordinating Center and Investigators. The Collaborative Islet Transplant Registry 2008 Annual Report. www.citregistry.org/reports/reports.htm.

The Diabetes Control and Complications Trial Research Group. The effect of intensive treatment of diabetes on the development and progression of long- term complications in insulin – dependent diabetes mellitus. New England Journal of medicine 1993; 329 977 – 986.

Thermos K: (2008): Novel signals mediating the functions of somatostatin: The emerging role of NO/cGMP: Mol Cell Endocrinol.; 286(1-2):49-57

Tiedge M and Lenzen S: (1996): Effects of sodium butyrate on glucose transporter and glucose-phosphorylating enzyme gene expression in RINm5F insulinoma cells: J Mol Endocrinol.; 17(1):19-26

Tiedge M, Höhne M and Lenzen S: (1993): Insulin secretion, insulin content and glucose phosphorylation in RINm5F insulinoma cells after transfection with human GLUT2 glucose-transporter cDNA: Biochem J.; 296 (Pt 1):113-8

Tiedge M, Lortz S, Munday R and Lenzen S: (1998): Complementary action of antioxidant enzymes in the protection of bioengineered insulin-producing RINm5F cells against the toxicity of reactive oxygen species: Diabetes; 47(10):1578-85.

Trimble E.R, Halban P.A, Wollheim C.B and Renold A.E: (1982): Functional differences between rat islets of ventral and dorsal pancreatic origin: J Clin Invest.; 69(2):405-13

Tsang J.C and Lo Y.M: (2007): Circulating nucleic acids in plasma/serum: Pathology; 39(2):197-207

Tsiotra P.C and Tsigos C: (2006): Stress, the endoplasmic reticulum, and insulin resistance: Ann N Y Acad Sci.; 1083:63-76

Tso A.W, Xu A, Sham P.C, Wat N.M, Wang Y, Fong C.H, Cheung B.M, Janus E.D and Lam K.S: (2007): Serum adipocyte fatty acid binding protein as a new biomarker predicting the development of type 2 diabetes: a 10-year prospective study in a Chinese cohort: Diabetes Care.; 30(10):2667-72.

Tsui N.B, Ng E.K and Lo Y.M: (2002): Stability of endogenous and added RNA in blood specimens, serum, and plasma: Clin Chem.; 48(10):1647-53.

Tsui N.B.Y and Lo Y.M.D: (2006): Placental RNA in maternal plasma toward noninvasive fetal gene expression profiling: Ann N Y Acad Sci.; 1075:96-102.

Turturro F, Friday E and Welbourne T: (2007): Hyperglycemia regulates thioredoxin-ROS activity through induction of thioredoxin-interacting protein (TXNIP) in metastatic breast cancer-derived cells MDA-MB-231: BMC Cancer.; 7:96

Tuschl T, Zamore P.D, Lehmann R, Bartel D.P and Sharp P.A: (1999): Targeted mRNA degradation by double-stranded RNA in vitro: Genes Dev.; 13(24):3191-7

Ueda K, Kawano J, Takeda K, Yujiri T, Tanabe K, Anno T, Akiyama M, Nozaki J, Yoshinaga T, Koizumi V, Shinoda K, Oka Y and Tanizawa Y: (2005):

Endoplasmic reticulum stress induces Wfs1 gene expression in pancreatic beta-cells via transcriptional activation: Eur. J. Endocrinol.; 153: 167-176.

Vairapandi M, Balliet A.G, Hoffman B and Liebermann D.A: (2002): GADD45b and GADD45g are cdc2/cyclinB1 kinase inhibitors with a role in S and G2/M cell cycle checkpoints induced by genotoxic stress: J Cell Physiol.; 192(3):327-38.

Van der Krol A.R, Mur L.A, Beld M, Mol J.N and Stuitje A.R: (1990): Flavonoid genes in petunia: addition of a limited number of gene copies may lead to a suppression of gene expression: Plant Cell.; 2(4):291-9.

van der Werf N, Kroese F.G, Rozing J and Hillebrands J.L: (2007): Viral infections as potential triggers of type 1 diabetes: Diabetes Metab Res Rev.; 23(3):169-83.

van Greevenbroek M.M, Vermeulen V.M, Feskens E.J, Evelo C.T, Kruijshoop M, Hoebee B, van der Kallen C.J and de Bruin T.W: (2007): Genetic variation in thioredoxin interacting protein (TXNIP) is associated with hypertriglyceridaemia and blood pressure in diabetes mellitus: Diabet Med.; 24(5):498-504.

Varadi A and Rutter G.A: (2002): Dynamic imaging of endoplasmic reticulum Ca2+ concentration in insulin-secreting MIN6 Cells using recombinant targeted cameleons: roles of sarco(endo)plasmic reticulum Ca2+-ATPase (SERCA)-2 and ryanodine receptors: Diabetes;5 1 Suppl 1:S190-201

Vionnet N, Hani E.H, Dupont S, Gallina S, Francke S, Dotte S, De Matos F, Durand E, Leprêtre F, Lecoeur C, Gallina P, Zekiri L, Dina C and Froguel P:

(2000): Genomewide search for type 2 diabetes-susceptibility genes in French whites: Evidence for a novel susceptibility locus for early-onset diabetes on chromosome 3q27-qter and independent replication of a type 2-diabetes locus on chromosome 1q21-q24: Am J Hum Genet.; 67: 1470–1480.

Viparelli F, Cassese A, Doti N, Paturzo F, Marasco D, Dathan N.A, Monti S.M, Basile G, Ungaro P, Sabatella M, Miele C, Teperino R, Consiglio E, Pedone C, Beguinot F, Formisano P and Ruvo M: (2008): Targeting of PED/PEA-15 molecular interaction with phospholipase D1 enhances insulin sensitivity in skeletal muscle cells: J Biol Chem.;283(31):21769-78

Voigt S, Jungnickel B, Hartmann E and Rapoport T.A: (1996): Signal sequence-dependent function of the TRAM protein during early phases of protein transport across the endoplasmic reticulum membrane: J Cell Biol.; 134(1):25-35

Vukkadapu S.S, Belli J.M, Ishii K, Jegga A.G, Hutton J.J, Aronow B.J and Katz J.D: (2005): Dynamic interaction between T cell-mediated beta-cell damage and beta-cell repair in the run up to autoimmune diabetes of the NOD mouse: Physiol Genomics.;21(2):201-11.

Waeber G, Hurlimann J, Nicod P and Grouzmann E: (1995): Immunolocalization of neuropeptide Y in human pancreatic endocrine tumors: Peptides. 16:921-926.

Waeber G, Thompson N, Waeber B, Brunner H.R, Nicod I and Grouzmann E: (1993): Neuropeptide Y expression and regulation in a differentiated rat insulinsecreting cell line: Endocrinology. 133:1061-1067.

Wang Q and Bag J: (2008): Induction of expression and co-localization of heat shock polypeptides with the polyalanine expansion mutant of poly(A)-binding protein N1 after chemical stress: : Biochem Biophys Res Commun.;370(1):11-5

Wang Y, De Keulenaer G.W and Lee R.T: (2002): Vitamin D(3)-up-regulated protein-1 is a stress-responsive gene that regulates cardiomyocyte viability through interaction with thioredoxin: J. Biol. Chem.; 277: 26496–26500.

Wang Z.L, Bennet W.M, Wang R.M, Ghatei M.A and Bloom S.R: (1994): Evidence of a paracrine role of neuropeptide-Y in the regulation of insulin release from pancreatic islets of normal and dexamethasone-treated rats: Endocrinology.135:200-206.

Webb G.C, Akbar M.S, Zhao C and Steiner D.F: (2000): Expression profiling of pancreatic beta cells: glucose regulation of secretory and metabolic pathway genes: Proc Natl Acad Sci U S A.; 97(11):5773-8.

Webb P.G and Bonser A.M: (1981): Basal C-peptide in the discrimination of type I from type II diabetes: Diabetes Care.; 4(6):616-9.

White S.A, James R.F, Swift S.M, Kimber R.M and Nicholson M.L: (2001): Human islet cell transplantation--future prospects: Diabet Med.; 18(2):78-103

Wieczorek A. J, Sitaramam V., Machleidt W., Rhyner K, Perruchoud A. P and Block L. H: (1987): Diagnostic and prognostic value of RNA-proteolipid in sera of patients with malignant disorders following therapy: first clinical evaluation of a novel tumor marker: Cancer Res: 47: 6407-6412.

Wieczorek A.J, Rhyner C and Block L.H: (1985): Isolation and characterization of an RNA-proteolipid complex associated with the malignant state in humans: Proc Natl Acad Sci USA.; 82: 3455-3459.

Wiederkehr A and Wollheim C.B: (2006): Minireview: implication of mitochondria in insulin secretion and action: Endocrinology.; 147(6):2643-9

Winter J, Klappa P, Freedman R.B, Lilie H and Rudolph R: (2002): Catalytic activity and chaperone function of human protein-disulfide isomerase are required for the efficient refolding of proinsulin: J Biol Chem.; 277(1):310-7

Wollheim C.B and Maechler P: (2002): Beta-cell mitochondria and insulin secretion: messenger role of nucleotides and metabolites: Diabetes.; 51 Suppl 1:S37-42

Wong S.C.C, Lo S.F.E, Cheung M.T, Ng K.O.E, Tse C.W, Lai B.S.P, Lee K.C and Lo Y.M.D: (2004): Quantification of plasma beta-catenin mRNA in colorectal cancer and adenoma patients: Clin Cancer Res.; 10:1613–7.

World C.J, Yamawaki H and Berk B.C: (2006): Thioredoxin in the cardiovascular system: J Mol Med.; 84(12):997-1003.

World Health Organisation Department of Noncommunicable Disease Surveillance (1999). Definition, Diagnosis and Classification of Diabetes Mellitus and its Complications.

Wu J.J, Roth R.J, Anderson E.J, Hong E.G, Lee M.K, Choi C.S, Neufer P.D, Shulman G.I, Kim J.K and Bennett A.M: (2006): Mice lacking MAP kinase

phosphatase-1 have enhanced MAP kinase activity and resistance to diet-induced obesity: Cell. Metab.; 4: 61-73.

www.betacell.org **:** 14 Apr. 08

Xu X, Kahan B, Forgianni A, Jing P, Jacobson L, Browning V, Treff N and Odorico J: (2006): Endoderm and pancreatic islet lineage differentiation from human embryonic stem cells: Cloning Stem Cells.;8(2):96-107.

Xu X, Zeng W, Popov S, Berman D.M, Davignon I, Yu K, Yowe D, Offermanns S, Muallem S and Wilkie T.M: (1999): RGS proteins determine signaling specificity of gq-coupled receptors: J. Biol. Chem.; 274: 3549-3556.

Yamawaki H, Pan S, Lee R.T and Berk B.C: (2005): Fluid shear stress inhibits vascular inflammation by decreasing thioredoxin-interacting protein in endothelial cells: J Clin Invest.; 115(3): 733-8.

Yao A, Takahashi T, Aoyagi T, Kinugawa K, Kohmoto O, Sugiura S and Serizawa T: (1995): Immediate-early gene induction and MAP kinase activation during recovery from metabolic inhibition in cultured cardiac myocytes: J Clin Invest.; 96(1):69-77

Yasumura Y and Kawakita M: (2003): The research for the SV40 by means of tissue culture technique: Nippon Rinsho.: 21 (6): 1201–1219.

Yoo S.H, You S.H, Kang M.K, Huh Y.H, Lee C.S and Shim C.S: (2002): Localization of the secretory granule marker protein chromogranin B in the nucleus. Potential role in transcription control: J Biol Chem; 277(18):16011-21

Yoshida H, Ohagi S, Sanke T, Furuta H, Furuta M and Nanjo K: (1995): Association of the prohormone convertase 2 gene (PCSK2) on chromosome 20 with NIDDM in Japanese subjects: Diabetes.; 44(4):389-93

Young H.Y, Zucker P, Flavell R.A, Jevnikar A.M and Singh B: (2004): Characterization of the role of major histocompatibility complex in type 1 diabetes recurrence after islet transplantation: Transplantation.; 78(4):509-15.

Yu M, Geiger B, Deeb N and Rothschild M.F: (2007): Investigation of TXNIP (thioredoxin-interacting protein) and TRX (thioredoxin) genes for growth-related traits in pigs: Mamm Genome.; 18(3):197-209

Zhang B, Hosaka M, Sawada Y, Torii S, Mizutani S, Ogata M, Izumi T and Takeuchi T: (2003): Parathyroid hormone-related protein induces insulin expression through activation of MAP kinase-specific phosphatase-1 that dephosphorylates c-Jun NH2-terminal kinase in pancreatic beta-cells: Diabetes.;52(11):2720-30.

Zhang H.J, Walseth T.F and Robertson R.P: (1989): Insulin secretion and cAMP metabolism in HIT cells. Reciprocal and serial passage-dependent relationships: Diabetes.; 38(1):44-8

Zhong S, Li C and Wong W.H: (2003): ChipInfo: Software for Extracting Gene Annotation and Gene Ontology Information for Microarray Analysis. Nucleic Acids Research.; 31, 3483-3486.

Zhong X.Y, Holzgreve W and Huang D.J: (2008): Isolation of cell-free RNA from maternal plasma: Methods Mol Biol.; 444:269-73

Zimmer Y, Milo-Landesman D, Svetlanov A and Efrat S: (1999): Genes induced by growth arrest in a pancreatic beta cell line: identification by analysis of cDNA arrays: FEBS Lett.; 457(1):65-70.